1.0

2.8 | 2.5

3.2 | 2.2

3.6

4.0 | 2.0

1.1

1.8

1.25 | 1.4 | 1.6

MICROCOPY RESOLUTION TEST CHART

NATIONAL BUREAU OF STANDARDS

Proceedings of a Workshop
on the

Properties of Snow

DTIC
SELECTED
OCT 8 1982

D

8–10 April 1981, Snowbird, Utah

82 020

COMPONENT PART NOTICE

THIS PAPER IS A COMPONENT PART OF THE FOLLOWING COMPILATION REPORT:

(TITLE): ___Proceedings of a Workshop on the Properties of Snow, 8-10 April 1981,___

___Snowbird, Utah.___

(SOURCE): ___U.S. Army Cold Regions Research and Engineering Laboratory___

___Hanover,   NH___

TO ORDER THE COMPLETE COMPILATION REPORT USE ___AD-A120 517___.

THE COMPONENT PART IS PROVIDED HERE TO ALLOW USERS ACCESS TO INDIVIDUALLY AUTHORED SECTIONS OF PROCEEDINGS, ANNALS, SYMPOSIA, ETC. HOWEVER, THE COMPONENT SHOULD BE CONSIDERED WITHIN THE CONTEXT OF THE OVERALL COMPILATION REPORT AND NOT AS A STAND-ALONE TECHNICAL REPORT.

THE FOLLOWING COMPONENT PART NUMBERS COMPRISE THE COMPILATION REPORT:

Accession For

DTIC GRA&I

DTIC T::

Unannounced

Justification

Distribution/

Availability Codes

Avail and/or

Special

A

DTIC
ELECTE
OCT 2 9 1982

A

AD#:   TITLE:

Proceedings of a Workshop
on the
Properties of Snow

8-10 April 1981, Snowbird, Utah

Edited by:

R.L. Brown   Department of Civil Engineering and Engineering Mechanics
Montana State University, Bozeman, Montana

S.C. Colbeck   U.S. Army Cold Regions Research and Engineering Laboratory
Hanover, New Hampshire

R.N. Yong   Department of Civil Engineering, McGill University,
Montreal, Quebec, Canada

PREFACE

The Joint U.S.-Canadian Workshop on the Properties of Snow was held 8-10 April 1981 at the Snowbird Recreational Area, Snowbird, Utah. The workshop was sponsored jointly by the National Science Foundation, the U.S. Army Research Office, and the National Research Council of Canada. The persons associated with those institutions are Charles Babendreier (NSF), Steven Mock (ARO) and Lorne Gold (NRCC). Without their support and cooperation, this workshop would never have taken place. Particular appreciation is extended to Charles Babendreier for his advice and constructive criticisms during the workshop organization and planning period. Finally, we gratefully acknowledge the work of Donna Murphy and Stephen Bowen in editing and otherwise preparing these proceedings for press.

This workshop was organized specifically for the purpose of discussing current problems associated with the properties and processes of snow. As such, we did not intend to make this a conference in which presentations on recent research findings were merely given by the participants. Open discussion of current research and engineering problems in an informal manner was encouraged. This was felt to be best accomplished by the informal committee sessions which were conducted during most of the workshop.

In addition to the above reason for the committee structure, we also hoped to accomplish several other objectives with this arrangement.

First, as with any technical field, there has been a lack of active communication between the scientific and engineering fields. This is to be expected, since the training, capabilities and interests of these two groups are distinct. However, we felt the committee format would encourage an open discussion in which each group could come to understand and learn what the other group has to offer.

Second, we felt that this format provided a unique opportunity for the introduction and consideration of new ideas and methods. For this to work, the participants had to be willing to openly greet new ideas, although acceptance could only come after these ideas had been shown to be valid through analytical and experimental investigation. However, under the scrutiny of an informal group meeting of engineers and scientists such as at this workshop, any physically unsound ideas could be shown to be wrong.

Third, we intended to stress the engineering relevance of current problems associated with snow. In the final analysis, increased knowledge obtained through basic and applied research should eventually lead to solution of practical engineering problems.

The workshop began with a series of seven review papers, each of which covered a major area of study on the properties of snow. These presentations were designed to indicate the current state of the art in each area and to give each reviewer's opinions on what the current important problems are. In reality, they also formed a basis upon which the committee sessions could begin. Each committee discussed only one of the major areas listed below and generally convened after six hours of discussion. The five committees discussed the following topics:

1. Mechanical properties of snow
2. Acoustical, optical and electrical properties of snow
3. Metamorphism of snow
4. Properties of surface friction, flowing snow, and blowing snow
5. Experimental methods and snow classification systems

Other topics could have certainly been added, but with the funds and time allocated, the above was felt to be a more than adequate number of topics for consideration.

All in all, we must consider the workshop a success, although there certainly were difficulties. For one, the committees initially had difficulty addressing problems in a systematic manner. This may be partly attributed to the fact that the scientists and engineers considered different problems to be of major importance. For example, where an engineer might consider the development of a mathematically tractable constitutive law important for application to engineering problems, the physicist would be more concerned about granular and intergranular flow mechanisms, their characterization, and their effect on the properties of snow. Such contrasts did occur, but in the final analysis this intermixing of concepts left most of us a little wiser and with some new ideas to work with.

In the end, no grand consensus was reached, nor did we expect it. We all have our own way of looking at problems and our own methods of study, experimentation, and solution. In the long run, if we can do our own thing a little more effectively as a result of this workshop, it was worth the effort.

Steeering Committee

R.L. Brown, Montana State University
S.C. Colbeck, CRREL
R.N. Yong, McGill University

CONTENTS

WORKSHOP PROGRAM

7 April

7:00–10:00 p.m.	Cocktail reception at the Magpie Room, Cliff Lodge

8 April

8:00 a.m.	Welcoming Speech, *R.L. Brown*
8:15	Mechanical Properties of Snow, *B. Salm*
9:00	Viscous Flow and Frictional Properties of Snow, *T.E. Lang*
9:30	Properties of Blowing Snow, *R.A. Schmidt*
10:00	Coffee Break
10:15	Thermodynamic Properties of Snow, *S.C. Colbeck*
11:00	Electrical Properties of Snow, *W.H. Stiles*
11:30	Optical Properties of Snow, *S. Warren*
12:30–2:00 p.m.	Lunch
2:00–5:00	Committee Meetings on:
	1. Mechanical Properties (Chairman: *R. Oakberg*)
	2. Acoustical, Electrical and Optical Properties (Chairman: *H. Gubler*)

9 April

8:00–10:00 a.m.	Committee Meetings on:
	1. Mechanical Properties
	2. Acoustical, Electrical and Optical Properties
10:00	Coffee Break
10:15–12:00	Committee Meetings on:
	1. Viscous Flow, Frictional Properties and Blowing Snow (Chairman: *D. McClung*)
	2. Thermodynamical Properties (Chairman: *E. LaChapelle*)
12:00–1:30 p.m.	Lunch
1:30–5:00	Continuation of Committee Meetings
7:30–10:00	Open Meeting on Experimental Methods, Reporting of Data, and Snow Classification (Chairman: *F. Smith*)

10 April

8:00–12:00 a.m.	Free Time
1:00–3:00 p.m.	Committee Chairmen Reports to General Meeting
3:00	Coffee Break
3:30–5:30	General Workshop Discussion
5:30	Closing Remarks and General Conclusions, *R.N. Yong*
7:00	Banquet

K. Tusima
Institute of Low Temperature Science
Hokkaido University
Sapporo 060, Japan

S.G. Warren
National Center for Atmospheric
Research
P.O. Box 3000
Boulder, Colorado 80307

W.J. Wiscombe
National Center for Atmospheric
Research
P.C. Box 3000
Boulder, Colorado 80307

Raymond Yong
McGill University
817 Sherbrooke St. West
Montreal, P.Q., Canada H3A 3K6

ATTENDEES

Donald Alford
Box 3067
University Station
Laramie, Wyoming 82071

W. Ambach
Institut fur Medizinische Physik
Mullerstrasse 44
A-6020 Innsbruck, Austria

Betsy R. Armstrong
WDC-A, INSTAAR
University of Colorado
Boulder, Colorado 80309

Richard Armstrong
INSTAAR
University of Colorado
Box 450
Boulder, Colorado 80309

Craig F. Bohren
Department of Meteorology
Pennsylvania State University
University Park, Pennsylvania 16802

Harold S. Boyne
Department of Earth Sciences
Colorado State University
Fort Collins, Colorado 80523

Duain Bowles
Avalanche Forecaster
United States Forest Service
Salt Lake City, Utah 84112

R.L. Brown
CE/EM Department
Montana State University
Bozeman, Montana 59717

A. Chang
11029 Rutledge Drive
Gaithersburg, Maryland 20760

Samuel C. Colbeck
U.S. Army Cold Regions Research
and Engineering Laboratory
72 Lyme Road
Hanover, New Hampshire 03755

Armin Denoth
Schoepfstr 41
Institut fur Experimentalphysik
University of Innsbruck
Innsbruck, Austria

Jimmie Dent
CE/EM Department
Montana State University
Bozeman, Montana 59717

J. Dozier
Department of Geography
University of California
Santa Barbara, California 93106

G.L. Freer
Ministry of Highways
Parliament Buildings
Victoria, B.C., Canada V8W 3E6

Bard Glenne
Civil Engineering
University of Utah
Salt Lake City, Utah 84112

B. Goodison
Atmospheric Environmental Service
Downsview, Ontario, Canada

Hardy Grandberg
McGill University
Montreal, P.Q., Canada H3A 2K6

Hans Gubler
Eidg. Institut fur Schnee-und
Lawinenforschung
CH-7260 Weissfluhjoch
Davos, Switzerland

William L. Harrison, Jr.
U.S. Army Cold Regions Research
and Engineering Laboratory
72 Lyme Road
Hanover, New Hampshire 03755

G.J. Irwin
Defence Research Establishment Suffield
Ralston, Alberta, Canada T0J 2N0

C. Jaccard
Eidg. Institut fur Schnee-und
Lawinenforschung
7260 Weissfluhjoch
Davos, Switzerland

Jerome B. Johnson
Geophysics Institute
University of Alaska
Fairbanks, Alaska 99701

H.Y. Ko
Department of Civil Engineering and
    Environmental Engineering
University of Colorado
Boulder, Colorado 80302

J.A. Kong
36-383
Massachusetts Institute of Technology
Cambridge, Massachusetts 02139

Edward R. LaChapelle
Department of Atmospheric Sciences
University of Washington
Seattle, Washington 98195

Theodore Lang
CE/EM Department
Montana State University
Bozeman, Montana 59717

D. Marbouty
Domaine Universitaire
Centre d'Etudes de la Neige
3800 Grenoble, France

D. Marks
Computer Systems Laboratory
University of California
Santa Barbara, California 93106

Mario Martinelli
Rocky Mountain Forest and Range
Experiment Station
240 W. Prospect
Fort Collins, Colorado 80526

Doug McCarty
United States Forest Service
State & Private Forestry
Box 1628
Juneau, Alaska 99802

David McClung
P.O. Box 282
Canmore, Alberta, Canada T0L 0M0

Arthur Mears
222 E. Gothic Avenue
Gunnison, Colorado 81230

Robert G. Oakberg
CE/EM Department
Montana State University
Bozeman, Montana 59717

Ron Perla
Box 313
Canmore, Alberta, Canada T0L 0M0

Charles Raymond
Geophysics Program
University of Washington
Seattle, Washington 98195

B. Salm
Eidg. Institut fur Schnee-und
Lawinenforschung
7260 Weissfluhjoch
Davos, Switzerland

R.A. Schmidt
Rocky Mountain Forest and Range
Experiment Station
240 W. Prospect
Fort Collins, Colorado 80526

F.W. Smith
Mechanical Engineering Department
Colorado State University
Fort Collins, Colorado 80526

Richard Sommerfeld
Rocky Mountain Forest and Range
Experiment Station
240 W. Prospect
Fort Collins, Colorado 80526

William Herschel Stiles
1205 Schwarz Road
Lawrence, Kansas 66044

William St. Lawrence
U.S. Army Cold Regions Research
and Engineering Laboratory
72 Lyme Road
Hanover, New Hampshire 03755

COMMITTEE MEMBERS

1. Mechanical Properties	2. Acoustical, Electrical & Optical Properties	3. Viscous Flow, Frictional Properties & Blowing Snow	4. Thermodynamic Properties
R. Oakberg, *Chairman*	H. Gubler, *Chairman*	D. McClung, *Chairman*	E. LaChapelle, *Chairman*
D. Alford	W. Ambach	D. Alford	W. Ambach
B. Armstrong	J. Bergen	H. Boyne	B. Armstrong
R. Armstrong	C. Bohren	J. Dent	R. Armstrong
R. Brown	H. Boyne	A. Denoth	J. Bergen
J. Dent	A. Chang	B. Glenne	C. Bohren
B. Glenne	S. Colbeck	H. Gubler	R. Brown
W. Harrison	A. Denoth	W. Harrison	A. Chang
G. Irwin	J. Dozier	J. Johnson	S. Colbeck
E. LaChapelle	B. Goodison	T. Lang	J. Dozier
T. Lang	J. Johnson	N. Maeno	B. Goodison
P. Martinelli	J. Kong	A. Mears	G.J. Irwin
D. McClung	N. Maeno	P. Martinelli	J. Kong
A. Mears	D. Marks	R. Oakberg	D. Marbouty
R. Perla	D. Marbouty	W. St. Lawrence	D. Marks
W. St. Lawrence	R. Sommerfeld	R. Schmidt	R. Perla
R. Schmidt	W. Stiles	F. Smith	W. Stiles
F. Smith	S. Warren	R. Sommerfeld	G. Wakahama
K. Tusima	W. Wiscombe	K. Tusima	S. Warren
R. Yong		R. Yong	W. Wiscombe

Mechanical Properties of Snow

B. SALM

Swiss Federal Institute for Snow and Avalanche Research
7260 Weissfluhjoch/Davos, Switzerland

The investigation of the mechanical properties of seasonal snow cover aims mostly at applications in avalanche release and avalanche control but also at no less important problems such as vehicle mobility in snow, snow removal, or construction on snow. Primary needs are (1) constitutive equations, that is, relations between the stress tensor and the motion, and (2) fracture criteria which limit the region of validity of constitutive equations. Both can be tackled from the aspect of continuum theories and structure theories. With modern continuum theories the characteristic nonlinear behavior of snow can be taken into account and also the strong dependence on stress and strain history. When thermodynamics is introduced, more insight into the deformation and fracture processes can be gained. High initial deformation rates cause low dissipation, elastic behavior, and brittle fracture, whereas when dissipative mechanisms can develop, ductile fracture occurs. The advantage of structural theories lies in the immediate physical insight into deformation mechanisms, but the disadvantage is that only simple states of stresses acting macroscopically on a snow sample can be considered. Different approaches have been elaborated: for low-density snow the concept of chains (a series of stress-bearing grains) or the neck growth model (consideration of stress concentrations in bonds between grains) and for high-density snow the pore collapse model (snow idealized as a material containing air voids). Structural constitutive equations were applied to the calculation of stress waves in snow. Recorded acoustic emissions, indicating intergranular bond fractures, can also be used for the construction of constitutive equations. Structural failure theories model brittle fracture with series elements, where the weakest link causes fracture of the entire body, and ductile fracture by parallel elements, where fracture of one element leads merely to a redistribution of stresses and only after a sufficiently high increase of the load to a total failure. In this method the statistical distribution of link strength plays an important role. The mechanics of wet snow (snow containing liquid water) is considerably different from dry snow mechanics. While deformation of dry snow is dominated by (slow) creep and glide of ice grains and bonds, the densification of wet snow is mainly due to the (fast) process of pressure melting at stressed contacts of a grain.

CONTENTS

1. INTRODUCTION

Mechanical properties mean the result of investigations about deformation and strength encountered under different conditions, such as the natural snowpack under gravitation or with man-induced effects such as explosions, oversnow vehicles, or snow removal.

Since we are concerned with the special material snow and not with materials in general, we presume that one is interested in results applicable to engineering problems. As this review is more or less restricted to the seasonal snow cover, applications to avalanche release and avalanche control are of prime but certainly not exclusive importance.

One can look on snow at different levels. On a microscopic scale, snow consists of a skeleton of ice grains. The grains can be single ice crystals or groupings of several crystals. The three-dimensional skeletal arrangement is characterized by the grains (shape, dimensions, crystallographic orientation of the crystals), the bonds (area), the mean number of bonds per grain (including their spatial distributions relative to the grain), and

finally the spatial arrangement of chains formed by several grains.

A structure defined as above, to be completed by the conditions of temperature and the air (or meltwater) filling the pores, constitutes a homogeneous snow. In other words, if in a certain snow sample the described quantities obey the same statistical distributions, then this snow is homogeneous.

In the natural snowpack, homogeneous snow exists in snow layers, originating from uniform snowfall periods. The individual layers have different physical and mechanical properties. From the stated definition of homogeneity it follows that flaws in a layer, originating from wind action, vegetation, skier, or mechanical effects (e.g., partial failure), are not distributed according to a statistical law and have to be treated differently from homogeneous snow.

The interfaces between individual layers or between ground and a layer play an important role when avalanche formation or snow gliding are considered. Such interfaces sometimes differ considerably in their properties from both neighboring layers, depending on the weather conditions between two snowfalls (e.g., formation of surface hoar). In some cases they are thin and may have a thickness of only a few grains or crystals.

To understand mechanically the snowpack as a whole, one has to know all the properties of the individual layers and the interfaces and how they interact with each other.

Obviously, for an understanding of material properties, both theory and experiment are needed. Without a physically sound theory, one will never be able to bring some order to the chaos of observed phenomena. Here a contrast often exists between analysts and scientists with more practical interests. The final goal, however, should be to obtain applicable results based on a

physically sound theory. This is exactly what *Mellor* [1975] pointed out: 'Elegant simplification of complicated behaviour is very much needed.'

The first and most important part of a theory is that one has to construct ideal models which reflect the predominant properties of the material. Today an 'ideal material' no longer exclusively means a linearly and infinitesimally elastic material or a linearly viscous fluid. Rational mechanics, mainly developed in the 1960's, provided a powerful tool for constructing nonlinear models of any degree.

For a mechanical description of a material, one has first to consider general principles common to all materials, such as the balance or conservation of mass, linear momentum, moment of momentum, and energy. A further principle, that of irreversibility, expressed in terms of entropy, is nowadays still debated among the 'giants' of modern continuum physics [*Truesdell*, 1965].

These general principles do not, however, suffice to describe the behavior of a body. A constitutive equation is needed to specify the material, that is, a relation between stress tensor and the motion, generally also including temperature. There are rules to be obeyed by all constitutive equations. The first is that of determinism, stating that all properties of a material can depend only on the past. This introduces the important notion of history, which influences the properties at present. A second is the rule of material frame indifference. It states that a constitutive equation has to be independent of the system from which quantities are observed (important for large rotations).

From this treatment it will become clear that there exists no universal constitutive equation for snow, only equations reflecting the behavior under special conditions, for example, conditions of stress, strain, or density.

Fracture criteria are related directly to constitutive equations in that they predict their region of validity beyond which fracture occurs. Consequently, they also have to obey the rules stated above.

It is obvious that the mechanical behavior of snow can be tackled from the aspect of continuum theories and structural theories (i.e., at the level of grains and bonds). The former procedure is confined to relations of gross phenomena in the sense that average effects are considered, whereas in the latter case the observed averaged behavior of a snow sample is explained by structural properties. As the same principles apply, no contradiction between the two approaches should appear. On the contrary, both seem necessary in order to increase understanding of the phenomena. A limitation for structural theories seems to exist in that only the behavior under simple states of stress or deformation can be predicted (e.g., hydrostatic pressure or uniaxial stress).

At any rate the experiment represents the only means of determining if a certain perception is valid. The ultimate goal is then nothing less than to be able to predict the behavior of our material, snow, under the different circumstances mentioned at the beginning of this section. At present we are still far from this ultimate goal. It will be shown in this review that fairly general (but nonuniversal!) constitutive equations and fracture criteria are known. But there is a snag, because the constants defining the relations are only valid for the particular snow that has been tested. With different snow samples they vary considerably, maybe over orders of magnitudes. Only the type of relation is unchanged (which is not proved strictly, but so far no observation contradicts this statement). Universal constants valid for any arbitrary snow (with the exception of some basic

physical ones for ice, water and water vapor or gravity) do not exist! Therefore all the numerical relations presented in this review are limited to the exact type and state of the snow tested. But this does not invalidate theories and does not depreciate specific tests, because they can demonstrate accurately the validity of a certain theory. To reach our ultimate goal, however, we should test the full variety of natural snow and at the same time define it not merely by density but also by a set of structural parameters and temperature. In such a way a 'dictionary' could be established which would make possible an accurate prediction of the behavior. In the immediate future, however, the establishment of such a dictionary cannot be of primary importance in research. First we must understand what really happens when snow deforms and fractures. In view of applications it seems highly desirable to select the snow types to be investigated according to their importance. For avalanche formation, for instance, these are new snow with a density of 100–200 kg/m³ and interfaces between snow layers. Unfortunately, big gaps still exist here because experiments are difficult to perform.

This paper deals with investigations performed roughly later than those included in the brilliant review papers by *Mellor* [1975, 1977].

We are following a series of papers which seemed relevant to the topics. No claim of completeness can be made. (References to work done in the USSR are missing because of language problems. To remedy this deficiency, we cite the recent review paper by *Voitkovsky* [1977].) Probably, this review seems less transparent than earlier ones dealing with more classical theories, where material constants could be directly compared. In the nonlinear theories, however, the constants are replaced by material functions or functionals, which often impedes a direct comparison.

2. CONSTITUTIVE EQUATIONS AND FAILURE CRITERIA BASED ON CONTINUUM THEORIES

As already stated, a failure criterion necessarily contains parameters from the constitutive equation. Both of them are therefore needed in continuum theories. When the criterion reaches a defined critical value, possibly a number, a magnitude of a stress, or an energy, failure occurs.

The classical failure criteria work well for materials with time-independent properties. They are usually formulated in terms of maximum stress or critical stored energy. Usually, strength is only influenced by deviatoric deformations, because unlimited volumetric strength is assumed. In rheological criteria [*Reiner*, 1958], ultimate strain, strain rates, and stress rates are introduced as parameters in fracture criteria.

For snow, *Salm* [1971] formulated strength in terms of critical elastic strain energy (reversible part) and critical rate of dissipation work (irreversible part). A nonlinear viscoelastic constitutive equation at high stresses was used in the failure criterion. The history was not introduced, but changes in properties during deformation paths were taken into account by a function of total deformation.

Snow strength dependence on a general history of deformation was first introduced by *Brown et al.* [1973]. In the following years the same group at Montana State University worked on the problem, based on nonlinear mechanics. This pioneering work culminated in the introduction of modern thermodynamic aspects as described by *Truesdell* [1965].

The theory by *Brown et al.* [1973], following *Pipkin* [1964], is a strictly mechanical one and does not consider the ther-
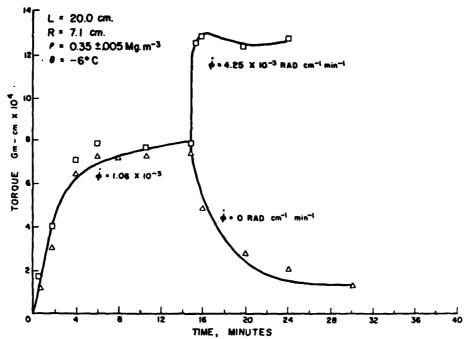
Fig. 1. Constitutive equation: comparison of torque response curve for theory and experiment. L is the length and R the diameter of tested circular cylinder, ρ is density, θ is temperature, and φ means the twist rate per unit length [Brown et al., 1973].

modynamic history. The criterion is based on the deformation history up to the time of fracture and was evaluated by separate tests for deviatoric and volumetric deformations (torsion and uniaxial compression, respectively). For the formulation of the criterion the intrinsic idea is that failure depends on the history of work rates, separated into volumetric and deviatoric stress powers, $P_v(\tau)$ and $P_d(\tau)$, respectively (τ is a variable time in the past). The failure functional, taking unity for fracture, is defined as a multiple integral representation approaching nonlinearity in work rates to third order. For example, the second-order part contains terms such as

$K_3\ P_d(\tau_1)\ P_d(\tau_2)$ purely deviatoric terms;

$K_4\ P_d(\tau_1)\ P_v(\tau_2)$ coupled terms;

$K_5\ P_v(\tau_1)\ P_v(\tau_2)$ purely volumetric terms.

The kinematical quantity upon which the above terms depend is the Lagrangian strain tensor (measures finite strain with respect to the undeformed state). The coefficients K_i of the terms in P, the failure memory functions, are chosen as functions containing $D \exp(-\gamma t)$, where the constants D and γ are obtained in tests. The constitutive equation, relating the Cauchy stress tensor to the deformation gradient and the history-dependent Lagrangian strain rate tensor, is represented by sums of multiple integrals up to the third order. The relaxation memory functions, the history-dependent coefficients in the constitutive equation, are chosen as functions of the form $A \exp(-\lambda t)$, where the decrease in time represents the principle of fading memory. Again the constants A and λ were determined in tests (Figure 1).

The tests proved a significant effect of the history on failure and, furthermore, that the failure process is mainly associated with volumetric deformation. For tests without deformation history, that is, a sudden increase of the deformation rate from zero to the nominal value, failure stress decreased with increasing deformation rate. As soon as a critical, that is, slow enough, rate was reached, no failure occurred, and snow exhibited a fluid nature. This is consistent with results by, for example, Salm [1971].

In tests where fracture was preceded by a constant deformation rate, that is, when after a certain time of deformation a higher strain rate leading to fracture was suddenly applied, fracture stresses were very high, whereas in other tests, in which the preceding deformation was terminated for a while and then the higher strain rate was applied, fracture stress decreased approximately in the same way as the stress-time relaxation curve (Figures 2 and 3).

Physically, this points to the following features:

1. With high strain rates, snow shows brittle fracture.
2. With low strain rates, a flow mechanism is established in the grain lattice. Intergranular bond rupture, local melting, and slip within crystals and grains enable a higher mobility of the lattice in that case.
3. With advancing relaxation, snow tends increasingly to a brittle state. Refreezing of the local melting points and disappearance of the slip can account for this phenomenon.
4. A significant part of the failure process is due to the collapse of the matrix of ice grains, that is, to the volumetric part.

A question may be raised about the degree of nonlinearity that has to be taken into account for snow in constitutive equations. Brown et al. [1973] chose an expansion of the multiple integral representation up to the third degree. Brown and Lang [1973] investigated two further constitutive equations of a lower degree in nonlinearity. One is the finite linear viscoelastic theory, where separate linear terms in strain and strain rates occur (elastic terms were dropped). Here the nonlinearity builds up with the proceeding deformation because of products of strain and strain rate. The other is the second-order
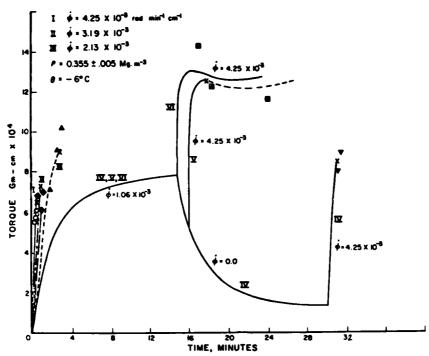
Fig. 2.   Failure tests: comparison of theoretical and experimental values for torsion. In load path III, nearly fluid nature
is reached; fracture was achieved on only three of six runs. In path VI, failure never occurred, and in path V, on only three of
five tests. In path IV, failure occurred on every test [*Brown et al.*, 1973].

theory, which is linear in strain and contains linear and quad-
ratic terms in strain rate. From tests with constant rate com-
pression it was found that the multiple integral constitutive
equation with a third-order expansion was in best agreement
with the results. Stress varied with the cube of strain rate. This,
however, does not invalidate theories with lower degrees for
cases of small or intermediate strain rates.

More insight into the phenomena of deformation and frac-
ture of snow than a purely mechanical theory can give can be
obtained by introducing the principle of irreversibility, because
snow is a highly dissipative material.

Salm [1975, 1977] made an attempt to describe the quasi-
stationary creep of snow by the principle of maximum entropy
production, as stated by *Ziegler* [1963]. With this principle a
constitutive equation of the Reiner-Rivlin type [*Reiner*, 1958]
but depending only on one function, the dissipation function,
was constructed. However, this did not include history effects
explicitly.
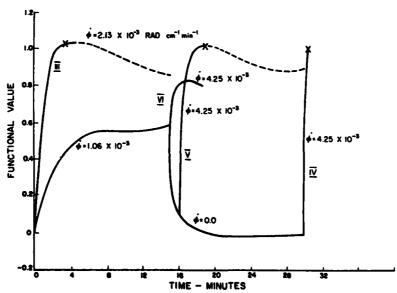
Fig. 3.   Variation of failure functional for deformation paths of Figure 2. A functional value of 1.0 means fracture [*Brown et
al.*, 1973].
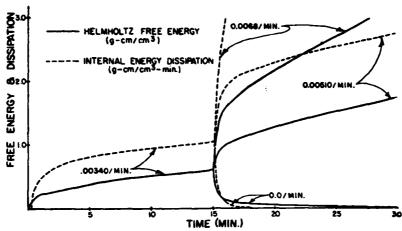
Fig. 4. Constitutive equation: demonstration of how energy is dissipated and stored with constant deformation rates in three different load paths. Note the initiation of deformation with negligible dissipation and the large increase of dissipation on the path with a rate of 0.0068 min^{-1} [Brown, 1976]. (Reprinted by permission of Pergamon Press.)

A general approach to the introduction of thermodynamics was made by Brown [1976], based on the important work of Coleman [1964]. With this theory the thermomechanical state can be studied during deformation and just prior to fracture. To do so, the histories of the strain tensor, of the Helmholtz free energy (the portion of internal energy which is recoverable under isothermal conditions), and of the dissipation rate have to be formulated. Brown's [1976] theoretical investigations resulted in a thermodynamic theory equivalent to Pipkin's [1964] mechanical one. The main result of Coleman [1964] is that a relation between the Helmholtz free energy ψ, stress, and specific entropy does exist by means of the first and second laws of thermodynamics. It is a relation between the three different functionals, each mapping the history of strain and temperature (temperature gradient drops out) into the stress tensor, ψ, and specific entropy. To derive it, the use of a highly complex mathematical apparatus is required, lying far outside the scope of this paper. Brown [1976] showed that a complete determination of the free energy is possible when the memory functions are evaluated by tests. Exponential forms similar to that of

Brown et al. [1973] are assumed. This is the impo.tant progress compared to pure mechanical theories, since with the calculated free energy and dissipation more insight into the deformation and fracture processes can be gained.

Uniaxial compression tests were performed to evaluate the memory functions. Axial strain (up to 15%), lateral strain, and load response were recorded. A snow type with faceted grain surfaces and weak intergranular bonding, having a density of 335 kg/m^3, was tested at cold room temperature of $-10°C$. With the thermodynamic theory the behavior in deformation and failure can now be expressed in terms of energy (Figures 4 and 5) as follows:

1. When deformation starts at a constant strain rate of 0.0034 min^{-1}, dissipation is negligible until a stress of about 0.2–0.3 bar is reached, which is in qualitative agreement with the one-dimensional Burger's body used by de Quervain [1946] or even better with the non-Burger's body introduced by Salm [1971]. It is interesting that acoustic emissions in the 50- to 100-kHz range, observed by Bradley and St. Lawrence [1975], become stronger when stresses of 0.2 bar are attained. This may
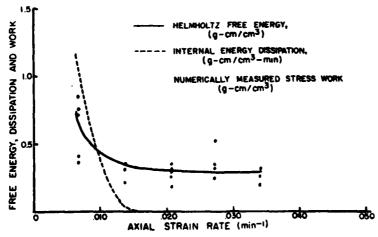

Fig. 5. Fracture values of free energy and dissipation for deformation paths with high initial deformation rate from the undeformed configuration. At higher rates, dissipation is negligible. Circles represent the total work calculated from strain rate and measured stress response [Brown, 1976]. (Reprinted by permission of Pergamon Press.)
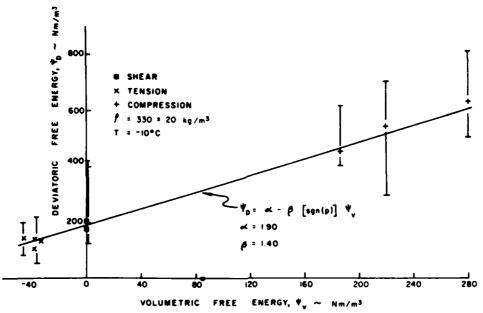
Fig. 6.   Failure criterion for brittle fracture: comparison with experimental results [*Brown*, 1977]. (Reprinted by permission
of the International Glaciological Society.)

be attributed to bond fractures representing dissipative pro-
cesses.

2. The nature of fracture is closely associated with dis-
sipation. A high initial deformation rate from the undeformed
state causes low dissipation, elastic behavior, and therefore
relatively low brittle fracture stresses, whereas with high rates
preceded by lower ones, dissipative mechanisms can develop,
and the energies causing ductile fracture are much higher.
Dissipation increases the internal energy ε necessary for frac-
ture and hence increases the strength of snow.

It now becomes clear that a fracture criterion can be written
in terms of free energy and internal dissipation. *Brown and Lang*
[1975] mentioned a possible form, relating the critical value of
free energy ψ_c with the elastic value ψ_0 and the history of
dissipation, but without giving a quantitative formulation of it.

This was then done by *Brown* [1977], who expressed failure
criteria by purely deviatoric and purely volumetric parts of the
free energy and by the internal energy dissipation σ. From tests
under tension, compression, and shear he arrived at criteria for
brittle and ductile fracture. For the first case, no dissipation is
assumed, and a linear relationship between the critical devi-
atoric and critical volumetric free energies ψ_D and ψ_v, respect-
ively, was obtained. In the second case, as an approximation of
the dissipation history the dissipative state σ_0 just after the high
strain rate leading to fracture was applied. Here, too, a linear
relation was obtained by adding a dissipation term to the
deviatoric free energy of brittle fracture (Figures 6 and 7).

So far we have discussed a series of papers dealing rigorously
with the concepts of modern continuum theories as set forth by,
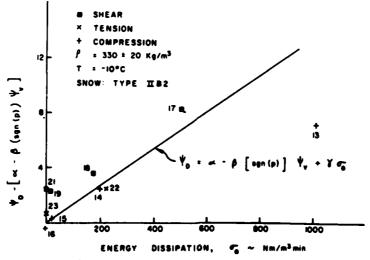for example, *Malvern* [1969] and *Truesdell* [1965]. However,

Fig. 7.   Failure criterion for ductile fracture: comparison with experimental results [*Brown*, 1977]. (Reprinted by permission
of the International Glaciological Society.)

to the author's knowledge none of the theories presented have ever been used to solve engineering problems. This does not mean that they are superfluous. On the contrary, only with a rigorous physical theory can insight into the processes involved be obtained.

In the following paragraphs a selection of papers is presented which are partly based on empirical findings and are therefore simpler and more suitable for solving practical problems.

Desrues et al. [1980] present a paper which aims not only to find a realistic constitutive equation for snow under slow deformation rates but also to use it for the investigation of the seasonal snowpack under gravity loading and specified boundary conditions. The applicability of the resulting type of constitutive equation to the finite element method has been demonstrated by *Boulon et al.* [1977]. The authors assume isotropy and consider the importance of volumetric creep. For a small deformation increment $d\varepsilon$ in a small time increment dt the response consists of a small stress increment $d\sigma$ which is expressible as

$$f(d\varepsilon, d\sigma, dt) = 0$$

The Boltzmann's superposition principle is now applied, which may be questionable because it holds strictly only for linear stress-strain relations. To construct a realistic model, separate nonlinear terms for the increments are introduced. For elasticity this is a linear stress-strain relation, assuming constant Poisson's ratio and a nonlinear Young's modulus (increasing with the first invariant of the stress tensor). The viscous deformation rate is linear in stress increments (or stress rate) and decreases nonlinearly with the total current viscous deformation and with time. The latter represents the history in a simple way. With infinitesimal increments the strain rate is given by a simple integral. Tests with a triaxial apparatus were performed under isotropic compression and constant axial strain rates with constant lateral pressure. In a first set of tests the eight constant parameters were measured. A second set, considerably different from the first in the stress history, was run to check how accurately the resulting constitutive equation predicts the response of the samples ('verification paths'). The result is good in spite of some scatter, which in part may also be attributed to the inhomogeneity of the tested snow (new snow, density 150–200 kg/m³, temperature −10°C to −2°C).

A completely different approach to a constitutive relation for the viscous creep of a natural snowpack was proposed by *McClung* [1980]. The idea behind his approach is that field data indicate conditions that are natural and difficult to reproduce in laboratory tests. The relation is derived from field tests in the neutral zone of a slope. Mostly, triangular creep profiles were observed, suggesting that shear strain rate and the strain rate perpendicular to the slope are each approximately independent of depth. With an assumed constant ratio of shear to normal stress in the neutral zone, the author arrives at a generalized three-dimensional relation. An approximately linear shear and bulk viscosity in depth and a constant depth-independent viscous Poisson's ratio is predicted. Laboratory tests support the linear increase of viscosity with increasing normal stress.

Probably the simplest constitutive equation which has been proposed recently is that of *Watanabe* [1980] for creep under uniaxial tension. The influence of stress σ, time t, and temperature T (in degrees Celsius) on strain e (defined as elongation of the sample) is given in the form

$$e \propto \sigma^{3/2}(t/-T)^{2/3}$$

which seems to fit the test results extremely well. History degenerated to $t^{2/3}$, which holds, of course, only for the monotonically increasing loads applied in the tests. The low exponent of σ demonstrates the stiffness of snow under tension. Of interest is the coupled effect of time and temperature, where equal ratios always result in the same strain (thermorheological simplicity). Certainly, the above relation is by no means a general one. It is to be expected that the exponents will depend on snow type. Furthermore, the maximum strain never exceeded 1%, which demonstrates nonlinearity of snow even under very small strains.

To conclude this section an observation by *Singh and Smith* [1980] should be mentioned which could question the continuum mechanical approach to snow mechanics. Samples were tested under constant strain rate in tension with strain gages mounted onto snow. In such a way the true strain and strain rate could be measured within the snow and not from the displacements of the ends of the sample as it is usually done. The authors discovered nonuniform deformations which could not have been detected with the usual measurement. A 'ratcheting' in the stress-strain curve was observed, which seems to be in agreement with *Narita's* [1980] discovery of small cracks (see section 5).

3. CONSTITUTIVE EQUATIONS BASED ON THE STRUCTURE

For the construction and use of structural theories it is necessary to know the significant parameters describing the structure. This is also of some importance for continuum theories (see section 1). In tests for the evaluation of constants appearing in constitutive relations, the snow type investigated should be precisely identified. Unfortunately, many investigators ignore this and describe snow at best by density.

Good [1975] described a way of identifying snow structure by automatic thin section analysis, using an automatic scanning microscope in combination with a software package to perform subsequent data analysis. He defined 21 parameters of the structure, for instance, point density (ratio of 'ice' points to all points), grain surface per unit volume, mean grain and void diameter, and mean radius of convex grain boundaries. The technique of factorial analysis is used to find a geometrical interpretation of these parameters. Independent factors, formed as linear combinations of the parameters, span a vector space. In this space, 62% of the total information of the parameter set is represented by two factors, and 70% by three factors. With this tool, subtle changes of structure can be recorded.

Grain bonds are critical for the mechanical properties of snow. To obtain insight into their geometrical nature, *Kry* [1975a] used a section plane preparation technique to allow a quantitative stereological analysis. This technique is ideal for the use of quantitative stereology, where from a two-dimensional projection the three-dimensional structure can be calculated with certain assumptions. Kry presents values for the three-dimensional grain size, grain bond size, number of bonds per unit volume, and related bonding measurements. These results from mutually othogonal section planes show that the assumptions of randomness and isotropy of grain and grain bond location and orientation, necessary for stereological analysis, are satisfied to within 10% even after 30% uniaxial viscoelastic deformation of a snow sample. The idealization of a grain bond as a circular plane disk yielded self-consistent results. An accurate determination of the number of bonds per grain was hindered because of variations in the shape and size

of snow grains within a given sample. Kry's results may not be generally valid for snow, because he only tested equi-temperature-metamorphosed snow in a density range 270–340 kg/m^3.

Kry [1975b] was the first to investigate relations between the viscoelastic properties and structure. The methods for structural investigations were the same as those described above [*Kry*, 1975a], and the same snow type was tested. He showed how the Young's modulus and viscosity vary when the structure of single samples is changed by nondestructive uniaxial compression up to 30% of deformation. The important conclusion is that viscosity increases much more rapidly than Young's modulus for an increase in density. The first increased nearly exponentially, whereas the latter increased only about linearly. Stereological analysis of sections from the samples showed a linear increase in number of grain bonds per unit mass, while the average grain bond size remained constant during densification. It is concluded that only a fraction of the grain bonds transmit an applied stress and that the new grain bonds formed during deformation determine the change of the viscoelastic properties. To explain these observed variations, the hypothesis of chains, a series of stress-bearing grains, is introduced and used in a quantitative way. In this way the importance of individual bonds is combined with the connectivity of grains. The experiments have established the validity and usefulness of this concept.

The advantage of structural theories lies in the immediate physical insight into deformation mechanisms. For the development of structural constitutive equations, one has to assume simple states of stresses acting macroscopically and on average on a snow sample large enough in comparison to grain diameters. The reason is that only in simple stress states can a relatively simple model for transferring the macroscopic stresses to the lattice be constructed. An introduction of complex states of stresses would imply a general relative movement in grain bonds, such as gliding and rotations, and also temporal variation of bond and grain dimensions, including separation and formation of bonds. All this would then have to be put in relation to the transfer of macroscopic stresses.

In the following paragraphs, two types of equations, one derived for hydrostatic pressure and the other for uniaxial deformation, are discussed. The influence of history is considerably simplified by a restriction to monotonically increasing loads.

Brown [1979a, 1980c] developed two constitutive equations for large strain and strain rates under hydrostatic pressure, one for medium- to high-density snow and the other for low-density snow. As the matrix material of snow consists of ice, a constitutive relation for this material first has to be derived. An elastic-viscoplastic behavior of the material is assumed, based on the experimental results of *Dillon and Andersland* [1967] and F. D. Haynes (unpublished data, 1976). According to these studies, ice behaves elastically in compression until a rate-dependent yield stress Y, the principal difference value of the deviatoric stress tensor,

$$Y = S_0 + C \ln (AD)$$

is reached. S_0, C, and A are material constants, and D is the principal difference value of the deviatoric deformation rate tensor (ice is assumed to be incompressible). For strain rates above 10^{-5} s^{-1} this law is more accurate than that of Glen.

For medium- to high-density snow, *Brown* [1979a] developed the pore collapse model. In this model, snow is idealized

as a material containing air voids (pores); a change of density is due exclusively to the collapse of the voids. The model is a thick-walled hollow sphere of polycrystalline ice. Therefore pores are considered separately, and no interaction takes place among them, as in low-density snow. The stress intensification, a consequence of the skeletal nature of snow, is taken into account by a scale factor which expresses that the average pressure in the porous material, $\hat{p}$, is smaller than the actual pressure in the matrix material, P: $\hat{p} = P/\alpha$, where $\alpha = \rho_m/\rho$ is the density ratio. Here ρ_m and ρ are the densities of the matrix material (ice) and of the porous material (snow), respectively. Further assumptions are that no fracture occurs and that the air pore pressure is negligible. The increase of stiffness under plastic deformation (work hardening) is taken into account by a term $J \exp(-\phi\alpha/\alpha_0)$, where J and ϕ are material constants and α_0 is the initial density.
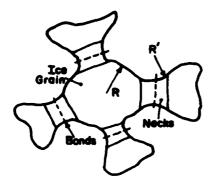
When the external pressure increases beyond that in the stress-free state, the hollow sphere deforms in three phases. These are (1) a purely elastic phase, then (2) an elastic-plastic phase (plastic flow starts at the inner side of the hollow sphere, where elastic stresses are maximum), and finally (3) a fully plastic phase. In all applications, only the last phase was considered (Y much smaller than the elastic shear modulus). In the most general case of the resulting constitutive equation the average pressure $\hat{p}$ depends on the three material constants of ice, the current and initial density ratios α and α_0, respectively, the rate $\dot{\alpha}$, and the work-hardening term. For very high rates of loading and the additive acceleration term containing geometrical parameters and $\dot{\alpha}$, $\ddot{\alpha}$ has to be included. A good agreement of the simplified constitutive equation for quasi-static loads (ignoring acceleration terms) with the experimental results of *Abele and Gow* [1975, 1976] could be found.

For low-density snow, that is, snow with densities less than about 300 kg/m^3, it would be unrealistic to model air pores by a sphere; the reverse has to be done by idealizing the ice grains as some specific shape including their connections to the lattice by necks. In general, the grains do not act separately, as they are arranged in chains of arbitrary form, which determines the state of stress and deformation in the neck region.
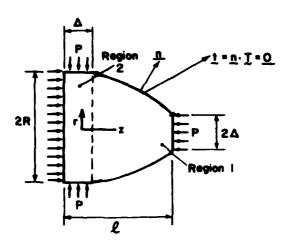
To establish a constitutive equation for low-density snow, *Brown* [1980c] considered a spherical grain of radius R acting separately and loaded by normal stresses in several (more than two) necks of length L and minimum radius Δ perpendicular to L (Figure 8). Glide in the necks (and in the grain) is therefore ignored in comparison to normal stress-induced plastic deformations of necks and grains. This is justified by the assumed hydrostatic pressure. However, an empirical adjustment is added later to account for intergranular slip. The calculation of stress and deformation in grains and necks is based on the idea that for each grain there exists a predominant axial state of stress with equally distributed directions of axes in the space. A first region of the grain is therefore idealized to carry solely this axial stress P with a stress-free lateral boundary. P is related to the macroscopically measured pressure $\hat{p}$ by

$$P \simeq \hat{p}\alpha(R/\Delta)^2$$

that is, the density ratio and the ratio of grain and neck areas. From this first region an expression for the rate of change of neck radius $\dot{\Delta}$ was found. This rate of change, a purely mechanical effect not including material transport to the neck, depends on the axial stress, on Δ, and on the three material constants of ice. In a second region of the grain, lateral surface loading by adjacent grains over a certain fraction of the total surface, f, is

a. TYPICAL GRAIN AND NECK GEOMETRY

b. IDEALIZED GRAIN GEOMETRY

Fig. 8. Geometry of granular structure of low-density snow and an idealized geometrical model [Brown, 1980c]. (Reprinted by permission of the American Institute of Physics.)

assumed to dominate. From the average state of stress in this region, the rate of change of the grain radius $\dot{R}$ is formulated in an expression containing R, Δ, f, $\dot{p}$, and the three material constants of ice. From this, in principle, the rate of change of density ratio $\dot{\alpha}$ can be expressed in the form

$$\dot{\alpha} = A_1 \exp (\beta_1 \, \dot{p}/F) + A_2 \exp (\beta_2 \, \dot{p}/F)$$

The coefficients A_1, A_2, β_1, and β_2 depend on the properties of ice and the structure of snow. The empirical term F was introduced for a better fit to experimental data [Abele and Gow, 1975, 1976] and is explained by taking into consideration the effects of intergranular glide, work hardening, and random neck and grain geometry. F is assumed to depend on density and varies considerably during densification, demonstrating the necessity of an important correction to the theoretical model. The evaluation of the above equation showed that $\dot{R}$ is much less than $\dot{\Delta}$, so that the deformation of the grain can be neglected and consequently also the second term in this relation. The most important structural parameter seems to be Δ/R. N, the mean number of bonds per grain, was taken as a function of density alone. In a later paper [Brown, 1980d] a density relation for f was given. Finally, it seems natural that the theory loses accuracy when Δ approaches the value of R.

It is possible to obtain a realistic constitutive relation with-

out detailed analysis of stress and strain in a grain or generally in chains. It is to be expected that stress at a microscopic level is not equally distributed over grains or chains, so that some grains participate more intensively in the deformation process than others, because they carry a much bigger portion of the overburden stress.

On this basis, St. Lawrence and Lang [1981] developed a constitutive relation for uniaxial deformation and intermediate values of deformation rates, that is, 10^{-6}-10^{-5} s^{-1}, where intergranular bond fracture is detectable as acoustic emissions. Adjacent ranges, such as low strain rates with little rearrangement of ice grains or high rates where fracture of grains becomes a large-scale fracture, are not considered. In the model presented, linear elastic and additive 'plastic' deformations are considered, where the latter deformation includes irreversible flow in and between grains and grain boundary fracture.

The plastic part of the strain rate $\dot{\epsilon}_p$ is attributed to the fraction of grains mobile in a given direction, N_m. It is given by

$$\dot{\epsilon}_p = N_m V/B$$

where V is the particle velocity during a mutual movement of adjacent ice grains separated by a center to center distance of B. The differential equation derived relates applied stress and total strain and strain rate substantially by the Young's modulus E and the quantities on the right-hand side of the above equation. The main task now is the evaluation of V and N_m, for which the basic assumption is made that V is a function of stress and N_m a function of strain and strain rate. In a relaxation phase (fixed strain), therefore, N_m remains constant, and V is a function of the decreasing stress alone. From relaxation tests it was found that V varies exponentially with the stress. To determine N_m, it was expected that this quantity depends on the intensity of acoustic emissions, representing fractures of bonds, represented as a function of total strain. With the inclusion of stereological parameters, N_m can then be related to the acoustic emissions. From this, one can see that the percentage of mobile grains decreases with progressive strain. With known velocity and mobility functions, the differential equation can be solved. The resulting stress-strain relation fits the experimental data well if, in tension, a work-softening coefficient is introduced, expressing the weakening of the material with progressive strain.

The paper by St. Lawrence and Lang [1981] is the latest of a series dealing with deformation and fracture of snow on the same principle of acoustic emissions. Each of these papers deserves more attention, but because of lack of space, they are merely listed here: St. Lawrence and Bradley [1975, 1977], St. Lawrence [1977, 1980], Sommerfeld [1977], and Gubler [1979a].

4. STRESS WAVES IN SNOW

Brown [1979a, 1980c] applied his volumetric constitutive equations to two practical problems, which proves that they can be used as an engineering tool. One is an application to vehicle mobility in snow. Here the required power for snow compaction under the track of a vehicle as a function of vehicle speed, track pressure, or initial snow density is of special interest [Brown, 1979a, c, 1981]. The other is an application to stress waves in snow, which is very useful for estimating the effectiveness for avalanche release by explosives. Here the effect is optimal when sufficiently large additional stresses are exerted on the snowpack over an area which should be as large as possible. Gubler [1977] compared the effectiveness of explosives placed above, on, and below the snowpack surface in field tests.
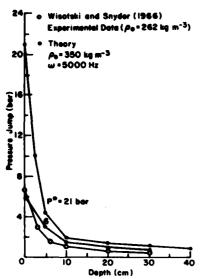
Fig. 9. Variation of peak pressure p^* with distance from snowpack surface [Brown, 1979b].

Fig. 11. Effect of explosive speed (frequency) on attenuation of shock wave [Brown, 1979b].

He observed the best effect by placing it above snow, because a high percentage of energy associated with the air pressure wave is transmitted to snow over large areas, whereas the effective plastic wave traveling in the snow is dissipated within a very short range.

Brown [1979b, 1980a, b, d] considered only pressure waves traveling in the snow and not air pressure-induced effects.

On the basis of the volumetric constitutive law for medium- to high-density snow (pore collapse model), Brown [1979b] established a general theory for plastic shock waves. In the constitutive law, only the fully plastic phase has to be taken into account. It is clear that the acceleration term containing α, $\dot{\alpha}$, $\ddot{\alpha}$ also has to be included. With the use of the balance laws (equation of motion and continuity equation) and compatibility laws (geometrical conditions at singular surfaces) he derived the jump conditions, for instance,

$$[p] = \rho_0 V[v]$$

or

$$[p] = -\frac{\rho_0 V^2}{\alpha_0}[\alpha]$$

Fig. 10. Variation of shock wave speed with distance below surface [Brown, 1979b].

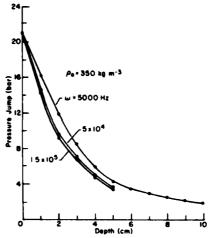V is the propagation velocity of the wave, and $[p]$, $[v]$, and $[\alpha]$ are the jumps in pressure, velocity, and density ratio, respectively. A numerical solution of the nonsteady wave problem is presented below and gives some interesting information. In a nonsteady wave the front profile, wave speed, and amplitude all change with time. This is realistic, but the calculations, for which a finite difference method was used, are rather complicated. For an explosion at the snow surface, simulated by a single pressure pulse with a maximum pressure p^* and a frequency ω, the following results were obtained: The pressure jump decreases very rapidly with depth, and the advantage of a higher pressure is nearly eliminated within the first 10 cm (Figure 9)! A strong plastic wave (high p^*) has a large wave speed, which can be explained by the work-hardening effect making the material stiffer. With lower pressure the wave speed increases with depth as the dissipative effect becomes less important and the wave tends to a more elastic wave (Figure 10). Plastic waves are considerably slower than elastic waves, the first having speeds in the range 50–150 m/s and the latter 500–2500 m/s [Mellor, 1977] for initial densities of 300–600 kg/m³. The frequency of plastic waves is not a dominant factor for attenuation (Figure 11). Whereas in elastic waves a high-frequency wave attenuates more rapidly than a low-frequency wave [Mellor, 1977; Lang, 1976].

Brown [1980a] considered steady waves in medium- to high-density snow, and again the high capacity of snow to dissipate energy was demonstrated. To compact snow of an initial density of 300 kg/m³ to a final density of 900 kg/m³ absorbs 3 times more energy than starting from an initial density of 600 kg/m³.

Practical aspects in regard to avalanche release are discussed by Brown [1980b]. Because only hydrostatic pressures are considered in all of the theories, one may ask which type of stress is most effective in releasing an avalanche. No definitive answer can be found as long as the predominant mode of failure remains unknown, but certainly, a fracture caused by hydrostatic pressure cannot be excluded. According to the above results and those of Gubler [1977], air-detonated explosives are needed with systems already existing in Europe and probably will be developed in the United States (SLUFAE, surface launched unit fuel air explosive).

Plastic waves in low-density snow, particularly relevant for artificial avalanche release in the seasonal snow cover with
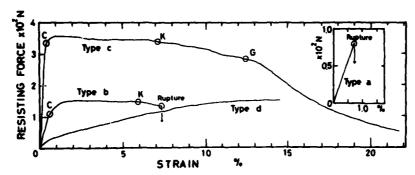
Fig. 12. Typical resisting force–strain curves [Narita, 1980]. Type a: strain rate 8.33×10^{-4} s^{-1}; rapid growth of a crack without plastic deformation. Type b: strain rate 9.15×10^{-5} s^{-1}; no rupture after critical point C; after point K, increasing growth of invisible small cracks until catastrophic fracture. Type c: strain rate 2.96×10^{-5} s^{-1}; similar to type b; at point G, two or three of the many small cracks grew larger. Type d: strain rate 9.54×10^{-7} s^{-1}; no maximum of resisting force nor cracks were observed. (Reprinted by permission of the International Glaciological Society.)

densities very often smaller than 300 kg/m^3, are treated by Brown [1980d]. With the volumetric constitutive law based on the neck growth model [Brown, 1980c], the equation of motion, and the continuity equation a relation between the pressure jump and the density ratio is obtained for steady waves. No definitive conclusions could be drawn about the validity of this theory for low densities. The only available data (by Napadensky [1964]) were obtained with high-density (500 kg/m^3) snow, which the present theory fits well. In agreement with the pore collapse model [Brown, 1979a] a local minimum in wave velocity was found for low pressures: Toward lower pressures, the increase is due to a more elastic wave; with higher pressures, necks rapidly thicken, and therefore there is more resistance to compaction, which results in a higher wave speed V. This can be readily seen from

$$V^2 = -\frac{\alpha_0}{\rho_0}\frac{p^*}{\alpha^* - \alpha_0}$$

where p^* and α^* are the pressure jump and the density ratio behind the wave, respectively. The above relation is more complicated than that for waves that produce infinitesimal strains, that is,

$$V^2 = (E/\rho)[(1 - v)/(1 + v)(1 - 2v)]$$

where v is Poisson's ratio and E is a strong function of ρ [Mellor, 1977].

5. FAILURE CRITERIA BASED ON STRUCTURE

The advantage of structural theories over continuum theories is evident in view of applications, for example, in the assessment of the stability of the sloping snow cover. Besides the fact that one gets immediate insight into physical fracture mechanisms, one does not have to know a complex constitutive relation which must be combined with a failure criterion. Rather, one starts with a given structure, the final result of a history, and tries to relate significant structural parameters and fracture stresses measured in field or laboratory tests.

For fracture of homogeneous snow, as defined in section 1, one has to distinguish between the nucleus of fracture and fracture propagation. The nucleus of fracture is a process in a relatively small area, whereas fracture propagation can cause a catastrophic failure of the natural snowpack over large areas (see section 6). It is clear that fractures of single bonds (as detected, for example, by acoustic emissions) do not represent

fracture nuclei. Rather, nuclei are formed when elements (e.g., chains) of the matrix which carry a main part of the overburden load fracture. How these elements fracture and how many have to fracture to cause an effective nucleus depends on the strain rate and on the state of stress. One has therefore to consider the behavior of an ensemble of elements with defined properties under certain load conditions. In general, one must also admit the fast formation of new bonds during the process. Flaws, as discussed in section 1, have to be treated in a different way, because they lie outside the laws of a defined structure.

To illustrate fracture in snow clearly, we use observations by Narita [1980]. Under uniaxial tensile stress he tested different types of natural snow with constant strain rates, ranging from 10^{-6} to 10^{-3} s^{-1} (Figure 12). In the recorded stress-strain relations he observed, from higher to lower strain rates, brittle fracture in the elastic region, a transition from increasing to nearly constant or decreasing stress ('plastic' behavior), and, at the lowest strain rates, monotonically increasing stresses up to about 15% strain. By thin section analysis (Figure 13) it is shown that the plastic behavior is due to the formation of cracks with average diameters of 1–2 mm and lengths of 5–6 mm. With smaller strain rates the sizes of cracks were smaller than with larger strain rates, and the number of cracks increased with smaller rates. Fracture occurred mostly at intergranular necks. It seems that at the lowest rates, snow can undergo tensile deformations without crack formation, just with a rearrangement of grains, which can even strengthen the grain lattice.

Similar results were obtained by de Montmollin [1981], who made shear tests with variable shear rates. With increasing strain rates he distinguished three types of behavior: viscous without failure, brittle of the first kind (cycles of failure), and brittle of the second kind (only one stress peak with failure followed by a lower constant residual stress). These observations are explained as the rapid formation of new bonds or a reduced formation due to the large strain rate. With the first kind of brittle fracture, considerable strength builds up within a few seconds.

For the establishment of a quantitative statistical model of snow strength the force-transmitting elements or links can be arranged in two ways: as series elements, where the weakest link causes fracture of the entire body, analogous to a failure of a chain, and as parallel elements, where fracture of one element leads merely to a redistribution of the stresses and only after a sufficiently high increase of the load to a total failure. It is
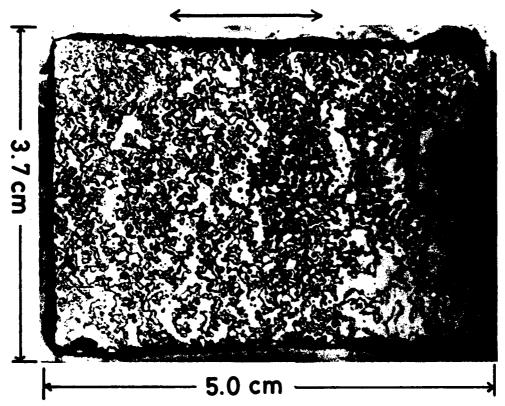
3.7 cm

|← —— 5.0 cm ——— →|

Fig. 13. Thin section of snow sample under natural tensile conditions in the vicinity of a tension crack on a mountain slope. The arrows show the direction of maximum inclination of the slope [Narita, 1980]. (Reprinted by permission of the International Glaciological Society.)

self-evident that the probability density of the link strengths has to be defined.

Sommerfeld [1973, 1974, 1976, 1980] and Sommerfeld and King [1979] were the first to establish such statistical models. As a series element theory he quotes Weibull, who proposed a probability of failure depending on the applied stress and sample volume. A minimum strength in the relation can be considered as the strength of an infinite volume. For small volumes the failure stress increases to unrealistically high values because Weibull based his theory on the existence of flaws which weaken the material. An element which is so small that it does not contain any flaw is assumed to have infinite strength. For this reason, Sommerfeld postulates a minimum volume for which the theory is still valid. The limit would be an element including at least one flaw. From experiments this minimum is about $5 \cdot 10^{-4}$ m^3 ((0.08 m)^3). It should be mentioned that here the concept of flaw is not introduced by a structural analysis, only by the fit of test results.

A parallel element theory is that of Daniel, who derived for the probable strength S of n links, each loaded by s,

$$S = ns \int_0^\infty f(\sigma) \, d\sigma$$

where $f(\sigma)$ is the probability density of the strength σ of the links. The highest probability is reached with the maximum of S, given by $dS/ds = 0$. The two theories represent extreme failure mechanisms. It seems obvious that for high strain rates with elastic behavior causing brittle fracture, Weibull's theory

is realistic, whereas for ductile fracture under low strain rates making relaxation possible, Daniel's theory should be applied.

For an interpretation of shear frame data, Sommerfeld using Daniel's model, arguing that cracks under shear remain in contact and resintering occurs accompanied by relaxation effects, so that strain rate effects disappear. He justifies this idea with shear frame data on avalanche sliding layers where the results of the model coincided well with the actual measured stress of the overburden snow. Also, size effects, as predicted by Daniel's theory, were checked with tests performed by Perla [1977] with different shear frame areas. The measured decrease of the mean strength with increasing area coincides with the theory.

Sommerfeld's models could certainly be improved with a determination of strength distribution of the microscopic links, which would be more appropriate than interpreting the shear frame sample strength to be the link strength. This is of some importance because the extrapolation to larger volumes depends strongly on the chosen link strength distribution [Gubler, 1979b].

For a satisfactory quantitative description of the structure which ultimately determines strength, it does not suffice to consider separate grains; rather, one has to consider grains and their surrounding matrix to obtain average properties for the overall aggregate. For this, quantitative stereology can be used to characterize numerically the three-dimensional geometrical properties observed in two dimensions. This is the starting point of Gubler [1978a, b] in establishing strength-structure

relations for snow. His basic concept is that external forces are transmitted through chains of snow grains. In a chain, grains have only two effective force-transmitting contacts (effective coordination number 2). A chain is terminated by grains with higher connectivities (effective coordination number higher than 2). This chain, characterized by a number of grains, is the fundamental unit. By the analysis of section planes, Gubler arrived at a determination of the mean coordination number per grain, of the mean number of grains per chain, and of the number of fundamental units per unit volume. By comparing these parameters to measured tensile strength a much better fit could be obtained than, for example, with density. Such parameters were, for example, mean number of contacts per grain or mean number of grains per chain (expressing the possible eccentricity of chains).

Gubler [1978b] applied the concept of fundamental units to brittle fracture (series element theory) and ductile fracture (parallel element theory). He tested both fracture modes with Weibull, normal, and log normal distributions of link strength. Various reasons favor, however, the log normal distribution (this type of distribution is characteristic of bonds and grain diameters in many sintered materials). In agreement with Sommerfeld he obtained for brittle fracture a decrease of the most probable strength of a body with increasing links (or volume). For the ductile fracture, however, he found a strength independent of the test volume, dependent only on the relative width of the link strength distribution. It must be mentioned that the fundamental units in Gubler's tested snow were quite small; they varied between 10 and 10^{-1} mm^{-3}. This theory may be improved by investigations of bond strength between ice grains [Gubler, 1981].

6. FRACTURE PROPAGATION

From the observations by Narita [1980] it became clear that the formation of small fracture nuclei is a question of forced strain rates upon snow. If this rate is not too small, that is, probably when the number of bond fractures exceeds that of bond formation, cracks will be formed. Even when these cracks are small, snow has already fractured because catastrophic failure is just a delayed action, the time lag being a function of strain rate.

Fracture propagation in snow slabs is still a matter of speculation. A description of reasonable ideas is given by Perla [1980]. McClung [1979] was the first to establish quantitative aspects for shear fracture. He based his model on tests with a simple shear apparatus with which constant shear strains and vertical loads are produced. Besides the horizontal shear force, horizontal and vertical displacement were recorded [McClung, 1977]. His results, compatible with those of Narita [1980] and de Montmollin [1981], are as follows:

1. Low-density samples strained at slowest rates showed no definite failure level, shear stresses continuously increased, and settling occurred throughout the tests.

2. Low-density samples strained at fastest rates showed strain softening, that is, shear stresses raised to a peak strength, and further displacement showed a gradual loss of resistance until roughly a constant residual shear stress was reached. After an initial settling, vertical dilatation occurred which persisted roughly until peak stress was reached.

McClung [1979] postulates, on the one hand, fracture lines of slab avalanches in thin weak layers in between two relatively harder layers and, on the other hand, strain softening. With these assumptions a model developed by Palmer and Rice [1973] for overconsolidated clay masses, exhibiting similar properties, can be applied. A reservation about this theory is that snow is nonlinear viscoelastic and not an elastic material as assumed generally in the Palmer-Rice theory. An important feature of the model is that snow slabs can fail under shear stresses smaller than the peak shear strength. This could be an additional or alternative explanation for slab failures occurring at body weight stresses less than the measured shear frame strength (if all this is indeed peak strength), a problem discussed by Sommerfeld [1976] and Sommerfeld and King [1979].

Palmer and Rice presuppose the existence of a weakened layer of limited length. Unfortunately, in a snow cover no obvious formation process is available for such a weakness (recrystallization?). The stress conditions in the model are as follows: Far from the weakened layer or shear band the shear stress is that of the body weight stress τ_g. Closer to the band tip, stress increases to the peak value τ_p, and then drops in the shear band to the residual value τ_r, which is smaller than τ_g and τ_p. The end zone over which τ reduces from τ_p to τ_r is assumed to be small in comparison to the total shear band length $2L$. The intrinsic part of the theory is the formulation of energy balance. The gravitational work performed by the overburden slab during an extension of the shear band, dL, is set equal to (1) the work of the slope-parallel normal stresses due to the extension dL, (2) the friction work done by τ_r within the band, and (3) the work against that part of shear strength in excess of τ_r. With a linear elastic constitutive equation a criterion for crack propagation is found, containing L as the only free parameter. This means that a certain critical length has to be reached before propagation is possible. The criterion equates a driving force term, containing $(\tau_g - \tau_r)$, and a resistance term, containing $(\tau_p - \tau_r)$. The driving force represents the net energy surplus to drive the band and is the release of elastic energy when τ_g drops to τ_r. Here the discrepancy between the elastic model and snow appears in that the stress work cannot be obtained fully during unloading from τ_g to τ_r. One part is dissipated, and the gained work has to be taken from the unloading stress-strain curve, as noted by Palmer and Rice. According to McClung, there are now three possible modes for slab release:

1. The shear band progresses slowly until the critical length is reached, and a further extension leads to rapid propagation.

2. A fixed local failure exists. With deposit of new snow the driving force term is increased, and the criterion can be satisfied. Here one should state more precisely that τ_g has to increase more than τ_r, because τ_r too increases with the vertical load [McClung, 1977].

3. Added loading by new snow causes stresses τ_g approaching τ_p. In this case a rapid catastrophic fracture is expected, making the criterion meaningless.

In the first mode it is questionable how the shear band can progress slowly if the critical length is not yet reached. R. G. Oakberg (personal communication, 1980) is attempting to solve this problem with the use of Shapery's theory, which relates far-field stress σ to the delayed fracture time t_f for linear viscoelastic materials. He obtained

$$t_f = (\text{lumped parameter}) a_0^{-2} \sigma^{-6}$$

where a_0 is the initial half-crack length and the lumped parameter is to be determined by tests (e.g., creep compliance $J_{(t)}$ of the relation $\varepsilon_{(t)} = J_{(t)}\sigma_0$). With the above relation our postulate about fracture would be justified (see the beginning of this section).

7. SNOW GLIDING

Very little work has been done in recent years on snow gliding, although this is an important phenomenon of the alpine snowpack. Applied problems such as snow pressure on supporting structures, protection of trees in afforestations, or formation of avalanches due to accelerated gliding attest to the fact that more information about this process is needed.

Glide is defined as the snow slip of the snowpack on a wetted interface over the ground (gliding within the snowpack seems questionable).

It is clear that for this phenomenon some sort of a constitutive equation is needed.

McClung [1980] distinguishes two conditions at the interface when gliding takes place:

1. The snowpack conforms to the ground surface over which it is gliding (i.e., no separation). This movement can be subdivided into two mechanisms, creep over asperities at the interface and motion by regelation.
2. The snowpack is separated from the ground by a thin water film.

The theory presented is based on field observations, theories of glacier gliding, and lubrication theory.

For creep over asperities without separation, snow is modeled as an incompressible Newtonian fluid (i.e., with constant viscosity). The resulting constitutive equation is of the form $\tau = \mu U_0/D$, where τ is the average basal shear stess, μ the viscosity of snow, U_0 the constant velocity of the snowpack sufficiently far from the boundary, and D the stagnation depth. The last is a function only of the geometry of the boundary.

Glide by regelation means, as usually discussed in glacier sliding, that melting occurs at the upstream high-pressure side of asperities followed by a refreezing on the downstream sides. Probably, regelation plays a minor role in the gliding process of snow, but a quantitative evaluation will not be possible until the processes with snow are better understood by experiments.

If creep and regelation are considered as competing effects, one can show that for short-wavelength asperities (e.g., those given by a simple sine wave) the drag is very high for creep, while for long-wavelength asperities it is high for regelation processes. The resulting shear stress can then be written for both processes as above with $D = D_c + D_r$, the sum of the parts originating from creep and regelation.

Separation probably starts at the downstream sides of asperities when the pressure fluctuations of normal stresses on the upstream and downstream sides of the asperities begin to approach the overburden pressure. This condition is realized on steep slopes where the 'roughness parameter,' that is, the ratio of amplitude to wavelength of the ground surface, is small.

McClung's theory contains hypotheses which should be checked by field and laboratory tests. There are severe limitations in applying glacier gliding theories to snow, such as the considerably lower body weight of snow and its compressibility.

8. WET SNOW MECHANICS

To understand the mechanics of dry snow is especially important in high alpine regions where the threat of catastrophic avalanches occurs during midwinter when the snowpack is dry. The urgency of avalanche control in such situations was probably one of the reasons for pushing forward dry snow mechanics. At present, wet snow mechanics, mechanics of snow containing liquid water, lags behind. Clearly, this is not because wet snow is less important. In regions such as the main island of Japan, Honshu, wet snow problems are by far predominant. In general, the mechanical properties of wet snow govern such practical matters as the release of wet snow avalanches, oversnow vehicle performance, traffic on snow-covered roads, and construction on snow, for example, in polar regions.

Progress in wet snow mechanics is hindered because experiments are difficult to control and a theory has to involve, in addition to the dry snow processes, complex surface phenomena in the three-phase system.

Failure criteria for wet snow are not yet established, neither those based on continuum theories nor those based on structure. What we have today are experimental observations and a constitutive equation for hydrostatic pressure based on the structure, mainly due to Japanese investigators and the extensive work by the group at the U.S. Army Cold Regions Research and Engineering Laboratory (especially S. Colbeck).

It is not surprising that the Japanese started with wet snow investigations. *Kinosita* [1963] was the first to test such snow mechanically. He compressed snow samples of different liquid water content under constant rates of deformation and noticed that the registered forces changed with time in the same manner as with dry snow. The big difference, however, was that this force was about 1 order of magnitude smaller than that for dry snow. Furthermore, the important observation was made that the more liquid water was present in a sample, the easier the snow could be deformed. In other words, the higher the saturation, the smaller the force required to obtain a certain compaction. *Ito* [1969] made similar tests and observed a decrease of shear strength analogous to the decrease of compaction force when more pore water is present.

Tusima [1973], considering snow on roads compressed by moving vehicles, made experimental studies on the compression of both dry and wet snow under periodically repeated loads (frequency of 36 min^{-1}). Here again the influence of the amount of free water has been demonstrated: The higher it is, the easier the snow is compressed. A plot of the variable density versus number of strokes, N, shows a similar shape for dry and wet snow (Figure 14). A much smaller increase in density can be observed after 10 strokes in dry snow and after 20 strokes in wet snow, where density increases in proportion to the logarithm of N. The density value attained after the same number of loads and about same initial density increased rapidly with free water content. A plot of density versus viscosity shows drastic increases of viscosity with increasing density for both dry and wet snow; however, the gradient is gradually reduced when more liquid water is present (Figure 15). This sharp growth of snow stiffness was explained by very quick rebonding of grains after failure in structure, readily seen from thin sections taken at different stages of compression.

Wakahama [1968, 1975], an investigator who made important observations on wet snow, noticed a drop of 2 orders of magnitude in Kinosita's hardness of a surface layer in the natural snowpack from the morning before melting to noon, when the free water content was 20–25%. He also made microscopic observations of densification and metamorphism, which later served as a basis for the theoretical model by Colbeck and collaborators. From a motion picture he observed the following phenomena:

1. Larger grains grew at the expense of smaller ones and became rounded ice particles. The smaller grains finally disappeared. Therefore the total number of grains decreased with the lapse of time.
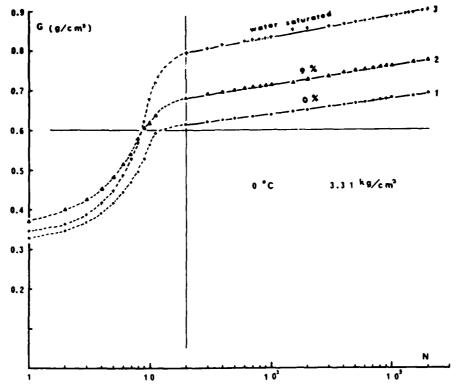
Fig. 14. Density G versus number N of loadings (3.31 kg cm^{-2}) for wet snow at 0°C with different free water contents [Tusima, 1973]. (Reprinted by permission of the Institute of Low Temperature Science.)

2. The growth rate of grains gradually decreased from 0.02 mm/h to practically zero after 3 days.

3. The number of bonds between grains became smaller with the lapse of time.

4. With the compression of wet snow, in the first phase the grains were displaced by gliding at bonds without appreciable deformation of grains until the closest packing was attained. In the second phase, further compression resulted in large deformations of grains with growing bonds until the snow turned into bubbly ice.

5. At an ambient temperature of +20°C the grain growth rate was approximately 50% larger than at 0°C.

6. Growth rate is impurity dependent: It becomes smaller when NaCl concentration is greater than 0.1 g/l, and vice versa when the concentration is less.

Colbeck [1973, 1975, 1976, 1979], Colbeck and Parssinen [1978], and Colbeck et al. [1978] present an exemplary investigation of the mechanical behavior based on complex physical phenomena of the structure. It is an obvious example of a case in which a pure continuum mechanical approach could never give as much insight into the processes involved. One is positively surprised that at the end it was unnecessary to introduce correction factors, taking into account differences between the idealized model and the real conditions. The model in its last version proved to be in fair agreement with experimental observations. This, of course, gives some confidence in the theory presented.

In contrast to dry snow, where deformation is due to creep of ice, here the major deformation mechanism is pressure melting at stressed contacts of a grain and refreezing of the meltwater (regelation) at stress-free grain boundaries. This mechanism is dominated by extremely small temperature differences (thousandths to hundredths of a degree Celsius) between stressed and stress-free surfaces of a particle.

Colbeck et al. [1978] and Colbeck [1979] consider experimentally and theoretically the compaction of wet snow under hydrostatic pressure. The main intention is to find an expression for the time-dependent ice density of snow, ρ (excluding pore fluids), in terms of the initial density ρ_0 and packing geometry. Approximately, this is given by

$$\rho = \rho_0 \left[\bar{r}/(\bar{r} - D) \right]^{n/2}$$

which becomes an exact relation for simple cubic packing where n, the average number of contacts per grain, is an integer. The average radius of unstressed spherical particles is denoted by $\bar{r}$, and the depth of the melted cap of the sphere by D (Figure 16).

In the presence of meltwater, larger particles grow rapidly at the expense of smaller ones, because the melting temperature decreases with the particle radius. Smaller particles melt therefore because of the heat flow from warmer, larger particles. For the increase of $\bar{r}$ with time, to be introduced in the above formula, an empirical expression is adopted because no comprehensive theory exists.

The most delicate problem is the determination of an expression for D or for the rate of increase of D. This depth and the bond radius r_b increase because the equilibrium temperature in the stressed interparticle contact area is reduced with increasing pressure (Figure 17). Stressed contact surfaces therefore exist at lower temperatures than do the particles' stress-free surfaces. A heat flow occurs which causes melting of the stressed surfaces. The meltwater is removed in a thin film, and
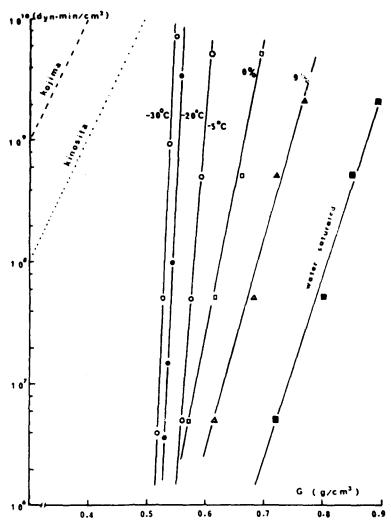
Fig. 15. Apparent viscosity for dry and wet snow versus density G [*Tusima*, 1973]. (Reprinted by permission of the Institute of Low Temperature Science.)

refreezing takes place on the stress-free surfaces. This refreezing represents the only available heat source, not only for melting of the stressed surfaces but also for the shrinking particles. Thus the rate of increase of D is

$$\frac{dD}{dt} = \frac{q}{L\rho_s} - \frac{75.9}{n^2 + 6n}\left[\frac{r_p}{r_b}\right]^2 \frac{r_t - r_0}{\tau} \exp\left(-t/\tau\right)$$

and consists of two terms, the first due to the heat flow q from the stress-free surfaces and the second representing the heat diverted to the shrinking particles. L is the latent heat, ρ_s the ice density, n the number of contacts per particle, t the time, and τ a characteristic time. The indices of the radii are p, particle; b, bond; 0, initial; and τ, radius at time τ.

Heat flow q is proportional to the phase equilibrium temperature difference between stress-free and stressed surfaces ($T_s - T_b$). Hence the larger this difference is (the higher T_s and the lower T_b), the easier snow is compacted.

For lower saturation (pendular regime), T_s is proportional to the capillary pressure and to the salinity; thus the lower both values, the more rapidly density increases (lower capillary pres-

Fig. 16. Cross-sectional view of a typical particle symmetrically developing four melt caps. The smaller circle r_0 represents the initial particle radius, and the larger circle r_p represents the increased particle radius due to refreezing on the stress-free surfaces [*Colbeck et al.*, 1978].

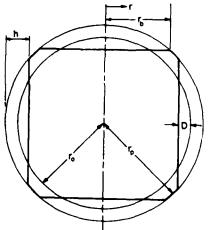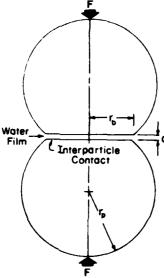Fig. 17. Two particles pushed together melting at the stressed surfaces. The meltwater is removed in a thin film, and refreezing takes place on the stress-free rounded surfaces [*Colbeck et al.*, 1978].

Fig. 19. Ice density versus time for various sodium chloride contents (gram moles NaCl per kilogram of solution times dissociated ions per molecule) for experimental and computed results [*Colbeck et al.*, 1978].

sure means higher water saturation). In Figures 18 and 19, measured and calculated results are plotted.

On the other hand, T_b is lowered with increased stress at bonds σ_b. A first term of σ_b is of a mechanical nature. This stress is higher than the bulk stress on snow. That is higher to the same extent that the number n of stressed contacts per particle is smaller and the ratio of particle to bond radius is larger. An important effect is taken into account by a second term, namely, that the pure mechanical stress is considerably reduced

by repulsive electrostatic forces due to the double charged layers at each solid-liquid boundary within the water film of the interparticle contact. These repulsive forces increase with decreasing concentration of dissolved salt at bonds, so that at low salinities, σ_b, and ultimately also the compaction rate, is effective much lower. A further question of critical importance to the compression is how and to what extent impurities (dissolved salt and air) penetrate into the water film between stressed particles. This delicate problem of the movement of impurities with the meltwater (moving radially outward in a bond) and the diffusion of impurities against this flow is discussed too.

A last question brings us back to dry snow mechanics. It is obvious that with wet snow, nonlinear viscous creep in the stressed contacts of grains must also exist. Assuming a power law relationship between stress and strain rate (exponent of stress taken as 3), it is demonstrated that this mechanism is of almost no importance. However, its relative importance increases with stress because the temperature depression, causing regelation, depends only linearly on stress (Figure 20). Generally, it appears that the regelation mechanism in wet snow is a fast process, whereas deformation rates of dry snow a e limited by the slow creep at stressed contacts of particles.

The theory described is in accordance with the Japanese observations cited above and gives a quantitative understanding of the phenomenon. Although a relatively simple packing geometry is assumed (in principle, simple cubic packing) with the simplest grain shape (sphere), the results are in fair
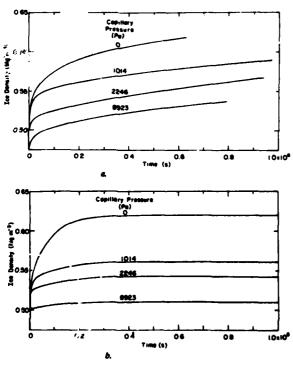

a.

b.

Fig. 18. Ice density versus time for various capillary pressures for both (a) experimental and (b) computed results [*Colbeck et al.*, 1978].
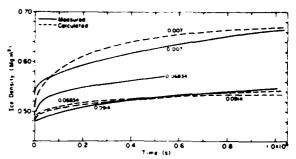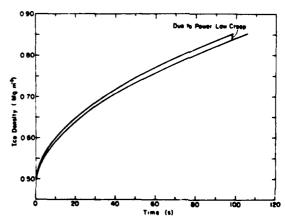

Fig. 20. Ice density versus time for regelation plus nonlinear viscous creep and regelation alone. The difference between the two curves is the contribution of the power law creep [*Colbeck et al.*, 1978].

accordance with experimental observations. It is clear that this accordance can only be valid for dense snow. The difficulties of the structural investigation of low-density snow, in which arbitrary grain shapes, sliding at bonds, or bending of chains occur, do not appear in that case (although *Wakahama* [1975] mentions gliding at bonds).

A foundation for the understanding of wet snow mechanics now exists in a theory based on physical phenomena on the scale of individual particles. Without this understanding it would hardly be conceivable that a reasonable continuum theory of wet snow could be constructed. Deterministic structure theories seem to be, at least in some cases, a prerequisite for continuum theories. There is still a long way to go until, for example, the release of a wet snow avalanche can be fully understood. We would need for this a stress-strain relation incorporating all the significant parameters and valid for general states of stress and also a corresponding failure criterion.

REFERENCES

Abele, G., and A. Gow, Compressibility characteristics of undisturbed snow, *Rep. 336*, U.S. Army Cold Reg. Res. and Eng. Lab., Hanover, N. H., 1975. (Available as AD A012113 from the Natl. Tech. Inf. Serv., Springfield, Va.)

Abele, G., and A. Gow, Compressibility characteristics of compacted snow, *Rep. 76-21*, U.S. Army Cold Reg. Res. and Eng. Lab., Hanover, N. H., 1976. (Available as AD A028622 from the Natl. Tech. Inf. Serv., Springfield, Va.)

Boulon, M., R. Chambon, and F. Darve, Loi rhéologique incrémentale pour les sols et application par la méthode des éléments finis, *Rev. Fr. Geotech.*, *1*(2), 5–22, 1977.

Bradley, C. C., and W. F. St. Lawrence, Kaiser effect in snow, *IAHS AISH Publ.*, *114*, 145–154, 1975.

Brown, R. L., A thermodynamic study of materials representable by integral expansions, *Int. J. Eng. Sci.*, *14*(11), 1033–1046, 1976.

Brown, R. L., A fracture criterion for snow, *J. Glaciol.*, *19*(81), 111–121, 1977.

Brown, R. L., A volumetric constitutive law for snow subjected to large strains and strain rates, *Rep. 79-20*, 13 pp., U.S. Army Cold Reg. Res. and Eng. Lab., Hanover, N. H., 1979a.

Brown, R. L., An analysis of plastic shock waves in snow, *Rep. 79-29*, 14 pp., U.S. Army Cold Reg. Res. and Eng. Lab., Hanover, N. H., 1979b.

Brown, R. L., A study of vehicle performance in snow, *J. Terramechanics*, *16*(4), 153–162, 1979c.

Brown, R. L., Pressure waves in snow, *J. Glaciol.*, *25*(91), 99–107, 1980a.

Brown, R. L., An analysis of non-steady plastic shock waves in snow, *J. Glaciol.*, *25*(92), 279–287, 1980b.

Brown, R. L., A volumetric constitutive law for snow based on a neck growth model, *J. Appl. Phys.*, *51*(1), 161–165, 1980c.

Brown, R. L., Propagation of stress waves in alpine snow, *J. Glaciol.*, *26*(94), 235–243, 1980d.

Brown, R. L., An analysis of vehicle power requirements in deep snowpack, *J. Terramechanics*, *18*(3), 164–181, 1981.

Brown, R. L., and T. E. Lang, On the mechanical properties of snow and its relation to the snow avalanche, *Proc. Annu. Eng. Geol. Soils Eng. Symp. 11th*, 19–36, 1973.

Brown, R. L., and T. E. Lang, On the fracture properties of snow, *IAHS AISH Publ.*, *114*, 196–207, 1975.

Brown, R. L., T. E. Lang, W. F. St. Lawrence, and C. C. Bradley, A failure criterion for snow, *J. Geophys. Res.*, *78*(23), 4950–4958, 1973.

Colbeck, S. C., Theory of metamorphism of wet snow, *Res. Rep. 313*, 11 pp., U.S. Army Cold Reg. Res. and Eng. Lab., Hanover, N. H., 1973.

Colbeck, S. C., Grain and bond growth in wet snow, *IAHS AISH Publ.*, *114*, 51–61, 1975.

Colbeck, S. C., Thermodynamic deformation of wet snow, *Rep. 76-44*, 9

pp., U.S. Army Cold Reg. Res. and Eng. Lab., Hanover, N. H., 1976.

Colbeck, S. C., Sintering and compaction of snow containing liquid water, *Philos. Mag. A*, *39*(1), 13–32, 1979.

Colbeck, S. C., and N. Parssinen, Regelation and the deformation of wet snow, *J. Glaciol.*, *21*(85), 639–650, 1978.

Colbeck, S. C., K. A. Shaw, and G. Lemieux, The compression of wet snow, *Rep. 78-10*, 17 pp., U.S. Army Cold Reg. Res. and Eng. Lab., Hanover, N. H., 1978.

Coleman, B. D., Thermodynamics of materials with memory, *Arch. Ration. Mech. Anal.*, *17*, 1–46, 1964.

de Montmollin, V., Shear tests on snow explained by fast metamorphism, *J. Glaciol.*, in press, 1981.

de Quervain, M., Kristallplastische Vorgänge im Schneeaggregat, II, *Int. Rep. 24*, pp. 1–41, Swiss Fed. Inst. for Snow and Avalanche Res., Weissfluhjoch/Davos, 1946.

Desrues, J., F. Darve, E. Flavigny, J. P. Navarre, and A. Taillefer, An incremental formulation of constitutive equations for deposited snow, *J. Glaciol.* 25(92), 289–307, 1980.

Dillon, H. B., and O. B. Andersland, Deformation rates of polycrystalline ice, in *Physics of Snow and Ice, Proceedings of International Conference on Low Temperature Science*, vol. 1, part 1, edited by H. Oura, pp. 313–327, Institute of Low Temperature Science, Hokkaido University, Sapporo, Japan, 1967.

Good, W., Numerical parameters to identify snow structure, *IAHS AISH Publ. 114*, 91–102, 1975.

Gubler, H., Artificial release of avalanches by explosives, *J. Glaciol.*, *19*(81), 419–429, 1977.

Gubler, H., Determination of the mean number of bonds per snow grain and of the dependence of the tensile strength of snow on stereological parameters, *J. Glaciol.*, *20*(83), 329–341, 1978a.

Gubler, H., An alternate statistical interpretation of the strength of snow, *J. Glaciol.*, *20*(83), 343–357, 1978b.

Gubler, H., Acoustic emission as an indication of stability decrease in fracture zones of avalanches, *J. Glaciol.*, *22*(86), 186–188, 1979a.

Gubler, H., An alternate statistical interpretation of the strength of snow: Reply to comments by R. A. Sommerfeld, *J. Glaciol.*, *22*(88), 561–562, 1979b.

Gubler, H., Strength of bonds between ice grains after short contact times, *J. Glaciol.*, in press, 1981.

Ito, H., Unconfined compression test of wet snow, *Jpn. J. Snow Ice*, *31*(9), 7–18, 1969.

Kinosita, S., Compression of snow immersed in water of 0°C, I, *Low Temp. Sci., Ser. A*, *21*, 13–22, 1963.

Kry, P. R., Quantitative stereological analysis of grain bonds in snow, *J. Glaciol.*, *14*(72), 467–477, 1975a.

Kry, P. R., The relationship between the visco-elastic and structural properties of fine-grained snow, *J. Glaciol.*, *14*(72), 479–500, 1975b.

Lang, T. E., Measurements of acoustic properties of hard-pack snow, *J. Glaciol.*, *17*(75), 269–276, 1976.

Malvern, L. E., *Introduction to the Mechanics of a Continuous Medium*, 713 pp., Prentice-Hall, Englewood Cliffs, N. J., 1969.

McClung, D. M., Direct simple shear tests on snow and their relation to slab avalanche formation, *J. Glaciol.*, *19*(81), 101–109, 1977.

McClung, D. M., Shear fracture precipitated by strain softening as a mechanism of dry slab avalanche release, *J. Geophys. Res.*, *84*(B7), 3519–3526, 1979.

McClung, D. M., Creep and glide processes in mountain snowpacks, *Pap. 6*, 66 pp., Natl. Hydrol. Res. Inst., Ottawa, Ont., 1980.

Mellor, M., A review of basic snow mechanics, *IAHS AISH Publ. 114*, 251–291, 1975.

Mellor, M., Engineering properties of snow, *J. Glaciol.*, *19*(81), 15–66, 1977.

Napadensky, H., Dynamic response of snow to high rates of loading, *Res. Rep. 119*, U.S. Army Cold Reg. Res. and Eng. Lab., Hanover, N. H., 1964.

Narita, H., Mechanical behavior and structure of snow under uniaxial tensile stress, *J. Glaciol.*, *26*(94), 275–282, 1980.

Palmer, A. C., and J. R. Rice, The growth of slip surfaces in the progressive failure of over-consolidated clay, *Proc. R. Soc. London, Ser. A*, *332*, 527–548, 1973.

Perla, R. I., Slab avalanche measurements, *Can. Geotech. J.*, *14*(2), 206–213, 1977.

Perla, R. I., Avalanche release, motion and impact, in *Dynamics of Snow and Ice Masses*, edited by S. C. Colbeck, pp. 397–462, Academic, New York, 1980.
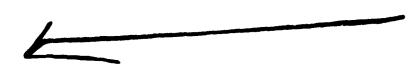
Pipkin, A. C., Small finite deformations of viscoelastic solids, *Rev. Mod. Phys.*, *36*(4), 1034–1041, 1964.

Reiner, M., Rheology, in *Encyclopedia of Physics*, vol. VI, *Elasticity and Plasticity*, edited by S. Flügge, pp. 434–550, Springer-Verlag, New York, 1958.

Salm, B., On the rheological behavior of snow under high stresses, *Contrib. Inst. Low Temp. Sci. Hokkaido Univ., Ser. A, 23*, 1–43, 1971.

Salm, B., A constitutive equation for creeping snow, *IAHS AISH Publ., 114*, 222–235, 1975.

Salm, B., Eine Stoffgleichung für die kriechende Verformung von Schnee, *Diss. 5861*, Eidg. Tech. Hochsch., Zürich, 1977.

Singh, H., and F. W. Smith, Constant strain-rate tensile testing of natural snow (abstract), *J. Glaciol., 26*(94), 519, 1980.

Sommerfeld, R. A., Statistical problems in snow mechanics, *U.S. For. Serv. Gen. Tech. Rep., RM-3*, 29–36, 1973.

Sommerfeld, R. A., A Weibull prediction of the tensile strength–volume relationship in snow, *J. Geophys. Res., 79*(23), 3353–3356, 1974.

Sommerfeld, R. A., A correction factor for Roch's stability index of slab avalanche release, *J. Glaciol., 17*(75), 145–147, 1976.

Sommerfeld, R. A., Preliminary observations of acoustic emissions preceding avalanches, *J. Glaciol., 19*(81), 399–409, 1977.

Sommerfeld, R. A., Statistical models of snow strength, *J. Glaciol., 26*(94), 217–223, 1980.

Sommerfeld, R. A., and R. M. King, A recommendation for the application of the Roch index for slab avalanche release, *J. Glaciol., 22*(88), 547–549, 1979.

St. Lawrence, W. F., A structural theory for the deformation of snow, Ph.D. thesis, 145 pp., Mont. State Univ., Bozeman, 1977.

St. Lawrence, W. F., The acoustic emission response of snow, *J. Glaciol., 26*(94), 209–216, 1980.

St. Lawrence, W. F., and C. C. Bradley, The deformation of snow in terms of a structural mechanism, *IAHS AISH Publ., 114*, 155–170, 1975.

St. Lawrence, W. F., and C. C. Bradley, Spontaneous fracture initiation in mountain snow-packs, *J. Glaciol., 19*(81), 411–417, 1977.

St. Lawrence, W. F., and T. E. Lang, A constitutive relation for the deformation of snow, *Cold Reg. Sci. Technol., 4*, 3–14, 1981.

Truesdell, C., The non-linear field theories of mechanics, in *Encyclopedia of Physics*, vol. III/3, edited by S. Flügge, 602 pp., Springer-Verlag, New York, 1965.

Tusima, K., Tests of the repeated loadings of snow, *Low. Temp. Sci., Ser. A, 31*, 57–68, 1973.

Voitkovsky, K. F., *Mechanical Properties of Snow* (in Russian), 126 pp., Nauka, Moscow, 1977.

Wakahama, G., The metamorphism of wet snow, in *IUGG, IAHS General Assembly of Bern, Sept.–Oct. 1967*, pp. 370–379, Paris, 1968.

Wakahama, G., The role of melt-water in densification processes of snow and firn, *IAHS AISH Publ., 114*, 66–72, 1975.

Watanabe, Z., Tensile strain and fracture of snow, *J. Glaciol., 26*(94), 255–262, 1980.

Wisotski, J., and W. Snyder, A study of the effects of snow cover on high explosive blast parameters, *Rep. 2303*, Denver Res. Inst., Univ. of Denver, Denver, Colo., 1966.

Ziegler, H., Some extremum principles in irreversible thermodynamics with application to continuum mechanics, in *Progress in Solid Mechanics*, vol. IV, pp. 91–193, edited by I. N. Sneddon and R. Hill, North-Holland, Amsterdam, 1963.

Review of Surface Friction, Surface Resistance, and Flow of Snow

T. E. LANG AND J. D. DENT

Civil Engineering/Engineering Mechanics Department, Montana State University
Bozeman, Montana 59717

Three related topics pertaining to surface properties of snow are reviewed: (1) surface friction between snow and other materials as applied to skis and sled runners, (2) surface resistance of snow to oversnow trafficability of vehicles, and (3) flow of snow over snow surfaces as occurs in avalanches. These topics were part of the presentations at the U.S.-Canadian Workshop on the Properties of Snow held at Snowbird, Utah, April 1981. The review is an update of work in these areas since the dates of previous reviews and focuses, particularly, on the work reported by attendees of the workshop.

CONTENTS

INTRODUCTION

In this review we summarize recent research work on snow related to surface effects. These effects are (1) surface friction between snow and other materials, (2) surface resistance of snow to trafficability of vehicles, and (3) flow of surface snow as in avalanches. Over the past 10 years the trend in research in these areas has been in the direction of increased use of analytical methodology and investigation of the mechanics of the processes involved. In part, the availability of computer analysis techniques and of advanced electronic instrumentation has contributed significantly to the trend toward analytical investigations.

Comprehensive reviews have previously been written that cover the topics of this review, and we note these rather than attempt to summarize all the earlier work. With regard to surface friction, *Mellor* [1964, 1974] summarizes many of the experimentally determined properties of snow and ice. On the subject of surface resistance and trafficability of vehicles over snow, a summary by *Mellor* [1963] includes performance characteristics of a number of oversnow vehicles. As to flow of snow in avalanches a recent summary has been prepared by *Perla* [1980] that updates on an earlier review by *Mellor* [1968]. Our attempt at review is to build upon the cited reviews, emphasizing research that has been completed more recently and, particularly, reports by attendees of the Joint U.S.-Canadian Workshop on the Properties of Snow held April 8, 1981, at Snowbird, Utah. Recognizing the extensive range of different means of publishing research work, we know that we have not included all references to work on the topics of this review.

SNOW SURFACE FRICTION
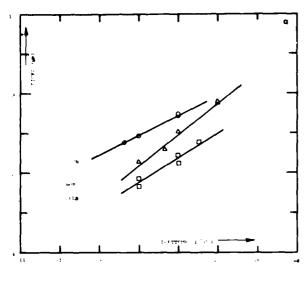
Various mechanisms have been used to describe the surface friction of snow when in moving contact with different materials. Among these mechanisms are dry or Coulomb friction, liquid film, plastic deformation, and adhesion, all of which appear in the literature up to the present time. Yet each represents different physical conditions, all of which can apparently exist in snow depending upon the temperature, moisture content, kinematics, etc. Coulomb

friction is normal load and velocity independent. Liquid film, if Newtonian, is velocity dependent, with force increasing with increase in velocity, just the opposite to adhesion theory, which, however, is velocity and normal force dependent also. Friction dependent upon plastic deformation is force dependent and requires a definition on the yield properties of the material. The fact that all these mechanisms can be applied to snow implies either that snow has regimes of behavior that are variable in relation to the friction mechanism or that a more complex mechanism of friction need ultimately emerge that contains essential elements of the various simpler mechanisms that have been listed. At the present state of the art, controversy continues on which of the simple mechanisms should be used. We can demonstrate this by citing some of the recent contributions in the field.

Early studies by *Kuroda* [1942], *Bucher and Roch* [1946], *Klein* [1947], *Ericksson* [1949], and *McConica* [1950] on the friction of snow, when in contact with different materials, centered on evaluations of ski and sled runner configurations involving traditional materials and coatings. The peculiar property that sliding friction on snow is an order of magnitude lower than usual values between dry materials was recognized, and the advantages noted. Reasons for this difference were derived from experiments that melting of contacting asperites produced a liquid film upon which the relative motion progressed. The heat necessary for melting was attributed to friction heating, generally, and to pressure melting at temperatures near 0°C. The recognition of a liquid film layer, which develops shear force in proportion to the velocity gradient and fluid viscosity, however, did not dissuade continued reporting of friction coefficient μ as the ratio of the friction force to the normal force. This ratio is measured with either initiation of motion (static coefficient μ_s) or sustaining of motion (kinetic coefficient μ_k).

Reasons for reporting the results of friction experiments in terms of a Coulomb mechanism are many. First, measuring the forces and weights is simple compared to measuring the viscosity and thickness of a thin film of fluid. Second, as temperature decreases below 0°C, a transition occurs to a dry friction process even with snow, but details on the temperatures and geometry of this transition are not known exactly. Third, question has been raised about the thin film fluid mechanism by *Niven* [1959], who gives reasons for a plastic deformation process at the tip of asperites due to intrinsic disorder and mobility of protons at temperatures slightly below melting. *Mayr* [1979], using a parallel plate capacitive pickup mounted to the running surface of a ski,
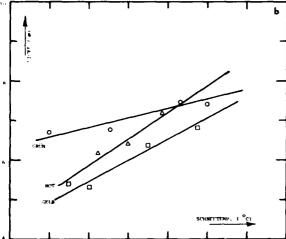
Fig. 1. Thickness (Dicke) of water film beneath waxed skis as a function of (a) air (Luft) and (b) snow (Schnee) temperatures [after Mayr, 1979].

reports measurements of water film thicknesses using different ski waxes as shown in Figure 1. The upper plot is water film thickness versus air temperature, and the lower plot is thickness versus snow temperature. Application of this technique to other problems in snow friction is encouraging. Both Jellinek [1957a] and Shimbo [1971] indicate dependence of friction of some plastics on the affinity of water with the surface. Some plastics show strong hydrophobic properties initially but increase in affinity to water as the plastic is slid on snow. From listing just these contributions to the recent literature we see that consensus on the friction mechanism with snow is far from resolved. Continued effort to identify regimes of application of the simple mechanisms is warranted at this stage until a more complete understanding of the processes is known.

To demonstrate the nonapplicability of any single friction mechanism, we have only to look at typical results from one researcher, with the idea of applying the results to a specific mechanism, say, Coulomb friction. Coulomb friction is

considered not to be temperature dependent, whereas snow and ice show a dependence, as depicted in Figure 2, taken from work by Eriksson [1949]. Clearly, distinction must be made between friction on ice, which is generally lower and more nearly constant, and friction on snow. The reversal in friction coefficient values between smooth and rough steel runners near 0°C is explained by Eriksson as due to geometric shape controlling the amount of meltwater in contact with the two types of surfaces.

Static friction of snow with other materials is generally much larger than the kinetic coefficient. Static friction variation with temperature is reported by Bowden [1955] for different ski facing materials (Figure 3). The near-constant and exceptionally low range of friction coefficient of Teflon (polytetrafluoroethylene) is reported also by Shimbo [1971] and is attributable to the high hydrophobic property of Teflon over a range of temperatures and for long durations of contact with snow. Static friction can be strongly time dependent owing to a process of adhesion of ice columns that continually form and grow through sublimation at the snow surface in contact with a ski or runner. Studies of the adhesion of ice to metals and polymers are reported by Jellinek [1957b, 1960], Raraty and Tabor [1958], and Landy and Freiberger [1967]. Carry-over from ice to snow is not necessarily straightforward because of the considerably lower ultimate strength of snow and hence the possibility of a different type of failure in snow than direct shear failure at the surface, which occurs with ice.

Another characteristic of Coulomb friction is a constant proportion between friction force and normal force. This characteristic is not strictly observed with snow, although
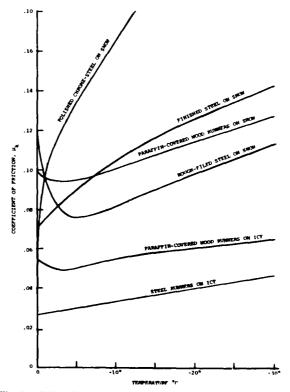
Fig. 2. Sliding friction of sled runners versus temperature [after Eriksson, 1949].
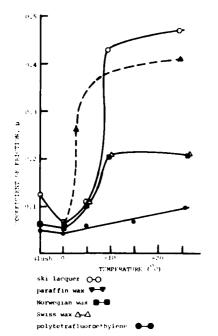
Fig. 3. Static coefficient of friction between snow and different coating materials applied to skis versus temperature [after *Bowden*, 1955].

data are far from complete. One factor that complicates tests with variable load is the possibility of friction coupling with compaction and sidewall shear mechanisms. *Shimbo* [1971] made considerable effort to separate these effects and shows a constant μ_k with load over a small range of loading corresponding to variation in skier loading on Teflon-coated skis (Figure 4). *Ericksson* [1949] shows a decrease in μ_k over a large load range corresponding to sled loading. Another related characteristic of Coulomb friction is independence of μ from contact area and from small variations in surface roughness. For snow, *Kuroda* [1942] measured a depen-

dence of kinetic friction on type and wetness of snow. This was later definitized more exactly for specific load, speed, and geometric configurations by *Eriksson* [1949] in regard to size of sled runners (Figure 5) and different dry snow grain sizes (Figure 6). Shimbo varied the roughness of phenolic resin sliders to show variation in static and kinetic friction as depicted in Figure 7. *Huzioka* [1962], in measurements of kinetic friction between snow and iron plates and between snow and metacrylic acid resin plates, classified three types of motion depending upon surface temperature and plate velocity (types A, B, and C in Figure 8). Type A is continuous, type B is saw-toothed, and type C is characterized by small irregular fluctuations. Huzioka reports kinetic friction to be twice as large for the resin as for the iron, which contradicts the idea of an insulator of heat having less friction than a comparable conductor of heat. Huzioka is also able to compute the thermal energy necessary to melt the ice asperites in contact with the plates and finds this energy to be only 1% of the total energy expended.

Tusima [1977] reports accurate measurement of the friction force on a steel ball 6.5 mm in diameter that was placed in contact at different normal pressures with a moving bicrystal ice plate. The surface of the ice plate was crystallographically half basal (0001) and half prismatic (01$\bar{1}$0). Changes in the values of μ_k on these surfaces as functions of applied load, frictional velocity, and temperature are shown in Figure 9. Values of μ_k on the (01$\bar{1}$0) surface are higher than values on the (0001) surface and are attributed to greater hardness and smaller shear strength of the (0001) surface compared to the (01$\bar{1}$0) surface. These results do not match behavior of dry friction theory nor that corresponding to pressure melting or frictional melting. Tusima indicates that the results fit the adhesion theory for ice.

A topic of current interest relating to friction on snow pertains to snow flowing on snow. This friction develops between the moving snow and the basal stationary snow in avalanches and is under study in regard to development of flow laws for moving snow. Discussion of this mechanism of friction is included in this review in the section on flowing snow.
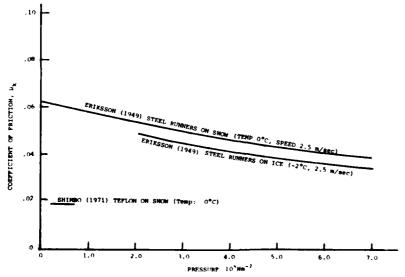
Fig. 4. Coefficient of kinetic friction versus contact pressure.
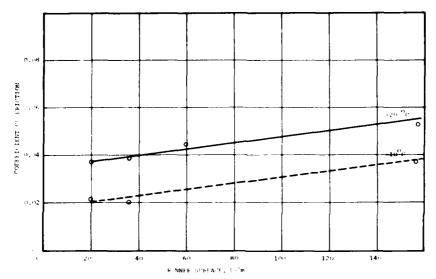
Fig. 5. Coefficient of kinetic friction on ice versus size of steel runner for a load of 40 kg and sliding speed of 2.5 m s⁻¹ [after *Eriksson*, 1949].

We conclude from these sets of data that snow friction deviates from a Coulomb model in numerous respects. However, until more definitized mechanisms of friction production with snow are determined, the practitioner is faced with using ranges in friction coefficients that may or may not encompass possible design conditions. This forces a dependence on experiment and empiricism that has earmarked advancement in friction-related design to date. For perhaps as complete a summary of data on friction coefficients for snow as is available the reader is referred to data compiled by *Mellor* [1964].

1/DIAMETER OF SNOW GRAIN
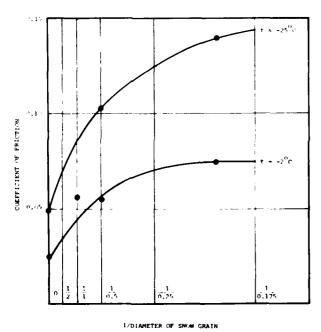
Fig. 6. Coefficient of kinetic friction of steel runners on snow of different grain sizes for a load of 20 kg and sliding speed of 2.5 m s⁻¹ [after *Eriksson*, 1949].

SNOW SURFACE RESISTANCE

At the International Society for Terrain-Vehicle Systems (ISTVS) meeting in 1978 in Vienna it was resolved that a strong need exists for identification and classification of snow in regard to its vehicular trafficability [*ISTVS*, 1978]. This emerged in part from the recent findings by *Yong and Harrison* [1978] that traditional techniques of analyzing vehicle trafficability on soils do not carry over to snow. That a new direction is necessary for snow is reflected in a classification system set up for snow at the ISTVS meeting. The classification system is structured in two parts, the simple and the complex, the simple based upon easily obtained data on snowpack, namely, (1) temperature profile and history, (2) density profile, (3) time of sampling, (4) grain size distribution at time of sampling, (5) grain geometry and initial assessment of bonding, (6) compressibility and density change under a single static load, (7) resistance to penetration (from a cone test or equivalent), and (8) shear resistance (from a vane cone test or equivalent). The ISTVS committee considers these types of data as basic to any attempt at
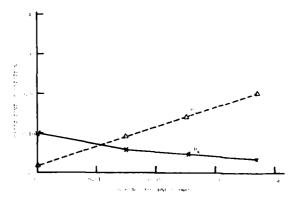
Fig. 7. Static and kinetic coefficients of friction on snow versus surface roughness of a phenolic resin slider for a temperature of 0°C [after *Shimbo*, 1971].
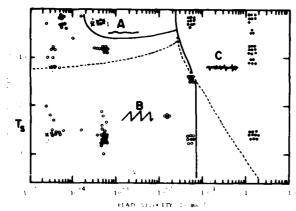
Fig. 8. Relation of friction type versus surface temperature T, and speed V for a methacrylic resin plate in contact with snow. Solid lines are boundaries between the friction types for the resin, while the dashed lines are boundaries for an iron plate [after *Huzioka et al.*, 1961].

Here ϕ' is not related to the internal friction as in the Coulomb-Mohr theory because of the velocity dependence of the test results. At a speed of 6.5×10^{-4} m s^{-1}, $\phi' = 46°$, and at a speed of 3.1×10^{-3} m s^{-1}, $\phi' = 33°$, so that shear resistance is decreasing with speed, in contrast to other materials. Yong and Fukue show further that in varying the type of snow tested, significant differences occur in shear response, and by implication the equation cited above does not apply (Figure 10b).

analytical modeling of trafficability of oversnow vehicles. The ISTVS report further lists some of the more complex properties of snow that in time need defintion and measurement. Among these are (1) constitutive and rheological performance, (2) yield/failure criterion, (3) viscous flow properties, (4) density changes under specific load conditions, (5) shear strength, and (6) water content, density, etc., at time of strength testing.

In reviewing these lists we see that the ISTVS committee is essentially saying that theory in oversnow trafficability of vehicles is very close to the starting point. This is not to say that technology is lacking in oversnow trafficability, but the technology has developed over the past 30 years by specific evaluation of designed vehicles, with comparisons made by relative performances. Results of experiments for drawbar loads, slope traction, horsepower requirements, speeds under different snow conditions, etc., are given for specific vehicles by *Rula et al.* [1955], *Nuttall and Finelli* [1955], *Lanyon* [1959], and *Rula* [1959, 1960]. A summary on vehicle performance has been compiled by *Mellor* [1963]. Most tests have been performed under controlled snow conditions in order to show comparisons between vehicles. *Harrison* [1975] shows that under certain snow conditions, results of tests are difficult to interpret and further work on testing methodology is warranted.
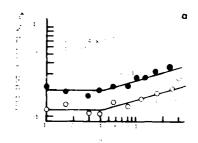
In the literature we see a recent trend in applying engineering mechanics principles to surface snow trafficability and handling problems and a gradual development of well-grounded theories and analysis techniques. *Yong and Fukue* [1978] demonstrate that snow, as a granular material under conditions that produce a shear plane failure, has characteristics of a Coulomb-Navier material. The relationship between normal and shear stresses at two shear speeds is shown in Figure 10a. The relationship is expressed as

$$\tau = \sigma_n \tan \phi'$$

where

τ shear strength;
σ_n normal pressure acting on the shear plane;
ϕ' apparent correlative angle.

Fig. 9. Kinetic coefficient of friction of basal (0001) and prismatic ice (01 $\bar{1}$0) versus (a) applied load, (b) velocity of sliding, and (c) temperature [after *Tusima*, 1977].

Fig. 10. Relationship between shear and normal stress for (a) granular snow and (b) different types of snow as noted [after *Yong and Fukue*, 1978].

In view of the above, it is apparent that properties of snow must be assessed separately, and no attempt to modify soil trafficability theory to model snow should be made. Additional differences between soils and snow are noted by *Yong and Harrison* [1978], including the following:

1. After initial pass by a vehicle to establish a track, follow-on vehicles further deteriorate inorganic soil, whereas compacted snow stabilizes.

2. The compaction of snow on initial and subsequent passes by vehicles is a large-deformation, rate-dependent process for which the Coulomb-Mohr failure theory is not applicable.

3. The properties of snow are time variable, except perhaps under Arctic conditions, and this large and sometimes rapid variation needs to be considered in regard to interaction with vehicles.

Material property investigations of snow that pertain to tracked vehicle performance have centered on compaction, shear, and plastic wave propagation. *Tusima* [1973] presents results of repeated loading on confined snow samples and measured densification of both dry and wet snow. The snow was loaded at 36 cpm, load limited to either 12.75 or 38.25 × 10^4 N m^{-2}. Densification versus number of cycles of loading of dry snow is shown in Figure 11, where a critical density around 600 kg m^{-3} is reached beyond which the snow has a tendency not to densify. This is consistent with earlier findings by *Bader* [1962] on snow densification and is further confirmed by *Yong and Fukue* [1977], using controlled deformation rates on confined cylinders of granular snow. Yong and Fukue define also threshold density as the minimum density of snow at which sawtooth failure under compression ceases to occur. Threshold density is found to depend upon initial density and grain size of the snow, whereas critical density is dependent only upon grain size for the tests performed (Figure 12). Yong and Fukue report approximately one-third total deformation of snow under incremental loading to a final load, compared to the deformation obtained from direct application of the final load in one increment. Thus type or sequence of loading influences total deformation. *Abele and Gow* [1975, 1976], in compression tests of natural undisturbed and precompacted snow at rates of deformation up to 0.4 m s^{-1}, also show a break in their data envelopes in the density range 400-600 kg m^{-3}, as shown in Figure 13. Abele and Gow report strong influence of initial density on densification of snow but little influence of snow temperature or deformation rate (under single-cycle loading).

On the basis of evidence from thin section studies by *Tusima* [1973], critical density is attributed to deformation that moves snow grains into a close-packed array. Deformation beyond this is related to deformation of the grains themselves, which occurs at higher loads and rates of energy. *Yong and Fukue* [1977] explain sawtooth load resistance of snow as local collapse followed by monotonic resistance of the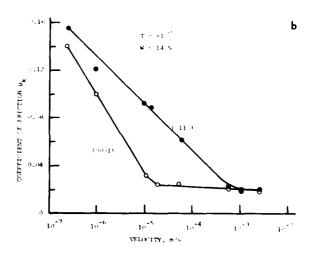 more densely packed snow. In an initial attempt at fitting a constitutive equation to compaction of snow, *Brown* [1979b] concentrates on snow of densities greater than those associated with sawtooth failure ($\rho > 300$ kg m^{-3}) and relates hydrostatic pressure to volumetric deformation by

$$p(t) = \frac{1}{3\alpha} \ln\left(\frac{\alpha}{\alpha - 1}\right)\left[2(S_0 - C) + C \ln \frac{(-\dot{\alpha}A)^2}{\alpha(\alpha - 1)}\right] J \exp\left(-\phi\alpha/\alpha_0\right)$$

where

α density of ice/density of snow, equal to ρ_m/ρ;
S_0, C, A material constants for ice;
J, ϕ empirically determined constants.

This equation lacks an inertial term, which is derived by Brown and can be added if needed. Brown compares this equation with the experimental data by *Abele and Gow* [1975, 1976] and obtains general correspondence for snow of initial density greater than 300 kg m^{-3}. Application of this equation to actual vehicle locomotion in snow is demonstrated by *Brown* [1979a] showing two ranges of performance (Figure 14). For a track pressure of 1×10^4 N m^{-2} the
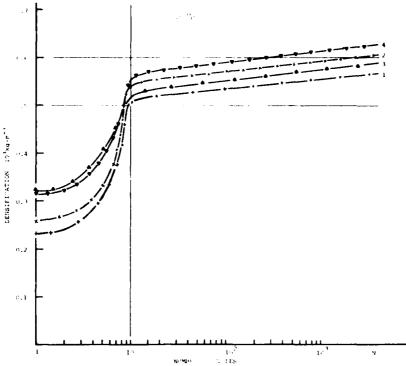
Fig. 11. Dry snow densification as a function of number of cycles of loading in uniaxial confined compression. Curves 1 and 3 correspond to maximum load of 1.3 kg/cm^2, and curves 2 and 4 to 3.9 kg/cm^2 [after *Tusima*, 1973].

tracked vehicle surface glides on the snow at greatly reduced energy dissipation as compared to vehicle advance at a track pressure of 5×10^4 N m^{-2}. *Brown* [1981] has extended his constitutive formulation of a tracked vehicle to include shear effects as well as to account for a suspended-in-snowpack pressure bulb beneath the track. In this constitutive equation formulation, Brown does not take explicit account of the critical density condition noted experimentally.
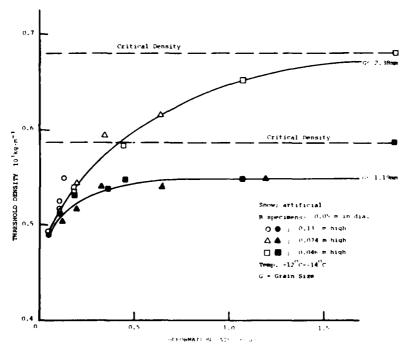
Fig. 12. Relationship between deformation (strain) rate and threshold density for natural aged granular snow with varying specimen heights [after *Yong and Fukue*, 1977].
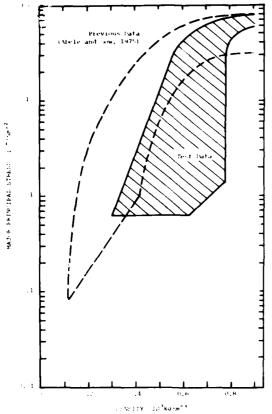
Fig. 13. Range in test data obtained with compression tests of natural snowpack at various rates of deformation. Previous data are of initially uncompacted snow, and the shaded test data are for precompacted snow [after *Abele and Gow*, 1976].

A series of tests by *Muro and Yong* [1980a, b] with rectangular plate and vane cone compression gages and shear penetrometers at high rates of deformation (up to 3.7×10^{-3} m s^{-1} compression and 3.49×10^{-3} m s^{-1} shear) were used to evaluate material properties of snow. From the compression tests they found that the deformation energy decreases with increase in the coefficient of propagation of plastic compression. In the shear tests, shear stress is related to deformation X by

$$\tau = \tau_0 e^{-2\lambda}$$

while the relation between shear stress τ and normal stress σ is found to coincide with the Coulomb-Mohr equation

$$\tau = C + \sigma \tan \phi$$

where C is cohesion strength and ϕ the angle of internal friction. For purposes of predicting drawbar pull of a tracked vehicle, Muro and Yong conclude that by making the rectangular plate compression and vane cone tests on snow, correlation is possible. *Muro and Yong* [1980c] demonstrate ability to correlate these test results with a particular tracked vehicle configuration, wherein traction force T is expressed by

$$T = \frac{1}{1-s} T_1 - \frac{s}{1-s} (T_3 + T_6) - (T_2 + T_5)$$

where

T_1 traction force of belt drive on vehicle;
T_2 compaction resistance (correlates with rectangular plate test);
T_3 snow terrain tractive resistance (vane cone test);
T_5, T_6 side friction resistances (vane cone test);
s slip ratio.

This equation is derived, but its application is not demonstrated.

Other studies that involve measuring material properties relating to vehicle performance include the work by *Kuriyama and Shiboya* [1978]. They develop a semitheoretical equation relating the power required for driving a rotary type snow blower based upon a vortex model of snow deposit on the blower casing. Calculated and experimental values approximately agree for a particular rotary blower (Niigata-652s). The effective throwing power for snow was found to be 30–45% of the power required to drive the blower. *Yosida* [1974a, b, 1975a, b, c] presented a five-part in-depth study of the performance evaluation of a high-speed railroad snowplough. Assumptions are made that allow definition of the kickup velocity of snow by the snowplough blade. Distinction is made between flow and spray types of kickup, defined in terms of plough speed V and the plastic wave speed c of the snow, namely,

Flow

$$\lambda = (V/c)^2 \qquad \lambda > 1$$

Spray

$$\lambda = (V/c)^2 \qquad \lambda < 1$$

Running resistance of the plough when snow kickup is of the flow type is expressed as

$$F = -C_1 h_0 \rho_0 V^2$$

where

$$C_1 = 1 - (v/V) \cos \alpha$$

and

h_0 depth of snow layer removed;
ρ_0 density of snow layer removed;
v kickup velocity;
α scoop angle of plough.

For spray-type kickup an equation similar to the above is defined, wherein C_1 is replaced by another constant

$$C_2 = 1 - (v_c/V) \cos \alpha_s$$

where

v_c velocity of snow at instant of pulverization;
α_s nominal spray angle of snow.

Special consideration of different speed ranges of the plough and plough geometry are investigated once the basic theory is developed.

The application of mechanics principles to snowplough and tracked vehicle problems described above involves in some form the propagation of plastic waves in snow. Recently, research on plastic waves in snow has been conducted that pertains directly to compaction by tracked vehicles and
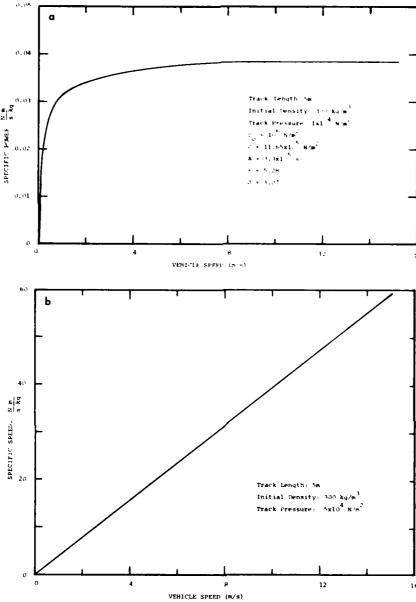
Fig. 14.   Specific power dissipation in snow as a function of vehicle speed for a track pressure of (a) 1×10^4 N m^{-2} and (b) 5×10^4 N m^{-2}.

to explosion response of snowpack [*Mellor*, 1965]. *Sato and Wakahama* [1976] investigate the propagation of a wave front in snow impacted by a falling weight. Both dry and wet snow results are given, with wide scatter in data, but indicating that wave speed in wet snow is lower than that in dry snow of the same density. At a falling block impact speed of 4.3 m s^{-1} the plastic wave is measured at 6.2 m s^{-1} in front of the block, dropping to 3.8 m s^{-1} when the wave front was 0.08–0.10 m ahead of the block. Plastic wave speed was found to increase with density of dry snow, from 6.5 m s^{-1} at an initial density of 200 kg m^{-3} to 12 m s^{-1} at twice the previous density. Significantly, the density of the material behind the plastic wave front was measured at 610 kg m^{-3}, which is in the range of critical density, as discussed previously. Sato and Wakahama found that application of

the Rankine-Hugoniot equations for density and pressure across the plastic wave front deviated from experiment; the higher the initial snow density, the greater the deviation. This result further emphasizes that the critical density property of snow needs to be factored into work pertaining to large deformation of snow. Other plastic wave work recently completed by *Brown* [1979b, 1980a, b], involving a form of the constitutive equation cited previously, pertains to high rate deformation as would be obtained in snow response to explosives.

Surface traction of snow is an important topic with respect to performance of pneumatic tires. *Browne* [1974] outlines equations for traction of treaded tires on compacted snow similar to the equation previously given by Muro and Yong but more complex in the account taken of tread effects.

/ versus depth in a small-scale avalanche
ig flow) [Dent and Lang. 1980].

licate the extent to which the different
n are known for a specific tire design.
irizes ranges of friction coefficients of
:ompact snow as measured by Abele
959]. However, the process of traction
irely frictional except in the case of a
rface and treadless tires. The Highway
i sponsored a number of studies on
ires; some of the work reported is by
and Clough [1972], Kinosita and Aki-
haerer [1970]. Additional tire traction
i manufacturer reports.

urface resistance of snow has been
attention in recent years because of
ctivity in cold regions. It is encouraging
se problems are tending more toward
eering mechanics principles and less
iluations.

Flowing Snow

ivity and development in the mountain-
orld have led to demands that govern-
nties be able to identify snow avalanche
out zones. In addtion, since it often
o build structures in these areas, ava-
must be determined to formulate build-
he study of flowing snow is motivated

otion is quite complex. It may generally
er flowing or airborne powdered or a
Flowing motion encompasses wet and

dry slab avalanches and is the tumbling, flowing motion
governed by the continuous interaction among snow clods.
Airborne powdered motion is found in powder avalanches
and dust clouds associated with flowing avalanches. In
powder motion most of the snow is swirling through the air,
with snow interactions being of lesser importance than the
properties of the air the material is entrained in. The relative
velocities and densities of different parts of an avalanche are
the subject of much speculation but are backed by few data.
Most velocity measurements have been of the leading edge
of the avalanche, and then only average velocities over
certain sections of the flow have been measured. Some
researchers [Shoda, 1966; LaChapelle and Lang, 1979;
Martinelli et al., 1980] have used motion picture footage of
avalanches to determine the leading edge velocity of the flow
as it starts from rest and accelerates down the slope.
Photogrammetry techniques have also been used to measure
the time-dependent leading edge velocity of avalanches
[Briukhanov et al., 1967; Van Wijk, 1967; Brugnot, 1979].

Measurements of interior transient velocities in ava-
lanches were achieved by Schaerer [1973], Schaerer and
Salway [1980], and Shimizu et al. [1973, 1975, 1977, 1980].
These researchers mounted sets of pressure transducers in
an avalanche path. By correlating pressure peaks between
separate sensors and the resulting time lag, internal veloci-
ties could be calculated. Systematic measurements, howev-
er, could not be made because of the difficulty in correlating
pressure peaks. Dent and Lang [1980, 1981] were able to
measure the velocity as a function of depth at one point in a
scaled-down snow avalanche (Figure 15). This was achieved
by photographing the snow flow as it passed a glass window
embedded in the avalanche track.

Another potentially powerful technique for measuring
both external and internal avalanche velocities is microwave
radar. Passive or active sensors may be placed in an ava-
lanche before it is released and monitored by a microwave
system for velocity as the avalanche descends the slope.
Ordinary Doppler measurements have already yielded lead-
ing edge velocities of flowing avalanches (H. Gubler, person-
al communication, 1980).

Since velocity data are so hard to gather by field measure-
ments, physical modeling can provide another means to get
useful avalanche data. In scaling down a natural phenome-
non such as an avalanche, dynamic similarity must be
maintained. In addition, boundary conditions must be faith-
fully reproduced. Dynamic similarity between model and
prototype is maintained by matching certain characteristic
dimensionless numbers, involving the flow parameters. The
more carefully these numbers are matched, the better the
model motion represents the real event. The densimetric
Froude number, which is the ratio of inertial forces to
gravity, is the commonly accepted parameter for plume
modeling. The Reynolds number must be high enough for
viscous effects to be neglected. Hopfinger and Tochan-
Danguy [1977] and Tochan-Danguy and Hopfinger [1975]
used gravity flow of salt solutions to model powder ava-
lanches. They used a 3-m-long inclined tank to allow a salt
brine to flow under a less dense ambient fluid. The qualita-
tive results strongly resembled the natural event. However,
the density ratios between the two fluids in the model did not
match the prototype, which casts suspicion upon the results.
Lang and Dent [1980] used a 1/100 scale geometric model of
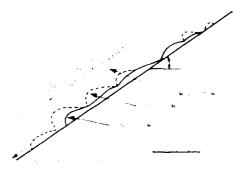snow impacting a barrier to study avalanche impact forces.

Fig. 16.   Profile of an avalanche derived from pressure sensors
[Schaerer and Salway, 1980].

Froude number was matched, but Reynolds number was not. The model impact results compared favorably to a computer simulation in which both Froude and Reynolds numbers were matched.

As sparse as the data are for velocities, they are much better than the data available for density. Direct density measurements have been very difficult to make for flowing snow. Eybert-Berard et al. [1978] used gamma rays to obtain some average density measurements in flowing snow. Indirect evidence based on flow depths has also been used to estimate the average density of an avalanche. These estimates range from 60–90 kg m⁻³ for dry snow avalanches to 300–400 kg m⁻³ for wet snow avalanches [Schaerer, 1975]. Schaerer and Salway [1980] concluded from evidence gathered from their pressure gauges located at Rogers Pass in British Columbia 'that well-developed dry snow avalanches have an unsteady wave motion similar to the slug flow observed in ultra-rapid flow of water, and that they consist of three stratified components: dense flowing snow at the bottom, light flowing snow, and powder snow' at the top (Figure 16). They go on to say that the dense zone was 0.5–1.2 m deep and formed the principal mass of the avalanche. The light flowing snow, with an average density from 10 to 30% of that of the dense zone, consisted of a mixture of powder and lumps of snow up to 60 mm in diameter. The speculation is that this 1- to 5-m layer of light snow is caused by lumps being tossed upward from the surface of the dense flowing snow by the turbulent motion at that surface. In the runout zone it is often possible for the light flow to separate from the dense flow either at bends in the avalanche track or during rapid deceleration. The third component of the avalanche reported by Schaerer and Salway is the powder cloud, which could not be detected by their instruments but was observed visually. Direct measurements of snow density in an avalanche will probably have to await development of remote sensing techniques.

In addition to determining the bulk density of flowing snow, the sizes of the particles that make up the avalanche would seem to have a marked effect on the motion. 'Almost immediately after a snow slab breaks away from the starting zone and begins accelerating down the track, the moving mass disaggregates into blocks, and then into round chunks and various sized particles' [Perla, 1980]. The sizes of these particles depend upon the type of snow released, the size of the avalanche, and the distance the avalanche runs. Schaerer [1973], from visual observations of moving and deposited snow, puts the particle size for dry snow avalanches in the range from 0.1 to 100 mm in diameter. Mears

[1980], from examination of avalanche debris, estimates this range to be 2.0–150 cm for hard slab avalanches. How particle size influences motion is not clear. However, the influences must depend upon the relative motion of the particles: how they slide past one another, bounce, collide, and rotate.

The relative motion of the various sized constituents of an avalanche and the stresses associated with that motion form the basis of avalanche dynamics. It has been said [Salm, 1966] that the exact development of a constitutive equation for snow flow may be impossible to determine. The relationships are very complex and dependent upon a large number of parameters. Thus certain empirical assumptions are necessary in order to achieve a working system for analysis, and selection of primary versus secondary parameters becomes an essential step in formulating the analysis technique. For example, since temperature is usually a function of altitude, the mass of an avalanche that has only descended several hundred meters may already be made up of snow of widely varying properties due to entrainment of snow of different temperatures.

If one were to try to characterize snow avalanches in general terms, a description might read: 'A snow avalanche is the transient, three-dimensional motion of a variable mass system made up of a nonrigid, nonrotund, nonuniform assemblage of granular snow fragments flowing down a nonuniform slope of varying surface resistance.' The driving force in an avalanche is always the force of gravity, but the resistive forces are all dependent upon the interactions between the individual snow fragments. Even if one knew the form of the interaction forces, the large number and highly variable nature of the particles would make analysis unmanageable, except in some statistical sense. Given, then, that the exact mechanical solution to the avalanche motion problem may be impossible, it is also unnecessary. The motion of individual snow fragments is of limited interest. The time and spatial transients are small for most purposes. A possible exception would be the impact of an individual snow clod upon an equal-sized or smaller area. It is the overall motion, in some sense the average motion, of the avalanche that is of interest. Approximations to the mechanics of the fragment interactions must be made so that analysis can be carried out. In this way, some appropriate average velocity may be determined from which runout distances and impact forces can be calculated. It is generally true that the more realistically the interaction forces are modeled, the more accurate and general will be the solution to the analysis. It has been the objective of the avalanche dynamicist to formulate avalanche flow models simple enough to solve, yet complicated enough to include as much of the mechanical behavior of the avalanche as possible.

Among the first to present an analytical formulation for avalanche flow was A. Voellmy in his classic monograph presented in 1955. Voellmy [1955] based his analysis on the equations developed to describe open channel fluid flow. He extended the open channel hydraulics approach, with all its implicit assumptions, to the flow of snow on a mountain slope. Voellmy, and many others since him, based their theories on the observation that snow avalanches seem to 'flow.' That is, the material deforms, conforms to the slope, and often flows around obstacles. This motion is much like the movement of water along a streambed—hence the analogy with open channel hydraulics. Implicit in the assumptions

of this approach is that flowing snow behaves as a fluid. In most continuum mechanical theories, fluids are considered to be continuous, homogeneous, and isotropic. That is, any granular nature of the material is ignored, and any spatial variation in the fluid is neglected. Furthermore, hydraulics deals with materials that can be considered incompressible. The degree to which all these effects influence snow avalanche movement determines the extent to which an incompressible fluid model can give useful results. The incompressible fluid model does, however, greatly simplify the analysis. Using a continuum mechanical theory, the problem is reduced to finding point values for the stresses within the material. This is most easily done by using a momentum balance analysis. The stresses are then related to deformations by a constitutive relation that takes the properties of the fluid into account.

The open channel hydraulics analysis that Voellmy applied contains, in addition to the fluid assumptions, approximations related to fluid motion in an open channel. Chief among these approximations is that the flow is steady, that is, that there is no time dependence to the motion. The idea is that an avalanche on a constant slope quickly accelerates to a terminal velocity and thereafter exhibits steady motion. The momentum balance equation is commonly integrated over the slope normal cross-sectional area so that only the boundary stresses need be considered. The dependent variable then becomes the average velocity of the material in cross section. In addition, a uniform motion is usually assumed, so that the flow experiences no variation along the slope. Under these assumptions the momentum balance equation becomes an equilibrium condition,

$$\tau = \rho g h \sin \theta \tag{1}$$

in which τ is the resistive shear stress at the fluid boundary, ρ is the average fluid density, g is the acceleration of gravity, h is the flow depth, and θ is the constant slope angle. In order to derive an equation for the velocity of the flow, an equation relating the velocity to the stresses on the boundary must be introduced. For this constitutive equation, Voellmy used the *Prantl mixing length approximation* [*Pao*, 1961]. In turbulent fluid flow, in which the velocity and stresses at any point fluctuate randomly, the boundary drag is approximately proportional to the square of the flow velocity: $\tau = k_1 v^2$. However, Voellmy postulated an additional friction force proportional to the acting normal force, so that the proposed equation became

$$\tau = k_1 v^2 + \mu g h \rho \cos \theta \tag{2}$$

The form of the additional term in this equation is the same as that of a conventional Coulomb friction force in which μ is the coefficient of friction. The addition of the friction term is necessary, because snow exhibits a cohesion or locking property. A minimum stress level must be exceeded before deformation occurs. Using this equation (2) for the shear stress at the avalanche-channel interface and equation (1) for the shear stress at the avalanche-atmosphere interface, the momentum balance equation may be solved for the flow velocity:

$$v = [\xi h(\sin \theta - \mu \cos \theta)]^{1/2}$$

where the drag coefficients have been combined into a single parameter ξ. The flow velocity v is the average terminal velocity that an avalanche is supposed to quickly attain

under uniform steady conditions along a constant slope, provided the stresses at the boundary of the avalanche can be modeled by the above stress equations. (In the case of open channel flow, the height of an avalanche, h, is replaced by the hydraulic radius, which is defined as the ratio of the cross-sectional area to the wetted perimeter.)

To calculate runout distances, the avalanche path is divided into three parts: (1) the starting zone, where the avalanche is initiated and accelerates to terminal velocity, (2) the avalanche track, with a constant slope which allows steady state flow, and (3) the runout area, where the slope of the track has decreased, causing the avalanche to decelerate. If it is assumed that the avalanche enters a constant-slope runout zone with the velocity calculated from the steady state conditions of the track flow, the runout distance S can be found from a simple energy balance equation. The equation Voellmy derived is

$$S = v^2/[2g(\mu \cos \theta - \tan \theta) + v^2 g/\xi h_m]$$

in which h_m is the mean deposition depth. By applying these equations to an avalanche path, avalanche runout may be calculated. The usual procedure is to subjectively break the avalanche track into its three sections. The important point is the transition into the runout zone. The steady velocity is calculated from the slope of the track, and then the runout distance is computed from the transition point. The result of the analysis is highly dependent upon exactly how the path is divided and where the transition point is chosen. Through experience, certain individuals have become very proficient at making these subjective decisions, and this method has yielded good results. As the avalanche paths become more complicated, the application of Voellmy's equations becomes more difficult; also, it is difficult for someone inexperienced in the method to apply it and get accurate results.

The material parameters appearing in Voellmy's equations are ξ, the turbulent friction coefficient, dependent upon terrain roughness, and μ, the dry friction coefficient. The coefficient ξ is given the range 400–600 m s^{-2} by Voellmy. Later investigators [*Mears*, 1976; *Schaerer*, 1975; *Leaf and Martinelli*, 1977; *Buser and Frutiger*, 1980; *Martinelli et al.*, 1980] have allowed ξ to become as large as 1600 m s^{-2} and recommend average values of ξ of about 1400 m s^{-2}.

Bucher and Roch [1946] were among the first to publish data for the dry friction coefficient μ. They found that for hard, wet snow sliding slowly over a hard, wet snow surface the friction coefficient ranged from 0.1 to 0.4. *Inaho* [1941] slid blocks of dry snow over a granular surface and found μ to range from 0.4 to 0.6. *Heimgartner* [1977] found values for μ from 0.22 to 0.39 when measured on a small test slide at Weissfluhjoch, Switzerland. *Sommerhalder* [1972] computed a maximum friction coefficient of 0.5 from snow flowing over snowsheds, with an average value of 0.32. Using data reduced from 16-mm movie film, *Martinelli et al.* [1980] computed the friction coefficient for a wet slab avalanche in the runout zone to be from 0.30 to 0.35.

Estimates of the friction coefficient can also be made from the static angle of repose for natural snow. *Perla et al.* [1980], using this method, give values for μ from 0.25 to 0.45 depending on factors such as snow type, path roughness, and the presence of trees and obstacles. *Mellor* [1978] puts the friction values between 0.2 and 0.6.

Many studies also have applied Voellmy's equations to avalanches that have already run, trying, from the known

results, to estimate the values of the friction coefficient. *Voellmy* [1955] suggests the use of the relation $\mu = \rho/2000$, where ρ is the density of the flowing snow in kilograms per cubic meter. Using values for ρ of 200–400 kg m^{-3}, the friction coefficient is in the range 0.1–0.2. *Salm* [1972] uses μ values from 0.15 to 0.50. *Leaf and Martinelli* [1977] found that values of 0.15–0.18 for the friction coefficient gave them the best results. *Schaerer* [1975] proposed to make μ velocity dependent and suggested the relationship $\mu = 5/v$ with v expressed in meters per second. *Martinelli et al.* [1980] found that this expression worked well for hard slab and slow wet avalanches when combined with a turbulent friction coefficient of $\xi = 700$–800 m s^{-2} but that for large-design avalanches a constant μ of 0.15 combined with a ξ of 1200–1600 m s^{-2} worked best.

Salm [1966] expanded upon Voellmy's theoretical treatment of an avalanche and derived a time-dependent equation for the velocity of the mass center. His resistive force was a Taylor series in velocity, truncated after the third term:

$$R = R_0 + R_1 \frac{v}{1!} + R_2 \frac{v^2}{2!}$$

The constant term R_0 represents a dry friction force; R_1 can be attributed to linear viscosity; the third term is due to turbulent friction and the ploughing of the avalanche into the stationary snow. Salm neglected the second term with respect to the third for high-speed flowing avalanches. He assumed that the energy dissipated by internal friction (the R_1 term) was small in comparison to the turbulent energy dissipation (the R_2 term). The resulting expression for maximum velocity on a constant slope has the same form as Voellmy's equation. Salm, in the same presentation, used energy considerations to derive an equation for runout distance. It is a more comprehensive treatment than Voellmy's and includes the possibility of artificial obstacles. The resulting equation is considerably more complicated than Voellmy's, but it does not contain the troublesome singularity that appears in Voellmy's equation.

Mellor [1968] presented an analysis similar to that of *Salm* [1966], but he also considered the possibility of having a variable mass system. The mass was allowed to vary linearly with the avalanche velocity:

$$m = m_0(1 + kv)$$

Here m_0 is the initial avalanche mass, and k is an entrainment coefficient. This is an empirical relation based upon a correlation between avalanche mass and velocity. The dynamic equations that result from this analysis are cumbersome and 'afford little insight into the effects of entrainment as they stand' [*Mellor*, 1968].

Perla et al. [1980] developed a center-of-mass model similar to the models discussed previously. A mass entrainment term proportional to the square of the speed was included in the dissipative forces. This term was combined with other v^2 terms into a single term having the coefficient D. The equation of motion was then solved successively over small intervals along the slope; in each interval the slope and the friction coefficients were considered to be constant. The expression for the maximum velocity over any interval has the same form as Voellmy's equation for terminal velocity,

$$v_{max} = [(mg/D)(\sin \theta - \mu \cos \theta)]^{1/2}$$

in which mg/D replaces Voellmy's ξh. In addition, at the juncture of two segments a correction for momentum loss at the slope transition is included.

Values for the parameters θ and m/D for this model are found in the same way that μ and ξ are found for Voellmy's model. *Perla et al.* [1980] and *Bakkeh\u00f8i et al.* [1981] discuss and give examples for these parameters.

In another work, *Perla* [1980] analyses the effects of snow entrainment that occur at a constant rate per unit length of avalanche travel: 'Initially entrainment and drag cooperate to oppose acceleration, but if entrainment continues the mass increase will eventually work against the drag and velocity will increase. However, . . . the velocity boost is only significant given continual entrainment on very long paths.'

A major drawback to the center-of-mass approach to avalanche dynamics is the lumping of the avalanche mass at one point. An avalanche is an extended mass of variable density and velocity. The use of the center-of-mass equations does not provide insight into the spatial properties of the flow. In particular, the flow depth, although it may appear as a parameter, is never calculated.

To account for the spatial characteristics, a general stress-deformation relation must be found. One of the simplest relations is the continuum-mechanical representation of a linear Newtonian fluid. It is very unlikely that snow in a moving avalanche deforms according to this flow law, but adoption of more sophisticated models leads to equations of motion that are unmanageable. As it is, the linear fluid assumption results in a nonlinear partial differential equation for the velocity, the so-called Navier-Stokes equation. For the flow geometries encountered in avalanche motion, only computer solutions to the Navier-Stokes equation can be obtained [*Brugnot*, 1979]. Using this technique, *Dent and Lang* [1980] match avalanche leading edge velocities and flow geometries for a small-scale test avalanche.

The principal parameter for linear fluid flow is the Newtonian viscosity. This coefficient is the constant of proportionality between shear stress and the linear velocity gradient. Estimated values for this constant range from the viscosity of air, 1.5×10^{-5} m^2 s^{-1} [*Perla*, 1980] to the viscosity associated with creep motion, 65.3 m^2 s^{-1} [*Shen and Roper*, 1970]. Actual measurements of viscosity for flowing snow do not exist. *Bucher and Roch* [1946], however, did measure the frictional resistance of hard wet snow sliding over a hard wet snow surface for speeds between 0.2 and 2.4 m s^{-1}. They found that the linear fit to their data yielded a constant of proportionality of 475 N s m^{-1}. If it is assumed that there was a 2-mm layer of granulated snow of density 300 kg m^{-3} between the sliding surfaces and that the velocity gradient was linear in this region, then the viscosity in this layer would be about 0.003 m^2 s^{-1}. Similar tests by *Lang et al.* [1981], using hard sintered snow over the velocity range 0.1–0.25 m s^{-1}, yielded a viscosity coefficient of 0.004 m^2 s^{-1}. These values will undoubtedly be different at higher speeds, but they do serve as possible order-of-magnitude estimates.

The viscosity of fluidized snow has been measured in Japan by *Maeno and Nishimura* [1979] and *Maeno et al.* [1980]. By passing air upward through a snow column they were able to suspend snow and create a fluidized bed: 'The general behavior of the fluidized snow resembles that of a liquid.' [*Maeno et al.*, 1980]. The dynamic viscosity was measured by standard techniques for a fully fluidized snow bed and found to be in the range 0.3–10^{-3} N s m^{-2},

TABLE 1.   Literature Lists for the Topics Reviewed

Snow Surface Friction	Snow Surface Resistance	Flowing Snow
Bowden [1955]	Abele [1963, 1966]	Bagnold [1954, 1956]
Bowden and Hughes [1939]	Abele and Gow [1975, 1976]	Bakkehøi et al. [1981]
Bowden and Tabor [1956, 1964]	Assur [1964]	Briukhanov et al. [1967]
Bucher and Roch [1946]	Bader [1962]	Brugnot [1980]
Budnevich and Deriagin [1952]	Bekker [1969]	Bucher and Roch [1946]
Eriksson [1949]	Brown [1979a, b, c,	Buser and Frutiger [1980]
Evans et al. [1976]	1980a, b, 1981]	Dent and Lang [1980]
Eybert-Berard et al. [1978]	Browne [1973, 1974]	Goodman and Cowin
Goldovskii [1953]	Diamond [1956]	[1971, 1972]
Huzioka [1957, 1959]	Dickson et al. [1961]	Heimgartner [1977]
Huzioka et al. [1954, 1955,	Gerdel et al. [1954]	Hopfinger and
1958, 1962, 1963]	Harrison [1957,	Tochon-Dangur [1977]
Jellinek [1957a, b]	1975]	Inaho [1941]
Keinonen et al. [1978]	ISTVS [1978]	Kanatani [1979]
Klein [1947]	Johnson [1978]	Korner [1980]
Kuroda [1942]	Kinosita and	LaChapelle and
Kuroiwa et al. [1969]	Akitaya [1970]	Lang [1979]
Landy and Freiberger [1959]	Lanyon [1959]	Lang and Dent [1980]
Mayr [1979]	Mellor [1963, 1965]	Lang et al. [1981]
McConica [1950]	Moyer [1947]	Leaf and Martinelli
Mellor [1964, 1966, 1974]	Muro and Yong	[1977]
Morphy [1913]	[1980a, b, c]	Maeno and Nishimura
Nakamura et al. [1966]	Napadensky [1964]	[1979]
Nakaya [1936]	Nuttall and	Maeno et al. [1980]
Niven [1959]	Finelli [1955]	Martinelli et al. [1980]
Palosuo et al. [1977, 1979]	Nuttall and McGowan	Mears [1976, 1980]
Raraty and Tabor [1958]	[1961]	Mellor [1968, 1978]
Seligman and	Rula [1959, 1960]	Nedderman and
Debenham [1943]	Rula et al. [1955]	Laohakul [1980]
Shimbo [1971]	Sato and Wakahama	Pao [1961]
Torgersen [1979]	[1976]	Pariseau [1980]
Tusima [1977]	Schaerer [1970]	Perla [1980]
University of Minnesota	Skinrood [1957]	Perla et al. [1980]
[1951, 1955]	Smith and Clough	Salm [1966, 1972]
	[1972]	Savage [1979]
	Taylor [1952]	Schaerer [1973, 1975]
	Thomson [1955, 1957]	Schaerer and Salway
	Tusima [1973, 1975]	[1980]
	Wakahama and Sato	Shen and Roper [1970]
	[1977]	Shimuzu et al.
	Wehner [1959]	[1973, 1975, 1977, 1980]
	Weiss et al. [1956]	Shoda [1966]
	Yokomore [1975]	Sommierhalder [1972]
	Yong [1973]	Tochon-Danguy and
	Yong and Fukue [1977, 1978]	Hopfinger [1975]
	Yong and Harrison [1978]	Van Wijk [1967]
	Yong and Muro [1980c]	Voellmy [1955]
	Yosida [1974a, b, 1975a, b, c]	

depending upon the particle size and the fluidization veloci-
ty. When these numbers are divided by the densities of the
snow, values of the kinematic viscosity are found to be in the
range 5×10^{-6} m^2 s^{-1} to 0.001 m^2 s^{-1}. As the fluidization air
velocity is decreased below the velocity necessary for com-
plete fluidization, the measured viscosity coefficients rise
sharply. At the minimum possible airflow velocity, below
which the incomplete fluidized bed becomes unstable and it
becomes impossible to measure the viscosity, the measure-
ments yield results in the range 0.0001–0.001 m^2 s^{-1}.

It is clear that the viscosity of avalanching snow is a
function of the degree to which the snow is fluidized. This, in
turn, depends upon the snow type and the velocity of the
flow. A high-speed powder avalanche may be fully fluidized,
with a viscosity very near that of air. For a slab avalanche of
the mixed type the dense flowing portion may have a
viscosity of 0.001 m^2 s^{-1} or larger. When flowing snow is

modeled as a linear viscous fluid, it may also be necessary to
use an artificially large viscosity to account for v^2 forces that
are not represented in the model.

Since flowing snow is made up of a granular material, it
may be possible to utilize some of the work being carried on
in the field of grain flow. Mears [1980] tries to apply some of
the results of Bagnold's [1954, 1956] work on cohesionless
grain flow in fluids to snow. Additional references in the
granular material area are articles by Goodman and Cowin
[1971, 1972], a monograph by Savage [1979], an article by
Nedderman and Laohakul [1980], and a paper by Kanatani
[1979]. Constitutive equations for granular materials are
formulated in these papers. The rheology of grain flow is
probed by experimental as well as theoretical techniques.
Only a partial list of the work in grain flow has been provided
(Table 1); other investigations either completed or in pro-
gress may have relevance to snow flow.

REFERENCES

Abele, G., Skid tests performed with a wheeled vehicle on a processed snow trench floor, internal technical note, U.S. Army Cold Reg. Res. and Eng. Lab., Hanover, N. H., 1963.

Abele, G., Performance testing of an air cushion vehicle on the Greenland Ice Cap, Spec. Rep. 91, U. S. Army Cold Reg. Res. and Eng. Lab., Hanover, N. H., 1966.

Abele, G., and A. Gow, Compressibility characteristics of undisturbed snow, Res. Rep. 336, 57 pp., U. S. Army Cold Reg. Res. and Eng. Lab., Hanover, N. H., 1975.

Abele, G., and A. Gow, Compressibility characteristics of compacted snow, Rep. 76-21, 47 pp., U. S. Army Cold Reg. Res. and Eng. Lab., Hanover, N. H., 1976.

Assur, A., Locomotion over soft soil and snow, Paper 782F, Soc. of Automot. Eng., New York, 1964.

Bader, H., The physics and mechanics of snow, monograph, part II, sect. B, U. S. Army Cold Reg. Res. and Eng. Lab., Hanover, N. H., 1962.

Bagnold, R. A., Experiments on a gravity-free dispersion of large solid spheres in a Newtonian fluid under shear, Proc. R. Soc. London, Ser. A, 225, 49–63, 1954.

Bagnold, R. A., The flow of cohesionless grains in fluids, Proc. R. Soc. London, Ser. A, 249, 29–297, 1956.

Bakkehøi, S., T. Cheng, V. Domaas, K. Lied, R. Perla, and B. Schieldrop, On the computation of parameters that model snow avalanche motion, Can. Geotech. J., 18(1), 121–130, 1981.

Bekker, M. G., Introduction to Terrain-Vehicle Systems, University of Michigan Press, Ann Arbor, 1969.

Bowden, F. P., Friction on snow and ice and development of some fast running skis, Nature, 176(4990), 946–947, 1955.

Bowden, F. P., and T. P. Hughes, The mechanism of sliding on ice and snow, Proc. R. Soc. London, Ser. A, 172, 280–298, 1939.

Bowden, F. P., and D. Tabor, Friction and Lubrication, Methuen, London, 1956.

Bowden, F. P., and D. Tabor, The Friction and Lubrication of Solids, vol. II, 544 pp., Clarendon, Oxford, 1964.

Briukhanov, A. V., et al., On some new approaches to the dynamics of snow avalanches, Phys. Snow Ice Conf. Proc., 1(2), 1223–1242, 1967.

Brown, R. L., A volumetric constitutive law for snow subjected to large strains and strain rates, Rep. 79-20, U.S. Army Cold Reg. Res. and Eng. Lab., Hanover, N. H., 1979a.

Brown, R. L., An analysis of plastic shock waves in snow, Rep. 79-29, U. S. Army Cold Reg. Res. and Eng. Lab., Hanover, N. H., 1979b.

Brown, R. L., A study of vehicle performances in snow, J. Terramechanics, 16(4), 153–162, 1979c.

Brown, R. L., Pressure waves in snow, J. Glaciol., 25(91), 99–107, 1980a.

Brown, R. L., An analysis of non-steady plastic shock waves in snow, J. Glaciol., 25(92), 279–288, 1980b.

Brown, R. L., An analysis of vehicle power requirements in deep snowpack, J. Terramechanics, in press, 1981.

Browne, A. L., Traction of pneumatic tires on snow, GM Res. Publ. GMR-1346, Gen. Motors, Detroit, Mich., March 1973.

Browne, A. L., Tire traction on snow-covered pavements, in The Physics of Tire Traction, edited by D. F. Hays and A. L. Browne, pp. 99–133, Plenum, New York, 1974.

Brugnot, G., Recent progress and new applications of the dynamics of avalanches, paper presented at Snow in Motion Symposium, Int. Glaciol. Soc., Fort Collins, Colo., Aug. 12–17, 1979.

Bucher, E., and A. Roch, Reibungs und Packungswiderstände bei raschen Schneebeweguagen, report, 9 pp., Eidg. Inst. fur Schnee und Lawinenforsch., Davos-Weissfluhjoch, Switzerland, 1946.

Budnevich, S. S., B. V. Deriagin, Sliding of solids on ice (in Russian), Zh. Tekh. Fiz., 22, 1967–1980, 1952.

Buser, O., and H. Frutiger, Observed maximum run-out distance of snow avalanches and the determination of the friction coefficients μ, and ξ, J. Glaciol., 26(94), 121–130, 1980.

Dent, J., and T. E. Lang, Modeling of snow flow, J. Glaciol., 26(94), 131–140, 1980.

Dent, J., and T. E. Lang, Experiments on the mechanics of flowing snow, Cold Reg. Sci. Technol., in press, 1981.

Diamond, M., Studies on vehicular trafficability of snow, Rep. 35, part I, Corps of Eng., U. S. Army Snow, Ice and Permafrost Res. Estab., Hanover, N. H., 1956.

Dickson, W. J., et al., A method of evaluating scaling factors and performance of tracked vehicles on snow, report, Def. Res. Board, Can. Armament Res. and Dev. Estab., Valcartier, Que., 1961.

Eriksson, R., Medens friktion mot sno och is, Rep. 34-35, Foren. Skogsarb., Kgl. Domanstyrelsens Arbetsstud., 1949. (Friction of runners on snow and ice, Transl. 44, U. S. Army Snow, Ice and Permafrost Res. Estab., Hanover, N. H., 1955.)

Evans, D. C., J. F. Nye, and K. J. Cheeseman, The kinetic friction on ice, Proc. R. Soc. London, Ser. A, 347, 493–512, 1976.

Eybert-Berard, A., P. Perroud, G. Brugnot, R. Mura, and L. Rey, Mesures dynamiques dans l'avalanche, in Comptes Rendus, Deuxieme Rencontre Internationale sur la Neige at les Avalanches, Grenoble, France, pp. 203–224, 1978.

Gerdel, R. W., et al., Some factors affecting the vehicular trafficability of snow, Res. Pap. 10, Corps of Eng., U. S. Army Snow, Ice and Permafrost Estab., Hanover, N. H., 1954.

Goldovskii, B. M., Sliding over snow (in Russian), Priroda Moscow, 42(6), 1953.

Goodman, M. A., and S. C. Cowin, Two problems in the gravity flow of granular materials, J. Fluid Mech., 45, 321–339, 1971.

Goodman, M. A., and S. C. Cowin, A continuum theory for granular materials, Arch. Ration. Mech. Anal., 44, 249–266, 1972.

Harrison, W. L., Study of snow values related to vehicle performance, Rep. 23, 31 pp., U.S. Army Ord. Corps Land Locomotion Res. Board, Detroit Arsenal, Mich., 1957.

Harrison, W. L., Vehicle performance over snow: Math model validation study, Tech. Rep. 268, U.S. Army Cold Reg. Res. and Eng. Lab., Hanover, N. H., 1975.

Heimgartner, M., On the flow of avalanching snow, J. Glaciol., 19(81), 347–363, 1977.

Hopfinger, E. J., and J. C. Tochon-Danguy, A model study of powder-snow avalanches, J. Glaciol., 19(81), 343–356, 1977.

Huzioka, T., Studies on ski, Low Temp. Sci., Ser. A, 16, 31–46, 1951.

Huzioka, T., Studies on ski, Low Temp. Sci., Ser. A, 18, 77–96, 1959.

Huzioka, T., et al., Studies on the resistance of a snow sledge, Low Temp. Sci., Ser., A, 13, 37–47, 1954.

Huzioka, T., et al., Studies on the resistance of a snow sledge, Low Temp. Sci., Ser. A, 14, 95–112, 1955.

Huzioka, T., et al., Studies on the resistance of a snow sledge, Low Temp. Sci., Ser. A, 17, 31–52, 1958.

Huzioka, T., et al., Studies on the resistance of a snow sledge, Low Temp. Sci., Ser. A, 20, 159–179, 1962.

Huzioka, T., et al., Studies on the resistance of a snow sledge, Low Temp. Sci., Ser. A, 21, 31–44, 1963.

Inaho, Y., Angle of kinetic friction of snow (in Japanese), J. Jpn. Soc. Snow Ice, 3, 303–307, 1941.

ISTVS Committee on Snow Mechanics Research Coordination, Requirement for identification and characterization of snow for mobility purposes, report, Sixth International Conference, Vienna, Austria, 1978.

Jellinek, H. H. G., Contact angles between water and some polymertic materials, Res. Rep. 36, U.S. Army Snow, Ice and Permafrost Res. Estab., Hanover, N. H., 1957a.

Jellinek, H. H. G., Adhesive properties of ice, I, Res. Rep. 38, U.S. Army Snow, Ice and Permafrost Res. Estab., Hanover, N. H., 1957b.

Jellinek, H. H. G., Adhesive properites of ice, II, Res. Rep. 62, U.S. Army Snow, Ice and Permafrost Res. Estab., Hanover, N. H., 1960.

Johnson, J. B., Stress waves in snow, Ph.D. thesis, Dep. of Geophys., Univ. of Wash., Seattle, 1978.

Kanatani, K., A micropolar continuum theory for the flow of granular materials, Int J. Eng. Sci., 17, 419–432, 1979.

Keinonen, J., E. Palosuo, P. Korhonen, and H. Suominen, Measurements of friction between snow and sliding materials of ski (in Finnish), Rep. Ser. Geophys. 10, 28 pp., Univ. of Helsinki, Helsinki, Finland, 1978.

Kinosita, S., and E. Akitaya, Classification of snow and ice on roads, Spec. Rep. 115, Highway Res. Board, Washington, D. C., 1970.

Klein, G. J., The snow characteristics of aircraft skis, Aeronaut. Rep. AR-2, Div. of Mech. Eng., Natl. Res. Counc. of Can., Ottawa, Ont., 1947.

Korner, H. J., Model conceptions for the rock slide and avalanche movement, in *Naturraumanalysen zum Zweck der Katastrophenvorbeugung in Schutzwasserbau and Raumordnung: Publikation International Symposium Interpraevent 1980, Bad Ischl, 8.-12. Sept.*, vol. II, pp. 15–55, Forschungsgessellschaft vorbeugende Hochwasserbekämpfung, Klagenfurt, Austria, 1980.

Kuriyama, H., and M. Shibuya, On the power required for driving the blower of a rotary type snow removal machine, *J. Jpn. Soc. Snow Ice, 40*(1), 16–23, 1978.

Kuroda, M., Resistance of snow to a sledge (in Japanese), *J. Jpn. Soc. Snow Ice, 4*, 42–48, 1942. (*Transl. 36*, U.S. Army Snow, Ice and Permafrost Res. Estab., Hanover, N. H., 1955.)

Kuroiwa, D., Wakahama, G. K. Fujino, and R. Tanahashi, The coefficient of sliding friction between skis and chemically treated or mechanically compressed snow surfaces, *Low Temp. Sci., Ser. A, 27*, 229–245, 1969.

LaChapelle, E. R., and T. E. Lang, A comparison of observed and calculated avalanche velocities, *J. Glaciol., 25*(92), 309–314, 1979.

Landy, M., and A. Freiberger, Studies on ice adhesion—Adhesion of ice to plastics, *J. Colloid Interface Sci., 25*, 321–344, 1967.

Lang, T. E., and J. Dent, Scale modeling of snow-avalanche impact on structures, *J. Glaciol., 26*(94), 189–196, 1980.

Lang, T. E., J. Dent, and R. G. Oakberg, Surface resistance measurements cooperative agreement, *Rocky Mt. For. Range Exp. Stn. For. Serv. Res. Pap. RM-81-165-Cu*, 1981.

Lanyon, J. H., Studies on vehicular trafficability of snow, *Rep. 35*, part II, Corps of Eng., U.S. Army Snow, Ice and Permafrost Res. Estab., Hanover, N. H., 1959.

Leaf, C. F., and M. Martinelli, Jr., Avalanche dynamics: Engineering applications for land use planning, *U.S. Rocky Mt. For. Range Exp. Stn. For. Serv. Res. Pap., RM-183*, 1977.

Maeno, N., and K. Nishimura, Fluidization of snow, *Cold Reg. Sci. Technol., 1*, 109–120, 1979.

Maeno, N., K. Nishimura, and Y. Kaneda, Viscosity and heat transfer in fluidized snow, *J. Glaciol., 26*(94), 263–274, 1980.

Martinelli, M., Jr., T. E. Lang, and A. I. Mears, Calculations of avalanche friction coefficients from field data, *J. Glaciol., 26*(94), 109–120, 1980.

Mayr, B., Ein Beitrag zur Physik des Schigleitens: Elektronische Messung des Wasserfilms beim Gleitvorgang, doktorgrad dissertation, Leopold-Franzens-Univ., Innsbruck, Austria, 1979.

McConica, T. H., Sliding on ice and snow, report to Res. and Dev. Di., Office of the Quartermaster Gen., U.S. Army, Washington, D. C., 1950.

Mears, A. I., Guidelines and methods for detailed snow avalanche hazard investigations in colorado, *Bull. Colo. Geol. Surv., 38*, 1976.

Mears, A. I., A fragment-flow model of dry-snow avalanches, *J. Glaciol., 26*(94), 152–164, 1980.

Mellor, M., Oversnow transport, *Rep. III-A4*, 58 pp., U.S. Army Cold Reg. Res. and Eng. Lab., Hanover, N. H., 1963.

Mellor, M., Properties of snow, Cold Regions Science and Engineering, report, part III-A1, U.S. Army Cold Reg. Res. and Eng. Lab., Hanover, N. H., 1964.

Mellor, M., Explosions and snow, Cold Regions Science and Engineering, report, part III, sect. A3a, U.S. Army Cold Reg. Res. and Eng. Lab., Hanover, N. H., 1965.

Mellor, M., Snow mechanics, *Appl. Mech. Rev., 19*(5), 379–389, 1966.

Mellor, M., Avalanches, *Monogr. III A3d*, U.S. Army Cold Reg. Res. and Eng. Lab., Hanover, N. H., 1968.

Mellor, M., A review of basic snow mechanics, *IAHS AISH Publ., 114*, 251–291, 1974.

Mellor, M., Dynamics of snow avalanches, in *Rockslides and Avalanches*, vol. 1, edited by B. Voight, pp. 753–792, Elsevier, New York, 1978.

Morphy, H., The influence of pressure on the surface friction of ice, *Philos. Mag., Ser. 6, 25*, 133, 1913.

Moyer, R., Braking and traction tests on ice, snow, and on bare pavements, in *Proceedings of the 27th Annual Meeting*, pp. 340–360, Highway Research Board, Washington, D. C., 1947.

Muro, T., and R. N. Yong, Rectangular plate loading test on snow—Mobility of tracked over snow vehicle. *J. Jpn. Soc. Snow Ice, 42*(1), 17–24, 1980a.

Muro, T., and R. N. Yong, Vane cone test of snow—Mobility of tracked oversnow vehicle, *J. Jpn. Soc. Snow Ice, 42*(1), 25–32, 1980b.

Muro, T., and R. N. Yong, On trafficability of tracked oversnow vehicle—Energy analysis for track motion on snow covered terrain, *J. Jpn. Soc. Snow Ice, 42*(2), 33–40, 1980c.

Nakamura, T., A water-like film produced by pressure on the surface of ice crystals, in *Physics of Snow and Ice*, pp. 247–258, Institute of Low Temperature Science Hokkaido Univ., Sapporo, Japan, 1966.

Nakaya, U., M. Tada, Y. Sekido, and T. Takano, Physics of skiing, *J. Fac. Sci. Hokkaido Univ., Ser. II, 1*, 265, 1936.

Napadensky, H., Dynamic response of snow to high rates of loading, *Res. Rep. 119*, AD 600075, U.S. Army Cold Reg. Res. and Eng. Lab., Hanover, N. H., 1964.

Nedderman, R. M., and C. Laohakul, The thickness of the shear zone of flowing granular materials, *Powder Technol., 25*, 91–100, 1980.

Niven, C. D., A proposed mechanism for ice friction, *Can. J. Phys., 37*(3), 247–255, 1959.

Nuttall, C. J., and J. P. Finelli, Vehicles in snow: A critical review of the state of the art, Trafficability of snow, *Rep. 1*, Waterways Exp. Stn., Vicksburg, Va., 1955.

Nuttall, C. J., and R. McGowan, Scale models of vehicles in soils and snows, paper presented at First International Conference on the Mechanics of Vehicle Soil Systems, Turin, Italy, 1961.

Palosuo, E., T. Hiltunen, J. Jokinen, and M. Teinonen, The effect of friction between snow and skis (in Finnish), *Rep. Ser. Geophys. 6*, 31 pp., Univ. of Helsinki, Helsinki, Finland, 1977.

Palosuo, E., J. Keinonen, H. Suominen, and R. Jokitalo, Measurement of friction between snow and ski running surfaces, (in Finnish), *Rep. Ser. Geophys., 13*, 42 pp., Univ. of Helsinki, Helsinki, Finland, 1979.

Pao, R. H. F., *Fluid Mechanics*, John Wiley, New York, 1961.

Pariseau, W. G., A simple mechanical model for rockslides and avalanches, *Eng. Geol., 16*, 111–123, 1980.

Perla, R. I., Avalanche release, motion, and impact, in *Dynamics of Snow and Ice*, edited by S. Colbeck, pp. 397–462, Academic, New York, 1980.

Perla, R. I., T. T. Cheng, and D. M. McClung, A two-parameter model of snow-avalanche motion, *J. Glaciol., 26*(94), 197–208, 1980.

Raraty, L. E., and D. Tabor, The adhesion and strength properties of ice, *Proc. R. Soc. London, Ser. A, 245*, 184–201, 1958.

Rula, A. A., Trafficability of snow, tests on a sub-Arctic snow, *Rep. 4*, Waterways Exp. St., Vicksburg, Va., 1959.

Rula, A. A., Trafficability of snow, Greenland studies, 1955 and 1957, *Rep. 4*, Waterways Exp. Stn. Vicksburg, Va., 1960.

Rula, A. A., E. S. Rush, and S. J. Knight, Trafficability of snow, Greenland studies 1954, *Rep. 2*, Waterways Exp. Stn., Vicksburg, Va., 1955.

Salm, B., Contribution to avalanche dynamics, *IAHS AISH Publ., 69*, 199–214, 1966.

Salm, B., Grundlagen des Lawinenverbaues. *Z. Buendner. Forstuer., 9*, 67–82, 1972.

Sato, A., and G. Wakahama, Plastic waves in snow, *Low Temp. Sci., Ser. A, 34*, 59–69, 1976.

Savage, S. B., Gravity flow of cohesionless granular materials in chutes and channels, *J. Fluid Mech., 92*(1), 53–96, 1979.

Schaerer, P., Compaction or removal of wet snow by traffic, *Spec. Rep. 115*, Highway Res. Board, Washington, D. C., 1970.

Schaerer, P. A., Observations of avalanche impact pressure, in *Proceedings of the Symposium on Advances in North American Avalanche Technology*, pp. 51–54, Rocky Mountain Forest and Range Experiment Station, U.S. Department of Agriculture, Fort Collins, Colo., 1973.

Schaerer, P. A., Friction coefficients and speed of flowing avalanches, *IAHS AISH Publ., 114*, 425–432, 1975.

Schaerer, P. A., and A. A. Salway, Seismic and impact-pressure monitoring of flowing avalanches, *J. Glaciol., 26*(94), 139–188, 1980.

Seligman, G., and F. Debenham, Friction of snow surfaces, *Polar Rec., 4*(25), 2–11, 1943.

Shen, H. W., and A. T. Roper, Dynamics of snow avalanches (with estimation for force on a bridge), *Bull. IAHS, 15*(1), 7–26, 1970.

Shimbo, M., Friction on snow of ski soles, unwaxed and waxed, in

Scientific Study of Skiing in Japan, pp. 99–112, Hitachi, Tokyo, 1971.

Shimizu, H., et al., Study of high-speed avalanches in Kurobe canyon, II (in Japanese), *Low Temp. Sci., Ser. A, 31*, 179–89, 1973.

Shimizu, H., et al., Study of high-speed avalanches in Kurobe canyon IV (in Japanese), *Low Temp. Sci., Ser. A., 33*, 109–116, 1975.

Shimizu, H., et al., Study of high-speed avalanches in Kurobe canyon, (in Japanese) *Low Temp. Sci., Ser. A., 35*, 117–132, 1977.

Shimizu, H., et al., A study on high-speed avalanches in the Kurobe canyon Japan, *J. Glaciol., 26*(94), 141–152, 1980.

Shoda, M., An experimental study on dynamics of avalanches snow, *IAHS AISH Publ., 69*, 215–229, 1966.

Skinrood, A. C., The effect of snow properties on vehicle trafficability in the Arctic, *Spec. Rep. 22*, Corps of Eng., U.S. Army Snow, Ice and Permafrost Res. Estab., Hanover, N. H., 1957.

Smith, R., and D. Clough, Effectiveness of tires under winter driving conditions, in *Proceedings of the 51st Annual Meeting, January 17-21*, Highway Research Board Washington, D. C., 1972.

Sommerhalder, E., Ablenkverbau, in *Lawinenschutz in der Schweiz—Bündnerwald*, Beih. 9, pp. 155–169, Genossenschaft der bündnerischen Holzproduzenten, 1972. (English translation, Avalanche Protection in Switzerland, *Gen. Tech. Rep. Rm-9*, U.S. Dep. of Agric., For. Serv., Washington, D. C., 1975.

Taylor, A., Snow compaction, report, Dir. of Eng. Dev., Can. Army Headquarters, Ottawa, Ont., 1952.

Thomson, J. G., The performance of tracked and wheeled vehicles in snow, Interservice Vehicle Mobility Symposium, Papers, vol. II, Land Locomotion Res. Lab., Detroit Arsenal, Detroit, Mich., 1955.

Thomson, J. G., A study of some factors influencing vehicle mobility in snow, report, Def. Res. Board, Ottawa, Ont., 1957.

Tochon-Danguy, J. C., and E. J. Hopfinger, Simulation of the dynamics of powder avalanches, *IAHS AISH Publ., 114*, 369–380, 1975.

Torgersen, L., Internal reports, summary, Astra-Wallco Corp., Skarer, Norway, 1979.

Tusima, K., Tests of the repeated loadings on snow, *Low Temp. Sci., Ser. A, 31*, 58–68, 1973.

Tusima, K., The temperature dependence of hardness of snow, *IAHS AISH Publ., 114*, 103–109, 1975.

Tusima, K., Friction of a steel ball on a single crystal of ice, *J. Glaciol., 19* (81), 225–235, 1977.

University of Minnesota, Review of the properties of snow and ice, *Rep. 4*, U.S. Army Snow, Ice and Permafrost Res. Estab., Hanover, N. H., 1951.

University of Minnesota, Friction on snow and ice, *Rep. 17*, U.S. Army Snow, Ice and Permafrost Res. Estab., Hanover, N. H., 1955.

Van Wijk, M. C., Photogrammetry applied to avalanche studies, *J. Glaciol., 6*(48), 917–933, 1967.

Voellmy, A., Uber die Zerstörungskraft von Lawinen, *Schweiz. Bauztg., 73*, 159–162, 212–217, 280–285, 1955. (English translation, On the destructive force of avalanches, *Transl. 2*, U.S. Dep. of Agric., For. Serv., Alta Avalanche Study Center, Wasatch Natl. For., Salt Lake City, Utah, 1964.)

Wakahama, G., and A. Sato, Propagation of a plastic wave in snow, *J. Glaciol., 19*(81), 175–184, 1977.

Wehner, B., Special observations on the resistance to sliding on snow covered or icy road surfaces, *Rev. Gen. Caoutch., 36*, 1959.

Weiss, S., W. Harrison, L. Abarca, and M. Bekker, Preliminary study of snow values related to vehicle performance, *Rep. 2*, Land Locomotion Res. Lab., Detroit Arsenal, Detroit, Mich., 1956.

Yokomore, M., Stability of motocycles on packed snow—with special reference to characteristics of tired wheels, *J. Jpn. Soc. Snow Ice, 37*(1), 21–31, 1975.

Yong, R. N., Analytical predictive performance for physical performance of mobility, *J. Terramechanics, 10*, 47–60, 1973.

Yong, R. N., and M. Fukue, Performance of snow in confined compression, *J. Terramechanics, 14*(2), 59–82, 1977.

Yong, R. N., and M. Fukue, Snow mechanics: Machine-snow interaction, paper presented at Second International Symposium on Snow Removal and Ice Control Research, U.S. Army Cold Reg. Res. and Eng. Lab., Hanover, N. H., 1978.

Yong, R. N., and W. L. Harrison, Snow trafficability—The knowledge gap, in *Symposium—ECONO-MOBILITY*, Canadian Society for Terrain-Vehicle Systems, Toronto, Ont., 1978.

Yong, R. N., and T. Muro, Plate loading and vane cone test measurements for fresh and sintered snow, *Soil Mech. Ser. 43*, McGill Univ., Geotech. Res. Center, Montreal, Que., 1980.

Yosida, Z., Theoretical studies on snow removal by a plough, I, Flow type kickup of snow caused by a plough moving at high speeds, *Low Temp. Sci., Ser. A, 32*, 39–53, 1974a.

Yosida, Z., Theoretical studies on snow removal by a plough, II, Spray type kickup of snow caused by a plough moving at high speeds, *Low Temp. Sci., Ser. A, 32*, 55–70, 1974b.

Yosida, Z., Theoretical studies on snow removal by a plough, III, Flow type kickup of snow caused by a plough moving at low speeds, *Low Temp. Sci., Ser. A, 33*, 39–55, 1975a.

Yosida, Z., Theoretical studies on snow removal by a plough, IV, Spray type kickup of snow caused by a plough moving at low speeds, *Low Temp. Sci., Ser. A, 33*, 57–73, 1975b.

Yosida, Z., Theoretical studies on snow removal by a plough, V, Kickup of snow caused by an acute angled plough, *Low Temp. Sci., Ser. A, 33*, 75–90, 1975c.

Properties of Blowing Snow

R. A. SCHMIDT

Rocky Mountain Forest and Range Experiment Station, USDA Forest Service, Fort Collins, Colorado 80526

The size and shape of windblown snow particles determine not only the mass transported by turbulent fluxes but also the rate of phase change from ice to water vapor that occurs in this multiphase flow. These properties and particle densities dictate particle fall velocity and therefore the vertical distribution of mass and surface area, which strongly influence the gradients and fluxes of sensible heat and water vapor within the transport layer. Initial movement at the snow surface depends more on availability and impact forces of loose particles than on aerodynamic drag. Cohesion between surface particles and particle restitution coefficient are important properties that determine threshold wind speeds for snow transport. Threshold speeds for blowing snow vary over such a large range in nature that formulations predicting transport rate as a function of wind speed should include threshold speed as a parameter. The expression derived by Iversen et al. (1975) is compared with low-level snow transport in the atmospheric boundary layer. Self-similarity of wind profiles in blowing snow is a property of the flow that has been exploited for scale modeling of snow deposition around obstacles, both outdoors and in wind tunnels. Good quantitative results are obtained by careful attention to similitude requirements.

This review of snow and flow properties in blizzards follows the detailed comparison by *Radok* [1977] of theory developed in the Russian and English literature. Before that, reviews by *Mellor* [1965, 1970] summarized measurements and theoretical developments very well, and *Male* [1980] provides quite a comprehensive look at our knowledge of blowing snow. In this review the phenomenon is considered as turbulent flow of a multiphase, incompressible fluid, so that in addition to properties of the snow particles, properties of the fluid and flow are also considered. Emphasis on flow over plane boundaries reflects the scarcity of recent studies on snow transport around obstacles.

BLOWING SNOW IS MULTIPHASE FLOW

Snow, the solid, and air, the fluid, make snow transport at least two phase, but during transport the solid also undergoes a phase change to vapor, and this is an important part of the process. Sublimation during transport was recognized by *Dyunin* [1959, 1967] and included in his transport equations. Temperature, humidity, and radiation are most important in determining the rate of phase change [*Schmidt*, 1972], but it is the vast particle surface area exposed during drifting that makes the process hydrologically momentous.

Over a horizontal surface, concentration of the solid phase is greatest at the surface, giving a bulk density of the mixture that is approximately twice the density of the air alone. A strong hydrostatic pressure gradient near the surface can be deduced from the interesting experiments of *Maeno and Nishimura* [1979] on fluidized snow. Drift particles are more rounded and much smaller than the original precipitation crystals, ranging from 20 to 500 μm in diameter, and size distributions measured at any height show slight positive skew. Mean diameters decrease with height and increase with increasing wind speed. These results are well documented by measurements at Byrd Station, Antarctica [*Budd et al.*, 1966], and by *Budd*'s [1966] analysis of those data. In transport over a frozen lake in southeastern Wyoming, *Schmidt* [1981] verified that the two-parameter gamma function fit size distributions in saltation, but *Budd*'s [1966]

relationship between size, wind speed, and height underestimated mean diameters.

Takeuchi [1980] describes an experiment on the growth of snow transport downwind from a boundary (a river which trapped snow from further upwind). The increase in mass flux with distance supports *Dyunin*'s [1967] observation of growth at a decreasing rate until oscillation occurs around some steady state transport rate. Dyunin gives distances required for full development of transport in the range from 200 to 500 m and more, depending on the state of snow cover surface. Takeuchi estimates 350 m from his measurements on snow-covered level terrain downwind of the Ishikari River in Hokkaido. At many locations in the mountains, it appears that snow transport by wind may not approach saturation rates because catchments are too closely spaced. Growth of transport should be predictable from the distribution of bond strengths of exposed surface particles and the probability that an exposed particle will be struck by a saltating grain. *Gessler* [1970] used a similar approach to predict hydraulic stability of channels from the distribution of surface particle sizes and the probability of fluid forces lifting surface particles. *Maeno et al.* [1979] also suggest a statistical approach to predicting the onset of blowing snow.

S. Kobayashi [1979] measured the wind turbulence in blowing snow with a sonic anemometer. The scale of turbulence determined from autocorrelation of longitudinal wind speed decreased in blowing snow. This scale corresponds to the horizontal dimension of the 'largest turbulons' and is approximately equivalent to the integral scale of turbulence. Spacing of snow waves corresponded closely to this scale. Perhaps more important is the slope of the autocorrelation coefficient with lag time. S. Kobayashi's measurements at Sapporo in 1969 with the sonic anemometer at heights below 1 m show large differences between drifting and nondrifting conditions. It appears that mechanical production of turbulence is greater with drifting. However, because the differences are over a range of lag times from 0.5 to 5 s, the increase in mechanical turbulence production is not associated directly with eddy shedding by individual particles but is more in the time scale of clouds or bursts of particles.

Measured vertical fluxes of heat and water vapor over snow surfaces without blowing snow show that turbulent

exchange coefficients for water vapor are less than exchange coefficients for sensible heat [*Male and Granger*, 1979]. If blowing snow occurs with sublimation, sensible heat transfer is usually directed toward the surface, while water vapor flux is away from the surface. The signs of the two gradients are therefore opposite, a condition which *Warhaft* [1976] concludes will produce a difference between eddy conductivity and eddy diffusivity for water vapor. It seems unlikely that the Monin-Obukhov similarity hypothesis would describe vertical profiles of temperature and humidity in the atmospheric surface layer with blowing snow, because it was not developed to account for multiphase flow.

The hypothesis that eddy diffusivity of snow K_s equals eddy viscosity K_m is of fundamental importance in the diffusion model of snow transport [*Radok*, 1977]. *Sommerfeld and Businger* [1965] question the hypothesis $K_s/K_m = 1$, but as *Radok* [1968] points out, their results depend on particle fall velocities (1.0–1.7 m/s) that are large in comparison to settling speeds for the particle sizes measured in the Antarctic. If we assume ice spheres and apply results for low Reynolds numbers [*Beard and Pruppacher*, 1969], the size corresponding to the fall velocity range 1.0–1.7 m/s is large in comparison to reported size distributions summarized by *Mellor* [1965]. *Businger* [1965] has also questioned the use of still-air settling velocities to test the hypothesis $K_s/K_m = 1$. Further consideration of the hypothesis $K_s/K_m = 1$ is in order in view of the above questions. An experiment that measured still-air settling velocities of individual particles sampled from drifting, and recorded their size, would determine particle density, which is assumed equal to that of ice but has not been measured. Direct measurement of vertical snow flux by eddy correlation, using a sonic anemometer and snow particle counter [*Schmidt*, 1977], would give another test of the hypothesis.

Dyunin [1967] observed periodic fluctuations in snow transport along an aerodynamic canal once saturated drifting rates were achieved. He suggested this as the origin of surface features such as dunes. This agrees with *Radok*'s [1968] argument that erosion and deposition are reflected by differences in vertical profiles of drift flux. The concept of a fully developed oscillating transport rate is strongly supported by *S. Kobayashi*'s [1979, p. 40] measured cospectrum of turbulent shear. During snow wave formation he noted that a remarkable peak is seen at the frequency of 0.07 Hz, but this peak disappeared as the wave-forming action weakened. *White and Schulz* [1977, p. 502] also noted an oscillation in wind tunnel saltation. *Maeno and Nishimura* [1977, p. 502] also noted an oscillation in wind tunnel saltation. *Maeno and Nishimura* [1978] recorded oscillations in pressure difference across fluidized snow, which may or may not be related to observations in horizontal transport, but *Dyunin* [1967, Figure 3] showed that changes in transport rate were associated with fluctuations of the quasi-static pressures in the boundary layer.

MEAN VELOCITY PROFILE DEPENDS ON DRIFT DENSITY

Several factors limit the region of flow in which the vertical profile of average velocity can be adequately described by the familiar logarithmic equation. Thermal stratification in the atmospheric surface layer, saltation, and nonuniform terrain all change the shape of the wind profile, yet this equation still provides the basis for descriptions of flow velocity.

Deviation from neutral atmospheric stability usually causes the difference between flow velocity and the logarithmic prediction to increase with height above the level of 2 m or so. Although the strong wind speeds associated with blowing snow increase turbulent mixing and tend to establish neutral stratification, sublimation and katabatic conditions require stable temperature gradients. Flow velocity profiles in light to moderate drifting snow do show deviations associated with stable stratification [*Shiotani and Arai*, 1967, Figure 3; *Lister*, 1960, Figure 14].

Saltation, on the other hand, creates deviations from the logarithmic wind profile in the region below 10 cm. These deviations increase approaching the snow surface [*S. Kobayashi*, 1969; *Maeno et al.*, 1979], and velocity vanishes at some depth below the surface [*Ôura et al.*, 1967]. *Bagnold* [1941] derived an expression for the velocity profile based on observations that profiles in saltation flow of sand in a wind tunnel pass through a 'focus' near the surface. The velocity at this focus is related to the velocity at the threshold of particle entrainment. A recent extension of this argument is presented by *White and Schulz* [1977]. Dyunin's measurements in saltation flow of snow in an aerodynamic canal lead him to accept Bagnold's velocity profile equation [*Dyunin*, 1967].

It appears that the log-linear wind profile [*Lumley and Panofsky*, 1964] may be combined with the saltation profile to give a description that will apply over horizontal or uniformly sloping terrain up to heights of several meters, in a wider range of thermal stability. Irregular terrain demands greater modification of the profile equations to account for streamwise pressure gradients [*Schmidt*, 1967]. Recent profiles in blowing snow at a ridge crest [*Föhn*, 1980] show velocity maxima at heights around 1 m. *S. Kobayashi* [1979] reports drift density profiles, and turbulence near an obstruction, where flow velocity profiles are much more complex than over plane horizontal surfaces.

COHESION DETERMINES THRESHOLD WIND SPEEDS

From experiments with sand in a wind tunnel, *Bagnold* [1941] concluded that the 'impact threshold' wind speed for particle movement when particles were injected into the flow was consistently lower than the 'fluid threshold' speed required to remove particles from the surface by aerodynamic forces. *S. Kobayashi* [1979] suggests that 'the ejection of snow particles from the snow surface by wind action may hardly occur in nature, (i.e., the generation of drifting snow in nature is explained by the mechanical impingement of a snow particle saltating on the snow surface).' He based this on the large discrepancy between measured threshold shear stresses for snow movement in the wind tunnel and over a natural snow surface. Comparison of calculated aerodynamic forces and forces of elastic impact with those required to overcome bonds on exposed surface particles leads to the same conclusion [*Schmidt*, 1980].

Precipitating snow, intercepted snow on vegetation, and hoar frost on a snow surface are sources of particles which, when injected into the wind stream, provide the impact to erode a snow surface otherwise stable in all but extremely strong winds. *Mellor* [1965] has suggested that defining threshold wind speed as the maximum speed at which particle motion ceases might provide a cleaner determination of this value.

Cohesive forces holding exposed particles to the surface include electrostatic forces, surface tension, and ice bonds. Even when particles are already in motion, cohesive forces must be overcome if the particle rebounds from the surface. The rate of bond growth is initially rapid, so that any 'rest period' between saltation jumps produces a significant increase in cohesion. Thus the 'lulls' of minima in horizontal wind speed may be as important as the gusts in determining the threshold wind speed, if the snow surface is being 'work hardened' at wind speeds only slightly above threshold values. *Yamada and Ôura* [1968] conclude, from their measurements of cohesion between ice spheres and an ice plate, that the 'liquid-like' layer theory explains initial cohesion and that sintering accounts for increasing bond strength with time after contact. As temperatures approach the melting point, cohesion increases, and threshold speeds increase [*Ôura et al.*, 1967]. The effect of humidity on cohesion has not been reported except at the extremes [*Hosler et al.*, 1957]. The restitution coefficients of an ice sphere rebounding from impact with a plane ice surface is in the range 0.8–0.9 if care is taken to avoid impurities in the ice [*Araoka and Maeno*, 1978]. Loss of kinetic energy during collision was larger if sodium chloride was added as an impurity. From calculations based on these experiments, plastic deformation is more effective in reducing kinetic energy than both crack formation and adhesion.

The impact velocity of a saltating particle is determined primarily by maximum trajectory height and mean flow velocity, since it is fluid drag that accelerates the particle in the direction of flow, and flow velocity increases rapidly with height, near the surface. *Kikuchi* [1981] has demonstrated that average horizontal acceleration of snow particles saltating in a wind tunnel is independent of trajectory height, however. *White and Schulz* [1977] show that saltation trajectories are higher than those predicted by equations of motion that included only drag forces. When additional lift forces created by particle spin (the Magnus effect) were included, theoretical trajectories were much closer to those measured. Snow saltation trajectory photographs presented by *D. Kobayashi* [1972] show periodic changes in brightness of the particle image that are similar to those described by White and Schulz and which they used to estimate particle spin rates.

THRESHOLD WIND SPEEDS DETERMINE TRANSPORT RATE

To simulate erosion around craters on Mars, *Iversen et al.* [1975] modified an equation derived by *Bagnold* [1941] for momentum loss during saltation of sand in air. If q_s denotes mass flow in saltation, with dimensions of mass per unit length across the flow, per unit time, for transport without obstructions, *Iversen* [1980] has suggested $q_s \sim (\rho u_*^2/g)(u_* - u_{*t})$. Friction velocity u_* is defined by $u_*^2 = \tau/\rho$, where τ is shear stress and ρ is fluid density. Gravitational acceleration is g, and u_{*t} denotes the threshold value of friction velocity, the highest value at which no particle motion occurs.

Iversen et al. [1975] argued that the proportionality factor relating saltation transport rate to the difference $(u_* - u_{*t})$ might also be a function of the ratio u_f/u_{*t}, where u_f is the particle terminal fall velocity. The equation

$$q_s = C(\rho/g)(u_f/u_{*t})u_*^2(u_* - u_{*t}) \qquad (1)$$

was the basis of a dimensionless erosion rate parameter that correlated wind tunnel data very effectively. Several other investigators have derived somewhat different forms of (1) [*Iversen et al.*, 1976].

The ratio u_f/u_{*t} is considered constant in wind tunnel experiments with particles of essentially uniform size. For snow, threshold friction velocity depends on age, temperature, and strength of the surface, and fall velocity u_f must represent a distribution of particle sizes. *Bagnold* [1966], in considering sediment transport, points out that because u_f is not a linear function of particle size, the fall velocity of the average-sized particle may not be substituted for u_f in general. Rather, the mean fall velocity must be computed from the integration of the size distribution. *Budd* [1966], however, assumes a linear relationship between diameter and fall velocity for blowing snow. The errors involved have been computed by *Lee* [1975].

To explore the usefulness of (1) in correlating snow transport rates in the atmospheric boundary layer, friction velocity can be expressed in terms of mean wind speed by using the logarithmic profile $U = (u_*/k) \ln z/z_0$. The roughness parameter z_0 is approximately proportional to u_*^2 in saltation transport [*Owen*, 1964; *Radok*, 1968; *Tabler*, 1980]. Therefore mean wind speed U at height z is not a linear function of friction velocity under these conditions. If U_t is the maximum wind speed at height z for which motion of particles does not occur, then $U_t = (u_{*t}/k) \ln z/z_{0t}$, where z_{0t} is less than z_0 during transport. Measured values in blowing snow on a frozen lake with snow cover greater than 75% show an order of magnitude increase in z_0 as u_* increases from 0.25 to 1.0 m/s [*Tabler*, 1980]. Using this result, (1) was evaluated in terms of velocities at 1 m to compare with measurements by several workers (Figure 1).

The striking point of Figure 1 is that the envelope of the data points is obtained without introducing a proportionality constant different from unity ($C = 1.0$). The value $U_f = 0.75$ m/s assumed for particle fall velocity corresponds to the settling velocity in still air of an ice sphere 220 μm in diameter (atmospheric pressure, 1000 mbar; temperature, $-10°C$). Since (1) applies to saltation transport, U_f was chosen to represent sizes near the surface. The relationship is relatively insensitive to U_f. To those whose field experience includes threshold friction velocity determinations, values of $u_{*t} = 0.1$ m/s (corresponding to 1 m wind speeds near 3 m/s) may seem a bit on the low side. However, part of this apparent underestimation of q_s may correspond to the definition of u_{*t} as the maximum occurring without particle motion. Values at which motion just begins are more often recorded in the field and would be somewhat higher than values given by the present definition. Since Sapporo is just above sea level, while Mizuho Camp is at 2230 m, assuming air density $\rho = 10^{-3}$ g/cm^3 more closely approximates Antarctic conditions. Stricter evaluation of (1) for these and other data, including Byrd Station measurements [*Budd et al.*, 1966], should be fruitful.

RIDGE CRESTS COMPLICATE VERTICAL DRIFT FLUX PROFILES

In the mountains, transport is complicated by terrain interactions. Distances between drift barriers are usually much shorter than on the plains, so that sublation has a shorter time to produce water vapor from the drifting particles. Although total winter precipitation is usually greater in the mountains, snow cover is completely eroded from windward ridge faces in some regions. Predicting transport
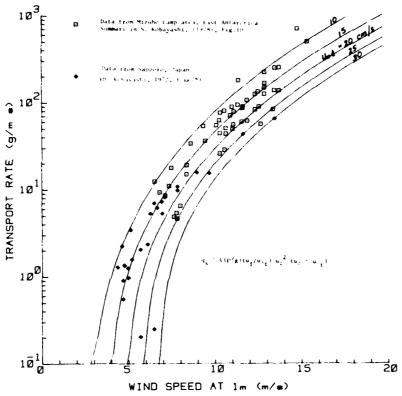
Fig. 1.   Comparison of blowing snow transport rate measured by drift traps, with prediction by *Iversen et al* [1975] assuming $\rho = 10^{-3}$ g/cm^3, $U_f = 75$ cm/s, and $C = 1.0$. The velocity at 1 m was computed from $U_1 = (u_*/k) \ln (100/z_0)$, based on *Tabler's* [1980] empirical result $z_0 = 1.35 \cdot 10^{-5} u_*^2$.

rate and both the amount and the distribution of deposition on lee ridge faces is part of the problem of predicting snow avalanches.

Föhn [1980] measured drift flux and wind speed profiles that show maxima of both at distances near 1 m above the crest of a sharp ridge. This is very significant for the location of deposition on the lee face and raises questions about the mechanism that lifts the drift flux. Roughness of the windward face may contribute.

Dyunin and Kotlyakov [1980] emphasize the convergence of precipitation flux in 'upper' snowstorm transport over mountain ridges. They demonstrate that during snowfall this contribution to total transport is much larger than deflation drift, in all but extremely strong winds (>50 m/s), and also note the general lack of saturated deflation transport rates, caused by limited distances between catchments.

OPTICAL PROPERTIES DETERMINE VISIBILITY IN BLIZZARDS

Mellor [1970] included the important aspects of visibility in blowing snow in his review. Particle sizes in blowing snow are large enough that Mie scattering can be ignored. Back-scattering of light by a snow particle is proportional to its projected area, so that attenuation in blowing snow is a direct function of the square of particle size and the number of particles per unit volume along the sight path. Recent work has applied the law of geometric optics to electronical-ly monitor visibility in blowing snow [*Schmidt*, 1977, 1979] and provide this information for traffic control on an inter-

state highway [*Tabler*, 1979]. This reviewer is not aware of any determination of albedo or emissivity of individual snow particles in transport. Such information is required to study the distribution of radiation within blowing snow.

NEW APPROACHES IMPROVE RESULTS FROM SMALL-SCALE MODELS

Because of the complex interactions between drifting snow and obstacles, small-scale models continue to be a very useful method in solving engineering problems of drift control. The laws of flow similitude have been reexamined [*Kind*, 1976], and new parameters tested [*Iversen*, 1980]. *Tabler and Jairell* [1981] simulated drifts around snow fences, buildings, highway guard rails, and terrain irregular-ities with scale models exposed to low-level drifting on a frozen lake, using the flow property that velocity profiles scale automatically in saltation flows [*Radok*, 1968; *Tabler*, 1980].

Iversen [1981] derives two modeling parameters that cor-relate wind tunnel results better than Froude number and other scaling parameters used previously. The transport rate parameter $(\rho U^2 / 2 \rho_p g H)(1 - U_0/U)$, derived from (1), is made equivalent in model and prototype. Here U is the free-stream tunnel velocity, and U_0 is the value of U at the threshold of transport.

An equivalent roughness parameter that reflects the influ-ence of saltation trajectory height on the flow velocity profile is derived from *Owen's* [1964] assumption that $z_0 \sim u_*^2/g$. *Iversen* [1981] writes this requirement for similitude as

equality between model and prototype of the parameter $\rho u_*^2/(\rho_p g H)$, where H is a characteristic reference height, such as the height of a fence, and the parameter includes the fluid to particle density ratio ρ/ρ_p.

Small glass spheres (49 μm average diameter) develop electrostatic charge during transport in the wind tunnel, which allows *Iversen* [1980] to simulate the cohesion of snow that produces cornices at some stages of deposition. He scales time by the transport rate parameter so that $\bar{t} = (\rho U^2/2\rho_p g H)(1 - U_t/U)(U_t/L)$, where t is time since the beginning of drift, L is a reference length which is scaled in model and prototype, and $\bar{t}$ is the dimensionless 'time.'

THESE EXPERIMENTS WOULD EXTEND OUR KNOWLEDGE

Most of the engineering problems we face in the prediction and control of blowing snow are in climates and regions other than polar. Therefore we are forced to take account of a wide and variable range of threshold speeds in equations that express transport rate as a function of wind speed. In many problems, fetch distances are too short to produce fully developed multiphase flow, so that useful engineering equations must also take account of the degree of drift development. To meet these requirements, more complete information on the relation of threshold wind speed to surface strength is required, including the effects of time, temperature, humidity, and radiation on bonding of the surface particle most exposed to saltation impacts. A theoretical model of growth of saltation transport would speed the design of these experiments.

Equations based on momentum transfer at the surface, such as (1), are useful when most of the transport is in saltation, but this must be considered analogous to 'bed load' in sediment transport by water. Attention to the problem of combining momentum and diffusion arguments is needed. The result should be a more general transport equation, without the need to specify a reference drift density that is presently required in the 'diffusion model'. Experiments using the sonic anemometers and snow particle counter will provide tests of improved theory. The first experiment should determine the ratio K_s/K_m under conditions where flow is saturated and vertical profiles of temperature, humidity, and wind speed are measured. If the result is definitely different from unity, the dependence of the ratio on other factors, such as stability, must be determined.

Radok [1977] noted the lack of progress in exploring the electrostatic effects in blowing snow. Forces developed from these charges must be included in calculations of cohesive forces. Experiments to quantify the electrostatic forces as a function of the several factors that determine their generation in blowing snow must be conducted in concert with the efforts on surface strength and threshold speeds.

Because of the application to loading of avalanches, wind erosion of snow on ski trails, and maintenance of mountain highways, systematic experiments to determine the mechanism that lifts drift flux to produce maxima above ridge crests must continue. The effects of crest geometry and surface roughness on height of drift flux maxima need to be defined.

REFERENCES

Araoka, K., and N. Maeno, Measurements of restitution coefficients of ice (in Japanese, English summary), *Contrib. Inst. Low Temp. Sci. Hokkaido Univ.*, Ser. A, no. 36, 55–65, 1978.

Bagnold, R. A., *The Physics of Blown Sand and Desert Dunes*, 265 pp., Methuen, London, 1941.

Bagnold, R. A., An approach to the sediment transport problem from general physics, *U.S. Geol. Surv. Prof. Pap.*, 422-I, 37, 1966.

Beard, K., and H. Pruppacher, A determination of the terminal velocity and drag of small water drops by means of a wind tunnel, *J. Atmos. Sci.*, 26, 1066–1072, 1969.

Budd, W. F., The drifting of non-uniform snow particles, in *Studies in Antarctic Meteorology, Antarctic Res. Ser.*, vol. 9, edited by M. Rubin, pp. 59–70, AGU, Washington, D. C., 1966.

Budd, W. F., R. Dingle, and U. Radok, The Byrd snow drift project: Outline and basic results, in *Studies in Antarctic Meteorology, Antarctic Res., Ser.*, vol. 9, edited by M. Rubin, pp. 71–134, AGU, Washington, D. C. 1966.

Businger, J., Eddy diffusion and settling speed in blown snow, *J. Geophys. Res.*, 70(14), 3307–3313, 1965.

Dyunin, A. K., Fundamentals of the theory of snowdrifting (in Russian), *Izv. Sib. Otd. Akad. Nauk SSSR*, no. 12, 11–24, 1959. (English translation by G. Belkov, *NRC-TT 952*, Natl. Res. Counc. of Can., Ottawa, Ont., 1961.)

Dyunin, A. K., Fundamentals of the mechanics of snow storms, in *Physics of Snow and Ice*, vol. 1, part 2, edited by H. Ôura, pp. 1065–1073, Institute of Low Temperature Science, Hokkaido University, Sapporo, Japan, 1967.

Dyunin, A. K., and V. M. Kotlyakov, Redistribution of snow in the mountains under the effect of heavy snow-storms, *Cold Reg. Sci. Technol.*, 3, 287–297, 1980.

Föhn, P., Snow transport over mountain crests, *J. Glaciol.*, 26(94), 469–480, 1980.

Gessler, J., Self-stabilizing tendencies of alluvial channels, *J. Waterways Harbors Div. Am. Soc. Civ. Eng.*, 96(WW2), 235–249, 1970.

Hosler, C. D., Jensen, and L. Goldshlak, On the aggregation of ice crystals to form snow, *J. Meteorol.*, 14, 415–420, 1957.

Iversen, J., Drifting-snow similitude—transport rate and roughness modeling, *J. Glaciol.*, 26(94), 393–403, 1980.

Iversen, J., Wind tunnel modeling of snow fences and natural snow fence controls, *Proc. 1980 East. Snow Conf.*, 106–124, 1981.

Iversen, J., R. Greeley, B. White, and J. Pollack, Eolian erosion of the Martian surface, 1, Erosion rate similitude, *Icarus*, 26, 321–331, 1975.

Iversen, J., R. Greeley, B. White, and J. Pollack, The effects of vertical distortion in the modeling of sedimentation phenomena: Martian crater wake streaks, *J. Geophys. Res.*, 81(26), 4846–4856, 1976.

Kikuchi, T., A wind tunnel study of the aerodynamic roughness associated with drifting snow, *Cold Reg. Sci. Technol.*, in press, 1981.

Kind, R., A critical examination of the requirements for model simulation of wind-induced erosion/deposition phenomena such as snow drifting, *Atmos. Environ.*, 10(3), 219–227, 1976.

Kobayashi, D., Studies of snow transport in low-level drifting snow, *Contrib. Inst. Low Temp. Sci. Hokkaido Univ.*, Ser. A, no. 24, 1–58, 1972.

Kobayashi, S., Measurements of the wind drag force of the snow surface (in Japanese, English summary), *Contrib. Inst. Low Temp. Sci. Hokkaido Univ.*, Ser. A, no. 27, 87–97, 1969.

Kobayashi, S., Snow transport by katabatic winds in Mizuho Camp area, East Antarctica, *J. Meteorol. Soc. Jpn.*, 56(2), 130–139, 1978.

Kobayashi, S., Studies on interaction between wind and dry snow surface, *Contrib. Inst. Low Temp. Sci. Hokkaido Univ.*, Ser. A, no. 29, 1–64, 1979.

Lee, L. W., Sublimation of snow in a turbulent atmosphere, Ph. D. dissertation, Univ. of Wyo., Laramie, 1975.

Lister, H., Solid precipitation and drift snow, *British TransAntarctic Expedition, 1955–1958, Sci. Rep. 5, Glaciol. 1*, 51 pp., 1960.

Lumley, J., and H. Panofsky, *The Structure of Atmospheric Turbulence*, 239 pp., Interscience, New York, 1964.

Maeno, N., and K. Nishimura, Studies of fluidized snow, 1, Formation of fluidized snow and its general properties (in Japanese,

English summary), *Contrib. Inst. Low Temp. Sci. Hokkaido Univ., Ser. A*, no. 36, 77–92, 1978.

Maeno, N., and K. Nishimura, Fluidization of snow, *Cold Reg. Sci. Technol., 1*, 109–120, 1979.

Maeno, N., K. Araoka, K. Nishimura, and Y. Kaneda, Physical aspects of the wind-snow interaction in blowing snow, *J. Fac. Sci. Hokkaido Univ., Ser. 8*, 6(1), 127–141, 1979.

Male, D., The seasonal snowcover, in *Dynamics of Snow and Ice Masses*, edited by S. Colbeck, pp 305–395, Academic, New York, 1980.

Male, D., and R. Granger, Energy mass fluxes at the snow surface in a prairie environment, in *Modeling of Snowcover Runoff*, edited by S. Colbeck and M. Ray, pp. 101–124, U.S. Army Cold Regions Research and Engineering Laboratory, Hanover, N. H., 1979.

Mellor, M., *Blowing Snow, U.S.A. CRREL Monogr.*, part 3, section A3c, 79 pp., U.S. Army Cold Regions Research and Engineering Laboratory, Hanover, N. H., 1965.

Mellor, M., A brief review of snowdrifting research, Snow Removal and Ice Control Research, *Spec. Rep.* 115, pp. 196–209, U. S. Army Cold. Reg. Res. and Eng. Lab., Hanover, N. H., 1970.

Óura, H., T. Ishida, D. Kobayashi, S. Kobayashi, and T. Yamada, Studies on blowing snow, II, in *Physics of Snow and Ice*, vol. I., part 2, edited by H. Óura, pp. 1099–1117, Institute of Low Temperature Science, Hokkaido University, Sapporo, Japan, 1967.

Owen, P., Saltation of uniform grains in air, *J. Fluid Mech., 20*, 225–242, 1964.

Radok, U., Deposition and erosion of snow by the wind, *Res. Rep. 230*, 23 pp., U.S. Army Cold Reg. Res. and Eng. Lab., Hanover, N. H., 1968.

Radok, U., Snow drift, *J. Glaciol., 19*(81), 123–129, 1977.

Schmidt, R., Wind flow over two alpine ridges, Ph.D dissertation, Colo. State Univ., Fort Collins, 1967.

Schmidt, R., Sublimation of wind-transported snow—A model, *U.S. For. Serv. Rocky Mt. For. Range Exp. Stn. Res. Pap., RM-90*, 24 pp., 1972.

Schmidt, R., A system that measures blowing snow, *U.S. For. Serv. Rocky Mt. For. Range Exp. Stn. Res. Pap., RM-194*, 80 pp., 1977.

Schmidt, R., Measuring visibility in blowing snow, Snow Removal and Ice Control Research, *Spec. Rep. 185*, pp. 200–207, Transp. Res. Board, Natl. Acad. of Sci., Washington, D. C., 1979.

Schmidt, R., Threshold windspeeds and elastic impact in snow transport, *J. Glaciol., 26*(94), 453–467, 1980.

Schmidt, R., Estimating threshold windspeeds from particle sizes in blowing snow, *Cold Reg. Sci. Technol., 4*, 187–193, 1981.

Shiotani, M., and H. Arai, On the vertical distribution of blowing snow, in *Physics of Snow and Ice*, vol 1, part 2, edited by H. Óura, pp. 1075–1083, Institute of Low Temperature Science, Hokkaido University, Sapporo, Japan, 1967.

Sommerfeld, R., and J. Businger, The density profile of blown snow, *J. Geophys. Res., 70*(14), 3303–3306, 1965.

Tabler, R., Visibility in blowing snow and applications in traffic operations, Snow Removal and Ice Control Research, *Spec. Rep. 185*, pp. 208–214, Transp. Res. Board, Natl. Acad. of Sci., Washington, D. C., 1979.

Tabler, R., Self-similarity of wind profiles in blowing snow allows outdoor modeling, *J. Glaciol., 26*(94), 421–433, 1980.

Tabler, R., and R. Jairell, Studying snowdrifting problems with small-scale models outdoors, *Proc. 1980 West. Snow Conf., 48*, 1–13, 1981.

Takeuchi, M., Vertical profiles and horizontal increase of drift snow transport, *J. Glaciol., 26*(94), 481–492, 1980.

Warhaft, Z., Heat and moisture flux in the stratified boundary layer, *Q. J. R. Meteorol. Soc., 102*(433), 703–707, 1976.

White, B., and J. Schulz, Magnus effect in saltation, *J. Fluid Mech., 81*(3), 497–512, 1977.

Yamada, T., and H. Óura, Studies of ice cohesion, I. A measurement of the cohesive force between an ice sphere and an ice plate (in Japanese, English Summary), *Contrib. Inst. Low Temp. Sci. Hokkaido Univ., Ser. A*, no. 27, 31–39, 1968.

An Overview of Seasonal Snow Metamorphism

S. C. COLBECK

J.S. Army Cold Regions Research and Engineering Laboratory, Hanover, New Hampshire 03755

The grains in seasonal snow undergo rapid and radical transformations in size, shape, and cohesion. These grain characteristics affect all of the basic properties of snow. Snow is characterized as either wet or dry depending on the presence of liquid water. Wet snow is markedly different at low and high liquid contents. Dry snow is characterized as either an equilibrium form or a kinetic growth form; that is, it is either well rounded or faceted. Of course, many snow grains display either transitional features between two of these categories or features which arise from other processes. Snow is classified depending on the dominant processes of its metamorphism.

1. INTRODUCTION

:-grained material with a high specific surface rally at or close to its melting temperature; ry active thermodynamically. It undergoes n grain size and grain shape with changes in ltent, temperature, and/or temperature gradi- f the important material properties are highly he metamorphic state of snow, a fundamental of snow metamorphism is essential for all ; and engineers. It is also of interest for the ovide into the study of crystal growth and the amic and metal powders.

;oes such interesting changes in its crystalline observations of the common crystal types ide for many years. Once on the ground, : the source material for the snow cover as :arting point for snow metamorphism. The ographs of *Bentley and Humphreys* [1931] are best known collection, partly because the chosen for beauty rather than for scientific

1936, early work in sampling and photograph-)ver in the Alps is also a widely known source i. Seligman invested considerable effort in ples on his many travels in the Alps. His croscopic and photographic equipment en- tserve and record the structure of the snow variety of conditions. *Seligman* [1936] dis- :rvations of others such as *Wolley* [1858], who ystal types in Lapland.

treatment of dry snow metamorphism proba- vitzerland with the work of *Bader et al.* [1939] with the work of *de Quervain* [1945]. The sublimation and vapor movement had been ch earlier, but the quantification of this mech- veloped first by the Swiss and then by the 'osida and colleagues (*Yosida*, 1955]).

s and descriptions of wet snow lagged far f dry snow perhaps because of the problems of at its melting temperature and because of the mulating a thermodynamic description when [vapor, solid, and liquid) are present. The f *Wakahama* [1965] on the growth of grains in d snow (i.e., the pore space is filled with

liquid) marked the beginning of a series of contributions on the metamorphism of wet snow. The most recent of these is my description of grain cluster geometry and thermodynam- ics in freely draining wet snow [*Colbeck*, 1979].

The overview of snow metamorphism given here does not cite all of the researchers whose observations and ideas have contributed to the present state of knowledge. Rather, this is one person's interpretation of the changes which take place once snow accumulates on the ground. We start with some illustrations of the dominant forms of snow crystals; the explanation for these forms is then given. An outline of seasonal snow as developed here is given in Table 1.

2. BASIC FORMS

It is common to classify snow as wet or dry depending on whether it is at or below its melting temperature as deter- mined by ionic impurities, elastic strains, and radius of curvature. Dry snow is subdivided here into two categories: the crystalline shape is characterized either as an equilibrium form or as a kinetic growth form. Wet snow is also subdi- vided depending on the liquid water content. Tightly packed grain clusters dominate wet snow at low liquid contents, whereas well-rounded, cohesionless particles appear at high liquid contents. These four basic forms are shown in Figures 1–4. Of course, the distinction among these forms is imper- fect, and therefore we consider some exceptions after dis- cussing the basic forms. We now turn to the task of explaining their formation.

3. EQUILIBRIUM FORMS

At slower rates of growth each site on the crystal surface is more or less equivalent, and thus there is no surface constraint on the kinetics of growth [*Hirth and Pound*, 1963]. This mode of growth occurs at higher temperatures and slower growth rates where the relaxation time for roughen- ing of a crystalline face is small in comparison to the time required for the addition of a monomolecular layer to the face. Since slow growth rates and high temperatures allow only slight departures from phase equilibrium, it is not surprising that the crystal shape developed under these conditions can be characterized by phase equilibrium ther- modynamics.

If we had precise knowledge of the surface free energies for ice as a function of orientation, we could uniquely define the equilibrium shape of ice crystals held in vapor or in liquid water through use of the Wulff plot [*Herring*, 1953]. In the absence of this knowledge we can only examine the crystals

TABLE 1. Seasonal Snow Outline

:signation	Description
I	snow precipitation
II	dry snow
IIa	equilibrium form
IIb	kinetic growth form
III	wet snow
IIIa	low liquid content
IIIb	high liquid content
IV	mixed processes
IVa	faceted crystals with rounded portions
IVb	rounded crystals with faceted portions
IVc	melt-freeze grains
IVd	surface melt crystals
IVe	melt-freeze layers
IVf	wind crusts
IVg	surface glaze
IVh	surface melt layer

nselves without being certain if they have had sufficient : to reach equilibrium. At the melting temperature, and :cially at high liquid contents, it is most likely that the erved crystals represent the true equilibrium shape. stals such as those shown in Figure 4 are nearly spheri-although many are distorted by the contacts among icles. The equilibrium shape should be a hexagonal m rather than a sphere [Krastanow, 1941], although a late spheroid is often suggested by the elongated grains in snow where slow growth rates prevail (see Figure 1). variation of surface free energies with orientation ap-rs to be small at high temperatures where the crysta! :s are covered by disordered layers. Golecki and Jaccard '8] suggest that these are as thick as 0.094 μ. According-we assume isotropy and treat the phase equilibrium ·modynamics isotropically.

a. *Wet Snow With a High Liquid Content*

Phase equilibrium thermodynamics appears in useful reference form for application to snow in several places, especially in the work of *Defay and Prigogine* [1951] and *Dufour and Defay* [1963]. It has been summarized for use in snow and other cold capillary systems by *Colbeck* [1980, 1981a], and, of course, much of the basis for its modern use appears in the *Collected Works of J. Willard Gibbs* [Gibbs, 1928]. Its application can be demonstrated most easily by considering the shape and growth of wet snow in which the pore space is liquid filled. This is a two-phase, single-component system in which the jth phase must obey the Gibbs-Duhem relation

$$d\mu_j = v_j \, dp_j - s_j \, dT \qquad (1)$$

When equilibrium exists, changes in the chemical potential μ of the two phases must be equal; hence

$$v_l \, dp_l - s_l \, dT = v_s \, dp_s - s_s \, dT \qquad (2)$$

where the difference in entropy s is

$$s_l - s_s = L/T$$

and the difference in pressure p is given by Laplace's equation

$$p_s - p_j = 2\sigma_{ij}/r_{ij} \qquad (3)$$

The mean radius of curvature, r_{ij}, is given by

$$\frac{2}{r_{ij}} = \frac{1}{r_1} + \frac{1}{r_2} \qquad (4)$$

where r_1 and r_2 are the two principal radii of curvature (or radii in any two mutually orthogonal planes). It follows that

0.4 mm
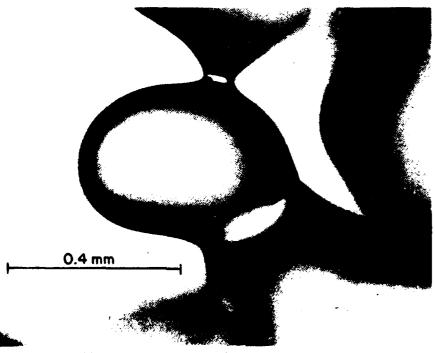
Fig. 1. Equilibrium form of dry snow. It is well rounded and appears at slower growth rates [from *Colbeck*, 1981b].
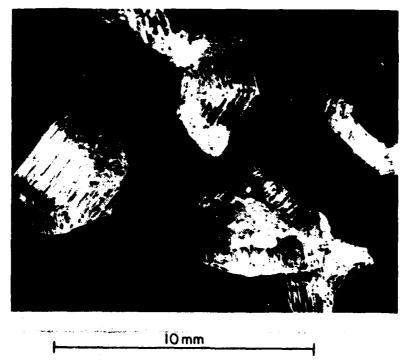
Fig. 2. Kinetic growth form of dry snow. It is distinctly faceted and appears at faster growth rates [from Colbeck, 1981b].

the melting temperature of an unstrained ice particle in pure, liquid water is given by

$$\ln (T/T_0) = -\frac{2}{L\rho_s} \frac{\sigma_{sl}}{r_{sl}} \tag{5}$$

or, approximately,

$$T_m = -\frac{2T_0}{L\rho_s} \frac{\sigma_{sl}}{r_{sl}} \tag{6}$$

where the melting temperature T_m is expressed in degrees Celsius and the reference temperature T_0 is the melting temperature of a flat surface.

Since the smaller particles are at lower temperatures in
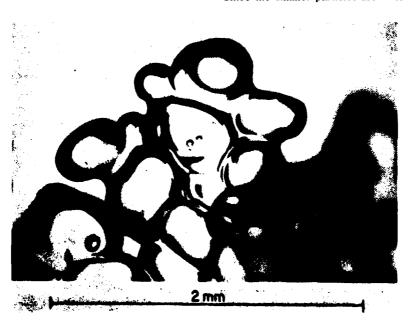
Fig. 3. Ice crystals gathered into tightly packed grain clusters in wet snow at low liquid contents. The individual grains are generally single crystals (photograph of young grain cluster growing in the laboratory).
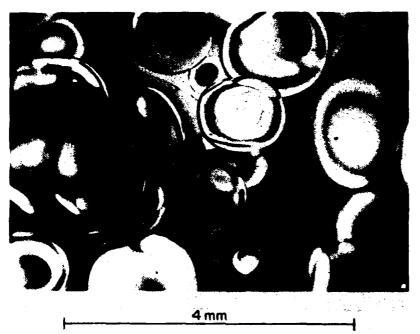
Fig. 4.   Well-rounded ice crystals in wet snow with high liquid contents. However, some distortions are caused by
grain-to-grain contacts (photographed through crossed polaroids).

liquid-saturated snow, heat flow to them causes their melting while the larger particles grow. *Wakahama* [1965] observed this grain growth process as shown in Figure 5. Inspired by Wakahama's experiments, I constructed a simple model of this process [*Colbeck*, 1973] which explained such things as the rapid disappearance of particles once they reach a critical minimum size (see Figure 6). Similar arguments would apply to grain growth in the simplest case of dry snow.

Raymond and Tusima [1979] developed a more sophisticated approach to understanding grain growth in the liquid-saturated case. They treated the entire population of grains through the conservation of total ice mass and thus were able to show certain featu.~ of the changing size distribution. They also found that dissolved impurities slow the rate of grain growth in a manner consistent with its effect on the melting temperature. This occurs because the temperature adjacent to a growing crystal is decreased by the rejection of dissolved impurities at the freezing surface, while the temperature adjacent to a melting surface is increased by dilution. Clearly, the temperature difference driving the grain growth process is reduced by this mechanism.

b.   *Wet Snow With a Low Liquid Content*

As opposed to the liquid-saturated case, highly unsaturated wet snow shown in Figure 3 is characterized by clusters of grains rather than by the individual spherical grains shown in Figure 4. Using a face-centered model of spherical grains, I suggested [*Colbeck*, 1973] that the transition between highly unsaturated wet snow (or pendular regime, where the air occupies continuous paths throughout the pore space) and highly saturated wet snow (or funicular regime, where the liquid occupies continuous paths throughout the pore space) occurs at a liquid saturation of about 14% of the pore volume. *Denoth* [1980] has experimentally observed this

transition to occur in the saturation range of 11–15% of the pore volume. This corresponds to a liquid water content (as a percentage of the total volume) of about 7%, just above the usual range of values (2–5%) observed by dielectric methods in freely draining snow.

Spherical grains are unstable in the lower range of liquid contents, just as grain boundaries are unstable in the higher range of liquid contents. Thus when the liquid is drained from the liquid-saturated snow shown in Figure 4, the tightly packed grain clusters shown in Figure 3 appear. The basic units of these grain clusters are the two- and three-crystal arrangements shown in Figure 7. A fourth grain is often attached to the three-grain arrangement to form a tetrahedral packing, but in low-density seasonal snow, the grain arrangements are seldom more regular than that. Neverthe-
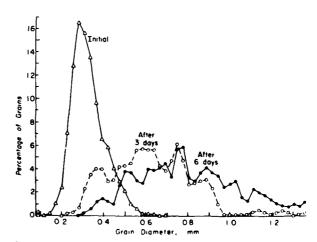

Fig. 5.   The changing distribution of grain size in liquid-saturated snow [from *Wakahama*, 1965].

less, hundreds of grains may be locked together to form a
single cluster with a density of 0.5–0.6 Mg/m^3, although the
bulk density of the snow may be much lower because of the
large voids among the clusters. As the air-filled voids among
the clusters are reduced, the bulk density increases until the
clusters are no longer individual units. At this point, such as
in the firn of a temperate glacier shown in Figure 8, the ice is
the continuous phase, while the air exists in distinct pores
and the liquid exists in isolated liquid veins (among three
grains) or fillets (between two grains as shown in Figure 7).

The clusters form quickly in snow when it is first wetted.
In dry seasonal snow where grain growth is proceeding
slowly, the rate of grain growth increases markedly when
even small quantities of water are added. For example,
Wakahama [1965] found that the rate of grain growth in wet
snow with 3–5% liquid was much greater than isothermal,
dry snow but much less than liquid-saturated wet snow. In
the liquid-saturated case described earlier the rate of grain
growth is rate controlled by heat flow among particles of
various sizes. In that case, mass flow among the growing and
shrinking particles occurs instantaneously through the liq-
uid-filled pores. However, grain growth in wet snow clusters
is slowed by both the reduced heat flow and the restricted
mass flow. The driving force for grain growth in clusters can
be determined from the equation for their phase equilibrium
temperature [*Colbeck*, 1973],

$$T_m = -\frac{T_0}{\rho_l L_s} p_c - \frac{2T_0}{\rho_s L_s} \frac{\sigma_{sg}}{r_p} \qquad (7)$$

where the capillary pressure p_c, the difference between the
pressures in the gas and liquid, increases as the liquid water
content decreases. Thus at a constant capillary pressure (and
assuming a constant ice pressure) the temperature is lower
for smaller particles, and in fact, the temperature difference

Fig. 7a. Equilibrium configuration for a two-unit cluster [from
Colbeck, 1979].

among particles in grain clusters could be greater than that
among particles in liquid-saturated snow because the ratio of
the interfacial energies $(\sigma_{sg}/\sigma_{sl})$ is about 3.3. Nevertheless,
both the heat and the mass flows among growing and
shrinking particles in grain clusters are reduced by the
absence of a liquid path. Also, it is unlikely that the
temperature differences among particles in a grain cluster are
as large as is suggested by (7) because some pressure
differences are likely to exist among the particles. In fact,
these pressure differences are required if the crystalline
boundaries are curved.

Mass flow among the particles in a grain cluster is difficult
to quantify because of the uncertainty of diffusion through
the quasi-liquid layers which cover the ice surfaces. Vapor
diffusion among particles occurs because of the larger vapor
pressure over smaller particles as given by Kelvin's equa-
tion,

$$p_R = p_0 \exp\left[\frac{1}{\rho_s R T_0} \frac{2\sigma_{sg}}{r_p}\right] \qquad (8)$$

However, this is a very restrictive mechanism for mass
transfer among particles. Vapor diffusion in dry snow is the
rate-limiting process [*Colbeck*, 1980], but in grain clusters in
wet snow, surface diffusion appears to greatly increase the
rate of mass transfer. While this qualitatively explains the
large increase in grain growth at low liquid contents as
compared to dry snow as observed by *Wakahama* [1965], a
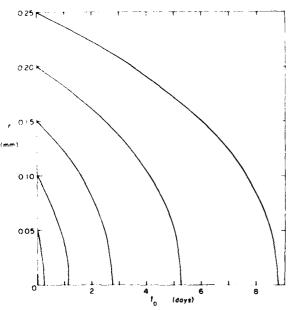quantitative description is still needed.

Fig. 6. The radius of the smaller particles of different initial radii
versus time as they are 'cannibalized' by the larger particles. The
smaller particles disappear while the larger particles grow [from
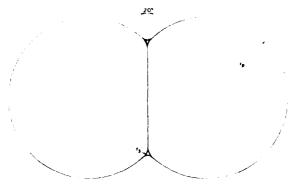*Colbeck*, 1973].
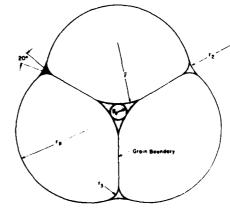
Fig. 7b. Equilibrium configuration for a three-unit cluster [from
Colbeck, 1979].

2 mm
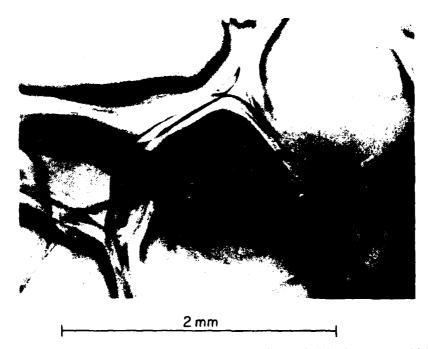
Fig. 8.   Cross-section of firn from the South Cascade Glacier. The individual crystals are visible.

c. Dry Snow

The equilibrium form generally dominates the grain shape in dry snow unless, as is discussed later, the snow cover is subjected to a large temperature gradient. The distinction between the conditions for the growth of the well-rounded, equilibrium grains and those for the kinetic growth of faceted grains is clear. When the rate of growth of grains in a dry snow cover is limited by vapor diffusion, the growth rate is so slow that the equilibrium form prevails. When an imposed temperature gradient increases the gradient in the vapor

pressure and possibly causes some thermal convection as well, the excess vapor pressure over the growing grains is much larger. The rate of crystal growth increases with increasing supersaturation [Burton et al., 1951], and if the growth rate is sufficient, a transition occurs to the faceted crystals of the kinetic growth form [Cahn, 1960].

In the absence of an imposed temperature gradient, a condition which can for significant periods of time occur only in the laboratory, snow metamorphism is exceedingly slow, as is shown in Figure 9. A comparison for snow in nature is shown in Figure 10. Clearly, snow metamorphoses
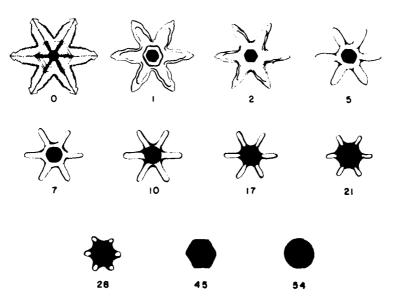
Fig. 9.   Decay of a snowflake in the absence of an imposed temperature gradient (drawn from Bader et al. [1939]). The equilibrium form develops slowly owing to slight temperature and vapor pressure differences around the snowflake. The times are in days!
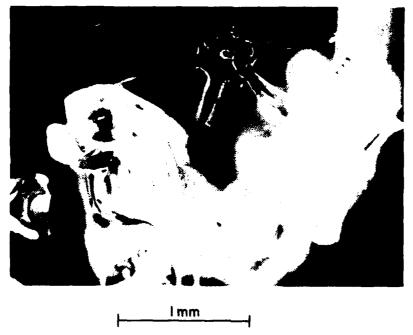
Fig. 10. Decay of a 20-hour-old snow in nature. The decay is greatly accelerated by the normal temperature and vapor pressure gradients in any dry snow cover. This is one of the few identifiable snowflakes remaining 20 hours after this layer was deposited.

much more rapidly in nature than in an adiabatic environment in the laboratory because of the normal temperature and vapor pressure fluctuations experienced by any dry snow cover. Thus temperature gradients are a normal part of the metamorphism of dry snow, even when only the well-rounded, equilibrium grains result. Although it has been suggested that the reduction in specific surface free energy is enough to drive grain growth, the change in surface free energy per unit change in latent heat, $2\sigma_{sg}/r_p L \rho_s$, is only about 10^{-6}. Thus some temperature gradient and heat flow among the particles is necessary.

In the absence of an imposed temperature gradient, snowflakes undergo 'destructive metamorphism,' while large grains grow at the expense of small grains (i.e., 'constructive metamorphism'). This occurs because, according to Kelvin's equation (8), the vapor pressure is larger over dendrite branches with small radii of curvature and over smaller ice grains. Perla [1978] showed that an imposed temperature gradient is necessary to get the commonly observed rates of grain growth even when only rounded crystals develop. Colbeck [1980] combined mass and heat flows to show that a local temperature gradient of about 10^{-2} °C/m would result from the metamorphism of 0.1-mm grains. Thus, as is suggested by Figure 11, the radius of curvature differences among ice surfaces cannot control the rate of metamorphism except possibly for brief periods immediately following a snowfall. when dendrite branches with a mean radius of 10^{-3} mm might occur. Of course, the radius of curvature differences do control the direction of metamorphism of the rounded grains.

In the absence of an imposed temperature gradient the rate of metamorphism is controlled by the slow diffusion of water vapor among the different grains. A temperature gradient increases the vapor flow J approximately as

$$J = -D \frac{\partial \rho}{\partial T} \frac{\partial T}{\partial z} + V\rho \qquad (9)$$

where the vapor density ρ can be approximated from equilibrium thermodynamics:

$$\rho = \rho_0 T_0 \exp\left[\frac{L_s}{R}\left(\frac{1}{T_0} - \frac{1}{T}\right)\right]/T \qquad (10)$$

This approximation is imperfect, however, since the actual vapor pressure during metamorphism without large density changes must lie between the equilibrium vapor pressure over the shrinking grains and the equilibrium vapor pressure
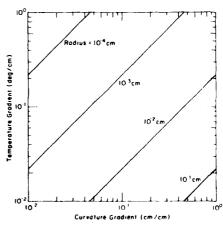
Fig. 11. Isopleths of equal contribution to the vapor flux from temperature and radius gradients for different particle radii. In the upper left, flux is dominated by temperature gradients, whereas in the lower right, flux is dominated by curvature gradients [after Colbeck, 1981b].

Fig. 12. Maximum possible excess vapor pressure during faceted crystal growth versus temperature when various sizes of rounded particles are present.

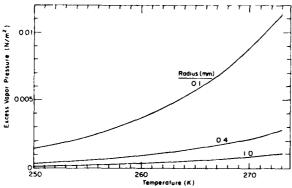over the growing grains. This complex system of sinks and sources with heat and mass flows has never been analyzed. Since this analysis is essential to understanding both the equilibrium and the kinetic growth forms of snow, heat and mass flow in snow are discussed before the growth of faceted crystals is reviewed.

4. KINETIC GROWTH FORM

The hexagonal snowflake is probably the best known example of the kinetic growth form of a crystal. At the very fast growth rates at which snowflakes form, a dendritic structure appears because protrusions sprout at the tips and edges where the supersaturation is greatest. The shape of any growing dendrite is ultimately determined by a balance between vapor diffusion to the growing facets and surface energy constrictions [*Frank*, 1958].

De Quervain [1958] observed the growth of faceted crystals at the expense of the rounded crystals in snow subjected to a large temperature gradient. The transition from the equilibrium (nonsingular or highly rounded) form of slow growth to the kinetic growth (singular or highly faceted) form of rapid growth occurs in the laboratory when the applied temperature gradient reaches about 20 °C/m depending on conditions like temperature and snow density [*de Quervain*, 1958; *Akitaya*, 1974; *Marbouty*, 1980]. At larger temperature gradients and higher vapor flow rates the vapor pressure over the growing crystals is larger, thereby resulting in faster
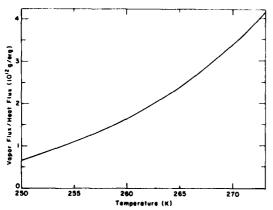
Fig. 13. Ratio of vapor flow to heat flow versus temperature [*Colbeck*, 1981b].
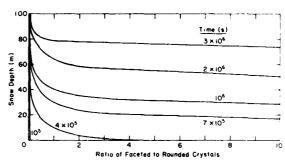
Fig. 14. Ratio of the bulk densities of faceted to rounded grains versus height in the snow cover at various times [*Colbeck*, 1981b]; 10^6 s is about 12 days.

growth. The heat and vapor flow within a snow cover are important aspects of this recrystallization process, and no doubt these processes depend somewhat on snow density and temperature. Many people believe that the critical temperature gradient of 20 °C/m is too high for most field situations. *Armstrong* [1980] states that the critical vapor pressure gradient is 0.05 mbar/cm, which corresponds to a temperature gradient of about 10 °C/m.

a. Heat and Mass Flows

Several people have described the heat and vapor flows in a snow cover; *Yen* [1969] and *de Quervain* [1973] reviewed most of this work and pointed to its significance. This earlier work provides an adequate understanding of heat and vapor flows for most engineering purposes, but its application to understanding the recrystallization of the snow cover is limited. In this regard there are three problems with much of this earlier work; the third problem will be quite difficult to correct. First, some of the early models assume arbitrarily that all of the moving vapor stops at a given horizon. Second, only *Palm and Tveitereid* [1979] try to handle the proper boundary conditions, sources, and sinks. Third, all of the earlier models assume that the vapor pressure is given by the Clausius-Clapeyron equation; *Palm and Tveitereid* [1979] also assume a linear relation between vapor density and temperature. Again, these models of heat and vapor flows are often adequate for most engineering purposes, but any attempt to model the formation of faceted crystals in a snow cover must recognize that the actual vapor pressure must lie between the equilibrium vapor pressure for the rounded, evaporating crystals and the vapor pressure for the flat-faced, growing crystals. According to Kelvin's equation (8), this fractional difference is about 10^{-5}, and thus it is readily understood why the actual process of the growth of faceted crystals has not been modeled. Accounting for both the boundary conditions and the growth of faceted crystals during evaporation of the rounded crystals in a heat and mass flow model will be quite difficult.

In the absence of a complete model there are some insights we can provide into the growth of the faceted crystals. While the faceted crystals grow, the rounded crystals evaporate because of their higher chemical potential. Thus the maximum excess vapor pressure P_{max} relative to a flat surface is

$$P_{max} = p(r, T) - p(\infty, T) \qquad (11)$$

where for any given temperature, $p(r, T)$ is given by Kelvin's equation (8) and $p(\infty, T)$ is simply the Clausius-Clapeyron

equation. As is shown in Figure 12, the maximum possible supersaturation increases with increasing temperature and decreasing radius of curvature. Thus the rate of growth of the faceted crystals should be higher in the lower, warmer portions of the snow cover and when the rounded particles are relatively small.

A further explanation for the growth of the faceted crystals in the warmer portion of the snow cover is provided by an examination of the ratio of vapor flux to heat flux. This is important because of the suggestion that vapor flow is the rate-limiting process in snow metamorphism [*Colbeck*, 1980]. This ratio, as determined from an equilibrium model of heat and mass flow [*Colbeck*, 1981b], increases rapidly with temperature as shown in Figure 13. Thus the supersaturation and the vapor flow necessary to sustain that supersaturation are both increased in the warmer, lower portions of the snow cover where depth hoar growth begins. Depth hoar also tends to form just below flow restrictions such as buried crusts. *De Quervain* [1958] found that flow restrictions in the presence of a temperature gradient caused deposition, presumably due to the increased supersaturation on the warm side of the restriction.

Even without a sophisticated calculation of the actual vapor pressure during the recrystallization of rounded to faceted grains in a snow cover, a model of the process can be constructed by assuming crystal growth and crystal evaporation rates proportional to the supersaturation and undersaturation respectively [*Colbeck*, 1981b]. It is also assumed that the bulk density remains constant during this process as suggested by *Armstrong* [1980]. The ratio of the bulk density of faceted to rounded grains, a measure of the stage of development of depth hoar, increases with time as shown in Figure 14. There is a fairly sharp transition between the overlying rounded crystals and the underlying faceted crystals which sweeps upward with increasing time. From this simple model it is also shown that the maximum value of the excess vapor pressure driving the growth of the faceted crystals moves upward with time. As is shown in Figure 15, the maximum rate of growth moves upward as the rounded crystals, the major source of the vapor, are depleted near the base of the snow cover. The growth of the faceted crystals can continue once the rounded crystals have been depleted. This continued growth requires a large temperature gradient, however, because the increased vapor pressure of the rounded grains is no longer available to drive the process.

The formation of faceted crystals near the upper surface is restricted, however, because of the lower temperature. While evidence of the recrystallization taking place near the
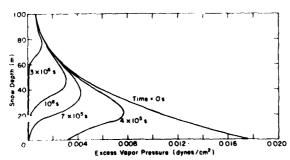
Fig. 15. Excess vapor pressure versus depth for various times during recrystallization [*Colbeck*, 1981b].

ground may never reach the surface, another type of faceted crystal known as surface hoar often forms there. These crystals appear to form by condensation from an atmosphere which is supersaturated as compared to the surface on cold, clear nights [*Seligman*, 1936].

Much remains to be learned about the complicated interaction of heat and mass flows during the recrystallization of the snow cover, especially on the scale of the grains. Likewise, much must be learned about the crystalline forms and growth processes of the faceted form. The kinetics of faceted crystal growth is addressed next.

b. Kinetic Growth Processes

When large supersaturations cause rapid growth rates, the growth occurs by the movement of molecular steps across the crystalline faces; hence the crystals develop distinctive shapes. This mode of growth of ice crystals is reviewed by *Hobbs* [1974], and further information about the application of these principles to snow is given by *Colbeck* [1981b]. A great deal of information exists about the growth of faceted crystals, and much of this information is directly applicable to the growth of crystals in a snow cover. Unfortunately, I am aware of only one study [*Eugster*, 1950] of the detailed crystal structure resulting from recrystallization in a snow cover; thus much remains to be learned about the details of the faceted crystals of the kinetic growth regime.

A wide range of faceted crystal types are found in the snow cover, including complex scrolls, cup-shaped crystals, plates, sheaths, and needles [*Bradley et al.*, 1977]. *Marbouty* [1980] found that the crystal habit–temperature relation in the atmosphere can be applied to the snow cover as well. Crystals in the snow cover, however, tend to display a more complex structure than ice crystals grown in other environments. Faceted crystals in the snow cover usually grow with a distinct step struture (see Figure 2) in which basal planes (0001) of ice are connected by either prismatic faces ($1\bar{1}00$) or what appear to be pyramidal faces ($1\bar{1}01$). *Hirth and Pound* [1963] state that rounded (nonsingular) crystals grow at low supersaturations but that rounded surfaces may become 'vicinal' at higher supersaturations (vicinal faces display a step structure in which basal or prism faces are separated by monomolecular risers). These surfaces remain vicinal up to the critical supersaturation where growth is dominated by the screw dislocation mechanism of *Burton et al.* [1951]. However, since the snow cover undergoes a recrystallization in which the faceted crystals grow at the expense of the rounded crystals, it appears that the supersaturation is less than the critical supersaturation required for growth by the dislocation mechanism [*Colbeck*, 1981b].

Cahn [1960] describes the differences between diffuse and sharp surfaces as well as singular and nonsingular surfaces. Diffuse surfaces have a gradual transition between phases and hence the liquidlike layer commonly thought to cover ice surfaces [*Golecki and Jaccard*, 1978]. Singular surfaces, or crystals displaying flat faces, have a minimum in the surface free energy at one or more orientations in the crystal. At temperatures close to the melting point, where an ice surface should be most diffuse, the presence of the liquidlike layer appears to eliminate or greatly reduce any effect of crystal orientation on surface free energy. Thus the equilibrium shape is well rounded, and according to *Cahn* [1960], nonsingular surfaces can advance normal to themselves without the
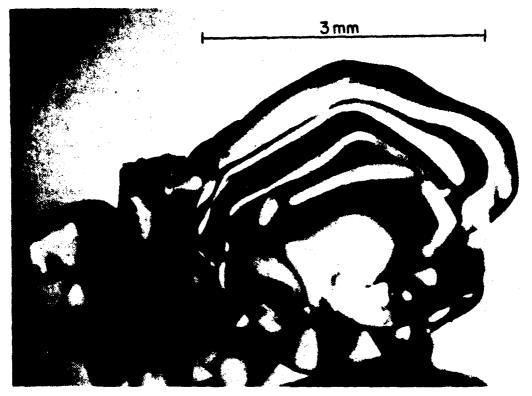
Fig. 16.   Faceted crystal in the act of rounding off after being held for a month at a constant temperature [*Colbeck*, 1981*b*].

lateral propagation of steps. At higher growth rates, however, the surfaces become singular because the kinetic growth processes on the surfaces control the shape of the crystal.

The temperature gradient in a snow cover plays a critical role in the growth only in the sense that vapor pressure over the growing crystals cannot be maintained at a sufficient level by isothermal diffusion alone. Thus the faster vapor movement associated with the temperature gradient is an essential part of the development of the faceted crystals. This is why *Armstrong* [1980] identified a critical vapor pressure gradient for the onset of faceted crystal growth.

So far we have discussed the growth of faceted crystals due to the upward migration of water vapor in the snow cover. Faceted crystals can also form by the condensation of

Fig. 17.   Faceted crystals in the act of rounding off after a few days of temperatures from $-3°$ to $-5°C$ in a shallow snow cover.

2 mm

Fig. 18. Dendrites growing on well-rounded crystals. These are the start of the recrystallization which leads to depth hoar.

water vapor when the atmosphere is supersaturated relative to the snow surface. This occurs most readily on cold nights when the snow surface is cooled by radiation loss through a clear atmosphere. Then the excess vapor pressure can be much greater than that found within the snow cover. Accordingly, larger growth rates and different crystal types should be expected on the surface. *Seligman* [1936] provides many examples of this crystalline form.

5. CRYSTAL FORMS FROM MIXED PROCESSES

Snow crystals falling from the atmosphere are characterized as simple plates, needles, etc., but in fact, snow particles often display mixtures of these characteristics depending on the particular path they follow through the atmosphere. Likewise, particles in the snow cover have generally experienced a variety of processes depending on

Fig. 19. Rapidly evaporating wet snow crystal displaying crystalline faces connected by a spinelike ridge (photograph of seasonal snow on the South Cascade Glacier).

the conditions since their deposition. Many snow grains cannot be well described by the basic cases shown in Figures 1–4 and must be described separately. Some of the more complicated cases are described here, although there are probably many cases of which I am not aware.

a. Faceted Crystals With Rounded Portions

There are two forms of these crystals. First, when the temperature gradient is removed, faceted crystals revert to the rounded form as shown in Figures 16 and 17. This process is probably accelerated in the presence of a small temperature gradient in much the same way that showflakes round off more quickly in nature than in an adiabatic environment in the laboratory (see Figure 9). Second, at higher temperatures, where thermal fluctuations are of greater importance [Herring, 1953], some faces on growing crystals can become rounded while others stay flat [Pavlovska and Nenow, 1972]. Lamb and Scott [1972] and Nenow and Stoyanova [1979] have grown such ice crystals individually in the laboratory, and they can be observed in the snow cover as well. These two cases are distingished on the basis of whether the faceted crystals are actively forming or decaying at the time of the observation. This case is distinguished from the next case (section 5b) on the basis of whether the faceted or the round form is dominant.

b. Rounded Crystals With Faceted Portions

There are two cases of rounded crystals with faceted portions which I have observed in seasonal snow. The most important one is shown in Figure 18, the incipient stage of faceted crystal growth in a snow cover consisting entirely of well-rounded grains. This example grew during a cold night in the fall when the snow cover was wetted during the day and the ground was warm. In fact, the snow cover did recrystallize into faceted grains owing to sustained cold weather after this photograph was taken.

The second type of rounded crystal with facets is shown in Figure 19. During conditions of a very dry atmosphere, wet snow crystals exposed to the atmosphere can evaporate rapidly enough to develop crystal faces connected by spine-like ridges. As with faceted crystal growth, the evaporation must occur with sufficient speed to overcome the tendency for thermal fluctuations to remove the molecular ledges which are propagating across the faceted surfaces. This is most difficult at the melting temperature, where a large liquidlike layer is assumed to exist over the solid surface during most conditions. The spines are probably remanent features of the formation of ledges at the crystal edges. Their regular spacing and size suggest some distinguishable mechanism, but that is not yet identified.

c. Melt-Freeze Crystals

Snow often undergoes cycles of freezing and thawing, thus causing an alternation of the clusters shown in Figure 3. The result is multicrystalline grains shown in the process of forming in Figure 20 and as they occur in nature in Figure 21. When subject to prolonged solar radiation, these grains may break down along the crystalline boundaries and revert to the original grain clusters. For this reason it is common to see a mixture of multicrystalline and single-crystal grains in wet snow. The existence of melt-freeze grains does not indicate that this process is inherent in the formation of the

normal grain clusters such as those shown in Figure 3. The formation of these grain clusters occurs without melt-freeze cycles [Colbeck, 1979].

d. Melt-Freeze Layers and Surface Melt Layer

These crusts form both on and below the surface. On the surface a thin layer can melt during the day (even at subfreezing air temperatures) and freeze at night, thus leading to a surface layer of higher density with a very complicated structure. At higher air temperatures when the melting is intense enough, the absorption of solar radiation can cause melting of the grain boundaries and lead to a cohesionless surface layer in snow which is otherwise characterized by the well-bonded grain clusters shown in Figure 3. This condition can be readily identified by the rapid increase in strength below the melting surface. At these melt rates, some of the pores may be filled with meltwater over a fair portion of the surface. Thus as is shown in Figure 22, the surface may have a very large liquid content which decreases rapidly in the first few millimeters below the surface. This large liquid content can lead to the growth of large, cohesionless crystals on the surface.

The melt-freeze process also operates below the surface when infiltrating meltwater is subsequently refrozen. Repeated cycles of melt-freeze of a large portion of the depth of the snow cover can lead to 'ice layers' of greatly reduced permeability and porosity as shown in Figure 23. These are rarely impermeable [Gerdel, 1954], although they can divert the infiltrating meltwater. They usually form at horizons where a fine-grained snow lay r overlies a coarse-grained layer because of the retentive capacity of the fine-grained material. As is shown in Figure 23, the crystals are often very large, probably because of crystal growth in the liquid-saturated snow prior to refreezing.

e. Wind Crusts

Another type of crust forms owing to the action of the wind on the surface of the snow cover. As the ice particles are carried along by the wind, they are broken into smaller fragments which can pack with a higher density. These crusts can develop a high strength due to their increased density and the faster sintering action of smaller particles [Hobbs and Mason, 1964]. No doubt the steep and rapidly changing temperature gradients associated with the surface are important as well.

f. Surface Glaze

Supercooled rainwater can refreeze onto the surface to form a glaze. As is shown in Figure 24, the crystal size of the surface glaze is about the same as grain size in the snow. The resulting surface tends to be smooth and impermeable.

6. SUMMARY

The overview of the metamorphism of seasonal snow given here is based on the processes which lead to the characteristic features of snow grains, especially their size, shape, and cohesion. Knowledge of these processes is quite incomplete, but enough is known to construct a meaningful outline based on the dominant processes. This outline, shown in Table 1, differs from that of Sommerfeld and LaChapelle [1970] in several important respects. First, their terms 'temperature-gradient' and 'equi-temperature meta-

Fig. 20b

Fig. 20d

Fig. 20a

Fig. 20c
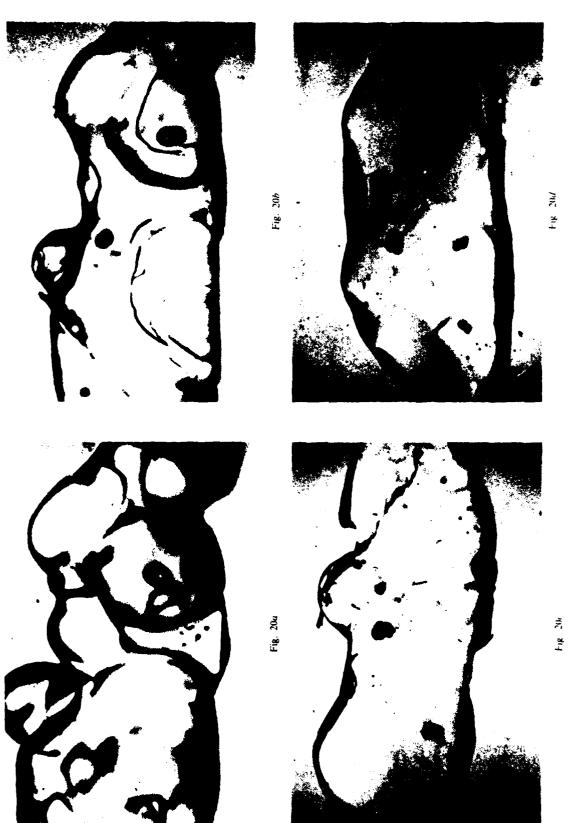
Fig. 20. Wet snow cluster (such as that shown in Figure 3) forming a multicrystalline grain when subjected to multiple freeze-thaw cycles. This shows a sequence of melt-freeze cycles in which a normal cluster forms a single melt-freeze grain. The original cluster is about 2.6 mm in length. The crystalline boundaries are visible in the last photograph.

2 mm
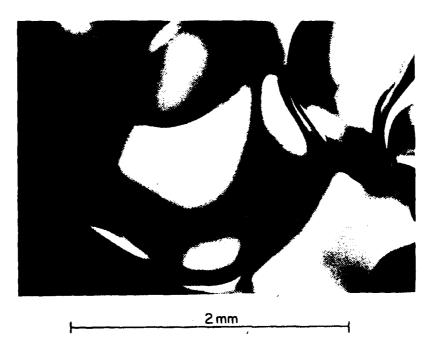
Fig. 21. Melt-freeze grain from the snow cover of the South Cascade Glacier.

morphism' are replaced by the crystallographers' terms 'kinetic growth' and 'equilibrium form' because all of these forms develop in the presence of a considerable temperature gradient. In fact, the temperature gradient controls the rate of grain growth even when the equilibrium form develops. Also, *Sommerfeld and LaChapelle* [1970] appear to use 'melt-freeze' in describing any freely draining wet snow. While they correctly point out the importance of these

cycles, the grain clusters of Figure 3 develop for reasons which have nothing to do with melt-freeze cycles or overburden pressure. The multicrystalline grains shown in Figures 20 and 21 do arise from these cycles, but most grain clusters in wet snow occur for other reasons [*Colbeck*, 1979].

The classification of snow logically begins with the precipitation. This occurs in many different forms, depending on the supersaturation and temperature of the atmosphere

2 mm
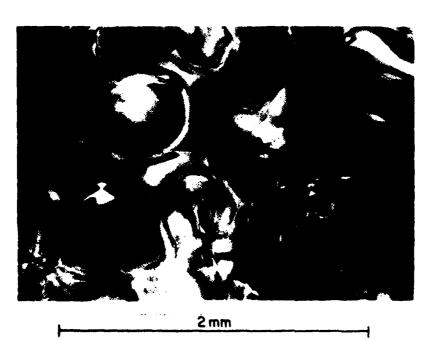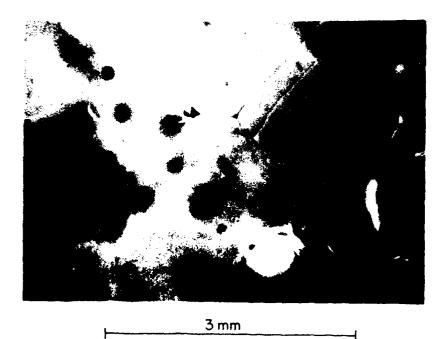
Fig. 22. Sample taken from the refrozen surface of a rapidly melting snow cover. Some of the spaces between the surface grains were filled with meltwater during the rapid melt. The meltwater refroze into crystals whose grain boundaries are visible.

3 mm
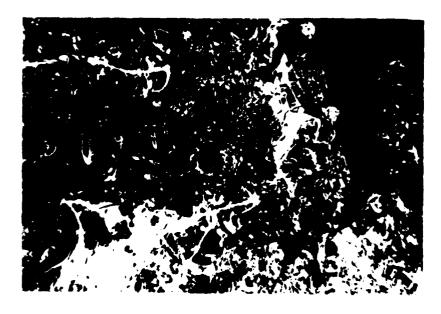
3. 23. View of an 'ice layer' formed below the surface in the seasonal snow of the South Cascade Glacier by ezing of infiltrating meltwater. The crystalline boundaries (on both the upper and the lower surfaces) and entrapped ubbles are visible.

54] and, of course, often displays a mixture of the various growth environments experienced l through the atmosphere. The best known ? snowflake, a thin plate displaying hexagonal

earlier classifiers [Commission on Snow and mmerfeld and LaChapelle. 1970]. I think of two

basic cases of dry snow. Dry snow is stable in either a well-rounded or a faceted form depending on the growth rate, although the transitional cases (IVa and IVb in Table 1) between these two states are very common. The well-rounded form can be understood approximately by phase equilibrium thermodynamics, hence the term equilibrium form. The kinetic growth form develops at rapid growth

10 mm

24. Supercooled rain freezing onto the snow surface as shown by the glassy reflection and ice crystal boundaries

where surface kinetics dictates the form of crystals are large enough to be seen with an optical micro- [Frank, 1958].

transitional forms between these two basic cases when a large temperature gradient is either removed or d to the snow cover. That is, the faceted form grows at :pense of the rounded form when a large temperature :nt (at least 10–20°C/m) is applied, while the rounded grows at the expense of the faceted form when smaller :rature gradients occur. One of the most interesting ples of dry snow is a grain undergoing faceted growth bottom side while evaporating from its rounded upper The crystals shown in Figures 9 and 16 are examples of pposite situation; these crystals are rounding off their :d portions because the large supersaturations respon- for their rapid growth have been removed.

the presence of all three phases at the melting tempera- snow undergoes rapid changes to achieve its equilibri- tate. At low liquid contents (case IIIa), the pendular ıe of saturation, the crystals are well rounded and join well-bonded grain clusters. These display some consid- e strength as compared to the relatively cohesionless cles at the high liquid contents of the funicular regime of ation (case IIIb). In fact, both cases IIb and IIIb are ively cohesionless forms of snow.

:yond the four basic states of wet and dry snow on the nd are many types of snow which display evidence of a bination of processes. The transitional cases of crystals laying both faceted and rounded portions are very mon, especially in shallow snow covers which are ected to changing weather patterns. Melt-freeze grains crusts also develop owing to changing conditions on the ace of the snow.

ıe metamorphism of snow has been reviewed with ect to both the important processes and the dominant talline shapes. The properties of snow are greatly affect- ıy crystal size, shape, and interactions. Accordingly, arch into this important area will continue, and our vledge of snow metamorphism will continue to evolve. key to a rapid increase in our knowledge of this subject understand both the processes and the results.

NOTATION

D	diffusion coefficient for water vapor in snow.
s	subscripts for gas, liquid, and solid phases.
j	indices.
J	vapor flux.
L	latent heat of fusion.
L_s	latent heat of sublimation.
p_c	capillary pressure, equal to $p_g - p_l$.
p_i	pressure of the ith phase.
p_0	reference pressure.
$_{A\Lambda}$	maximum possible pressure difference between a curved and a flat surface.
r_{ij}	mean radius of curvature between ith and jth phases.
r_p	particle radius.
r_2	principal radii.
s	entropy.
T	temperature, kelvins.
$_m$	melting temperature, degrees Celsius.
T_0	reference temperature, kelvins.

v_i	specific volume of ith phase.
V	mean air velocity.
z	vertical coordinate.
μ	chemical potential.
ρ_0	reference density.
ρ_i	density of ice.
σ_{ij}	surface free energy between ith and jth phases.

REFERENCES

Akitaya, E., Studies of depth hoar, *Low Temp. Sci.. Ser. A. 26*, 1– 67, 1974.

Armstrong, R. L., An analysis of compressive strain in adjacent temperature-gradient and equi-temperature layers in a natural snow cover, *J. Glaciol., 26*(94), 283–289, 1980.

Bader, H., R. Haefeli, E. Bucher. J. Neher, O. Eckel, and C. Thams, Der Schnee und seine Metamorphism, *Beitr. Geol. Schweiz, Geotech. Ser. Hydrol., 3*, 1939.

Bentley, W. A., and W. J. Humphreys, *Snow Crystals*, McGraw- Hill, New York, 1931.

Bradley, C. C., R. L. Brown, and T. R. Williams, Gradient metamorphism, zonal weakening of the snow-pack and avalanche initiation, *J. Glaciol., 19*(81), 335–342, 1977.

Burton, W. K., N. Cabrera, and F. C. Frank. The growth of crystals and the equilibrium structure of their surfaces. *Philos. Trans. R. Soc. London, Ser. A, 243*, 299–358, 1951.

Cahn, J. W., Theory of crystal growth and interface motion in crystalline materials, *Acta Metall., 8*, 554–562, 1960.

Colbeck, S. C., Theory of metamorphism of wet snow, *Res. Rep. 313*, U.S. Army Cold Reg. Res. and Eng. Lab., Hanover, N. H., 1973.

Colbeck, S. C., Grain clusters in wet snow, *J. Colloid Interface Sci., 72*(3), 371–384, 1979.

Colbeck, S. C., Thermodynamics of snow metamorphism due to variations in curvature, *J. Glaciol., 26*(94), 291–301, 1980.

Colbeck, S. C., An introduction to the basic thermodynamics of cold, capillary systems, *Spec. Rep. 81-6*, U.S. Army Cold Reg. Res. and Eng. Lab., Hanover, N. H., 1981a.

Colbeck, S. C., Growth of faceted crystals in a snow cover, submitted to *J. Cryst. Growth*, 1981b.

Commission on Snow and Ice, *The International Classification for Snow*, Tech. Mem. 31, Associate Committee on Soil and Snow Mechanics, National Research Council, Ottawa, Ont., 1954.

Defay, L., and R. Prigogine, *Tension Superficielle et Adsorption*, Desoer, Liège, France, 1951.

Denoth, A., The pendular-funicular transition in snow, *J. Glaciol., 25*(91), 93–97, 1980.

de Quervain, M. R., Schnee als kristallines Aggregat, *Experientia, 1*, 207, 1945.

de Quervain, M. R., On the metamorphism and hardening of snow under constant pressure and temperature gradient, *IAHS AISH Publ., 46*, 225–239, 1958.

de Quervain, M. R., Snow structure, heat and mass flow through snow, in *The Role of Snow and Ice in Hydrology*, vol. 1, pp. 203– 226, UNESCO, Paris, 1973.

Dufour, L., and R. Defay, *Thermodynamics of Clouds*, Academic, New York, 1963.

Eugster, H. P., Zur Morphologie und Metamorphose des Schnees, *Intern. Rep. 113*, Eidgenoess. Inst. fur Schnee und Lawinenfors- chung, Weissfluhjoch-Davos, Switzerland, 1950.

Frank, F. C., Introductory lecture, in *Growth and Perfection of Crystals*, edited by R. H. Doremus, B. W. Roberts, and D. Turnbell, pp. 3–10, John Wiley, New York, 1958.

Gerdel, R. W., The transmission of water through snow, *Eos Trans. AGU, 35*(3), 475–485, 1954.

Gibbs, J. W., *Collected Works of J. Willard Gibbs*, Yale University Press, New Haven, Conn., 1928.

Golecki, I., and C. Jaccard, Intrinsic surface disorder in ice near the melting point, *J. Phys. C.*, *11*, 4229–4237, 1978.

Herring, C., The use of classical concepts in surface-energy problems, in *Structure and Properties of Solid Surfaces*, edited by R. Gomer and C. S. Smith, pp. 5–7, University of Chicago Press, Chicago, Ill., 1953.

Hirth, J. P., and G. M. Pound, *Condensation and Evaporation: Nucleation and Growth Kinetics*, Macmillan, New York, 1963.

Hobbs, P. V., *Ice Physics*, Clarendon, Oxford, 1974.

Hobbs, P. V., and B. J. Mason, The sintering and adhesion of ice, *Philos. Mag.*, *9(98)*, 181–197, 1964.

Krastanow, L., Beitrag zur theorie der trophen-und kristall bildung in der atmosphäre. *Meteorol. Z.*, *58*, 37–45, 1941.

Lamb, D., and W. D. Scott, Linear growth rates of ice crystals grown from the vapor phase, *J. Cryst. Growth*, *12*, 21–31, 1972.

Marbouty, D., An experimental study of temperature gradient metamorphism, *J. Glaciol.*, *26(94)*, 303–312, 1980.

Nakaya, U., *Snow Crystals Natural and Artificial*, Harvard University Press, Cambridge, Mass., 1954.

Nenow, D., and V. Stoyanova, Appearance of non-singular surfaces on vapor grown ice crystals, *J. Cryst. Growth*, *46(6)*, 779–782, 1979.

Palm, E., and M. Tveitereid, On heat and mass flow through dry snow, *J. Geophys. Res.*, *84(C2)*, 745–749, 1979.

Pavlovska, A., and D. Nenow, Les surfaces non-singulières sur la forme d'équilibre de la naptaline, *J. Cryst. Growth*, *12*, 9–12, 1972.

Perla, R., Temperature-gradient and equi-temperature snow, in *Deuxième Rencontre Internationale sur la Neige et les Avalanches*, pp. 43–48, National Association for Study of Snow and Avalanches, Grenoble, France, 1978.

Raymond, C. F., and K. Tusima, Grain coarsening of water-saturated snow, *J. Glaciol.*, *22(86)*, 83–105, 1979.

Seligman, G., *Snow Structure and Ski Fields*, Macmillan, New York, 1936.

Sommerfeld, R. A., and E. R. LaChapelle, The classification of snow metamorphism, *J. Glaciol.*, *9(55)*, 3–17, 1970.

Wakahama, G., Metamorphisms of wet snow, *Low Temp. Sci., Ser. A*, *23*, 51–66, 1965.

Wolley, J., *Report of the British Association*, part II, pp. 40–41, London, 1858.

Yen, Y. C., Recent studies in snow properties, *Advan. Hydrosci.*, *5*, 173–214, 1969.

Yosida, Z., Physical studies of deposited snow, 1. Thermal properties, *Low Temp. Sci., Ser. A*, *7*, 19–74, 1955.

A Review of Snow Acoustics

R. A. SOMMERFELD

Rocky Mountain Experiment Station, U.S. Forest Service, Fort Collins, Colorado 80526

Snow acoustics can be divided into two major areas. One is the attempt to understand the acoustic properties of snow and to relate them to other material properties. In this area the major advance has been the recent understanding that snow must be treated as a porous medium and that the ice framework, the pore air, and their interaction all play important roles in acoustic propagation. It appears that a more realistic model of the ice framework must be used before the full range of snow's acoustic properties can be modeled adequately. The second area is acoustic emissions. High-frequency acoustic emissions have aided in the development of a texture-oriented constitutive relationship. Low-frequency acoustic emissions have been shown to have the potential for predicting avalanches, at least under some conditions.

INTRODUCTION

In this paper I will limit my use of the term acoustics to the study of stress waves in materials which do not cause permanent, macroscopic deformations. This somewhat arbitrary restriction excludes important but peripheral studies such as plastic waves [Brown, 1980], other effects close to explosives, and the stress wave triggering of material failure.

Studies of acoustic phenomena in materials fall naturally into two categories. The first includes attempts to understand and describe the acoustic properties of materials and relate the descriptions to other material properties. The second is the study of acoustic emissions from stressed materials.

The acoustic properties of materials are of interest for a variety of reasons. Since sound is propagated in a material through the motion of material particles, the propagation and attenuation of acoustic energy in a material is closely related to the mechanical properties of the material. Also, some combinations of stress rates and durations, for the determination of material properties, are most conveniently attained through acoustic experiments.

In the case of porous materials such as snow, sound propagation involves an extremely complex interaction between the pore fluid and the solid framework. It is obvious from much of the work in snow acoustics that this complexity was not fully appreciated for many years. In general, the complexity of sound transmission in porous media has hampered its understanding, and snow is certainly no exception.

The difficulty of theoretical treatment probably explains the relative lack of interest in snow acoustics. Although experiments on sound propagation in snow were conducted as early as 1952 [Ôura, 1952a, b], Mellor's [1964] review only mentions acoustic properties in relation to bulk mechanical properties. Furthermore, most of that work was on very high density snow, of little interest in work on seasonal snow cover. A glance at the reference list of this article reveals the slow pace of work until very recently. Perhaps the most important recent work is that of Johnson [1978], which unfortunately remains largely in unpublished thesis form. On the other hand, the fact that acoustic properties of porous materials are so strongly affected by the texture of the material holds the promise that acoustic properties can

be used to index the textural properties and perhaps categorize them.

Here I would like to inject a little semantics. I find that in most snow acoustic studies, the ice network is called the ice or snow 'structure.' This terminology is ambiguous. On one scale the snow structure is the layering and composition of a snow pack, in agreement with geological usage. There is no doubt that this snow structure has a strong effect on the propagation of sound in the snow pack. On another scale the ice structure is wurtzite type, in agreement with crystallographic usage. I strongly recommend that the interrelationship of the ice grains be called the texture, in agreement with a geological, mineralogical, and metallurgical usage developed to circumvent similar ambiguities.

Some acoustic properties are closely related to the stress state and history of a material specimen. In particular, most materials under stress emit acoustic energy related to the stress level and history. There are many mechanisms for generating this energy. They span a size scale from the molecular to the geological with a corresponding range in frequencies from tens of megahertz to tenths of millihertz.

Acoustic emission studies are of two types: Studies of the fundamental relationships between acoustic emissions and other materials phenomena are performed under controlled laboratory conditions using small samples and high frequencies. Studies to predict large-scale material failure are performed in the field on complex structures using low frequencies.

SNOW ACOUSTIC PROPERTIES

Historically, snow has been treated both as a continuous material and as a porous material. In general, there has been a serious lag between available technology and analysis. For example, it was 22 years before the work of Biot [1956] was applied to snow [Johnson, 1978]. Comparisons among work in this field are difficult and may not have much meaning. As Johnson [1978] points out, experimental techniques among various workers are variable, and most experiments were not completely adequate in their design. In this section some comparisons are made. Any conclusions drawn from the comparisons must be considered tentative and hypothetical. They are presented to indicate where further work is needed. At present, data are not available to make definite choices among competing hypotheses.
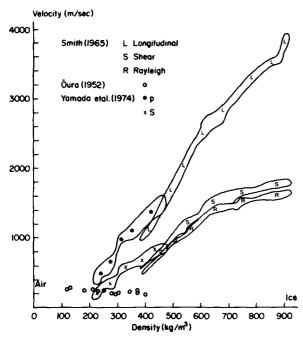
Velocity (m/sec)

Fig. 1. Comparison of the velocities of sound in the ice framework and pore air in snow.

Snow as a Continuous Medium

The treatment of snow as a continuous material is, of course, simpler in concept and can draw on a larger body of established work. The shortcomings of this viewpoint make it inadequate to answer some of the most important questions of snow acoustics: those involved with the two different propagation media. For example, Chae [1967] attempted to reproduce the frequency variation of the complex modulus, the viscosity coefficient, and the loss tangent using a series of Voight models. Agreement between theory and experiment of the complex moduli and the viscosity coefficients could not be obtained without using different relaxation time distributions in each case. Agreement of the loss tangents between theory and experiment could not be obtained at all.

However, acoustic techniques have been used with success in determining the bulk mechanical properties of snow. Estimates of Young's modulus and Poisson's ratio are best made with acoustic techniques, since they can provide short stress durations and small strains conveniently. The more recent measurements of these quantities [J. L. Smith, 1965; N. Smith, 1969] are in essential agreement with those collected by Mellor [1964] and will not be reproduced here. The major shortcoming of most of these measurements is that they do not reach into the density range of the seasonal snow cover, below 300 kg m^{-3}. Nakaya [1959a] encountered practical problems in performing his experiments on softer, less dense snow. N. Smith [1969] has calculated complex Young's and shear moduli, Poisson's ratios, and loss factors for snow in the density range 412–896 kg m^{-3}. Johnson [1978] presents data over the range 210–500 kg m^{-3}, still not adequately covering the range of seasonal snow, 80–300 kg m^{-3}. As we will see below, the density range less than 300 kg m^{-3} may also be much less amenable to continuum treatment than higher densities.

Snow as a Porous Medium

Studies from the viewpoint of snow as a porous medium have been encouraged both by intrinsic interest and by failures of the continuous medium viewpoint. In particular, the continuum viewpoint has not been able to account for the sound velocity and attenuation in lower-density snows, and the complicated phase relationships in snow do not seem amenable to a continuum approach.

Ōura [1952a, b] made the earliest acoustic measurements on snow that I have been able to find. Because of his technique, rather than his viewpoint, his measurements emphasized the porous nature of snow. He worked with low-density snow and excited and detected pressure waves in the air. It is interesting to compare his results with the most recent sound velocity measurements, those of J. L. Smith [1965] and Yamada et al. [1974] (Figure 1). They measured motions in the ice framework. Since shear waves cannot exist in the fluid, the comparison is between Ōura's velocities on the one hand and J. L. Smith's longitudinal and Yamada's P velocities on the other. A continuous, single-valued function of density which explains J. L. Smith's and Yamada's data cannot account for Ōura's. Ōura also mentions measurements of higher velocities in the range from 700 to 1000. He discounts these as being due to transmission through an ice layer underlying his sample. However, the possibility remains that he detected a wave in the ice framework which coupled back into the air [Johnson, 1978].

Ōura's data easily extrapolate to the velocity of sound in air, but it would strain J. L. Smith's and Yamada's data to do the same. Clearly, there are two modes of sound propagation operating here, one associated with the ice framework and one associated with the air. A possible hypothesis from this comparison is that below 200 kg m^{-3} the pore air is more important in sound propagation, while above 300 kg m^{-3}, propagation in the ice network is more important. H. Gubler (personal communication, 1981) believes that air propagation was more important in the lower densities he studied. However, the velocities seismically determined by Bentley et al. [1957] on higher-density snow substantially agree with those of J. L. Smith [1965] and Yamada et al. [1974]. It would be interesting to see some experiments specifically on this point.

Ishida [1965] was the first to treat snow explicitly as a porous medium. He was also the first to recognize the complex nature of the acoustic impedance of snow, an important point which has received too little attention. Ishida's [1965] analysis was not adequate for two reasons. First, he was not able to work around the fact that the sound propagation in air in snow is in an analytically difficult region. It cannot be characterized as either isothermal or adiabatic but falls in the intermediate region. Second, Ishida treated the ice framework as rigid, essentially removing it from the analysis. Undoubtedly, much of his agreement between analysis and experiment resulted from the fact that he only excited and measured air pressure waves.

It is interesting, in view of the above discussion, that Lang [1976] found an average transmission loss versus frequency similar to that found by Ishida [1965]. Lang's measurements were over a distance of 3 m, and his transducers were responsive to motions in the ice framework. As was mentioned above, comparisons among different experiments may not have much meaning because of different experimen-

tal techniques. However, as the data stand, the comparison supports the observation of H. Gubler (personal communication, 1981) that for lower-density snow the major part of the acoustic energy is carried in the pore fluid.

Yen and Fan [1966] calculated the attenuation in a porous medium of nonuniform permeability, intending application to snow. However, their assumptions of isothermal flow [see *Ishida*, 1965], rigid framework, and Darcy flow (see below) are not realistic. They present no experimental data.

Johnson's [1978] results indicate a different frequency function from that of *Ishida* [1965] and *Lang* [1976], which may be due to different experimental conditions or simply to inaccuracies in the data. *Johnson* [1978] did not specify his experimental error but appears to have attained fair agreement between theory and experiment, considering the problems usually involved in these measurements. He attributed the transmission loss-frequency function to the presence of two interacting dilatational waves, one in the ice network and one in the air. *Johnson* [1978] was the first to specifically address this complicated problem in snow. However, *Johnson*'s [1978] calculations indicate that the attenuation attributed to the ice network is much less than that of the pore fluid, the opposite conclusion from that indicated above. *Ōura*'s [1952a] measurements bear on this point. He found a decrease in velocity with increasing density, clearly indicating that the energy he was detecting was carried in the fluid [see *Johnson*, 1978, Figures 3 and 4]. Whether this is because of his experimental techniques or because most of the energy was transmitted in the fluid is a matter of conjecture, but it does raise the latter possibility. More accurate measurements of velocities at lower densities, with detection of both type of waves, are indicated to resolve this problem.

Johnson's [1978] analysis relied heavily on the analysis of *Biot* [1956] and assumed an elastic framework with a compressible viscous pore fluid, seemingly a realistic assumption. Although Johnson's conclusions on attenuation may be in conflict with some experimental evidence, his conclusion that two interacting modes of propagation exist in snow is probably correct. The possible disagreement between observations and Johnson's calculations might come from the fact that Biot includes no loss in the solid framework except through its coupling to the fluid. Perhaps a more complete constitutive model could be used in a sound transmission model similar to Biot's with better results.

The lack of definite statements in this discussion is symptomatic of this field. Comparisons among the various sets of experimental data are difficult and of limited value because of varying techniques and flaws in experimental design. Even with well-designed experiments the intrinsic variability of snow causes large scatter in the data and inconclusive results. *Johnson*'s [1978] analysis may be an adequate representation of sound transmission in snow. However, current experimental evidence is inadequate to prove that it is either adequate or inadequate. More experimental work with careful attention to experimental design, as Johnson recomends, is needed along with critical comparisons between experiment and theory. Also, some method of rationality dealing with the intrinsic variability of snow is needed in this as in most areas of snow research.

A final problem with porous media analyses must be mentioned. These types of analyses depend on Darcy's law. The assumption is always made that since the flow rates are

well below the turbulent range, Darcy's law holds and the permeability measured at higher flow rates (still below the turbulent range) can be used. The only permeability measurements at pressure gradients and flow rates in the sonic range are those of *Martinelli* [1971]. He found very serious deviations from Darcy flow. Martinelli cites similar results in soils but gives no explanation. This point further indicates a lack of complete understanding of the interactions between the solid and the fluid and clearly requires further theoretical and experimental work. Martinelli's observations must be explained before models based on Darcy flow can be relied on.

In addition to understanding the acoustic propagation in snow, the majority of workers hoped to index the snow texture with acoustic properties. The most complete work in this area was done by Nakaya [*Nakaya and Kuriowa*, 1967]. His results must be considered qualitative and tentative because his choice of thick sections (300–600 μm) led to inaccurate grain and pore size measurements [see *Underwood*, 1970]. Other work has been done by *Ishida* [1965], *Nakaya* [1961], *Yamada et al.* [1974], and *Johnson* [1978]. These attempts have not been successful for two reasons. First (with the possible exception of that of Johnson), the analysis of sound propagation as affected by snow texture has been inadequate for the problem. Second, there have been no independent, quantitative texture analyses done on snow to use for comparison. O. Buser (personal communication, 1981) believes he has made progress on the first problem. He is initiating some wave tube experiments to test his analysis. In addition, he has access to texture analysis equipment and techniques [*Good*, 1975] which can provide independent and quantitative measures of snow texture. His results will be of interest.

The possibilities for practical applications of these lines of research to seasonal snow cover problems seem remote at present. However, seasonal snow provides an interesting material in which the interactions of the two different propagation modes are very important. As such, it can be used to test the accuracy and completeness of porous media sound propagation theories.

Gubler [1976, 1977a, b] has completed a study of explosions on snow. His major conclusion is that most of the energy is injected into the snow by the air wave traveling over the surface. His work is of great practical interest in avalanche control and, as was mentioned above, has some fundamental implications.

A noticeable gap in this general field is quantitative experiments on the effect of structure on long-range acoustic propagation.

ACOUSTIC EMISSIONS

The field of acoustic emissions in general can be divided between fundamental and applied studies, and this is true in snow. Pioneering fundamental work has been done by *St. Lawrence and Bradley* [1973, 1975], *St. Lawrence et al.* [1973], and *Bradley and St. Lawrence* [1975]. They found that snow stressed under laboratory conditions emitted acoustic signals similar to those from other materials. The work showed that snow definitely exhibits a Kaiser effect. Later work showed that the Kaiser effect could not be used to determine stress state in an avalanche path, since the sign of the original stress could not be determined. However, continued effort has produced significant success in another

line. *St. Lawrence and Lang* [1981] recently described a constitutive relation for snow under uniaxial deformation. In their texture-oriented relationship they used the acoustic emission rate as a function of strain to determine the grain mobility function. The grain mobility function and a velocity function accurately modeled the plastic part of the stress-strain response of snow in their experiments.

On a practical level, *St. Lawrence and Williams* [1976], *Bowles and St. Lawrence* [1977] and *Sommerfeld* [1977] have investigated the possibility of using low-frequency acoustic emissions as a measure of snow slope stability. Initially, St. Lawrence and I obtained conflicting results. I concluded that there were detectable acoustic emissions preceding avalanches. St. Lawrence did not detect any precursors to an avalanche in his study area. He was able to clearly detect the avalanche itself, surface slides, cornice falls, etc. It now appears that the conflicting results came from a combination of different experimental technique and ambiguities inherent in the precursor data. St. Lawrence recorded his data on a drum recorder. This type of display is more sensitive to isolated, relatively high amplitude spikes. My data were displayed as both counts above a trigger level and as rms voltage levels. My method is more sensitive to persistent, low-level signals and tends to ignore isolated spikes. It is my opinion that any precursor signal must be sustained because unstable slope conditions are sustained for appreciable periods of time. The increases must also be low level because of the mechanical and acoustic properties of snow. It is impossible to introduce a high-amplitude elastic stress wave into snow: a reflection of its nonlinear behavior. Thus any precursor must start at a low amplitude. Then snow has a high attenuation coefficient, and attenuation is greater at high frequencies than low. The result is that individual spikes can only be detected if they occur very near the sensor. My opinion is that during an unstable period, many such spikes occur but, in general, they are quickly attenuated and merge into a low-level, persistent, incoherent increase in the noise at the sensor position.

Recently, *Gubler* [1979] obtained results similar to mine in that he also found a correspondence between the acoustic level and the slope instability. His sensor design was superior to mine in some aspects. We concluded that geophones (velocity gages) were superior in low-frequency response and cost but that for maximum sensitivity the sensor should be mounted in the snow and matched to the snow density with a foam plastic housing. We are now testing a further improvement.

An important question which remains only partially answered is: Are there any avalanches without usable precursors? Small, surface avalanches do not have usable precursors if there is more than 1–1.5 m of snow between the sliding surface and the sensor [*Sommerfeld*, 1980]. Intuitively, it seems likely either that some large avalanches release on the first detectble motion or that precursors are emitted for too short a time to be usable [*St. Lawrence*, 1980]. To date, examination of available data has not revealed an unambiguous case of this sort. The ambiguity comes from the fact that all avalanches which appeared to have no precursors were also avalanches that were triggered well outside the experimental area. The dynamics of the avalanche release may have propagated the instability into the sensor area where none previously existed.

I have observed that some large avalanches release after an unusually quiet period which has followed a period of prolonged high noise. Similar observations have been made in other areas of acoustic monitoring of geological structures [*Hardy and Leighton*, 1980]. Three hypotheses for this behavior are apparent: (1) An initial unstable condition starts near the sensor and then propagates to a different area where it subsequently causes a release. The original unstable area near the sensor has become stable but is then made to fail by dynamic propagation from the distant, unstable area at the time of release. (2) The local area is stressed, causing acoustic emissions. The stress relaxes and then increases again. The Kaiser effect prohibits acoustic emissions until the original stress level is surpassed, so that a slight increase in acoustic emissions indicates a much higher than normal stress level. (3) An instability slowly propagating under increasing stress encounters a hard spot and locks up. The stress increases until the instability can again propagate. At this point it moves into a weaker area where it has enough energy to propagate rapidly and cause complete slope failure. Testing of these hypotheses would require a major study with a very large sensor array, probably coordinated with displacement or strain sensors.

Related to the above is perhaps the most important outstanding question: What is the source of the signals? Source location experiments designed to answer this question have failed, primarily because of an insufficient sensor array. Only a very intensive experiment will provide a satisfactory answer.

SUMMARY AND CONCLUSIONS

Realization of the complexity of sound propagation in snow is aiding in the development of more satisfactory theoretical analyses. *Johnson*'s [1978] model is superior to previous models but still may not be able to represent sound transmission in snow accurately. The next step appears to be a more accurate modeling of the ice framework, particularly for low-density snow. It is also important in experimental work to pay careful attention to the two different models of sound propagation. The experimental results can be different depending on whether the pore fluid or the framework is excited and detected. Because of the complex impedance of snow the distinctions among phase, wave, and group velocities may be important in experiments. Some advances are probable in the relationships between acoustic properties and texture, since there are now techniques for the quantitative characterization of snow texture.

Even with well-designed experiments the intrinsic variability of snow presents severe problems in interpreting experimental data. So far, the variability has been ignored or treated in the most cursory manner.

Acoustic emissions are aiding in the difficult problem of developing constitutive relations for snow. Progress in this area is related to progress in the understanding of snow texture; the mutual interactions of these studies are very promising. The acoustic emissions prediction of avalanche slope instability is at a plateau. With current knowledge a system could be built which would predict major instabilities on particular slopes. Any significant increase of knowledge in this area will require a major increase in experimental complexity and sophistication.

for generous access to all their facilities and services. I am also grateful to H. Gubler for many discussions and help with the literature search on this subject.

REFERENCES

Bentley, C. E., P. W. Pomeroy, and H. I. Dorman, Seismic measurements on the Greenland ice cap, *Ann. Geophys., 13*(4), 253–285, 1957.

Biot, M. A., Theory of propagation of elastic waves in a fluid saturated porous fluid, *J. Acoust. Soc. Am., 28*(2), 168–191, 1956.

Bogorodskii, V. V., V. P. Gavrillo, and V. A. Nikitin, Characteristics of sound propagation in snow, *Sov. Phys. Acoust.,* Engl. Transl., *20*(2), 1974.

Bowles, D., and W. F. St. Lawrence, Acoustic emissions in the investigation of avalanches, *Proc. West. Snow Conf. Annu. Meet. 45th,* 88–94, 1977.

Bradley, C. C., and W. F. St. Lawrence, The Kaiser effect in snow, *IAHS AISH Publ., 114,* 145–154, 1975.

Brown, R. L., Pressure waves in snow, *J. Glaciol., 25*(91), 99–107, 1980.

Chae, Y. S., Frequency dependence of dynamic moduli of, and damping in snow, in *Physics of Snow and Ice,* edited by H. Oura, pp. 827–842, Institute of Low Temperature Science, Hokkaido University, Sapporo, Japan.

Furukawa, I., A study on the absorption of sound by snow (in Japanese), in *Yuki-to-seikatsu,* vol. 5, the Snow Association of Japan, Tokyo, 1953.

Good, W., Numerical parameters to identify snow structure, *IAHS AISH Publ., 114,* 91–102, 1975.

Gubler, H., Künstliche Auslösung von Lawinen durch Sprengungen (Zwischenbericht), *Rep. 32,* Eidg. Inst. für Schnee- und Lawinenforsch., Weissfluhjoch/Davos, Switzerland, 1976.

Gubler, H., Künstliche Auslösung von Lawinen durch Sprengungen, *Rep. 35,* Eidg. Inst. für Schnee- und Lawinenforsch., Weissfluhjoch/Davos, Switzerland, 1977a.

Gubler, H., Artificial release of avalanches by explosives, *J. Glaciol., 19*(81), 419–429, 1977b.

Gubler, H., Acoustic emissions as an indication of decrease in fracture zones of avalanches, *J. Glaciol., 22*(86), 186–187, 1979.

Hardy, H. R., Jr., and F. W. Leighton (Eds.), *Proceedings of the Second Conference on Acoustic Emissions/Microseismic Activity in Geological Structures and Materials,* pp. 459–464, Trans Technical, Clausthal, Federal Republic of Germany, 1980.

Ishida, T., Sound absorption by snow layer (in Japanese, English summary), *Contrib. Inst. Low Temp. Sci. Hokkaido Univ., Ser. A, 12,* 17–24, 1954.

Ishida, T., Acoustic properties of snow, *Contrib. Inst. Low Temp. Sci. Hokkaido Univ., Ser. A, 20,* 23–63, 1965.

Johnson, J. B., Stress waves in snow, thesis, Univ. of Wash., Seattle, 1978.

Lang, T. E., Measurements of acoustic properties of hard-pack snow, *J. Glaciol., 17*(16), 269–276, 1976.

Martinelli, M., Jr., Physical properties of alpine snow as related to weather and avalanche conditions, *U.S. For. Serv. Res. Pap., RM-64,* 1971.

Mellor, M., Properties of snow, Cold Regions Science and Engineering, part II, sect. A, U.S. Army Cold Reg. Res. and Eng. Lab., Hanover, N. H., 1964.

Nakaya, U., Visco-elastic properties of snow and ice in the Greenland ice cap, *Res. Rep. 46,* U.S. Snow, Ice and Permafrost Res. Estab., Hanover, N. H., 1959a.

Nakaya, U., Visco-elastic properties of processed snow, *Res. Rep. 58,* U.S. Snow, Ice and Permafrost Res. Estab., Hanover, N. H., 1959b.

Nakaya, U., Elastic properties of processed snow with reference to its internal structure, *Res. Rep. 82,* U.S. Army Cold Reg. Res. and Eng. Lab., Hanover, N. H., 1961.

Nakaya, U., and D. Kuroiwa, Physical properties and internal structure of Greenland snow, in *Physics of Snow and Ice,* edited by H. Oura, Institute of Low Temperature Science, Hokkaido University, Sapporo, Japan, 1967.

Oura, H., Sound velocity in the snow cover (in Japanese, English summary), *Contrib. Inst. Low Temp. Sci. Hokkaido Univ., Ser. A, 9,* 171–178, 1952a.

Oura, H., Reflection of sound at snow surface and mechanism of sound propagation in snow (in Japanese, English summary), *Contrib. Inst. Low Temp. Sci. Hokkaido Univ., Ser. A, 9,* 179–186, 1952b.

Smith, J. L., The elastic constants; strength and density of Greenland snow as determined from measurements of sonic wave velocity, *Tech. Rep. 167,* U.S. Army Cold Reg. Res. and Eng. Lab., Hanover, N. H., 1965.

Smith, N., Determining the dynamic properties of snow and ice by forced vibrations, *Tech. Rep. 216,* U.S. Army Cold Reg. Res. and Eng. Lab., Hanover, N. H., 1969.

Sommerfeld, R. A., Preliminary observations of acoustic emissions preceding avalanches, *J. Glaciol., 19*(81), 399–409, 1977.

Sommerfeld, R. A., Acoustic emissions from unstable snow slopes, in *Proceedings of the Second Conference on Acoustic Emissions/Microseismic Activity in Geological Structures and Materials,* edited by H. R. Hardy, Jr., and F. W. Leighton, pp. 319–330, Trans Technical, Clausthal, Federal Republic of Germany, 1980.

St. Lawrence, W. F., A structural theory for the deformation of snow, Ph.D. thesis, Mont. State Univ., Bozeman, 1977.

St. Lawrence, W. F., A phenomenological description of the acoustic emissions response in several polycrystalline materials, *J. Test. Eval., 7*(4), 223–228, 1979.

St. Lawrence, W. F., The acoustic emission response of snow, *J. Glaciol., 26*(94), 209–216, 1980.

St. Lawrence, W. F., and C. C. Bradley, Ultrasonic emissions in snow, *Advances in North American Avalanche Technology, U.S. For. Serv. Gen. Tech. Rep., RM-3,* 1–7, 1973.

St. Lawrence, W. F., and C. C. Bradley, The deformation of snow in terms of a structural mechanism, *IAHS AISH Publ., 114,* 155–170, 1975.

St. Lawrence, W. F., and C. C. Bradley, Spontaneous fracture initiation in mountain snowpacks, *J. Glaciol., 19*(81), 411–417, 1977.

St. Lawrence, W. F., and T. E. Lang, A constitutive relation for the deformation of snow, *Cold Reg. Sci. Technol., 4,* 3–14, 1981.

St. Lawrence, W. F., and T. R. Williams, Seismic signals associated with avalanches, *J. Glaciol., 17*(77), 521–526, 1976.

St. Lawrence, W. F., T. E. Lang, R. L. Brown, and C. C. Bradley, Acoustic emission at constant rates of deformation, *J. Glaciol., 12*(64), 144–146, 1973.

Underwood, E. E., *Quantitative Stereology,* Addison-Wesley, Reading, Mass., 1970.

Yamada, T., T. Hasemi, K. Izumi, and A. Sato, On the dependencies of the velocities of P and S waves and thermal conductivity upon the texture of snow, *Contrib. Inst. Low Temp. Sci. Hokkaido Univ., Ser. A, 32,* 71–80, 1974.

Yen, Y. C., and S. S. T. Fan, Pressure wave propagation in snow with nonuniform permeability, *Res. Rep. 210,* U.S. Army Cold Reg. Res. and Eng. Lab., Hanover, N. H., 1966.

Optical Properties of Snow

STEPHEN G. WARREN[1]

*Cooperative Institute for Research in Environmental Sciences, University of Colorado
Boulder, Colorado 80309*

Measurements of the dependence of snow albedo on wavelength, zenith angle, grain size, impurity content, and cloud cover can be interpreted in terms of single-scattering and multiple-scattering radiative transfer theory. Ice is very weakly absorptive in the visible (minimum absorption at $\lambda = 0.46$ μm) but has strong absorption bands in the near infrared (near IR). Snow albedo is therefore much lower in the near IR. The near-IR solar irradiance thus plays an important role in snowmelt and in the energy balance at a snow surface. The near-IR albedo is very sensitive to snow grain size and moderately sensitive to solar zenith angle. The visible albedo (for pure snow) is not sensitive to these parameters but is instead affected by snowpack thickness and parts-per-million amounts (or less) of impurities. Grain size normally increases as the snow ages, causing a reduction in albedo. If the grain size increases as a function of depth, the albedo may suffer more reduction in the visible or in the near IR, depending on the rate of grain size increase. The presence of liquid water has little effect per se on snow optical properties in the solar spectrum, in contrast to its enormous effect on microwave emissivity. Snow albedo is increased at all wavelengths as the solar zenith angle increases but is most sensitive around $\lambda = 1$ μm. Many apparently conflicting measurements of the zenith angle dependence of albedo are difficult to interpret because of modeling error, instrument error, and inadequate documentation of grain size, surface roughness, and incident radiation spectrum. Cloud cover affects snow albedo both by converting direct radiation into diffuse radiation and also by altering the spectral distribution of the radiation. Cloud cover normally causes an increase in spectrally integrated snow albedo. Some measurements of spectral flux extinction in snow are difficult to reconcile with the spectral albedo measurements. The bidirectional reflectance distribution function which apportions the reflected solar radiation among the various reflection angles must be known in order to interpret individual satellite measurements. It has been measured at the snow surface and at the top of the atmosphere, but its dependence on wavelength, snow grain size, and surface roughness is still unknown. Thermal infrared emissivity of snow is close to 100% but is a few percent lower at large viewing angles than for overhead viewing. It is very insensitive to grain size, impurities, snow depth, liquid water content, or density. Solar reflectance and microwave emissivity are both sensitive to various of these snowpack parameters. However, none of these parameters can be uniquely determined by satellite measurements at a single wavelength; a multichannel method is thus necessary if they are to be determined by remote sensing.

CONTENTS

---

[1] Now at Department of Atmospheric Sciences, University of Washington, Seattle, Washington 98195.

A. INTRODUCTION

An understanding of the reflection, absorption, and transmission of light by snow is important for two general applications. The first is the calculation of the radiation budget of snowpacks and the planetary radiation budget over snow-covered surfaces. This is important both for hydrology, because radiation is usually the dominant component in the surface energy budget of snow, and for global climate modeling. The second application is for planning the remote sensing of snowpack properties. This requires modeling of the optical properties at high spectral detail.

Considerable progress has recently been made in under-

standing the optical properties of snow in the solar and infrared regions of the spectrum. The most recent review article was that of *Mellor* [1977]. However, the modeling papers of *Wiscombe and Warren* [1980a] (hereafter WWI) and *Warren and Wiscombe* [1980] (hereafter WWII) included considerable review material. They reviewed earlier theoretical models, snow albedo observations, and the complex index of refraction of ice and reviewed (where necessary to compare with model results) observations of the dependence of snow albedo on wavelength, grain size or age, liquid water content, solar zenith angle, cloud cover, snowpack thickness, and snow density.

This article gives a more thorough review of observations and modeling than did WWI, treats flux extinction and bidirectional reflectance as well as albedo, but especially reviews the considerable work done since WWI and WWII were written, pointing out topics for further research where theories and observations are lacking or in conflict.

This review of optical properties is limited to the parts of the electromagnetic spectrum which are important for determining the climatic role of snow and for affecting snowmelt. These are the solar ($0.3 \le \lambda \le 5$ μm) and thermal infrared ($5 \le \lambda \le 40$ μm) wavelengths. (Radiation of wavelength shorter than 0.3 μm is absorbed in the upper atmosphere and does not reach the surface.) Other parts of the spectrum (microwaves) will be mentioned only for the purpose of contrastive analysis in the discussion of the far-field assumption in scattering theory and in the discussion of remote sensing.

B. DEFINITIONS

Definitions for reflectance are given by *Siegel and Howell* [1972, pp. 47–88] and by *Nicodemus et al.* [1977].

The reflected radiation is not perfectly diffuse but is unevenly distributed among the reflection angles according to the bidirectional reflectance distribution function (BRDF). This function R has units sr^{-1}:

$$R(\theta_0, \theta', \phi_0, \phi', \lambda) = \frac{dI(\theta', \phi', \lambda)}{\mu_0 dF(\theta_0, \phi_0, \lambda)}$$

where (θ_0, ϕ_0) is the incident (zenith, azimuth) angle, $\mu_0 = \cos \theta_0$, (θ', ϕ') the reflection angle, λ the wavelength, F the incident flux (on a surface normal to the beam), and I the reflected intensity. Unless the surface has azimuthally dependent surface features, such as the sastrugi oriented with their long axes parallel to the prevailing wind at the south pole [*Carroll and Fitch*, 1981], the dependence of R on both ϕ_0 and ϕ' reduces to a dependence only on the relative azimuth $\phi_0 - \phi'$.

The albedo a_s is the 'spectral directional-hemispherical reflectance'; it is the integral of R over all reflection angles:

$$a_s(\theta_0, \lambda) = \int_0^1 \mu' \, d\mu' \int_0^{2\pi} R(\theta_0, \theta', \phi', \lambda) \, d\phi'$$

More simply stated, the albedo is just the upflux divided by the downflux at a particular wavelength, usually measured just above the snow surface.

The albedo for hemispherically isotropic incident radiation is the diffuse albedo a_d:

$$a_d(\lambda) = 2 \int_0^1 \mu_0 a_s(\mu_0, \lambda) \, d\mu_0$$

In general, the albedo depends on the distribution of incident radiation with angle.

The spectrally integrated albedo is what is measured by unfiltered radiometers:

$$\bar{a}_s(\theta_0) = \frac{\int a_s(\theta_0, \lambda) F \downarrow (0, \lambda) \, d\lambda}{\int F \downarrow (0, \lambda) \, d\lambda}$$

where $F \downarrow (0, \lambda)$ is the spectral downflux of solar radiation at the surface. The value of $\bar{a}$ thus depends not only on the snow properties and on the sun angle but also on the atmospheric composition (water vapor content, cloud thickness, etc.), which affects the spectral distribution of the sunlight.

It is often convenient to normalize the bidirectional reflectance relative to the albedo. Thus in Figure 14 below is plotted not R but rather the anisotropic reflectance function f:

$$f(\theta_0, \theta', \phi' - \phi_0) = \pi R(\theta_0, \theta', \phi' - \phi_0)/a_s(\theta_0) \qquad (1)$$

The spectral emissivity $\varepsilon(\theta, \lambda)$ depends on emission angle θ and is equal to the absorptivity or the coalbedo $[1 - a_s(\theta_0, \lambda)]$ by Kirchhoff's law [*Siegel and Howell*, 1972].

Deep in a homogeneous snowpack (uniform density and grain size distribution and far from any boundaries) the spectral flux $F \downarrow (\lambda)$ is attenuated approximately exponentially:

$$F \downarrow (\lambda, z + \Delta z) \approx F \downarrow (\lambda, z) e^{-\kappa_s(\lambda) \Delta z}$$

where $\kappa_s(\lambda)$ is the flux extinction coefficient:

$$\kappa_s(\lambda) = -\frac{d \ln F \downarrow (\lambda)}{dz} = \frac{-1}{F \downarrow (\lambda)} \frac{dF \downarrow (\lambda)}{dz}$$

κ_s^{-1} is often reported in units of geometric depth, but it is better expressed in units of liquid equivalent depth in order to avoid effects of snow density variation.

The important quantities for calculating snowmelt are the surface albedo and emissivity. The important quantities for the earth radiation budget are the planetary albedo and the 8- to 12-μm window emissivity. None of these are measured by narrow field of view satellites, which instead measure the planetary bidirectional reflectance R over a particular wavelength band. This can be converted to planetary albedo for the same wavelength band if the anisotropic reflectance function f is known. Further conversion to a surface albedo requires knowledge of the atmospheric vertical structure.

Other symbols used in the paper are as follows:

$g(x, m)$	single-scattering asymmetry parameter;
$\kappa_i(\lambda)$	absorption coefficient of pure, bubble-free, polycrystalline ice;
$\kappa_s(\lambda)$	flux extinction coefficient for snow;
$m(\lambda) = m_{re}(\lambda) - im_{im}(\lambda)$ complex refractive index of ice;
$Q_{ext}(x, m)$	single-scattering extinction efficiency;
r	snow grain radius;
x	size parameter, equal to $2\pi r/\lambda$;
ρ_s	snow density;
$\bar{\omega}$	single-scattering albedo.

C. OPTICAL CONSTANTS OF ICE

Theoretical models of the optical properties of snow require as input the laboratory measurements of the refrac-

tive index m_{re} and absorption coefficient κ_i of pure ice as functions of wavelength. They are combined as the complex index of refraction $m = m_{re} - im_{im}$, where $\kappa_i = 4\pi m_{im}/\lambda$.

Of particular importance for solar albedo calculations are the recent measurements of $\kappa_i(\lambda)$, $0.4 \mu m \leq \lambda \leq 1.4 \mu m$, by *Grenfell and Perovich* [1981]. The absorption coefficient is so small in the visible wavelengths that, to measure it accurately, blocks of bubble-free ice as long as 2.8 m had to be grown in order to obtain sufficient light attenuation.

For $1.4 \leq \lambda \leq 2.8 \mu m$ we recommend the values of $m(\lambda)$ compiled by WWI, and for $2.8 \leq \lambda \leq 33 \mu m$ we recommend the measurements by *Schaaf and Williams* [1973]. The optical constants of ice from 45-nm to 8.6-m wavelength are reviewed by S. G. Warren (unpublished manuscript, 1981).

D. MEASUREMENTS OF REFLECTION AND TRANSMISSION OF LIGHT BY SNOW

1. Albedo

All-wave albedo has been routinely measured on polar expeditions for many years. Time series of albedo show high all-wave albedos (75–90%) in late winter and early spring, dropping as snowmelt begins to about 60%. Such time series have been reported for Greenland by *Ambach* [1963] and *Diamond and Gerdel* [1956]; for Barrow (Alaska) by *Maykut and Church* [1973]; for McCall Glacier (Brooks Range, Alaska) by *Wendler and Weller* [1974]; for McGill Ice Cap (Canada) by *Havens* [1964]; and for snow-covered sea ice in the Antarctic by *Weller* [1968] and in the Arctic by *Langleben* [1971]. Summaries of monthly average or seasonal average all-wave albedos have been reported for Antarctic stations by *W. Schwerdtfeger* [1970, p. 258] and for drifting ice islands in the Arctic by *Chernigovskii* [1963, p. 269]. For the Antarctic Plateau, where snow never melts, Schwerdtfeger found that 'a useful value of 0.8 as the lower limit of surface albedo appears to be certain.'

Apart from these routine measurements, problem-directed research has sought to identify the factors influencing snow albedo. The albedo of both dry snow and melting snow is normally found to increase as solar zenith angle increases, as measured by *Hubley* [1955], *Liljequist* [1956], *Rusin* [1961], *Bryazgin and Koptev* [1969], *Korff et al.* [1974], and *Carroll and Fitch* [1981]. These measurements are examined in section J2 below. Some workers, however, found the opposite trend. *Havens* [1964] reported highest albedos at mid-day, as did *Kondratiev et al.* [1964].

Cloud cover affects both the spectral distribution of irradiance and the effective incident zenith angle. It normally causes an increase in all-wave snow albedo. An increase of 5–10% relative to clear-sky albedo was found by *Liljequist* [1956] and 11% by *Weller* [1968], both on the Antarctic coast, and 5–7% by *Hanson* [1960] at the south pole. However, *Carroll and Fitch* [1981] have now found cloud cover to reduce albedo at the south pole; this can be attributed to the unusually steep dependence of albedo on zenith angle which they find, described in section J2 below. *Grenfell et al.* [1981] found snow albedo to increase with cloud optical thickness at a mid-latitude site.

The effect of snow thickness on the albedo of a thin snowpack over a black surface was investigated by *Giddings and LaChapelle* [1961] for monochromatic light at $\lambda = 0.59 \mu m$. They found the snow albedo to reach within 3% of its asymptotic value at a depth of 8 mm (liquid equivalent), as did *O'Neill and Gray* [1973] for broadband-filtered sunlight, $0.3-1.1 \mu m$. However, *Warren and Wiscombe* [1980, p. 2742] think that these snow samples were probably somewhat contaminated and that pure snow would require 4 times this thickness to reach within 3% of the semi-infinite albedo.

The reduction of albedo due to snow aging has been documented for visible wavelengths by *Holmgren* [1971] and *Grenfell and Maykut* [1977] and for the near IR by *O'Brien and Munis* [1975]. *Grenfell et al.* [1981] studied the progress of spectral albedo changes $(0.4 \leq \lambda \leq 2.5 \mu m)$ due to snow aging.

Spectrally detailed measurements are necessary for an understanding of the physical processes affecting snow albedo. Many of these measurements were reviewed by WWI and WWII. The most accurate measurements are probably the following. Albedo measurements in four spectral bands for clean Antarctic snow were made by *Liljequist* [1956]. High spectral resolution albedo measurements were reported for $0.4 \leq \lambda \leq 1.0 \mu m$ on the Arctic Ocean by *Grenfell and Maykut* [1977], for $0.4 \leq \lambda \leq 1.5 \mu m$ at South Pole Station by *Kuhn and Siogas* [1978], for $0.4 \leq \lambda \leq 2.5 \mu m$ in the Cascade Mountains by *Grenfell et al.* [1981], and for $0.34 \leq \lambda \leq 1.1 \mu m$ on the Great Lakes by *Bolsenga* [1981].

Grenfell and his colleagues have developed a portable (16 kg) scanning spectrophotometer for field measurements. The instrument described by *Roulet et al.* [1974] was useful for $0.4 \leq \lambda \leq 1.0 \mu m$; it has been improved by *Grenfell* [1981] with the use of a circular variable interference filter for $\lambda < 1.375 \mu m$ (resolution $\Delta\lambda \leq 0.03 \mu m$) and fixed wavelength filters to extend the wavelength range out to $2.45 \mu m$ ($\Delta\lambda \approx 0.1 \mu m$).

2. Bidirectional Reflectance

The bidirectional reflectance measurements of *O'Brien and Munis* [1975] were designed principally to investigate the spectral dependence of reflectance for $0.6 \leq \lambda \leq 2.5 \mu m$; only a narrow range of incidence and detector angles was employed. Although they are not albedo measurements, they were used as proxy evidence for near-IR spectral albedo and its dependence on snow age by the albedo-modeling efforts of *Choudhury and Chang* [1979a, b] and *Wiscombe and Warren* [1980a].

Measurements of spectrally integrated bidirectional reflectance over a large range of angles were made by *Dirmhirn and Eaton* [1975]. Measurements over a restricted range of angles but for a variety of snow types were reported by *Middleton and Mungall* [1952]. Section L below reviews these as well as the aircraft measurements of *Griggs and Marggraf* [1967] and *Salomonson and Marlatt* [1968a, b]. The dependence of the BRDF on wavelength, grain size, and surface irregularity has not been adequately studied either experimentally or theoretically.

3. Flux Extinction

The monochromatic flux extinction coefficient $\kappa_i(\lambda)$ decreases rapidly with depth near the surface where a significant fraction of the upwelling radiation escapes the snowpack. Below a few centimeters depth the effect of the top boundary is no longer noticeable, and one measures an 'asymptotic' monochromatic flux extinction coefficient which is independent of depth for a homogeneous snowpack. The asymptotic flux extinction coefficient has been mea-

TABLE 1. Models for the Optical Properties of Snow

Reference	Input Parameters	Grain Size Enters	Wavelength Dependence Examined	Anisotropic Scattering Considered	Sun Angle Dependence	Thin Snow Treated	Comments
Dunkle and Bevans [1956]	t, m	as t	yes				yes	for diffuse incidence and high albedo
Giddings and LaChapelle [1961]	l, m_{im}	as l					yes	for diffuse incidence and high albedo
Barkstrom [1972]	ω, θ_0				yes		must be tuned
Barkstrom and Querfeld [1975]	ω, g, θ_0	yes		yes	yes	yes	unrealistic g
Bohren and Barkstrom [1974]	r, m	yes		yes			for diffuse incidence and high albedo
Berger [1979]	m, ρ_s	yes	yes	yes			for high infrared emissivity
Choudhury and Chang [1979a, b]	r, m, β	yes	yes	yes		yes	for diffuse incidence and albedo ≥ 0.1
Wiscombe and Warren [1980a]	r, m, θ_0	yes	yes	yes	yes	yes	used in this paper
Choudhury and Chang [1981]	r, m, θ_0, s^2	yes	yes	yes	yes		'surface reflection' included

Symbols used are as follows: g, single-scattering asymmetry parameter; l, photon mean path length through ice; $m = m_{re} - im_{im}$, complex index of refraction of ice; r, snow grain radius; s^2, variance of surface facet slopes; t, ice lamina thickness; β, single-scattering backscattered fraction; θ_0, solar zenith angle; ρ_s, snow density; and ω, single-scattering albedo.

sured as a function of wavelength by *Liljequist* [1956] and with better spectral resolution by *Grenfell and Maykut* [1977] and *Kuhn and Siogas* [1978]. These relatively monochromatic measurements are better suited to testing theoretical models than are all-wave extinction measurements and are discussed below in section 12.

Only a few such monochromatic measurements of flux extinction have been reported. Far more commonly measured is the attenuation of all-wave solar radiation in snow, which has been reported by (among others) *Ambach and Habicht* [1962], *Ambach* [1963], *Weller* [1969], and *Schwerdtfeger and Weller* [1977]. A number of other measurements were reviewed by *Mellor* [1977], who also clearly explained intuitively the fact that κ_s decreases as grain size increases. Unlike the monochromatic $\kappa_s(\lambda)$ the all-wave κ_s does not quickly reach an asymptote. It decreases with depth because of the changing spectral composition of sunlight with depth. At great depth, where all but the blue light is filtered out by the snow, κ_s will reach the asymptotic value corresponding to $\lambda = 0.46 \mu m$.

4. Intensity Extinction

The extinction and scattering of a directed beam of monochromatic radiation as a function of angle and depth in the snowpack has been studied by Ambach and his coworkers [e.g., *Ott*, 1974]. These measurements could be useful for testing future models which may attempt to calculate intensities as well as fluxes within the snowpack.

E. MODELING THE OPTICAL PROPERTIES OF SNOW

Modeling of the reflection and transmission of light by snow has nearly a 30-year history. A rather oversimplified summary is given in Table 1. The early models of *Dunkle and Bevans* [1956] (hereafter DB) and *Giddings and LaChapelle* [1961] did not explicitly compute scattering by individual ice grains but set up a two-stream radiative transfer framework which required two input parameters. These two parameters can be loosely related to an effective grain size and an absorption coefficient, but they are normally found by fitting

experimental data. Because these models are computationally simple, they have been used extensively for fitting albedo and flux extinction data [e.g., *Weller*, 1969; *P. Schwerdtfeger*, 1969; *Bergen*, 1970, 1971, 1975; *Schlatter*, 1972; *O'Neill and Gray*, 1973]. However, they are not generally applicable outside the wavelength range where they are tuned.

The application of modern radiative transfer theory to snow was pioneered by Barkstrom and Bohren, who started with the single scattering by individual ice sphere and used a number of approximations to relate these to observable quantities. *Bohren and Barkstrom* [1974] (hereafter BB) obtained very simple equations which (as shown below) are applicable only for the visible wavelengths. *Choudhury and Chang* [1979a] also started with single scattering by ice particles and used a two-stream method for radiative transfer. They did not attempt to derive simple parameterizations as had BB. Their model is applicable over a wider wavelength range than is BB's and is more accurate than the model of DB.

The most accurate model now available for computing radiant fluxes in snow (short of a much more costly doubling or discrete ordinates method) is the delta-Eddington/Mie theory model used by WW1. Although we sometimes use it in this section as a benchmark to criticize other models, one should keep in mind that the WW1 model still has shortcomings, which are discussed in later sections of this paper: it neglects effects due to close packing (which restricts its validity to $\lambda \leq 20 \mu m$) and nonsphericity of snow grains (which may cause errors at very large solar zenith angles $\theta_0 \rightarrow 90°$), and it calculates only fluxes, not intensities, so it says nothing about the BRDF. However, it has proven very useful in explaining quantitatively the influence of snow parameters and environmental parameters on spectral albedo.

1. Early Two-Stream Models

Dunkle and Bevans modeled the snowpack as a stack of horizontal ice layers. They calculated the Fresnel reflection

at normal incidence on each layer, as well as the absorption of light passing vertically through the layer according to Sauberer's [1950] measurements of κ_i. Given these reflection and absorption coefficients, as a function of wavelength, they used the Schuster two-stream method to examine the dependence of albedo on the thickness of the ice layers. In Figure 1 we reproduce Figure 3 of DB together with the more accurate calculations of the Wiscombe-Warren model, assuming that DB's layer thickness represents the snow grain diameter. The DB model gives the correct qualitative behavior of a_d/r, λ), showing the decrease of albedo due to increased grain size as the snow ages, as well as the fact that albedo is lower in the near IR than in the visible. However, there are substantial errors. These errors are due to treating the ice as sheets rather than as particles, the assumption of normal incidence Fresnel reflectivity, and the use of two-stream theory (An additional small part of the discrepancy is due to the WWI model's use in Figure 1 of the new measurements of m_{im} by Grenfell and Perovich [1981].)

DB gave formulas for both albedo and transmittance for both thin snow and semi-infinite snow. Although they obtained their absorption and reflection coefficients from laboratory mesurements on pure ice, later users of their model have treated these coefficients as two adjustable parameters to be fit to field observations of snow.

Giddings and LaChapelle [1961] (hereafter GL) used a diffusion model which, like DB's, also employs two adjustable parameters, a diffusion coefficient and an absorption coefficient. The GL model is actually equivalent to the DB model, because the diffusion approximation is a form of two-stream approximation. (Recently, both Meador and Weaver [1980] and Zdunkowski et al. [1980] have shown that all two-stream approximations are equivalent and can be put into a common framework.) The diffusion coefficient was related to a length l which is the average distance a photon travels through ice between air-ice interfaces, so it is interpreted as the effective grain diameter. GL estimated that the simple diffusion model was accurate if there were a large number of scatterings before the absorption of a photon, that is, if $a_d \gtrsim 0.8$. Correcting for 'nondiffuseness' (taking into account the nonunit ratio of downflux to upflux, $F\uparrow/F\downarrow < 1$) was thought to extend the validity of the model down to albedo as low as 0.5.
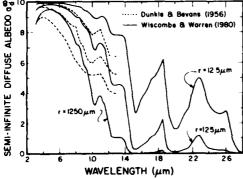

Fig. 1. Model calculations of semi-infinite diffuse albedo as a function of wavelength for various snow grain radii. Dashed lines are calculations by Dunkle and Bevans [1956, Figure 3]. Solid lines are calculations using the model of WWI, with the new m_{im} (λ) measured by Grenfell and Perovich [1981].

For small absorption (large albedo), equations 13 and 21 of GL imply that $1 - a_d \propto r^{1/2}$, a result also obtained later by Bohren and Barkstrom [1974].

GL made measurements of albedo and transmission of thin snow over a black background for monochromatic light ($\lambda = 0.59$ μm) to determine the two free parameters in the diffusion model. They found the same two parameters to fit both the albedo data and the transmission data. However, the value of l obtained was 20 times the grain radius estimated by eye, $l = 20r$, whereas it should be $l = 2r$ according to the interpretation of l as grain diameter.

GL also analyzed the disturbance of the radiation field due to a radiometer inserted into the snow. The instrument measures less downflux than would be present in the undisturbed snow because it is blocking some of the upflux that otherwise could be scattered back down. This is one of the reasons why transmission measurements are more difficult than albedo measurements.

2. Single-Scattering by Ice Grains Introduced

The scattering and absorption of radiation by a single ice particle are described by three quantities:

1. Extinction efficiency Q_{ext} is the ratio of the extinction cross section to the geometric cross section. For large particles ($r \gg \lambda$), Q_{ext} is close to its geometric optics limit of 2.

2. Single-scattering albedo $\tilde{\omega}$ is the ratio of scattering efficiency to extinction efficiency. It is the probability that a photon intercepted by a particle will be scattered rather than absorbed.

3. Phase function $P(\Omega_1, \Omega_2)$, when multiplied by $\tilde{\omega}$, gives the probability that a photon incident from angle $\Omega_1 = (\theta_1, \phi_1)$ will be scattered into angle $\Omega_2 = (\theta_2, \phi_2)$. For a spherical particle, P is a function only of the cosine of the scattering angle $\Omega_2 \cdot \Omega_1$. The complete phase function is needed for computing intensity, but for computing fluxes normally only a single measure of the anisotropy of P is needed, commonly the asymmetry parameter g, which is the mean value of $\Omega_2 \cdot \Omega_1$, or the backscattered fraction β [Wiscombe and Grams, 1976; Zdunkowski et al., 1980].

Both $\tilde{\omega}$ and g are dimensionless with ranges $0 \leq \tilde{\omega} \leq 1$ and $-1 \leq g \leq 1$; $g = 0$ corresponds to isotropic scattering, and $g = 1$ to completely forward directed scattering.

Barkstrom [1972] assumed the snowpack to be semi-infinite, grey, and isotropically scattering. He introduced a zenith angle dependence by solving the radiative transfer equation for intensity. This was then integrated to get flux in terms of the X functions of radiative transfer. He calculated that albedo would increase with zenith angle in approximate agreement with measurements of Rusin [1961] and Liljequist [1956]. He also showed that the (monochromatic) flux should decrease faster than exponentially at the surface but at great depth should decrease exponentially, $dF\downarrow/dz = -\kappa_s F\downarrow$, with κ_s independent of solar zenith angle.

The first consideration of the anisotropic scattering by ice grains was that of Barkstrom and Querfeld [1975], who attempted to explain the bidirectional reflectance measurements of snow by Middleton and Mungall [1952]. Barkstrom and Querfeld used the adding-doubling method for radiative transfer. However, in order to match Middleton and Mungall's measurements they required quite unrealistic values of asymmetry parameter ($g = 0.5$, corresponding to $r = 0.1$ μm,

whereas $g \approx 0.9$ for a realistic grain size $r > 50 \mu m$).

Bohren and Barkstrom [1974] used geometrical optics in the limit of small absorption to calculate the scattering by individual ice spheres. They obtained $g = 0.874$, close to the asymmetry parameter found in exact Mie calculations for a wide range of particle sizes ($g \approx 0.89$ for $\lambda < 1 \mu m$ in Figure 4 of WW1). The geometrical optics calculation also showed that the scattered light was due mostly to refraction rather than reflection.

BB made a number of approximations which used the assumption that $\kappa_i r \ll 1$, which means that their results apply only to the visible wavelengths. They obtained simple formulas for albedo under isotropic illumination.

$$a_d = 1 - 8.43(\kappa_i r)^{1/2} \qquad (2)$$

and for asymptotic flux extinction coefficient,

$$\kappa_* = 0.65(\kappa_i/r)^{1/2} \qquad (3)$$

where depth is measured as liquid-equivalent depth. Neither (2) nor (3) involves snow density. (BB's formula did show κ_* to be proportional to snow density, but this dependence disappears if we measure depth as liquid-equivalent depth. We do this in order to investigate possible near-field effects which are ignored in all published models and which would introduce a density dependence into (2) and (3), as discussed in section E5 below.)

Figures 2 and 3 compare equations (2) and (3) with the more accurate results of WW1 for several wavelengths. Figure 2 shows that the albedo is indeed proportional to $r^{1/2}$ for $\lambda < 0.8 \mu m$. Accordingly, BB found good agreement of (2) with *Liljequist*'s [1956] observations of high visible albedos ($a_d \approx 0.96$) using Liljequist's measured grain size $r = 150 \mu m$; this is the wavelength region where (2) is applicable. However, (2) becomes useless as ice becomes more absorptive in the near IR. At $\lambda = 1.3 \mu m$, for example, (2) predicts negative albedos for $r > 110 \mu m$. Figure 3 shows that the flux extinction formula (3) is better behaved than the
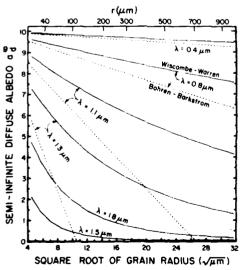
Fig. 3. Asymptotic flux extinction coefficient κ_* versus $(1/r)^{1/2}$ for three discrete wavelengths. Solid lines are calculated using WW1 model. Dashed lines are calculated using equation (37) of *Bohren and Barkstrom* [1974].

albedo formula. The results of the WW1 model show that κ_* $\propto r^{-1/2}$, as (3) predicts, but that the WW1 model increasingly deviates from (3) as $\kappa_i(\lambda)$ increases ($\kappa_i(1.5) > \kappa_i(1.8) > \kappa_i(1.3$ μm)). It may be that snow albedo and flux extinction can be parameterized by simple formulas like (2) and (3), but more work is needed to develop parameterizations that are applicable over wider wavelength ranges.

Berger [1979] adapted the Bohren-Barkstrom theory for the limit of large absorption, assuming that any photon entering an ice sphere is absorbed by it. This assumption makes the optical properties independent of grain size. Berger's interest was to model the infrared emissivity of snow, and his large-absorption approximation is reasonable for $r > 100 \mu m$ in the thermal infrared, as we show below in section M1. Berger found the emissivity ϵ to depend on snow density ρ_s, with ϵ increasing as ρ_s decreases, owing to the reduced average angle of incidence on spheres in a regular array. This may be unrealistic, because the derivation depends on the particular spherical shape of ice grains and on the assumption that they are in a regular array. However, Berger found the dependence of ϵ on ρ_s to be weak (Figure 17 below).

The next experimental advances which stimulated further modeling were the spectral bidirectional reflectance measurements of *O'Brien and Munis* [1975]. *Choudhury and Chang* [1979a, b] (hereafter CCa and CCb) used the Sagan-Pollack two-stream model, which was rather good at all wavelengths, and they obtained tolerable agreement with O'Brien and Munis' measurements (uncorrected for the reflectance of the BaSO₄ standard). In contrast to the models of DB, GL, and BB, none of which were applicable for $a_d >$ 0.5, the Choudhury-Chang model became inaccurate only for $a_d < 0.1$ (compare Figure 4 of CCa with Figure 1 of CCb). In their two-stream model, CC assumed a backscatter fraction (7.5%) independent of wavelength, using single-scatter-


Fig. 2. Diffuse albedo versus square root of grain radius for six discrete wavelengths. Solid lines are calculated using WW1 model. Dashed lines are calculated using equation (42) of *Bohren and Barkstrom* [1974].
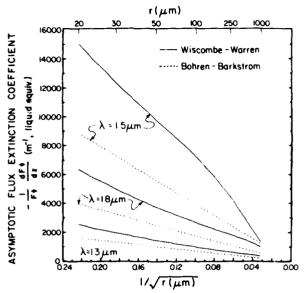
:ulated from r and m_{im} by means of a param-
: to *Sagan and Pollack* [1967]: $\omega - \frac{1}{2} + \frac{1}{2} \exp$
b is an adjustab. parameter taken as $b - 1.67$
$b = 2.0$ by CCb. These approximations make
ream model more accurate than the DB two-
. In CCb a 'surface reflection' term was
iich calculated the Fresnel reflection from a
:e at the snow surface. However, the perfor
two CC models were not compared with each
of these papers, so the effect of the hypotheti-
/er is not clear.

-Warren Model

es in modeling made by WWI were to use Mie
ory. which made the single-scattering calcula-
at all wavelengths and for all grain sizes, and
·lta-Eddington approximation [*Joseph et al.*,
lle the anisotropic phase function, which al-
xdel to calculate albedo for any solar zenith
an arbitrary mix of diffuse and direct radiation.
measurements of visible spectral albedo by
Maykut [1977] further inspired WWII to adapt
calculate the effect of absorptive impurities on

ack was modeled as ice spheres, and it is
WI why the effects of nonsphericity should be
ion to the effects of grain size variation. The
J absorption of light by single ice spheres is
Mie theory. Mie calculations, even using the
ns of *Wiscombe* [1980], are extremely time
ir the larger snow grain sizes. However, for
ains (actually for any grains whose size param-
0, where x is the ratio of the circumference of
the wavelength of light). asymptotic formulae
:veloped [*Nussenzveig and Wiscombe*, 1980]
ficiently accurate and much faster than the Mie

assumes that the particles behave as isolated
they are not sufficiently separated, then near-
/ill be observed that are not predicted by Mie
examined this question in their section 7 and
it the near-field effects are probably negligible
he solar spectrum. They become important at
:ngths, and a criterion for estimating them is
ow in section E5.
scattering quantities Q_{ext}, ω, and g at a particu-
h are functions of the complex refractive index
'ective snow grain radius r. (This is the area-
an radius, which is always larger than the
ited mean radius.) These single-scattering
:ome the input to a multiple-scattering model.
xdel for snow albedo is the delta-Eddington
iuse it can adequately handle the extreme
' scattering by ice particles in snow, in which a
of the scattered light is only slightly deflected.
lington method is designed to be efficient and
:alculating radiant fluxes.
can also be used to calculate snow infrared
described below in section M.
ngth dependence of snow albedo is controlled

snow spectral albedo is highly sensitive to grain size and
moderately sensitive to solar zenith angle and, in the visible
wavelengths only, to trace amounts of absorptive impurities.
The principal results of the model are summarized in the
appropriate sections below.

4. Choudhury-Chang Model

Choudhury and Chang [1981] (hereafter CC81) and
Choudhury [1981] have now abandoned the two-stream
approach in favor of the delta-Eddington method. (*Dozier et
al.* [1981] have shown that although not obvious, equation
(28) of CC81 is indeed equivalent to equation (4) of WWI.
This is the special case of direct incidence on a semi-infinite
snowpack, where a_v' is a function of only the three parame-
ters ω, g, and μ_o.)
Instead of doing Mie calculations, CC81 used the Sagan-
Pollack approximation for ω mentioned above and a param-
eterization for g which they devised to mimic some pub-
lished results from Mie theory. However, these
approximations are quite good at mimicking the Mie results,
at least for the larger grain sizes. Thus the spectral albedo
calculations of CC81 would be nearly identical to those of
WWI, except for the use by CC81 of a special 'surface
reflection' term. This feature of the CC81 model has been
criticized by *Warren and Wiscombe* [1981], who think that
CC81's special accounting of surface reflection is unneces-
sary for ordinary snow in the solar spectrum. Warren and
Wiscombe's main points are as follows: (1) The nature of the
interaction of electromagnetic radiation with a snowpack
depends on the ratio d/λ, where d is the interparticle (center
to center) separation; snow does exhibit a 'surface' to radio
waves but not to sunlight. (2) Even if one does want to
include a surface reflection treatment for special situations
that would require it, it is formulated incorrectly by CC81.
(3) The reason for introducing surface reflection, namely, to
match wavelength-integrated albedo observations, is insuffi-
cient, because the model-measurement discrepancy could in
this case be due to errors in the atmospheric radiation model
instead of the snow albedo model.
There is also no need to invoke a special surface reflection
to explain the enhanced specular reflection peak at low sun
angle. The explanation for specular reflection in terms of
standard single-scattering and multiple-scattering theory is
included below in the section on zenith angle dependence
(section J).
Although CC81's use of a surface reflection term for a
homogeneous snowpack of small, randomly oriented grains
seems inappropriate, such a separate modeling of surface
reflection could indeed be required for a highly nonrandom
surface, in particular for the case of glazed crust, or 'firn-
spiegel' [*LaChapelle*, 1969, Figures 59 and 60].

5. Neglected Effects

a. *Near-field effects.* Because snow particles are close-
ly packed, they may be in each other's 'near field,' meaning
that Mie scattering theory is inapplicable. The problem of
near-field interference was mentioned by BB, who cited
experiments by *Blevin and Brown* [1961] on the density
dependence of the albedo of pigments as evidence that near-
field effects would be unimportant for snow of ρ, < 0.45 g

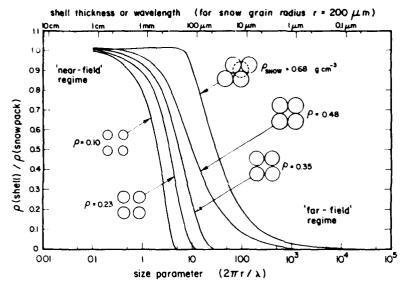shell thickness or wavelength   (for snow grain radius r = 200 μm)

Fig. 4. Transition from region of validity of far-field approximation to near-field regime. The assumption is made that single-scattering properties of a sphere are influenced only by that part of the surrounding medium which is within one wavelength distance of the surface of the sphere. A spherical shell of thickness λ (surrounding the ice particle of radius r) contains mostly the matrix material (air) if the shell is thin ($\lambda \ll r$) but contains an increasing fraction of ice fro: other spheres as the shell expands. The ratio of the density in the shell to the density of the bulk medium (spheres plus air) is plotted as a function of size parameter or shell thickness for five different regular arrangements of spheres: (1) hexagonal close packing (ρ_{snow} = 0.68 g/cm³), (2) simple cubic packing, spheres in contact (ρ_{snow} = 0.48), (3) simple cubic packing, spheres not quite in contact, interparticle gap of 0.22r (ρ_{snow} = 0.35) (4) interparticle gap of 0.56r (ρ_{snow} = 0.23), (5) interparticle gap of 1.33r (ρ_{snow} = 0.10).

ity. WWI reviewed the possible near-field effects and ted out that interparticle interference should be neglect- or particles whose center-to-center separation d is large mparison to the wavelength λ. Since $d \gg \lambda$ in the solar trum. no interference should be observed, and this is irmed by Bohren and Beschta's [1979] observation that albedo of a thick snowpack is independent of density. microwaves, where $d \leq \lambda$, interference effects will arise, ing snow microwave emissivity a function of snow ity. Both $\bar{\omega}$ and g are altered. It is possible to make a h estimate of the effect using Gate's [1973] adjustment lie theory to investigate this dependence on density. simply altered m_{re} of the medium to be not that of air ather a volume-weighted mean of m_{re} (air) and m_{r_i} (ice). 'medium' should probably be taken to be a shell. one or w wavelengths thick. surrounding the particle. The ition from the far-field regime to the near-field regime ld then be described qualitatively by Figure 4. Roughly d. snow is safely in the far-field regime for $\lambda < 1\ \mu$m and e near-field regime for $\lambda > 1$ cm, with a transition region se location depends on snow density.

is possible that near-field effects could become impor- for flux extinction (and for the albedo of thin snow) even n they do not affect the albedo of deep snow. This is use the albedo of deep snow depends on g and $\bar{\omega}$ but not $?_{ext}$, whereas the asymptotic flux extinction coefficient nds on Q_{ext} as well. Whether the near-field approach of v grains could in some wavelength region significantly t Q_{ext} but not g or $\bar{\omega}$ is an open question.

Surface irregularity. The model calculations of albe- ll assume that the snow surface is flat. Surface irregular- can reduce the albedo relative to that of a flat surface if

the height scale of the irregularities is comparable to or larger than the length scale and if both scales are comparable to or larger than the penetration depth of light (which depends on μ_o). This means that surface roughness of $\gtrsim 10$-cm amplitude (such as suncups) is required to reduce visible albedo but that much smaller irregularities can affect near-IR albedo. The albedo is reduced relative to that of a flat surface because some of the light reflected from a slope does not escape to space but instead is intercepted by the slope facing it. There is, of course, no enhancement of absorption if the albedo of the flat surface is 0.0 or 1.0; the enhancement must reach a maximum at some intermediate value of albedo. Pfeffer [1982] has developed a model for use in calculating the enhanced absorption due to glacier crevassing, and his model might be adapted to the study of smaller irregularities.

F. Effect of Snow Grain Size on Albedo

Figure 1 shows the calculated spectral albedo of snow for diffuse incident radiation for three different grain sizes expressed as spherical radii r. These radii were chosen for comparison with Figure 3 of DB. but the smallest size is probably unrealistic. To match reflectance measurements of O'Brien and Munis [1975] for new snow. WW1 never needed grain sizes smaller than $r = 50\ \mu$m. What the optically equivalent sphere would be for a nonspherical snow particle is discussed below.

The albedo is very high in the visible wavelengths. corre- sponding to the minimum in m_{im}, and lower in the near infrared. The albedo drops at all wavelengths as the grain size increases. It is easy to understand why albedo should decrease with increasing grain size. Roughly stated. a pho- ton has a chance to be scattered (or a ray to be bent) when it

crosses an air-ice interface. It has a chance of being absorbed only while it is passing through the ice. An increase in grain size causes an increase in the path length that must be traveled through the ice between scattering opportunities. (A similar dependence of reflectance on sand grain size was found by *Leu* [1977] for beach sand, which is in some ways analogous to snow.)

On the basis of matching the model results to observations of *O'Brien and Munis* [1975] (see Figures 10 and 15 of WW1) the optical grain size of the snow surface generally varies in the range from 50 μm for new snow to 1 mm for old melting snow. This increase of grain size with increasing age is the normal situation, but there can be curious exceptions. *Liljequist* [1956] routinely observed the albedo at Maudheim (on a small ice shelf at the coast of Antarctica) to be low after a new snowfall and to rise after a windstorm. At the very cold temperatures of Maudheim, snow metamorphism apparently proceeds so slowly that grain size changes may be due to other effects. Wind probably caused a reduction in grain size by breaking the crystals and possibly also by gravitational sorting. The latter sould cause the smallest particles to settle out last, so they would end up at the surface, where they would dominate the albedo.

1. The Optically Equivalent Sphere

How a field measurement of snow grain size translates into the radius of the optically equivalent sphere is a subject of current research. *O'Brien and Koh* [1981] found that the 'equal projected area' assumption gave an overestimate of the radius of the equivalent sphere. Comparison of *Grenfell et al.*'s [1981] albedo measurements with Figure 1 shows that their report of grain radius as half the minimum dimension of the snow grain is a factor of 2–5 smaller than the optical grain size. The best conversion procedure must lie between these two extremes and is probably that suggested by *Dobbins and Jizmagian* [1966] (and by WW1). Namely, the optically equivalent sphere is that which has the same volume-to-surface ratio V/S as the nonspheri snow particle. The results of *Pollack and Cuzzi* [1980] also suggest this. (In the case of a sphere, of course, all three definitions of grain size converge.)

However, any attempt to treat a nonspherical particle as an equivalent sphere involves a compromise, because the sphere with the correct ω may not have the correct g. Furthermore, the sphere which gives the correct ω at one wavelength may not do so at another wavelength. The sphere with the same V/S is likely to be most appropriate at wavelengths where absorption is small, $\kappa_i r \ll 1$.

2. Grain Size Increasing with Depth

The albedos in Figure 1 are for a homogeneous snowpack, that is, one whose average grain size does not vary with depth. Grain size is observed to increase with depth in a predictable manner in the Antarctic but can, of course, both increase and decrease with depth at mid-altitudes. In order to affect the shape of the spectral albedo curve the grain size must change rapidly with depth; the most likely situation where this effect would be noticed is for a very thin layer of new snow on a thick layer of old snow. This effect has been calculated by S. G. Warren and W. J. Wiscombe (unpublished data, 1981). An increase of r with depth corresponding to about one-third the rate of increase found in the top

centimeter at the south pole [*Stephenson*, 1967, Figure 8], causes a greater decrease in visible albedo than in near-IR albedo. This is due to the greater penetration depth of the visible light, which thus 'sees' a larger average grain size. For faster rates of radius increase with depth, however, another effect takes over. The albedo drops more in the 1-μm region than in the 0.4-μm region. Reference to Figure 1 explains this: the albedo is insensitive to grain size where albedo is very high (0.4 μm) or very low (2.8 μm) but highly sensitive in the region of intermediate albedo (1 μm).

3. Snow Density

There have been many reports of snow albedo decreasing as density increases. Neither BB nor WW1 nor CC obtained a density dependence in their models. The observed dependence of albedo on density might actually be a dependence on grain size, since density normally increases as grain size increases. *Bohren and Beschta* [1979] isolated the two parameters, finding albedo unchanged when density was artificially increased at presumably constant grain size.

Density enters *Bergen*'s [1975] model as a parameter used in computing the air permeability, which is used to compute V/S, which in turn is used to compute the reflection coefficient in the DB model. We interpreted grain size above as proportional to V/S, so it appears that Bergen's dependence of albedo on density could actually be translated into a grain size dependence, when grain size is defined as above.

G. EFFECT OF LIQUID WATER CONTENT

WW1 cited both experimental and theoretical evidence that the effect of liquid water on snow albedo is simply to increase the effective grain size, because the refractive index contrast between water and ice is very small. We wish only to add a footnote to that statement here. *O'Brien and Koh* [1981] have pointed out that the slight differences (a few percent at some near-infrared wavelengths) in reflectance noted between wet melting snow and the subsequently refrozen snow (Figure 5) are in the right direction and of the right magnitude to be attributed to the difference in spectral m_{im} of water and ice. This is most obvious between 1.2- and 1.4-μm wavelength.

H. EFFECT OF IMPURITIES ON SNOW ALBEDO

WW1 modeled an impure snowpack as a mixture of ice particles and dust or soot particles. They showed that small amounts of impurities affect snow albedo only in the spectral region where absorption of light by ice is weakest, mainly in the visible ($\lambda < 1$ μm). Reductions of visible albedo by a few percent can be caused by ~10 parts per million by weight (ppmw) of desert dust or ~0.1 ppmw of carbon soot. A given amount of an absorptive impurity causes a greater reduction in albedo for coarse-grained snow than for fine-grained snow, as will be illustrated in Figure 7.

1. Soot

WW1 and WW2 showed that some published low values of visible spectral albedo for apparently clean snow could be explained by the model only if the measured snow sample had contained a grey absorber such as soot. Discrepancies between model and observation were obvious for the recent careful spectral albedo measurements of *Grenfell and May-*
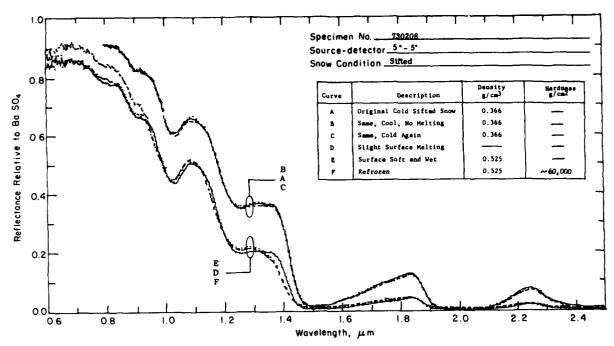
Fig. 5. Effect of liquid water on snow spectral reflectance. (Figure 6 cf *O'Brien and Munis* [1975].)

kut [1977] at Arctic ice island T-3 and *Kuhn and Siogas* [1978] at the south pole.

Figure 6 shows that the model for pure snow may predict albedos up to 15% higher than those which are actually observed. Unrealistically large grain sizes could reduce the calculated visible albedo but would destroy the agreement with observation in the near IR. The two major effects which are neglected in the model, namely, nonsphericity of snow grains and near-field scattering, were judged (section 7 of WWI) to be orders of magnitude too small to be responsible for the discrepancy. Insufficient snow depth and error in laboratory-measured ice absorption coefficient were also ruled out as the explanation, leaving impurities as the remaining hypothesis. In order to match the spectral shape of albedo at T-3 (Figure 6) a grey absorber such as soot was implicated, and desert dust was ruled out.

The soot in snow at T-3 may result from pollution, either local or distant. There is soot in the Arctic air [*Rosen et al.*, 1981] which may come from industrial sources in Europe [*Rahn*, 1981], but it is questionable whether the high soot concentrations found necessary to explain snow albedo at T-3 (~0.2 ppmw soot) are representative of the entire Arctic. H. Rosen (personal communication, 1981) found soot amounts in the range 0.01–0.06 ppmw in a preliminary experiment on snow samples from Barrow, Alaska.

We can be fairly certain that any soot at the south pole would be the result of local contamination from the permanent camp. For representative visible spectral albedos for the Antarctic, one should therefore use *Liljequist*'s [1956, Figure 45] high values, which agree with the pure-snow model, rather than Kuhn and Siogas' low values. For $\lambda > 1$ μm, soot has no effect (Figure 1 of WWII), and Kuhn and Siogas' measurements for these wavelengths should be representative of Antarctic snow. They correspond to an average grain radius of 100 μm, which agrees fairly well with *Stephenson*'s [1967, Figure 8] grain size measurements at Southice.

Grenfell et al. [1981] have recently made simultaneous measurements of spectral albedo, grain size, and soot for a snowpack in the Cascade Mountains. We can compare these results with the model of WWII. The measured grain size in this case is much smaller than the effective optical grain size, as mentioned above, so we ignore the grain size data and instead determine the optical grain size from the albedo measurements at $\lambda > 1$ μm, where soot has no effect on albedo. It then appears that in order to explain the visible albedos the WWII model would need 2–5 times as much soot as was actually found in the snow. A factor of 2 difference can be explained by reconciling the definitions of soot amount. (The effect of a given weight fraction of soot on snow albedo depends on the assumed values of absorption coefficient and density for soot. Grenfell et al. used an operational definition of soot concentration which assumes a mass absorption coefficient of 8 m^2 g^{-1} at $\lambda = 0.55$ μm. In fact, all of the graphs in WWII for soot-containing snow are labeled with soot amounts that are probably a factor of 2 too large. This was due to an overestimate of soot density, which was pointed out in footnote 3 of WWII (see also *Roessler and Faxvog* [1979]). Figure 6 of this review is taken from WWII but with the soot amounts now altered to the more likely values.) The remaining discrepancy may be due to five causes.

1. The new accurate laboratory measurements of m_{im} by *Grenfell and Perovich* [1981] differ somewhat from the values of *Sauberer* [1950] used by WWI and WWII. Their use causes no difference in the maximum albedo value (although its position is at 0.46 μm rather than 0.40 μm) but causes a rise of ~0.01 in albedo at 0.9 μm.

2. Agreement between measurement and calculation can be further improved by speculating that grain size increases with depth (which was observed in one case).

3. Soot which is reported as an average concentration in the snow may actually be concentrated at the surface (which was also observed in one case) where it has more effect on albedo.

4. The measurement of soot concentration may have been in error. Grenfell et al. estimated an uncertainty of a factor of 2-3 in soot concentration.

5. There may be an incorrect assumption in the modeling. The calculations assumed that both soot particles and ice particles were surrounded by air. The possible location of soot particles inside the ice grains might enhance their absorption of light. However, it has not been demonstrated that a significant fraction of the soot could be inside the ice grains. Soot could be located inside a snow particle if it were attached to a dust particle which served as an ice nucleus. But it seems unlikely that soot collected by scavenging or dry fallout would end up inside ice grains.

2. Volcanic Ash

Volcanic ash currently seems to affect snow albedo only locally, but at times in the past it has probably reduced the albedo of the entire Antarctic continent (Gow and Williamson [1971], reviewed by WWII).

The most common magma is basalt, and the most common volcanic ash is andesite (R. Cadle, personal communication, 1980). Both of these rocks have very similar optical properties for short waves: $m_{im} \approx 1 \times 10^{-3}$, constant across the visible spectrum [Pollack et al., 1973]. Thus their effect on snow albedo is qualitatively similar to that of soot, that is,

Fig. 7. Effect of Mount St. Helens ash on snow albedo for diffuse incidence: (a) snow grain size $r = 100$ μm: (b) $r = 1000$ μm. Ash parameters are described in the text.

giving no color to the snow; but in order to mimic a given concentration of soot, the andesite concentration must be 200 times higher.

For this review article we have done a special calculation of the effect on snow albedo of Mount St. Helens ash (Figure 7), using the model of WWII, for diffuse incident radiation. The ash particle size distribution is taken to be that measured from aircraft at 3200-m elevation, 130 km downwind of the volcano on May 19, 1980 [Hobbs et al., 1981, Figure 2c]. This size distribution has about the same effect on snow albedo as does a uniform size of $r = 5$ μm. The real refractive index is taken as that of andesite ($m_{re} = 1.47$) from Pollack et al. [1973]. The imaginary index m_{im} (λ) was measured by Patterson [1981] for $0.3 \leq \lambda \leq 0.7$ μm. We take the values he gives for the ash which fell at Bozeman, Montana, and then interpolate from his value at 0.7 μm to the value for andesite at 1.2 μm. For $\lambda > 1.2$ μm we use the andesite values reported by Pollack et al. In the visible wavelengths the Mount St. Helens ash is measured to be more absorptive ($m_{im} \approx 4 \times 10^{-3}$) than was the andesite sample of Pollack et al. ($m_{im} \approx 1 \times 10^{-3}$) and also to be slightly reddish colored rather than perfectly grey.

The snow albedo in Figure 7 is reduced for $\lambda < 1$ μm by addition of ash. At longer wavelengths the albedo is unaffected unless the ash content exceeds 0.1%, in which case the albedo is increased for $\lambda > 1.15$ μm.

The eruption of Mount St. Helens has provided an opportunity to study the effects of volcanic ash on snowmelt. A curious puzzle reported by R. Armstrong (personal communication, 1980) is that although the melting rate on Mount Olympus in summer 1980 was enhanced by the Mount St. Helens ash, the formation of suncups [Post and LaChapelle, 1971, pp. 71-73] was dramatically inhibited. The solution to this puzzle may lead to further insight into the nature of the snowmelt process.

Fig. 6. Comparison of calculated snow albedo with observations at visible wavelengths. Solid lines are measurements of Grenfell and Maykut [1977, Figure 1] made in summer 1974 at ice island T-3 in the Arctic Ocean. In order of decreasing albedo they are (1) dry, cold snow, wind packed, deep drift, $\rho = 0.4$ g/cm³, (2) 5-cm wet new snow over multiyear white ice, and (3) old melting snow, 28 cm thick. Circles are calculated albedo of semi-infinite pure snow for diffuse illumination, with grain radii to match observations at $\lambda = 0.9$ μm. In order of decreasing albedo they are (1) $r = 110$ μm, (2) $r = 300$ μm, and (3) $r = 1300$ μm. Plus signs are for snow containing the specified concentrations of soot, using for the imaginary index of refraction m_{im} (soot) $= 0.5$ independent of wavelength; $m_{re} = 1.8$. (Taken from Figure 6b of WWII but with soot amounts corrected according to footnote 3 of WWII).

Fig. 8. Measurements of the downward flux of solar radiation in the snow at Plateau Station, Antarctica. The horizontal axis is geometric depth, not liquid-equivalent depth. (Figure 1 of *Schwerdtfeger and Weller* [1977].)

I. TRANSMISSION OF LIGHT THROUGH SNOW

1. *Spectrally Integrated Flux Extinction*

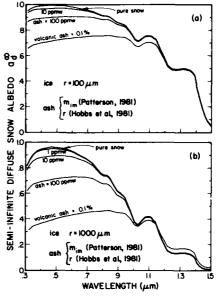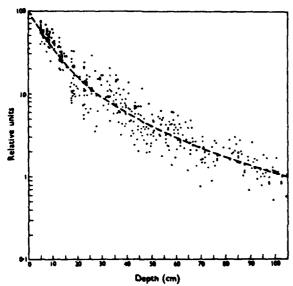Figure 8, taken from *Schwerdtfeger and Weller* [1977] shows the extinction of all-wave solar radiation flux in clean, dry snow ($\rho_s = 0.3$ g cm^{-3}) of the Antarctic Plateau. The extinction is due to both scattering and absorption. It does not follow an exponential decay in the top 40 cm or so because the spectral composition of the downflux changes rapidly in this region. Only the visible radiation penetrates deeply. At a depth of 100 cm (30 cm liquid equivalent), 1% of the incident downflux remains unextinguished. This 1% is probably entirely blue light, concentrated in a narrow wavelength band about $\lambda = 0.46$ μm, where κ_i reaches its minimum.

The absorption of solar radiation is greatest near the surface and is due almost entirely to near-IR radiation [*Wiscombe and Warren*, 1980b, Figure 3] because most of the visible light eventually reemerges after multiple scatterings. *Choudhury* [1981, Figure 14] has calculated the solar flux divergence and the associated heating rates in the snow using an atmospheric radiation model coupled to his snow albedo model. He finds the heating rate at the surface to be about 20 times that at 5-mm depth for $r = 300$ μm but dependent on grain size. The factor is larger for smaller grains because radiation is attenuated more rapidly in fine-grained snow.

These calculated solar heating rates will, of course, be compensated by infrared cooling rates. The κ_s for thermal IR radiation is much larger than that for near-IR radiation, so the cooling is more concentrated at the surface than is the heating. This leads to the observation of temperature maxima at some depth below the surface in polar snowfields during the sunlit seasons. The temperature maximum at Pionerskaya (Antarctica) in December was located 8 cm below the surface [*Schlatter*, 1972, Figure 2]. Similar results

are found in Greenland (W. Bow, personal communication, 1981). The depth of maximum net heating rate should vary with solar zenith angle, approaching the surface as $\theta_0 \rightarrow 90°$.

2. *Spectral Flux Extinction*

For the testing of theoretical models, monochromatic flux extinction measurements are more useful than the spectrally integrated measurements of Figure 8 because of the changing spectral composition with depth and the uncertain spectral composition of the incident sunlight.

Flux extinction measurements are more difficult to do accurately than are albedo measurements for diffuse incidence. (Albedo measurements under clear sky are also subject to error, as is explained in section J below.) The presence of the radiometer in the snowpack disturbs the radiation field more than it does above the snowpack; this disturbance was analyzed by *Giddings and LaChapelle* [1961]. A second difficulty which is more severe for extinction measurements than for albedo is 'leakage,' the detection of unwanted light from the wings of the filter function (T. C. Grenfell, personal communication, 1979). Leakage is least important at the wavelength of smallest absorption, $\lambda = 0.47$ μm. For example, one may nominally be measuring radiation flux at λ_1 because the filter function is centered at λ_1, but some small fraction of the light at λ_2 in the wing of the filter function also enters the detector. Unfortunately, the downflux at λ_2 deep in the snowpack may be orders of magnitude larger than that at λ_1, so that most of the light one reports at λ_1 was actually light of the wrong wavelength. This is a problem for extinction measurements but not for albedo measurements: for example, whereas the ratio of blue albedo ($\lambda = 0.46$ μm) to red albedo ($\lambda = 0.7$ μm) may be close to 1.0 (see Figure 1), the ratio of blue downflux to red downflux (for $r = 110$ μm in Figure 9a) may be ~60 at a depth of 10 cm (liquid equivalent) and ~4000 at 20 cm.

Figure 9 compares measurements with calculations of κ_i (λ). *Liljequist* [1956] used four filters to study the visible spectrum in Antarctic snow whose grain size he measured as $r \approx 150$ μm. *Kuhn and Siogas'* [1978] (hereafter KS) measurements in south polar snow probably had good spectral resolution throughout the range, whereas *Grenfell and Maykut*'s [1977] (hereafter GM) spectral resolution became poorer with increasing wavelength. Deconvolution was used for the longer wavelengths in an attempt to improve the resolution (T. C. Grenfell, personal communication, 1981). The data of GM in Figure 9 are probably reliable for $\lambda < 0.6$ μm.

Albedo had also been measured for these snow samples, and grain size was obtained by WWI and WWII by matching the calculated and observed albedo at $\lambda \geq 0.9$ μm, where impurities have negligible effect on albedo. (This was done for the albedos of KS and GM; Liljequist's albedos indicate that the snow at Maudheim was uncontaminated.) The grain sizes thus obtained (Figure 6) were $r = 1300$ μm for GM's old melting snow and $r \approx 110$ μm for both GM's 'dry compact snow' and KS's south polar snow ($r = 110$ μm also tolerably matches Liljequist's albedos).

The model parameters necessary to explain the albedo agreed with the parameters necessary to explain κ_i only for Liljequist's measurements. (However, his measurements are unreliable for $\lambda \geq 0.6$ μm because of leakage as described above.) The presence of 0.5 ppmw of soot was found

necessary by WWII (after taking into account footnotes 3 and 4 of WWII) to explain the KS albedo measurements, yet Figure 9a shows that KS's flux extinction measurements are characteristic of pure snow, as can also be seen in Figure 11 of *Choudhury* [1981].

The calculations (circles and plus signs) in Figure 9 correspond to the circles and plus signs in Figure 6; the plus signs give κ_s for the soot amount necessary to explain the albedos of GM. Considering only $\lambda < 0.6$ μm for reasons mentioned above, the measured κ_s falls between the pure-snow κ_s and the sooty-snow κ_s. This might be explained if the soot concentration at the surface at T-3 had been higher than its subsurface concentration. This is possible if the soot was the result of combustion of heating fuel, because the nearby building had been unoccupied until shortly before the measurements were made (T. C. Grenfell, personal communication, 1981). However, this argument probably cannot explain the data of Kuhn and Siogas; it is difficult to see how soot could be concentrated at the surface 1 km from the South Pole Station, rather than uniformly distributed.
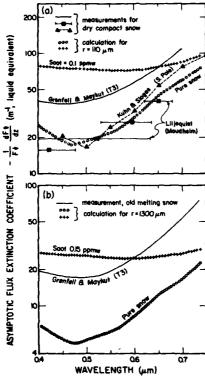

Fig. 10. Direct-beam albedo of a semi-infinite snowpack versus wavelength for several values of direct-beam zenith angle $\theta = \cos^{-1}$ μ_0. (Figure 11a of WWI. Reprinted by permission of the American Meteorological Society.)

These discrepancies indicate the need for more spectrally detailed measurements of both $\kappa_s(\lambda)$ and $a_d(\lambda)$ on the same snowpack. As *Choudhury* [1981] emphasized, a good theoretical model must explain both albedo and extinction measurements. With the currently available data we place more emphasis on explaining the albedo measurements than on explaining the κ_s measurements, because the latter are more susceptible to experimental error.

J. DEPENDENCE OF SNOW ALBEDO ON SUN ANGLE

1. Spectral Snow Albedo

As is true for most surfaces, the albedo of snow increases as the sun nears the horizon. Figure 11a of WWI is reproduced here as Figure 10, showing model-calculated albedo for four zenith angles. The albedo is predicted to be sensitive to zenith angle in the near IR but not in the visible, in qualitative agreement with measurements of *Bryazgin and Koptev* [1969]. However, addition of trace amounts of impurities to the snow would allow a zenith angle dependence in the visible as well. (These calculations are for the extreme case of 100% direct-beam radiation. Even under clear sky the diffuse sky radiation would make the observed zenith angle dependence weaker than that shown in Figure 10.)

The reason that the albedo is higher for low sun is that a photon on average undergoes its first scattering event closer to the surface if it entered the snow at a grazing angle. If the scattering event sends it in an upward direction, its chance of escaping the snowpack without being absorbed is greater than it would be if it were scattered from deeper in the pack. This would be observed even if the ice particles scattered light equally in all directions. But the phenomenon is greatly enhanced by the extreme asymmetry of the scattering, whereby scattering within a few degrees of the forward direction is much more probable than scattering to other angles.

In all radiative transfer problems for a plane-parallel slab, as the direction of incidence goes toward grazing, the albedo becomes increasingly dominated by single scattering. As the sun goes down, the shoulder of the forward peak of the single scattering phase function begins to emerge more and more from the snowpack (Figure 11), whereas when the sun was higher it was buried because of its 5°–10° width. Naturally, it is the grains at the surface that are doing most of the scattering in this case. Figure 11 is purely schematic, be-

Fig. 9. Asymptotic flux extinction coefficient for snow as a function of wavelength in the visible spectrum. Solid lines are measurements of *Grenfell and Maykut* [1977, Figure 3]. Squares are Antarctic measurements of *Liljequist* [1956] for snow of measured grain size $r = 150$ μm. Bandwidths of Liljequist's filters are obtained from his Figure 48 and plotted here as the positions of half-maximum transmittance. Triangles are measurements of *Kuhn and Siogas* [1978] at South Pole Station. (All depth values have been converted here from snow depth to liquid-equivalent depth.) Circles are calculations using WWI model, with grain radii chosen to match albedo at $\lambda = 0.9$ μm for snowpacks shown in Figure 1 of *Grenfell and Maykut* [1977]. These are the same model snowpacks described by the top and bottom lines of the circles in Figure 6 of this paper. Plus signs are model calculations for snowpacks corresponding to the top and bottom lines of the plus signs in Figure 6.
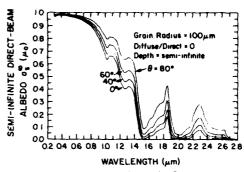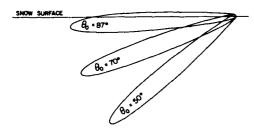
Fig. 11. Polar diagram of the scattering phase function of a snow particle at the surface of the snowpack for three solar zenith angles. This shows the probability that a scattered photon will go into any particular direction. For display purposes this phase function was calculated for an unrealistically small snow grain size (r = 10 μm, λ = 5 μm). The asymmetry of the phase function becomes much more extreme as r increases or λ decreases.

cause it was calculated for spherical ice particles. For hexagonal columns or plates the 22° halo may contain as much energy as the forward peak [*Wendling et al.*, 1979, Figure 5], and this halo begins to emerge from the snowpack already at $\theta_0 \approx 65°$.

With very low sun we approach a pure single-scattering situation, so that the bidirectional reflectance becomes just the single-scattering phase function.

At the same time the assumption of sphericity of snow grains breaks down. The effects of angular details are smeared out with multiple scattering, so that the grains can be treated as spheres. But the angular effects become dominant as $\theta_0 \rightarrow 90°$.

Besides the breakdown of the sphericity assumptions as $\theta_0 \rightarrow 90°$, the delta-Eddington approximation also becomes poor, for reasons which are given by *Wiscombe* [1977]. The disagreement between model and observation as $\theta_0 \rightarrow 90°$ is attributed (below) to this breakdown of delta-Eddington approximation.

All of this can be discussed in terms of standard single-scattering and multiple-scattering theory. There is no need to invoke a separate 'surface reflection.' Specular reflection is an acceptable natural part of the single-scattering pattern of hexagonal plates and prisms and other ice crystal forms. Hence if one would use a fully correct single-scattering phase function instead of the spherical Mie phase function, and an exact radiative transfer method for multiple scattering, one could properly model the albedo as $\theta_0 \rightarrow 90°$.

There are no nomochromatic measurements against which to test the model. This is unfortunate, because the discrepancies in spectrally integrated albedo between model and observation described below might be pinned down if measurements would be made at discrete wavelengths.

2. *Spectrally Integrated Snow Albedo $\bar{a}$ (μ_0)*

This is a controversial subject at present. The reasons for the confusion are (1) modeling error, (2) instrument error, (3) inadequate observation of snow grain size, impurity content, and surface roughness, all of which should affect the slope of $\bar{a}$ (μ_0), and (4) inadequate knowledge of the spectral distribution of the incident radiation.

A number of clear-sky measurements of spectrally integrated snow albedo as a function of the cosine μ_0 of the solar zenith angle θ_0 are plotted in Figure 12, along with model results. (The only reason for plotting the data on the two

separate frames (Figures 12a and 12b) is to avoid clutter.) Considering first Figure 12a, we note that the model calculations of *Wiscombe and Warren* [1980b] (for the atmospheric conditions of the Antarctic Plateau and r = 100 μm) show a much weaker dependence of $\bar{a}$ on μ_0 than do the observations by *Hubley* [1955] on the Juneau Icefield, *Korff et al.* [1974] in Colorado, and *Rusin* [1961] in Antarctica. (Note that the model does not account for the sphericity of the atmosphere, which probably makes it unreliable for $\mu_0 < 0.1$ or so.)

The responses of all commercial radiometers deviate from a proper 'cosine law' [*Liljequist*, 1956; *Dirmhirn and Eaton*, 1975]. They are usually less sensitive at large incident zenith angles. If not corrected for, this causes albedos at low sun to be overestimated. This is because the reflected radiation is more diffuse than the incident radiation. The steep dependence of $\bar{a}$ on μ_0 reported by Rusin and by Hubley might be explained as this type of error. But the measurements of Korff et al. must be considered reliable because they calibrated their instrument and applied a correction at large zenith angles.

Hubley's results show an interesting hysteresis, with higher albedo in the morning than afternoon at the same zenith angle. Hubley speculated that this might be attributed to specular reflection from firnspiegel in the morning before the melting began.

In Figure 12b are plotted several Antarctic measurements and calculations. *Carroll and Fitch's* [1981] (hereafter CF) measurements extended to larger zenith angles than anyone else has reported and show a much steeper dependence of $\bar{a}$ on μ_0 than *Liljequist* [1956] found. Liljequist's instruments had been extensively calibrated for the dependence of their response on both the zenith and the azimuth solar angles [*Liljequist*, 1956, pp. 45–55]. CF did not report such calibrations for their instrument, so it is possible that their dramatic disagreement with Liljequist is at least partly caused by an experimental bias in CF's measurements.

CF's measurements were complicated by surface irregularity. The faces of oriented sastrugi present different angles to the sun as it moves around the horizon. Accordingly, CF noted a diurnal cycle of albedo, as had *Kuhn and Siogas* [1978], with higher values when the sun was oriented parallel to the sastrugi, so that the effective zenith angle was larger. The measurements of CF plotted in Figure 12b are the averages of four solar azimuths 6 hours apart. A representative error bar is drawn on one of the points.

There are actually several effects of surface roughness on albedo. In a field of randomly oriented surface roughness features (or in the daily average at the south pole) when the sun is low, the effective zenith angle is always smaller for a rough surface than for a flat surface (section 5c of WW1). This means that CF's observed dependence of $\bar{a}$ on μ_0 would be even steeper if μ_0 were taken as the effective value instead of the flat surface value, and their results would deviate even more dramatically from the results of other experimenters plotted in Figure 12.

However, this is further complicated by the fact that the effective zenith angle is a function of wavelength. In order for surface roughness to moderate the zenith angle effect its typical length and depth must not be much smaller than the average penetration depth of light into snow. Surface irregu-
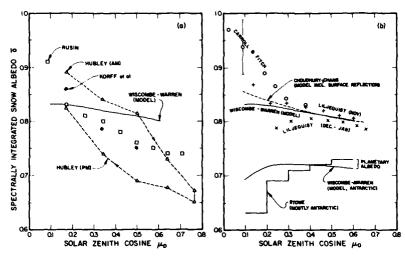
Fig. 12. Spectrally integrated clear-sky snow albedo as a function of μ_o according to various investigators. The result of the Wiscombe and Warren [1980b] Antarctic model is plotted in both frames for reference. The lower two plots in Figure 12b are for Antarctic planetary albedo.

larities on smaller scales are less important because a significant amount of radiation penetrates right through a peak and emerges on the other side. Thus whereas surface roughness of millimeter scale affects the reflection of visible light by soil particles, it does not affect the reflection of visible light by snow.

Besides altering the effective zenith angle, surface roughness will also decrease the albedo further by trapping some radiation in the troughs, as described in section E5b.

In addition to these systematic effects there is a sampling error which arises in albedo measurements of a rough surface. One should ideally make measurements from high towers [Langleben, 1968] so as to get a representative view of the surface. Close to the ground the field of view may contain only one or a few sastrugi and will thus contain more or less than its fair share of shadow, depending on solar azimuth.

The delta-Eddington snow albedo model of WW1 was coupled to the atmospheric radiation model of Wiscombe for cloud-free January conditions of the Antarctic Plateau [Wiscombe and Warren, 1980b]. The zenith angle dependences of both surface albedo and planetary albedo are shown in Figure 12b. The model adequately explains the $\bar{a}(\mu_o)$ observed by Liljequist [1956] but clearly fails to reproduce that of CF. (The reduction of December-January albedo at large zenith angles which shows up in Liljequist's daily averages was only observed in the afternoon and was attributed by Liljequist to metamorphism rather than to zenith angle. This is a possible complicating factor in all of these studies.)

Choudhury and Chang [1981] added 'surface reflection' to their model, as described in section E4 above, in order better to match the November measurements of Liljequist. But in order to get even this slight steepening of the $\bar{a}(\mu_o)$ shown in Figure 12b they had to use what seems an unreasonably small slope variance $s^2 = 0.01$, which would be more appropriate for a glazed crust than for the dry snow grains of Antarctica. The point we wish to emphasize here is that the addition of even this extreme amount of surface reflection is

dramatically inadequate to bring the delta-Eddington model in line with CF's observations. If these observations must be matched instead of those of Liljequist, a problem with the delta-Eddington model is indicated that cannot be corrected by adding an ad hoc surface reflection.

Delta-Eddington is known to underestimate the albedo of a plane-parallel layer at large zenith angles. It agrees very well with the exact doubling calculations [see Joseph et al., 1976, Figure 3] for $\mu_0 \geq 0.4$ ($\theta_0 \leq 66°$), but albedo errors of up to 10% can occur at $\mu_0 = 0.1$ ($\theta_0 = 84°$) for particular values of g and $\tilde{\omega}$. In order to quantify the errors of the delta-Eddington method for snow at low sun, it will be necessary to do some albedo calculations which give a more exact account of the radiative transfer process.

3. Spectrally Integrated Planetary Albedo

Model calculations of spectrally integrated planetary albedo over the Antarctic Plateau plotted in the lower part of Figure 12b show planetary albedo to increase slightly from $\mu_0 = 0.6$ to $\mu_0 = 0.3$ because of the μ_0 dependence of surface albedo. But when the sun goes even lower, a second effect comes into play to reduce the albedo. This is the increased H_2O and O_3 absorption in the atmosphere due to the longer slant path of the sunlight.

The zenith angle dependence of planetary albedo of the snow-atmosphere system is being measured by Stowe et al. [1980, personal communication, 1980] using the scanning radiometer of the Nimbus 7 satellite. For that work all snow-covered scenes at the same zenith angle are considered equivalent, regardless of geographic location. However, for the 1 month of data available so far (November 1978), nearly all of the scenes were over Antarctica. These observations of Stowe et al. plotted as the histogram in Figure 12b show a steeper decrease in albedo as μ_0 decreases. It is probably premature to comment on the differences between Stowe's observations and the model predictions, since many factors remain to be considered, but it is noteworthy that both model and observation agree on a range of about 70-73% for
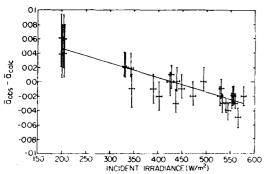
Fig. 13. Effect of cloud cover on spectrally integrated snow albedo. The difference between observed and calculated spectrally integrated albedos is plotted versus incident irradiance (which is here approximately proportional to atmospheric transmissivity, because the measurements were all made between 1100 and 1400) for snow in the Cascade Mountains. 'Calculated' albedos were calculated by *Grenfell et al.* [1981] using observed spectral albedos with a fixed incident spectral distribution characteristic of an intermediate cloud thickness. The straight line is a least squares fit to the data points. (Figure 5 of *Grenfell et al.* [1981]. Reprinted by permission of Elsevier.)

$\mu_0 \geq 0.2$. Of all the surface types examined by Stowe et al., snow was the only one in which the atmospheric path length effect was able to dominate over the surface albedo effect. In order to be consistent with these planetary albedos, the μ_0 dependence of the snow surface albedo would have to be even smaller than the modest dependence given by the delta-Eddington model.

In summary, (1) the delta-Eddington method underestimates albedo at low sun (the magnitude of this underestimate could be determined by doing a more exact calculation), and (2) the Antarctic planetary albedo measurements of Stowe et al. and the Antarctic surface albedo measurements of Carroll and Fitch are mutually inconsistent.

Our detailed discussion here of extreme zenith angles ($\theta_0 \rightarrow 90°$) is important for focusing on discrepancies between model and observation, but it has very limited relevance for the snow energy budget. Even at the north and south poles, only 3% of the annual irradiance is received at $\mu_0 < 0.1$ ($\theta_0 > 84.3°$), and only 13% at $\mu_0 < 0.2$ ($\theta_0 > 78.5°$). At other latitudes these percentages are even smaller.

K. EFFECTS OF CLOUD COVER ON SNOW ALBEDO

1. *Monochromatic Albedo*

The only effect of cloud cover on monochromatic albedo is to diffuse the radiation, changing the effective zenith angle. The effective zenith angle for purely diffuse radiation is about 50°. Thus as shown in Figure 12 of WW1, the interposition of a cloud layer between sun and snow causes spectral snow albedo to increase for $\theta_0 < 50°$ and to decrease for $\theta_0 > 50°$, the latter being the normal situation over snow-covered surfaces.

2. *Spectrally Integrated Albedo*

Cloud cover is normally observed to cause an increase in spectrally integrated snow albedo. This is because clouds absorb the same near-infrared radiation that snow would absorb, leaving the shorter wavelengths (for which snow albedo is higher (cf. Figure 1)) to penetrate to the surface.

This was pointed out by *Liljequist* [1956, p. 88], *Grenfell and Maykut* [1977, p. 457], and WW1 (section 5d). This 'spectral shift' effect (named by CF) dominates the contrary 'zenith angle alteration' effect discussed above but is moderated by it, as seen in Table 173 of *Rusin* [1961].

An example of the spectral shift effect is shown in Figure 13, which is taken from *Grenfell et al.* [1981]. The difference $a_{obs} - a_{calc}$ is plotted, where a_{calc} was based on the spectral albedo measurements and was calculated by Grenfell et al. assuming a fixed spectral distribution of incident radiation characteristic of an intermediate cloud thickness. Under a thick overcast the albedo is found to be 1–9% higher than it would have been under an intermediate cloud condition.

An interesting exception to the general rule that snow albedo is higher under cloud cover has been reported by CF to occur at very low sun and can be directly traced to the much steeper dependence of a on μ_0 that they found at these sun angles (Figure 12b). At the low solar elevations encountered by CF at the south pole, the change in effective zenith angle caused by clouds is apparently more than able to compensate for the spectral shift effect.

L. BIDIRECTIONAL REFLECTANCE OF SNOW

1. *Complete Description (for Satellite Measurements)*

The radiation reflected by a snow surface is not distributed uniformly into all angles. If it were, then the principle of reciprocity [*Siegel and Howell*, 1972] would indicate that snow albedo was independent of θ_0. The pattern of reflection is described by the anisotropic reflectance function f, which depends on the source zenith angle θ_0, detector nadir angle θ', and the relative azimuth $\phi' - \phi_0$. The bidirectional reflectance R is the product of the albedo and f, as given by equation (1). If the surface conditions depend on azimuth, as is the case for the oriented sastrugi at the south pole, f is actually a function of the two individual azimuth angles ϕ_0 and ϕ' rather than merely of their difference, but this complication is usually ignored; f may also depend on snow grain size and snow depth.

Satellite detectors with narrow fields of view measure R at only one or a few angles. In order to obtain the planetary albedo from individual satellite measurements it is thus necessary to have prior knowledge of f. Measurements of f have been made at the surface by *Middleton and Mungall* [1952] and *Dirmhirn and Eaton* [1975], from low-flying aircraft by *Griggs and Marggraf* [1967] and *Salomonson and Marlatt* [1968b] (with more details by *Salomonson and Marlatt* [1968a]), and from satellite by *Stowe et al.* [1980, personal communication, 1980].

Because the single-scattering phase function varies with wavelength, f could additionally be a function of wavelength. However, *Griggs and Marggraf* [1967] have found f to be independent of λ, at least for $0.44 \leq \lambda \leq 0.96$ μm. If this holds also at longer wavelengths (which seems unlikely), it means that f can be obtained from spectrally integrated measurements.

Figure 14 shows the results of the two most comprehensive sets of measurements. (The other reports cited above included measurements at only a few angles.) *Dirmhirn and Eaton* [1975] measured f for a melting snowpack five times (i.e., at five sun angles) on a single afternoon in Utah. (They reported that snow appeared glazed at sunrise and sunset,
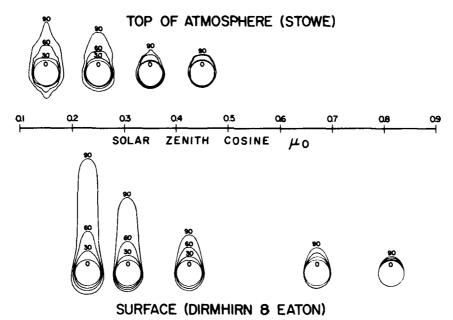
TOP OF ATMOSPHERE (STOWE)

SOLAR ZENITH COSINE μ_0

SURFACE (DIRMHIRN & EATON)

Fig. 14. Anisotropic reflectance functions for snow at the surface [from *Dirmhirn and Eaton*, 1975, Figure 3] and at the top of the atmosphere (replotted from data of *Stowe et al.* [1980, personal communication, 1980]).

but since it was melting in the afternoon when measurements were taken, we doubt that glazing affected the measurements.) A separate diagram is given for each solar zenith angle θ_0; at each θ_0, f was measured at eight azimuths $\phi' - \phi_0$ for four nadir angles θ': 0°, 30°, 60°, and 90°. In each diagram, f is proportional to the distance from the center of the inner circle to the appropriate point on the curves, but for use it must be normalized for each diagram so that

$$\frac{1}{\pi} \int \int_{\text{hemisphere}} f(\mu_0, \mu', \phi' - \phi_0) \mu' d\mu' d\phi' = 1 \quad (4)$$

The solar beam is taken to be incident from below. There is enhanced reflectance in the forward direction, and the anisotropy increases as μ_0 decreases (i.e., as the sun goes down).

Stowe et al. [1980] have taken scanner data from the Nimbus 7 satellite and grouped them into bins of $(\theta_0, \theta, \phi' - \phi_0)$. Since the satellite did not examine a single target at all angles, the measurements from all snow surfaces on earth were treated together and assumed to have the same f. However, at the time of this pilot experiment (November 1978) most of the earth's sunlit snow area was actually in the Antarctic, so the results of Stowe et al. (top of Figure 14) are really representative of a snow surface uncontaminated by vegetation. They show less anisotropy than do the measurements at the surface. This difference may partly be due to the diffusing effect of the intervening atmosphere, but there may also be an actual difference in f between the two snow types (dry, clean, fine-grained Antarctic snow versus old, melting, somewhat glazed mid-latitude snow). These results were from only a small sample of the satellite data and will be augmented in the future.

The bidirectional reflectance of snow has not been modeled since the work of *Barkstrom and Querfeld* [1975] reviewed in section E2 above. The doubling [*Hansen*, 1969] or discrete ordinates [*Stamnes and Swanson*, 1981] radiative

transfer solutions would be useful in this connection, although surface roughness may be as important as doing the plane-parallel radiative transfer correctly, because of its two effects discussed above: altering the effective zenith angle by putting some of the snow in shadow and trapping light by multiple reflections among troughs and peaks.

2. Azimuthally Averaged Bidirectional Reflectance (for Flux Calculations)

For radiation budget calculations which produce only fluxes and not intensities, the full BRDF is not needed. One only requires the albedo and the azimuthally averaged anisotropic reflectance factor $\bar{f}$:

$$\bar{f}(\theta_0, \theta') = \frac{1}{2\pi} \int_0^{2\pi} f(\theta_0, \theta', \phi' - \phi_0) d\phi'$$

S. G. Warren and W. J. Wiscombe (unpublished data, 1980) derived a parameterization for $\bar{f}$ from observations of snow reflectance. They then used it to apportion the model-calculated snow albedo among the reflection nadir angles θ'.

In Figure 15 are plotted values of $\bar{f}$ they obtained from azimuthal averaging of measurements of f from four reports. Each set of connected points corresponds to a particular zenith angle θ_0. A straight line was fit to each of these 10 plots:

$$\bar{f} = 1 + b(\mu' - 1) \quad (5)$$

(The data in Figure 15 have been normalized so that the least squares lines all pass through the point (1, 1).)

The slopes b of these lines are plotted versus the solar zenith cosine μ_0 in Figure 16. They show approximately a linear dependence on μ_0, so the resulting parameterization for $\bar{f}$ is
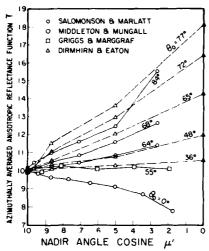
$$\bar{f}(\mu_0, \mu') = [3/(3 - b)][1 + b(\mu' - 1)] \quad (6)$$

Fig. 15. Azimuthally averaged anisotropic reflectance function $\bar{f}$ of snow as a function of nadir angle cosine μ', scaled so that $\bar{f}(1) = 1.0$ for the least squares linear fit of each data set. The data points were obtained by azimuthally averaging charts published in four reports, as follows: *Salomonson and Marlatt* [1968a, b]: Measurements of f for snow (depth unspecified) in Utah and Wyoming from aircraft 120 m above the surface, wavelength channel 0.55–0.85 μm. Results were very similar for the 2- to 4-μm channel. *Middleton and Mungall* [1952]: Measurements at the surface using artificial incandescent lighting. Plotted here are results derived from their Figure 3a for wind-packed snow. The anisotropy exhibited by this snow sample was greater than for new snow fallen in calm. Observations were made only in the plane of incidence, so there are insufficient observations to do an azimuthal average for any zenith angles except $\theta_0 = 0°$, which is the case plotted here. *Dirmhirn and Eaton* [1975]: Measurements made at the surface under natural sunlight, April afternoon in Utah, melting snow. *Griggs and Marggraf* [1967, p. 153]: Measurements from aircraft, 120 m above the surface of a snow-covered lake, Oregon, snow depth of ≈ 1 m. Measurements were made at coarse azimuthal resolution ($\Delta\phi = 60°$) but at eight discrete wavelengths between 0.44 and 0.96 μm; f appeared to be independent of wavelength.

where $b = 1.07\mu_0 - 0.84$. The prefix $3/(3 - b)$ is a nor...lizing factor, chosen so that (4) is satisfied. The dependences of f on μ_0 and μ' are different, so (6) does not satisfy the reciprocity principle and is only a first attempt to parameterize available data.

The measurements used to obtain (6) were made under a variety of snow conditions with unspecified grain size, and it is likely that (6) is not really correct for all wavelengths and grain sizes. However, *Wiscombe and Warren* [1980b] found that their radiant flux calculations were actually insensitive to the functional form of f; they obtained almost identical fluxes whether they used (6) or, alternatively, assumed isotropic reflectance. The largest differences in fluxes at the surface occurred in the visible wavelengths and were at most 0.6%.

M. THERMAL INFRARED EMISSION FROM SNOW

1. Emissivity

We have taken many pages to discuss the solar reflectance of snow, yet its infrared emission deserves only a few paragraphs. The reason for this is that the infrared emissivity of snow is quite insensitive to snowpack parameters. For many purposes one can simply assume a snow emissivity of about 99%, as was measured by *Griggs* [1968].

Berger [1979] adapted the derivations of *Bohren and Barkstrom* [1974] to the limit of large absorption as described in section E2 above. His calculated emissivity (Figure 17) is independent of grain size but decreases slightly with increasing density. This calculated density dependence may depend on the particular regular array of spheres assumed by Berger, as noted above.

The albedo model of WWI was used to calculate emissivity (Figures 8b and 11b of WWI) by virtue of Kirchhoff's law [*Siegel and Howell*, 1972, p. 70]:

$$\epsilon(\theta_0, \lambda) = 1 - a_s(\theta_0, \lambda)$$

where a_s is the albedo for zenith angle θ_0 and ϵ is the directional thermal emissivity at the same wavelength into the viewing (nadir) angle θ_0. Figure 18 shows the calculated dependence of snow emissivity on wavelength, averaged over emission angle for five grain sizes (Figure 18a) and for a single grain size $r = 100$ μm at four emission angles (Figure 18b). Since these calculations were done without a near-field correction, we do not show results beyond 40-μm wavelength, and the results plotted may already be somewhat inaccurate at $\lambda = 20$ μm, especially for $r = 50$ μm.

The emissivity is sensitive to grain size only at certain wavelengths. In particular, it is completely insensitive to grain size over most of the Planck function for normal terrestrial temperatures, centered near $\lambda = 10$ μm. The Mie results thus support *Berger*'s [1979] assumption of no transmission of IR radiation through ice spheres in this spectral range, which led to his prediction that emissivity would be independent of grain size.

The model of WWI does not compute a dependence of ϵ on ρ_s. However, because of the small penetration depth of thermal IR radiation in ice, 'surface roughness' on the scale of millimeters may affect emissivity. *Berger*'s [1979] dependence of ϵ on ρ_s is actually caused only by the relation he obtained between ρ_s and 'projected areas of surface and subsurface particles' (his equations 27 and 28), which seems actually to be a measure of surface roughness.

Because of the large m_{im} of ice throughout the thermal infrared, only a very thin layer of snow is already effectively
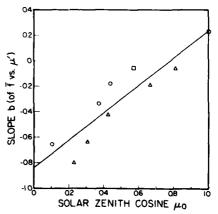

Fig. 16. Slopes (b in equation (5)) of the lines in Figure 15 are plotted here versus μ_0. The line is a least squares fit to the points. Symbols refer to the data sources given in Figure 15.

semi-infinite, so ε is independent of snow layer thickness. Small amounts of impurities will also not affect ε.

Figure 18b shows that the emissivity is near 100% for overhead viewing ($\theta_{out} = 0°$) but is significantly lower for large nadir angles. Thus the satellite viewing angle should be taken into account when inferring snow temperatures from satellite infrared channel ($\lambda \sim 11 \mu m$) emission measurements. The results in Figure 18 were obtained using the delta-Eddington approximation, so for $\theta_{out} = 80°$ the true emissivity may actually be lower than that shown.

2. Brightness Temperature

If $\varepsilon < 1$, the brightness temperature T_B at a single wavelength will be smaller than the true temperature T. The difference $T_B - T$ depends not only on ε but also on wavelength because of the variation of the Planck function with wavelength. J. Dozier (personal communication, 1981) has calculated $T_B - T$ for $3 \le \lambda \le 14 \mu m$ for snow near the melting temperature, plotted in Figure 19. The assumption that snow is a blackbody could lead to an underestimate of temperature by as much as 2.5 K at $\lambda = 14 \mu m$ and $\theta' = 75°$. However, the estimation of snow temperature from satellites will likely be subject to more error from uncertainty in atmospheric transmissivity than from uncertainty in snow emissivity.

N. REMOTE SENSING OF SNOW

1. Snowpack Properties From Albedo Measurements

Dozier et al. [1981] have used the model of WW1 to calculate snow albedos integrated over channels 1 and 2 of the NOAA Tiros N satellite (0.5–0.7 μm and 0.7–1.0 μm, respectively). The hope is to deduce grain size from a near-IR channel, where depth and contaminants have no effect on albedo, and then use the deduced grain size together with the channel 1 data to infer snow water equivalent depth below some threshold value around 100 mm. Among the difficulties in this approach are (1) the conversion of bidirectional reflectance to albedo, (2) the poor location of channel 2 for this purpose (an ideal channel would be located in the region 1.0–1.2 μm, where the sensitivity of albedo to grain size is greatest), and (3) the fact that visible albedo reduction can be due to impurities as well as to thinning of the snowpack.

Dozier et al. were apparently able to detect the thinning of the snowpack at the end of the melting season on some Canadian lakes. Figure 20 is taken from their work. On the
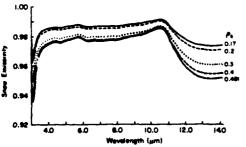
Fig. 18. Thermal infrared emissivity of snow as a function of wavelength, according to the model of WW1. (a) Hemispherically averaged emissivity for snow grain sizes $r = 50, 100, 200, 500, 1000$ μm. (b) Directional emissivity for four detector nadir angles.

earlier date, April 12, the snow-covered lakes are brighter than the intervening forest in both channels. Two weeks later, much of the snow had melted, so that on April 27 there was less contrast in both channels between lake and forest. On both of these dates it is apparent that for snow the near-IR reflectance is smaller than the visible reflectance, in agreement with Figure 1. The forest exhibits the opposite behavior, in agreement with the known spectral reflectance of green plants [Gates, 1980]. Hopefully, in the future this work will be combined with ground truth measurements of snow depth.

Some experiments at the surface which are relevant to this problem are being done by O'Brien and Koh [1981]. They observed the change in spectral reflectance (using a few narrow-band filters) as a thick snow cover decayed, documenting the transition from the spectral reflectance of snow to the spectral reflectance of grass. As is expected (Figure 13 of WW1), the underlying surface first begins to 'show through' in the visible wavelengths and is evident in the near IR only when the snow cover is much thinner. Because of the somewhat crude experimental setup, these results are as yet only qualitative.

Detection of the dust content of snow has been attempted by Sydor et al. [1979] for polluted snow in Duluth harbor. However, dust was reported as rates of deposition rather than as weight fractions in snow, so no direct comparison with a model can be made.

Matson and Wiesnet [1981] describe the routine global mapping of snow cover using visible-channel imagery from

Fig. 17. Emissivity as a function of wavelength for various snow densities, according to the model of Berger [1979]. (Figure 7 of Berger [1979].)
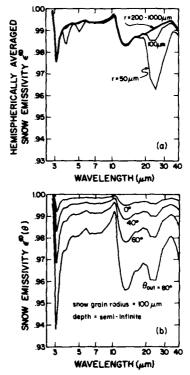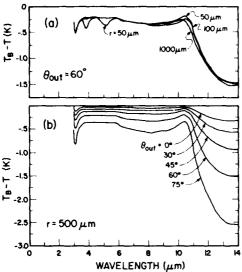
Fig. 19. Difference between brightness temperatures T_B and snow temperature T as a function of wavelength (a) for three different snow grain sizes at viewing angle $\theta' = 60°$ and (b) for snow grain radius $r = 500$ μm at five different viewing angles. Figure from J. Dozier (personal communication, 1981).

NOAA satellites. This monitoring program has been useful in describing the interannual variability of regional snow cover.

2. Snow Cloud Discriminator (1.6 μm)

Measurements from aircraft of spectral reflected intensity in the 1.4- 1.8-μm wavelength region have shown that clouds
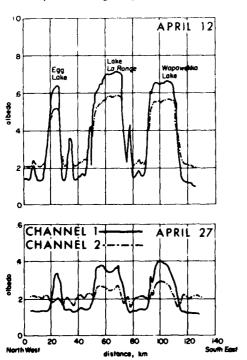
Fig. 20. Traces of reflectance measured from satellite by NOAA scanning radiometer across three lakes in Saskatchewan on two different days in visible channel 1 (0.5–0.7 μm) and near-IR channel 2 (0.7–1.0 μm). (Figure 10 of Dozier et al. [1981].)
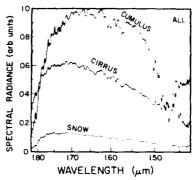
Fig. 21. Relative reflectance of snow and clouds as a function of wavelength from aircraft observations. (Figure 14 of Valovcin [1978].)

can be distinguished from snow. Figure 21 is taken from the report of Valovcin [1978]. The reflectance of cirrus clouds is shown to be greater than that of snow. This is because cirrus particles have a much smaller effective mean radius than do snow particles (perhaps 20 μm as opposed to 200 μm) and the albedo is higher for smaller ice grains (cf. Figure 1). The fact that cumulus clouds have even higher reflectance is due in part to each of three causes:

1. Cumulus clouds are thicker than cirrus.
2. Water is less absorptive than ice in this spectral region.
3. Cloud water droplets are smaller than cloud ice particles. (The cumulus clouds studied were all water droplet clouds, even at their tops.)

These aircraft observations have led to the employment of a 'snow cloud discriminator' channel at $\lambda = 1.6$ μm on a Defense Meteorological Satellite Program satellite. This channel cannot distinguish between thin cloud cover over bare ground and snow cover, but these can be distinguished in the visible channel; a bispectral method should therefore be quite reliable as a snow cloud discriminator. Tests of the utility of the 1.6-μm channel are under way by comparison with results from human analysis of satellite imagery, who use pattern recognition methods [Woronicz, 1981], or from ground-based observations of snow and cloud (R. Barry, personal communication, 1981).

3. Thermal Infrared

The temperature of a snowpack should be detectable from the thermal infrared emission, provided that the dependence of emissivity on viewing angle (Figure 18b) and the atmospheric transmissivity are accounted for.

4. Summary of Snow Parameters Detectable in Solar, Infrared, and Microwave Spectra

Table 2 offers a rough allocation of the snow parameters affecting solar spectral albedo, thermal infrared spectral emissivity, and microwave spectral emissivity. The microwave emissivity depends on three additional variables which are unimportant for the shorter waves: (1) liquid water content, because the m_{im} for ice and water are very different in the microwave; (2) temperature, because the m_{im} of ice (and of water) exhibits a significant temperature dependence for $\lambda \geq 0.2$ mm; and (3) density, because snow grains are in each others' near fields at these wavelengths.

ımeters Affecting Albedo and Emissivity of Snow

	Visible Solar Albedo	Near-IR Solar Albedo	Thermal Infrared Emissivity	Micro-wave Emissivity
	(+)	yes		yes
angle	(+)	yes	yes	yes
	yes			yes
	yes			
ıtent				yes
				yes
				yes

means only if snowpack is thin or impurities are

is made here to subdivide the microwave
is done, one may find that the emissivity is
some of the parameters in Table 1 at certain

l infrared emission can be used to obtain snow
But a multiplicity of factors are seen to affect
operties of snow in other spectral regions. In
:t individual snow parameters unambiguously
, one must therefore examine the snow at
engths simultaneously.

RECOMMENDATIONS FOR MODELING AND EXPERIMENTAL WORK

: theoretical radiative transfer models, more
:ar-IR measurements are needed of monochro-
inction and of the zenith angle dependence of
lic albedo in situations where all relevant snow
ee Table 2) are measured simultaneously. The
ivity in the thermal IR should be measured as a
:nsity and viewing angle. Reflectance measure-
usual snow conditions would also be useful,
' covered with firnspiegel and rapidly melting
nay have a high liquid water content. Special
uld be devoted to characterizing absorptive
snow.

' sensing applications, angularly detailed mea-
the bidirectional reflectance for various wave-
sizes, and surface conditions should be given

future modeling include the study of near-field
ıhericity, and surface irregularity and the pre-
irectional reflectance rather than merely fitting

.

d in proof. Ackerman and Toon [1981] have
ngle scattering from atmospheric ammonium
les containing soot and have shown that the
indeed enhanced by putting the soot particles
nsparent sulfate particles. To reduce the aero-
ttering albedo from 1.0 to 0.85 required 10-20%
lume) if the soot was present as separate
only 5% if the soot was located inside the
les. Similar results would be obtained for soot
bedded in ice grains, as was speculated in
love.

REFERENCES

Ackerman, T. P., and O. B. Toon, Absorption of visible radiation in
atmosphere containing mixtures of absorbing and nonabsorbing
particles, *Appl. Opt., 20*, 3661-3668, 1981.

Ambach, W., Untersuchungen zum Energieumsatz in der Ablations-
zone des Grönlandischen Inlandeises, in *Expedition Glaciologi-
que Internationale au Groenland,* vol. 4, pp. 76-78, Bianco
Lunos, Copenhagen, 1963.

Ambach, W., and H. L. Habicht, Untersuchung der Extinktionsei-
genschaften des Gletschereises und Schnees, *Arch. Meteorol.
Geophys. Bioklimatol., Ser. B, 11*, 512-532, 1962.

Barkstrom, B. R., Some effects of multiple scattering on the
distribution of solar radiation in snow and ice, *J. Glaciol., 11*, 357-
368, 1972.

Barkstrom, B. R., and C. W. Querfeld, Concerning the effect of
anisotropic scattering and finite depth on the distribution of solar
radiation in snow, *J. Glaciol., 14*, 107-124, 1975.

Bergen, J. D., A possible relation between grain size, density, and
light attenuation in natural snow cover, *J. Glaciol., 9*, 154-156,
1970.

Bergen, J. D., The relation of snow transparency to density and air
permeability in a natural snow cover, *J. Geophys. Res., 76*, 7385-
7388, 1971.

Bergen, J. D., A possible relation of albedo to the density and grain
size of natural snow cover, *Water Resour. Res., 11*, 745-746,
1975.

Berger, R. H., Snowpack optical properties in the infrared, *CRREL
Rep. 79-11,* U. S. Army Cold Reg. Res. and Eng. Lab., Hanover,
N. H., 1979. (Available as NTIS AD-A 071 004 6GA from the
Natl. Tech. Inf. Serv., Springfield, Va.)

Blevin, W. R., and W. J. Brown, Effect of particle separation on the
reflectance of semi-infinite diffusers, *J. Opt. Soc. Am., 51*, 129-
134, 1961.

Bohren, C. F., and B. R. Barkstrom, Theory of the optical proper-
ties of snow, *J. Geophys. Res., 79*, 4527-4535, 1974.

Bohren, C. F., and R. L. Beschta, Snowpack albedo and snow
density, *Cold Reg. Sci. Technol., 1*, 47-50, 1979.

Bolsenga, S. J., Spectral reflectances of freshwater ice and snow
from 340 through 1100 nm, Ph.D. thesis, Univ. of Mich., Ann
Arbor, 1981.

Bryazgin, N., and A. Koptev, Spectral albedo of snow-ice cover (in
Russian), *Probl. Arktiki Antarkt., 31*, 79-83, 1969. (*Probl. Arctic
Antarct., Engl. Transl., 29-32*, 355-360, 1970.)

Carroll, J. J., and B. W. Fitch, Dependence of snow albedos on
solar elevation and cloudiness at the south pole, *J. Geophys. Res.,
86*, 5271-5276, 1981.

Chernigovskii, N. T., Radiational properties of the ice cover of the
central Arctic (in Russian), *Tr. Arkt. Antarkt. Nauchno-Issled.
Inst., 253*, 1963. (*Hydrometeorology of the Polar Regions,* En-
glish translation, Israel Program for Scientific Translations, Jeru-
salem, 1967.)

Choudhury, B. J., Radiative properties of snow for clear sky solar
radiation, *Cold Reg. Sci. Technol., 4*, 103-120, 1981.

Choudhury, B. J., and A. T. C. Chang, Two-stream theory of
reflectance of snow, *IEEE Trans. Geosci. Electron., GE-17*, 63-
68, 1979a.
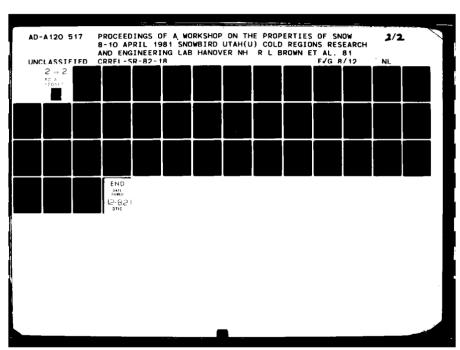
Choudhury, B. J., and A. T. C. Chang, The solar reflectance of a
snow field, *Cold Reg. Sci. Technol., 1*, 121-128, 1979b.
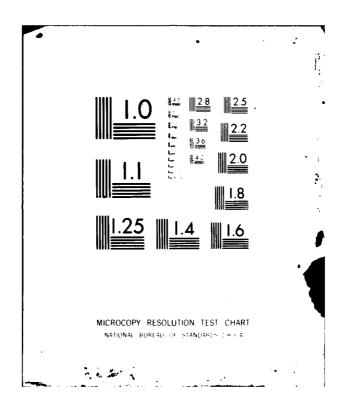
Choudhury, B. J., and A. T. C. Chang, On the angular variation of
solar reflectance of snow, *J. Geophys. Res., 86*, 465-472, 1981.

Diamond, M., and R. W. Gerdel, Radiation measurements on the
Greenland Ice Cap, *U.S. Army Snow, Ice Permafrost Res.
Estab., Res. Rep. 19,* U.S. Army Cold Reg. Res. and Eng. Lab.,
Hanover, N. H., 1956.

Dirmhirn, I., and F. D. Eaton, Some characteristics of the albedo of
snow, *J. Appl. Meteorol., 14*, 375-379, 1975.

Dobbins, R. A., and G. S. Jizmagian, Optical scattering ...

END
DATE
FILMED
12-82
DTIC

1.0

28
25

32
22

36

1.1

40
20

1.8

1.25
1.4
1.6

MICROCOPY RESOLUTION TEST CHART
NATIONAL BUREAU OF STANDARDS 1963 A

sections for polydispersions of dielectric spheres, *J. Opt. Soc. Am.*, *56*, 1345–1350, 1966.

Dozier, J., S. R. Schneider, and D. F. McGinnis, Jr., Effect of grain size and snowpack water equivalence on visible and near-infrared satellite observations of snow, *Water Resour. Res.*, *17*, 1213–1221, 1981.

Dunkle, R. V., and J. T. Bevans, An approximate analysis of the solar reflectance and transmittance of a snow cover, *J. Meteorol.*, *13*, 212–216, 1956.

Gate, L. F., Light-scattering cross sections in dense colloidal suspensions of spherical particles, *J. Opt. Soc. Am.*, *63*, 312–317, 1973.

Gates, D. M., *Biophysical Ecology*, Springer-Verlag, New York, 1980.

Giddings, J. C., and E. R. LaChapelle, Diffusion theory applied to radiant energy distribution and albedo of snow, *J. Geophys. Res.*, *66*, 181–189, 1961.

Gow, A. J., and T. Williamson, Volcanic ash in the Antarctic ice sheet and its possible climatic implications, *Earth Planet. Sci. Lett.*, *13*, 210–218, 1971.

Grenfell, T. C., An infrared scanning photometer for field measurements of spectral albedo and irradiance under polar conditions, *J. Glaciol.*, *27*, in press, 1981.

Grenfell, T. C., and G. A. Maykut, The optical properties of ice and snow in the Arctic basin, *J. Glaciol.*, *18*, 445–463, 1977.

Grenfell, T. C., and D. K. Perovich, Radiation absorption coefficients of polycrystalline ice from 400 nm to 1400 nm, *J. Geophys. Res.*, *86*, 7447–7450, 1981.

Grenfell, T. C., D. K. Perovich, and J. A. Ogren, Spectral albedos of an alpine snowpack, *Cold Reg. Sci. Technol.*, *4*, 121–127, 1981.

Griggs, M., Emissivities of natural surfaces in the 8- to 14-micron spectral region, *J. Geophys. Res.*, *73*, 7545–7551, 1968.

Griggs, M., and W. A. Marggraf, Measurement of cloud reflectance properties and the atmospheric attenuation of solar and infrared energy, *Rep. AFCRL-68-0003*, Air Force Cambridge Res. Lab., Bedford, Mass., 1967.

Hansen, J. E., Radiative transfer by doubling very thin layers, *Astrophys. J.*, *155*, 565–573, 1969.

Hanson, K., Radiation measurements on the Antarctic snowfield: A preliminary report, *J. Geophys. Res.*, *65*, 935–946, 1960.

Havens, J. M., Meteorology and heat balance of the accumulation area, McGill Ice Cap, Axel Heiberg Island, *Res. Rep. Meteorol. 2*, McGill Univ., Montreal, Que., 1964.

Hobbs, P. V., L. F. Radke, M. W. Eltgroth, and D. A. Hegg, Airborne studies of the emissions from the volcanic eruptions of Mount St. Helens, *Science*, *211*, 816–818, 1981.

Holmgren, B., *Climate and Energy Exchange on a Subpolar Ice Cap in Summer*, part E, *Radiation Climate*, Meteorologiska Institutionen, Uppsala Universitet, Uppsala, Sweden, 1971.

Hubley, R. C., Measurements of diurnal variations in snow albedo on Lemon Creek Glacier, Alaska, *J. Glaciol.*, *2*, 560–563, 1955.

Joseph, J. H., W. J. Wiscombe, and J. A. Weinman, The delta-Eddington approximation for radiative flux transfer, *J. Atmos. Sci.*, *33*, 2452–2459, 1976.

Kondratiev, K. Ya., Z. F. Miranova, and A. N. Otto, Spectral albedo of natural surfaces, *Pure Appl. Geophys.*, *59*, 207–216, 1964.

Korff, H. C., J. J. Gailiun, and T. H. Vonder Haar, Radiation measurements over a snowfield at an elevated site, *Atmos. Sci. Pap. 221*, Colo. State Univ., Fort Collins, 1974. (Available as NTIS N74-31878/3GI from the Natl. Tech. Inf. Serv., Springfield, Va.)

Kuhn, M., and L. Siogas, Spectroscopic studies at McMurdo, South Pole and Siple stations during the austral summer 1977–78, *Antarct. J. U. S. 13*, 178–179, 1978.

LaChapelle, E. R., *Field Guide to Snow Crystals*, University of Washington Press, Seattle, 1969.

Langleben, M. P., Albedo measurements of an Arctic ice cover from high towers, *J. Glaciol.*, *7*, 289–297, 1968.

Langleben, M. P., Albedo of melting sea ice in the southern Beaufort Sea, *J. Glaciol.*, *10*, 101–104, 1971.

Leu, D. J., Visible and near-infrared reflectance of beach sands: A study on the spectral reflectance/grain size relationship, *Remote Sens. Environ.*, *6*, 169–182, 1977.

Liljequist, G. H., Energy exchange of an Antarctic snow field: Short-wave radiation (Maudheim 71°03'S, 10°56'W), in *Norwe-gian-British-Swedish Antarctic Expedition, 1949–52, Scientific Results*, vol. 2, part 1A, Norsk Polarinstitutt, Oslo, 1956.

Matson, M., and D. R. Wiesnet, New data base for climate studies, *Nature*, *289*, 451–456, 1981.

Maykut, G. A., and P. E. Church, Radiation climate of Barrow, Alaska, 1962–66, *J. Appl. Meteorol. 12*, 620–628, 1973.

Meador, W. E., and W. R. Weaver, Two-stream approximations to radiative transfer in planetary atmospheres: A unified description of existing methods and a new improvement, *J. Atmos. Sci.*, *37*, 630–643, 1980.

Mellor, M., Engineering properties of snow, *J. Glaciol.*, *19*, 15–66, 1977.

Middleton, W. E. K., and A. G. Mungall, The luminous directional reflectance of snow, *J. Opt. Soc. Am.*, *42*, 572–579, 1952.

Nicodemus, F. E., J. C. Richmond, J. J. Hsia, I. W. Ginsberg, and T. Limperis, Geometrical considerations and nomenclature for reflectance, *NBS Monogr. 160, U. S.*, 52 pp., 1977. (Available as SD Cat. No. C13.44:160, U. S. Govt. Print. Office, Washington, D. C.)

Nussenzveig, H. M., and W. J. Wiscombe, Efficiency factors in Mie scattering, *Phys. Rev. Lett.*, *45*, 1490–1494, 1980.

O'Brien, H. W., and G. Koh, Near-infrared reflectance of snow-covered substrates, *CRREL Rep. 188*, U. S. Army Cold Reg. Res. and Eng. Lab., Hanover, N. H., in press, 1981.

O'Brien, H. W., and R. H. Munis, Red and near-infrared spectral reflectance of snow, *CRREL Res. Rep. 332*, U. S. Army Cold Reg. Res. and Eng. Lab., Hanover, N. H., 1975. (Available as NTIS AD-A007 732/1GI, from the Natl. Tech. Inf. Service, Springfield, Va.)

O'Neill, A. D. J., and D. M. Gray, Solar radiation penetration through snow, *IAHS AISH Publ.*, *107*, 227–241, 1973.

Ott, W., Strahlungsextinktion in homogenen Schneeschichten- Laserexperimente und Theorie des Strahlungstransportes, Ph.D. thesis, Univ. of Innsbruck, Innsbruck, Austria, 1974.

Patterson, E. M., Measurements of the imaginary part of the refractive index between 300 and 700 nanometers for Mount St. Helens ash, *Science*, *211*, 836–838, 1981.

Pfeffer, T., The effect of crevassing on the radiative absorptance of a glacier surface (abstract), *Ann. Glaciol.*, *3*, in press, 1982.

Pollack, J. B., and J. N. Cuzzi, Scattering by nonspherical particles of size comparable to a wavelength: A new semi-empirical theory and its application to tropospheric aerosols, *J. Atmos. Sci.*, *37*, 868–881, 1980.

Pollack, J. B., O. B. Toon, and B. N. Khare, Optical properties of some terrestrial rocks and glasses, *Icarus*, *19*, 372–389, 1973.

Post, A., and E. R. LaChapelle, *Glacier Ice*, University of Washington Press, Seattle, 1971.

Rahn, K. A., Relative importances of North America and Eurasia as sources of Arctic aerosol, *Atmos. Environ.*, *15*, 1447–1455, 1981.

Roessler, D. M., and F. R. Faxvog, Optoacoustic measurement of optical absorption in acetylene smoke, *J. Opt. Soc. Am.*, *69*, 1699–1704, 1979.

Rosen, H., T. Novakov, and B. A. Bodhaine, Soot in the Arctic, *Atmos. Environ.*, *15*, 1371–1374, 1981.

Roulet, R. R., G. A. Maykut, and T. C. Grenfell, Spectrophotometers for the measurement of light in polar ice and snow, *Appl. Opt.*, *13*, 1652–1658, 1974.

Rusin, N. P., *Meteorological and Radiational Regime of Antarctica* (in Russian), Gidrometeorologicheskoye Izdatel'stvo, Leningrad, 1961. (English translation, Israel Program for Scientific Translations, Jerusalem, 1964.)

Sagan, C., and J. B. Pollack, Anisotropic nonconservative scattering and the clouds of Venus, *J. Geophys. Res.*, *72*, 469–477, 1967.

Salomonson, V. V., and W. E. Marlatt, Anisotropic solar reflectance over white sand, snow, and stratus clouds, *Atmos. Sci. Pap. 120*, Colo. State Univ., Fort Collins, 1968a.

Salomonson, V. V., and W. E. Marlatt, Anisotropic solar reflectance over white sand, snow and stratus clouds, *J. Appl. Meteorol.*, *7*, 475–483, 1968b.

Sauberer, F., Die spektrale Strahlungsdurchlässigkeit des Eises, *Wetter Leben*, *2*, 193–197, 1950.

Schaaf, J. W., and D. Williams, Optical constants of ice in the infrared, *J. Opt. Soc. Am.*, *63*, 726–732, 1973.

Schlatter, T. W., The local surface energy balance and subsurface temperature regime in Antarctica, *J. Appl. Meteorol.*, *11*, 1048–1062, 1972.

Schwerdtfeger, P., Absorption, scattering and extinction of light in ice and snow, *Nature*, *222*, 378–379, 1969.

Schwerdtfeger, P., and G. E. Weller, Radiative heat transfer processes in snow and ice, in *Meteorological Studies at Plateau Station, Antarctica, Antarct. Res. Ser.*, vol. 25, edited by J. A. Businger, pp. 35–39, AGU, Washington, D. C., 1977.

Schwerdtfeger, W., The climate of the Antarctic, in *World Survey of Climatology*, vol. 14, edited by S. Orvig, pp. 253–355, Elsevier, New York, 1970.

Siegel, R., and J. R. Howell, *Thermal Radiation Heat Transfer*, McGraw-Hill, New York, 1972.

Stamnes, K., and R. A. Swanson, A new look at the discrete ordinates method for radiative transfer calculations in anisotropically scattering atmospheres, *J. Atmos. Sci.*, *38*, 387–399, 1981.

Stephenson, P. J., Some considerations of snow metamorphism in the Antarctic ice sheet in the light of ice crystal studies, in *Physics of Snow and Ice*, pp. 725–740, Bunyeido, Sapporo, Japan, 1967.

Stowe, L. L., H. Jacobowitz, and V. R. Taylor, Reflectance characteristics of earth and cloud surfaces as measured by the ERB scanning channels on the Nimbus-7 satellite, in *International Radiation Symposium Volume of Extended Abstracts*, pp. 430–432, Colorado State University, Fort Collins, 1980.

Sydor, M., J. A. Sorensen, and V. Shuter, Remote sensing of snow albedo for determination of dustfall, *Appl. Opt.*, *18*, 3574–3578, 1979.

Valovcin, F. R., Spectral radiance of snow and clouds in the near infrared spectral region, *Rep. AFGL-TR-78-0289*, Air Force Geophys. Lab., Hanscom Air Force Base, Bedford, Mass., 1978.

Warren, S. G., and W. J. Wiscombe, A model for the spectral albedo of snow, II, Snow containing atmospheric aerosols, *J. Atmos. Sci.*, *37*, 2734–2745, 1980.

Warren, S. G., and W. J. Wiscombe, Comment on "Radiative properties of snow for clear sky solar radiation," *Cold Reg. Sci. Technol.*, *5*, in press, 1981.

Weller, G. E., Heat-energy transfer through a four-layer system:

Air, snow, sea ice, seawater, *J. Geophys. Res.*, *73*, 1209–1220, 1968.

Weller, G. E., Radiation diffusion in Antarctic ice media, *Nature*, *221*, 355–356, 1969.

Wendler, G., and G. Weller, A heat-balance study on McCall Glacier, Brooks Range, Alaska: A contribution to the international Hydrological Decade, *J. Glaciol.*, *13*, 13–26, 1974.

Wendling, P., R. Wendling, and H. K. Weickmann, Scattering of solar radiation by hexagonal ice crystals, *Appl. Opt.*, *18*, 2663–2671, 1979.

Wiscombe, W. J., The delta-M method: Rapid yet accurate radiative flux calculations for strongly asymmetric phase functions, *J. Atmos. Sci.*, *34*, 1408–1422, 1977.

Wiscombe, W. J., Improved Mie scattering algorithms, *Appl. Opt.*, *19*, 1505–1509, 1980.

Wiscombe, W. J., and G. W. Grams, The backscattered fraction in two-stream approximations, *J. Atmos. Sci.*, *33*, 2440–2451, 1976.

Wiscombe, W. J., and S. G. Warren, A model for the spectral albedo of snow, I, Pure snow, *J. Atmos. Sci.*, *37*, 2712–2733, 1980a.

Wiscombe, W. J., and S. G. Warren, Solar and infrared radiation calculations for the Antarctic Plateau using a spectrally-detailed snow reflectance model, in *International Radiation Symposium Volume of Extended Abstracts*, pp. 380–382, Colorado State University, Fort Collins, 1980b.

Woronicz, R., The U. S. Air Force snow cover charts, *Glaciol. Data*, *11*, 63–69, 1981. (Available from World Data Center-A for Glaciology, University of Colorado, Boulder.)

Zdunkowski, W. G., R. M. Welch, and G. Korb, An investigation of the structure of typical two-stream-methods for the calculation of solar fluxes and heating rates in clouds, *Beitr Phys. Atmos.*, *53*, 147–166, 1980.

Dielectric Properties of Snow

W.H. Stiles and F.T. Ulaby

Remote Sensing Laboratory
University of Kansas Center for Research, Inc.
Lawrence, Kansas 66045

ABSTRACT

This paper is a review of the dielectric properties of snow in the radio frequency range from 100 kHz to 35 GHz. Applicable dielectric mixing formulas are discussed and compared to available experimental data. Below 1 GHz, the dielectric behavior of snow is well understood and has led to development of sensors to measure the liquid water content of snow, while above 1 GHz, the scarcity of experimental data and the discrepancies between the few available measurements, particularly when liquid water is present, are responsible for the rather sketchy understanding of the dielectric behavior of snow in the microwave region.

INTRODUCTION

As the importance of snow as a renewable resource becomes increasingly recognized, methods of assessing snow properties in a timely fashion over large areas become indispensable. It is clear that, for both timely observations or large areal coverage, the physical handling of the snow must be minimized. Remote sensing techniques satisfy the above requirement; however, interpretation of the remotely sensed data is not always straightforward. These data are usually in the form of processed quantities which are determined by the parameters of the measurement system and the characteristics of the observed scene (in this case, snow). In the radio region of the spectrum, the interaction of electromagnetic energy with snow is governed by its geometrical and electrical (dielectric) properties; therefore, a more complete description of the dielectric properties of snow should lead to a better understanding of remote sensing observations of snow.

Several review articles of the electrical properties of ice and snow have been published over the last 20 years [1–4]. The most recent of these reviews, by Glen and Paren [3], stressed the electrical behavior in the spectral range that is particularly suited to glacial sounding (DC to 100 kHz). This paper presents a review of the dielectric properties of snow, with special emphasis on its behavior at the radio frequencies above 100 kHz. Included in this review are: 1) a discussion of mixing formulas used to characterize the dielectric properties of a snow mixture in terms of its constituent parts—air, ice and liquid water (if present), and 2) a summary of experimental data reported in the literature.

PROPERTIES OF CONSTITUENTS

The electromagnetic propagation properties of a material are defined in terms of its magnetic permeability, μ, and its relative complex dielectric constant, ϵ. For most naturally occurring materials, including snow, $\mu \cong \mu_0$, the magnetic permeability of free space. Hence, the propagation is governed solely by ϵ, which has the complex form:

$$\epsilon = \epsilon' - j\epsilon'' \tag{1}$$

Since snow is a heterogeneous mixture of air, ice, and, under certain conditions, liquid water, the constituent dielectric properties must be examined first in order to understand the dielectric properties of the mixture. For practical purposes, the characteristics of air are indistinguishable from those of free space. Water and ice, however, exhibit dielectric behavior which can be described, at least to the first order, by the Debye equation:

$$\epsilon = \epsilon_\infty + \frac{\epsilon_0 - \epsilon_\infty}{1 + j2\pi f \tau} \tag{2}$$

or in terms of its real and imaginary parts:

$$\epsilon' = \epsilon_\infty + \frac{\epsilon_0 - \epsilon_\infty}{1 + (2\pi f \tau)^2} \tag{2a}$$

$$\epsilon'' = \frac{2\pi f \tau (\epsilon_0 - \epsilon_\infty)}{1 + (2\pi f \tau)^2} \tag{2b}$$

91
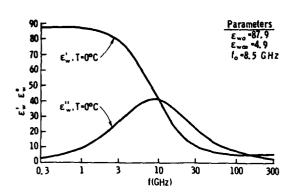
Figure 1. Complex dielectric constant of water at 0°C from the Debye equation.

Parameters
$\epsilon_{wo} = 87.9$
$\epsilon_{w\infty} = 4.9$
$f_o = 8.5$ GHz

Figure 2. Cole–Cole diagram of ϵ'' and ϵ' for ice samples at $-10.8°C$ in a) pure ice and b) ice with impurities. Points represent measurements at the indicated frequencies in kHz. (From Evans [1].)

where $\epsilon_0 = \lim_{f \to 0} \epsilon$ or the static dielectric constant, dimensionless

$\epsilon_\infty = \lim_{f \to \infty} \epsilon$ or the optical limit of dielectric constant, dimensionless

τ = relaxation time of the material (s)

f = electromagnetic frequency (Hz).

This equation describes the contribution to the polarizability of a polar molecule (H_2O) from the permanent dipole moment of that molecule. An applied electric field tends to align the dipole against the thermal forces which induce disorder or "relaxation" and are a function of the temperature and viscosity of the dielectric material. The relaxation tir e as derived by Debye for spherical polar molecules in a viscous medium is a good approximation for water [5]:

$$\tau = \frac{4\pi \eta a^3}{kT} \qquad (3)$$

where η is the viscosity, a is the molecular radius, k is Boltzmann's constant and T is the temperature.

Empirical expressions based on experimental results have been developed for the constants in equation 2 for water as functions of physical temperature [5-8] and are reviewed in [9]. Figure 1 illustrates the behavior of ϵ_ω' and ϵ_ω'' of water at 0°C as a function of frequency. The peak in ϵ_ω'' at 8.5 GHz results from the Debye dispersion being centered in the microwave region. The frequency at which the peak occurs is termed the relaxation frequency f_0 where $f_0 = (2\pi\tau)^{-1}$.

For the frequency interval of emphasis, 100 kHz to 35 GHz, the dispersion causes the dielectric properties of water to vary significantly. Below approximately 1 GHz, low frequency approximations to equations 2a and 2b yield $\epsilon_\omega' \cong \epsilon_{0\omega}$ and $\epsilon_\omega'' \cong 2\pi f T(\epsilon_{0\omega} - \epsilon_{\infty\omega})$, while

above 1 GHz the exact form must be used. For liquids or solids, interactions between molecules and viscosity variations tend to violate some of the assumptions of the Debye equation giving rise to a non-unique relaxation time. The Cole–Cole [10] modification to the Debye form (eq 2), i.e. raising the $j2\pi f\tau$ term to the power $(1 - \alpha)$, allows this equation to describe the dispersion for a distribution of relaxation times. For water, α has been determined to be less than 0.03 [8], indicating that the Debye form for a single relaxation time is adequate, but for ice and snow this is not always the case.

The dielectric properties of ice, at least over a large frequency interval, can also be described by the Debye equation of the same form as for water, equation 3. While the relaxation frequency of water lies in the microwave region, for ice (as a result of the higher viscosity compared to that of water) the relaxation frequency is reduced to the kilohertz region and as in the case for water, it is temperature-dependent. Auty and Cole [11] measured the dielectric coefficients for pure ice and found that $\epsilon_{i\infty} = 3.10$, that τ_i had a minimum value at 0° corresponding to $f_0 = 7.5$ kHz, and that ϵ_{i0} had a minimum value of 91.5 at $-1°C$.

A convenient form for examining the spectral behavior of a material describable by the Debye form is the Cole–Cole diagram which is a plot of the imaginary part ϵ'' versus the real part ϵ'. Curves defined by equation 2 are semicircles in this representation. Figure 2 from Auty and Cole's data [11] illustrates measurements of pure ice and ice with impurities along with their respective Debye curves. Each symbol corresponds to a measurement at frequencies denoted in kHz. Two observations are apparent from this figure: 1) the DC conductivity of sample (b) causes the behavior to deviate from the Debye form below 1.5 kHz and 2) since the optical limit is the left-most intersection of the semicircle with the ϵ'-axis, this representa-

92

Table 1. Measured values of the real part of the relative dielectric constant of pure or freshwater ice, ϵ_i' (from Ulaby et al. [9]).

Frequency (GHz)	Temperature range (°C)	ϵ_i'	Reference
0.15 to 2.5	−1 to −60	2.90 to 2.95	Westphal (in [1])
9.375	0 to −18	3.15	Cumming [14]
10	−12	3.17	Von Hippel [20]
10	0 to −35	3.14	Vant et al. [16]
10	−1 to −49	3.17	Lamb [17]
24	0 to −185	3.18	Lamb and Turney [18]
26.4 to 40.0	0 to −35	2.92	Vant et al. [16]
94.5	−28	3.08	Perry and Straiton [15]
1000	−173	3.20	Bertie et al. [21]
99	—	3.17	Blue [19]

tion is not very illuminating for the high frequency response because of the compression of the variation in ϵ''.

It should be noted that in the frequency range below 10 kHz, several loss mechanisms are present [3, 12, 13], primarily due to impurities, structural effects, and molecular or ionic defects. A good overview of these dispersions is given in the review by Glen and Paren [3] and in a paper by Paren and Glen [12]. These dispersions may be describable by the Debye form but do not occur at the same relaxation frequencies or have the same strengths. In the high-frequency limit, however, these values will each approach their optical limits and consequently will have very little contribution above 100 kHz. Therefore, the macroscopic dielectric behavior can be described by effective quantities that include contributions from all of the dispersion mechanisms.

For frequencies much greater than the relaxation frequency in ice, $f//f_0 = 2\pi f\tau_i >> 1$, the following high frequency approximations can be made to the rationalized form of the Debye equation (eq 2a and 2b):

$$\epsilon_i' = \epsilon_{i\infty} \qquad (4a)$$

$$\epsilon_i'' = \frac{\epsilon_{i0} - \epsilon_{i\infty}}{2\pi f\tau_i} = (\epsilon_{i0} - \epsilon_{i\infty})\frac{f_{i0}}{f} \qquad (4b)$$

From measurements for which these approximations are valid, between 10 MHz and 1000 GHz, the optical limit $\epsilon_{i\infty}$ has been found to be insensitive to temperature (below 0 °C) and independent of frequency. Values from several experimental investigations [1, 14–21] for $\epsilon_{i\infty}$ are given in Table 1 and excellent agreement generally is observed; hence, the value of $\epsilon_{i\infty} = 3.15$ from Cumming [14] will be used as being representative. While the real part is well-behaved, the imaginary part is dependent on both frequency and temperature as expected from equations 3 and 4b. Figure 3 is a survey of the available data on ϵ_i'' as a function of fre-

quency for pure or freshwater ice at two temperatures. For this frequency interval, equation 4b indicates that ϵ_i'' should decrease as f^{-1}; therefore on a log–log scale, the behavior should be linear with a negative slope. The experimental data given in Figure 3 show, however, that the Debye form is inapplicable above 1 GHz, indicating that the single resonance assumption is not valid. Evans [1] attributed the observed spectral behavior of ϵ_i'' to contributions by infrared dispersions.

Since the theoretical expressions for ϵ_i'' are not adequate in the microwave frequency range, experimental results must be relied upon even though considerable variability exists in the data above 10 GHz. This variation is at least in part a consequence of the problems associated with making accurate measurements of the loss factor of a very low-loss material, which ice is.
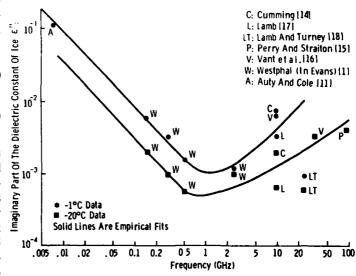
Figure 3. Imaginary part of the relative dielectric constant of pure and fresh water ice. (From Ulaby et al. [9].)

93

Table 2. Mixing formulae for snow.

Formula Number	Mixing Formula	Comments	Inclusion Shape	Reference
1	$$\frac{\epsilon_{ds} - 1}{3\epsilon_{ds}} = V_i \frac{\epsilon_i - 1}{\epsilon_i + 2\epsilon_{ds}}$$	Simplification of 6 for spherical with $V_w = 0$ $\epsilon_{ws} = \epsilon_{ds}$	Spherical	Cumming [14] Glen and Paren [3] (Bottcner)
2	$$\frac{\epsilon_{ds} - 1}{\epsilon_{ds} + F} = V_i \frac{\epsilon_i - 1}{\epsilon_i + F}$$	Dry snow only	F = 0 vertical to F = ∞ planar	Evans (Weiner for dry snow) [1]
3	$$\epsilon_{ws} = \frac{\epsilon_w V_w U + \epsilon_{ds}(1-V_w)}{V_w U + (1-V_w)} \quad \text{where } U = \frac{\epsilon_{ds} + F}{\epsilon_w + F}$$	Wet snow	F = 0 vertical to F = ∞ planar	Edgerton et al. [22] (Weiner)
4	$$\epsilon_{ds}^{1/3} - 1 = V_i(\epsilon_i^{1/3} - 1)$$	Dry snow	Spherical	Glen and Paren [3] (Looyenga)
5	$$\epsilon_{ws} - \epsilon_{ds} = \frac{V_w}{3}(\epsilon_w - \epsilon_{ds}) \sum_{j=1}^{3} \frac{1}{1 + (\frac{\epsilon_w}{\epsilon_n} - 1)A_{wj}}$$	ϵ_n - local dielectric constant accounts for particle interactions	Ellipsoidal	Sweeney and Colbeck [23] (de Loor)
6	$$\epsilon_{ws} = 1 + \frac{\epsilon_{ws}}{3} V_i(\epsilon_i - 1) \sum_{j=1}^{3} \frac{1}{\epsilon_{ws} + (\epsilon_i - \epsilon_{ws})A_{ij}}$$ $$+ \frac{\epsilon_{ws}}{3} V_w(\epsilon_w - 1) \sum_{j=1}^{3} \frac{1}{\epsilon_{ws} + (\epsilon_w - \epsilon_{ws})A_{wj}}$$	Different shape factors for water and ice	Ellipsoidal	Colbeck [24] (Polder and van Santen)
7	$$\epsilon_{ws} - \epsilon_{ds} = \frac{V_w}{3}(\epsilon_w - \epsilon_{ds}) \epsilon_{ws} \sum_{j=1}^{3} \frac{1}{\epsilon_{ws} + (\epsilon_w - \epsilon_{ws})A_{wj}}$$	Simplification of 5 with $\epsilon_n = \epsilon_{ws}$	Ellipsoidal	Ambach and Denoth [25] (Polder and van Santen)
8	$$\epsilon_{ds} = 1 + \frac{3V_i(\epsilon_i - 1)}{(2 + \epsilon_i) - V_i(\epsilon_i - 1)}$$	Simplification of 9	Spherical	Tinga et al. [26]
9	$$\epsilon_{ws} = 1 + \left\{ 3 \left[(\frac{r_w}{r_a})^3 (\epsilon_w - 1)(2\epsilon_w - \epsilon_i) - (\frac{r_i}{r_a})^3 (\epsilon_w - \epsilon_i)(2\epsilon_w + 1) \right] \right.$$ $$\times \left[(2 + \epsilon_w)(2\epsilon_w + \epsilon_i) - 2(\frac{r_i}{r_w})^3 (\epsilon_w - 1)(\epsilon_w - \epsilon_i) \right.$$ $$\left. - (\frac{r_w}{r_a})^3 (\epsilon_w - 1)(2\epsilon_w + \epsilon_i) + (\frac{r_i}{r_a})^3 (\epsilon_w - \epsilon_i)(2\epsilon_w + 1) \right]^{-1} \right\}$$		Spherical of ice coated with water	Tiuri and Schultz [27] (Tinga et al.)

MIXING FORMULAS

The dielectric properties of a heterogeneous mixture such as snow must be described by mixing formulas that incorporate the dielectric properties and proportions of the component materials. In the rigorous formulations, structure will also be a factor. Snow can be treated as either a two-component or three-component mixture consisting of ice, air and liquid water. The two-component formulation is usually applied to dry snow (air and ice) and sometimes to wet snow through an additional application of the formula for dry snow and water. In the three-component formulations, air, ice and water are each accounted for as individual components.

Both theoretical and purely empirical mixing formulas have been reported in the literature. In this section, the discussion will be limited to theoretical approaches,

94

while discussion of the regression models will be presented in the section on dielectric properties. The developments of mixing formulas have usually been restricted to modeling one component as regularly shaped inclusions uniformly distributed within a host or background material. The mathematical difficulties of handling inclusion shapes and inter-inclusion interactions have required the choice of ellipsoidal or spherical particles. This limitation poses no real problem for snow that has been wet since the particle shapes tend toward spherical anyway; however, very fresh snow is not usually even close to spherical. Applicability for fresh snow therefore may be suspect but also may be difficult to examine because handling requirements and the action of metamorphism immediately start modifying its structure towards more stable thermodynamic shapes.

Mixing formulas which have been applied to snow are given in Table 2. With the exceptions of Formulas 2 and 3, which are variations on the formulation due to Weiner [1, 22] and which attempt to use a single factor to describe a three-dimensional shape (and are therefore inherently unsound), all the other formulas can be related to one another.

Formulas 5, 6 and 7 are descriptive of ellipsoidal inclusions with axes a, b and c and associated depolarization factors A_{kj}, where k denotes the inclusion type, either ice or water, and j denotes the axis. Usually two of the axes are assumed equal, thus since the sum of the A_j must equal one, only one integration is needed. Formula 5 is the most rigorous in that ϵ_n (the effective dielectric constant in the immediate region of the particle) can be different from either of the constituents or the mixture average. This formulation is the most general; however, it is also the most complicated to apply. Formula 7 makes the approximation that $\epsilon_n = \epsilon_{ws}$, the dielectric constant of the mixture, and appears to provide an adequate fit to the available data. Both of these formulations assume that the dry snow dielectric properties are already known, while Formula 6 treats the three-component case. In applying Formula 6 to measured dielectric data, Colbeck [24] found that the ellipsoidal ice particles may be approximated as spherical in shape without incurring significant error in the results, but for the water inclusions the shape factor was found to be very important.

Formula 1, which applies to dry snow only, is a special case of Formula 5; if the particles are spherical (i.e., $A_1 = A_2 = A_3 = \frac{1}{3}$), Formula 5 reduces to Formula 1 upon replacing ϵ_{ws} and ϵ_{ds} with ϵ_{ds} and ϵ_i, respectively, and setting $\epsilon_n \approx \epsilon_{ds}$. Similarly, Formula 4 can be derived from Formula 5 for dry snow conditions.

The expressions given by Formula 9 are a special case of a more general formulation derived by Tinga et al. [26] for ellipsoids of dielectric ϵ_1 covered by a layer of

material of dielectric ϵ_2 contained in a host material of dielectric ϵ_3. As given in Table 2, Formula 9 is for spherical ice particles covered by a uniform layer of water. Formula 8 is the same as Formula 9 with no water present (i.e., dry snow). While Colbeck [24] states that the water distribution in the snowpack is not in spherical layers around the ice particles, Formula 9 has been found to give acceptable results when compared to experimental data, as discussed in a later section.

DIELECTRIC PROPERTIES OF SNOW

The dielectric properties of dry and wet snow are discussed in separate sections because the addition of liquid water to dry snow significantly alters its properties.

Dry snow

Because the relaxation frequency of ice is in the kilohertz range, dry snow is not expected to exhibit a dispersion behavior above 100 kHz. Although surface effects and other processes may cause additional low-frequency dispersions [5], the mixture with air, which can be considered to have $f_0 = \infty$, makes the relaxation frequency of snow always higher than that of ice. The relaxation frequency for natural dry snow remains below approximately 100 kHz. Dielectric measurements, conducted for densities ranging between 0.08 and 0.41 g cm^{-3} and for temperature between $-10\,°C$ and $0\,°C$, show that the relaxation frequency of dry snow, f_{ds}, is in the 5- to 60-kHz range [1, 12, 28].

Ambach and Denoth [25] measured the frequency dependence of ϵ_{ds}' and the loss tangent, $\tan \delta_{ds}$, for fine-grained (<0.25-mm radius) and coarse-grained (>0.25-mm radius) dry snow. The loss tangent is defined as the ratio of the imaginary part to the real part of the dielectric constant. Their results, given in Figure 4, indicate different relaxation spectra for the two samples; the coarse-grained sample exhibits a single Debye-type relaxation, while the fine-grained sample exhibits a wide relaxation spectrum indicative of a range of relaxation frequencies. This result does not imply that the size is the effect; the depolarization factors of the ice particles were very much different from the two cases: fine-grained $A \leq 0.03$ and coarse-grained $A \geq 0.20$. Above 10 MHz, the real part is independent of frequency and the effect of grain shape on the relaxation spectrum in the high-frequency limit is negligible.

For frequencies above 1 MHz, the dominant physical parameter that determines the dielectric constant of dry snow is its density. An alternate and useful expression for density is the volume fraction of ice V_i, which is related to the ice density ρ_i and the snow density ρ_s through:

95
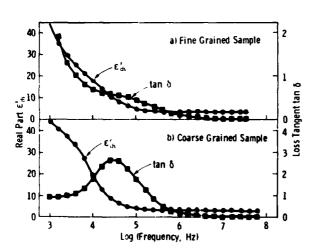
Figure 4. Dependence of the real part of the complex dielectric constant and loss tangent of dry snow with frequency for a) fine-grained and b) coarse-grained samples. (From Ambach and Denoth [25].)

	Formula	Frequency
Howorka [In 3]	$1+2.22\,\rho_s$	3.5 MHz
Ambach And Denoth [25]	$1+2.205\,\rho_s$	13.6 MHz
Kurioua [29] (Estimated)	$1+2.3\,\rho_s$	3 MHz
Looyenga Formula [In 3]	$(1+0.508\,\rho_s)$	—
● Cumming [14]	Experimental Data	9.375 GHz

Figure 5. Real part of the dielectric constant of dry snow as a function of snow density ρ_s along with empirical fits.

$$V_i = \varrho_s/\varrho_i. \tag{5}$$

Figure 5, from Cumming [14], depicts the dependence of ϵ_{ds}' on ϱ_s at 9.375 GHz, along with curves defined by mixing Formula 4 (in Table 2) and several empirical expressions [3, 25, 29]. Although this data set was measured at 9.375 GHz, it is applicable above 1 MHz where ϵ_{ds}' is frequency-independent. Cumming [14] also found ϵ_{ds}' to be independent of temperature as expected from ice and air properties. The empirical fits [3, 25, 29] are approximately what one would get from a volumetrically weighted average of the dielectric constants of the constituents. Any of the mixing formulas applicable to dry snow will also provide a good fit to these data. One useful simple formulation for the real part results from Formula 4 with $\epsilon_i = 3.15$

$$\epsilon_{ds}' = (1 + 0.508\,\varrho_s)^3. \tag{6}$$

While ϵ_{ds}' is independent of both temperature and frequency, ϵ_{ds}'' is sensitive to temperature as shown in Figure 6 and to frequency by inference from Figure 3 for ice. Although spectral measurements of dielectric properties have been made up to around 100 MHz, in the microwave region single-frequency measurement programs have predominated and precise determination of the spectral dependence is not available. As a result, one must rely on mixing formulas, which often lead to

Figure 6. The loss tangent of dry snow as a function of temperature at a frequency of 9.375 GHz. (From Cumming [14].)

96

inconsistencies. For example, Royer [2] found that if Formula 2 of Table 1 is used, different values of F are required to fit the real and imaginary parts of ϵ_{ds} to experimental data suggesting that a better model is needed and therefore Formula 2 should not be used.

An expression derived from Formula 8 (of Table 1) by Ulaby et al. [9] is given by

$$\epsilon_{ds}'' = \frac{0.34\,V_i\epsilon_i''}{(1-0.417V_i)^2} \qquad (7)$$

and provides a fit close to Cumming's [14] data.

For dry snow, if one avoids the low-frequency dispersion region, the real part of ϵ_{ds} is well-known and easily determined from density and the mixing formulas; for the imaginary part, however, the fits are approximate due to the limited accuracy of the available data on the imaginary part of the dielectric constant of ice.

Wet snow

As 0 °C is approached, liquid water appears in snow and causes a significant change in the dielectric properties of the mixture because both the real and imaginary parts of the dielectric constant of water are much greater than those of ice.

10-MHz to 1-GHz region

For the frequency interval between approximately 10 MHz and 1 GHz, propagation loss through dry or wet snow is very small. Consequently, most of the research activities conducted in this frequency range have concentrated on the dependence of ϵ_{ws}' on V_w, the volume fraction of water. The use of mixing formulas is facilitated by the fact that for $f > 10\,\text{M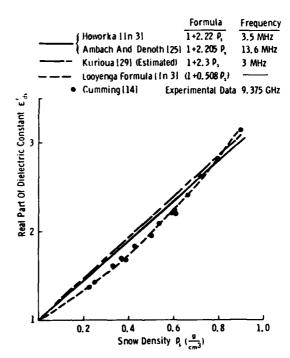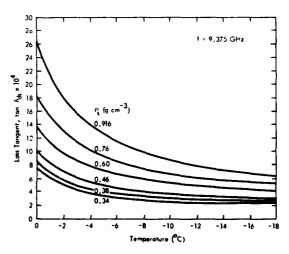Hz}$, $\epsilon_i' \approx 3.15$ and, as mentioned earlier, it is frequency- and temperature-independent, and for $f < 1\,\text{GHz}$, $\epsilon_w' \approx \epsilon_{wo}'$, the static

dielectric constant of water, which, of course, is frequency-independent and weakly dependent on temperature. Hence, the dielectric constant of the ice–air–water mixture is also frequency-independent and approximately temperature-independent.

The empirical expressions given in Figure 5 for dry snow have been extended to wet snow by adding a term that accounts for the water volume fraction, V_w,

$$\epsilon_{ws}' = 1 + a\varrho_s + bV_w \qquad (8)$$

where the constants (a, b) were found experimentally to have the values (2.22, 23.6) of Howorka [in 3] and similar values (2.205, 21.3) were determined by Ambach and Denoth [25].

The above expression provides a useful approximation of the relationship between ϵ_{ws}' and V_w, although a more exact representation using Formula 7 of Table 1 allows for modeling the water particles as ellipsoids. With the assumption that the depolarization factors A_1 and A_2 are equal, implying that $A_3 = 1 - 2A_1$, Ambach and Denoth [25] employed experimental data to compute A_1, by fitting the data to Formula 7. Their results are shown in Figure 7. It is observed that A_1 is a function of V_w; however, $A_1 \approx 0.05$ seems to be a good average depolarization factor.

In a more detailed modeling of liquid distribution, Colbeck [24] suggested that water actually appears in two basic shapes (fillets and veins) because of the geometry of wet snow ice-grains. All wet snow tends to form multiple crystal clusters and the fillets and veins of water form in the air spaces between three or two grains, respectively.

The practical application of dielectric measurements in this frequency range is in the measurement of liquid water, which will be covered in a later section.
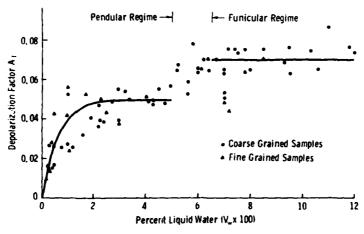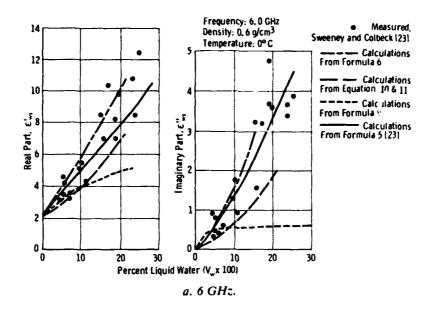
Figure 7. Depolarization factor A_{w1} for mixing Formula 7. (From Ambach and Denoth [25].)

97

a. 6 GHz.

b. 9.4 GHz.
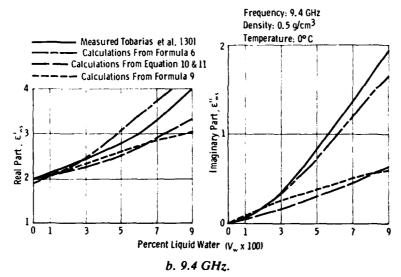
Figure 8. Real and imaginary parts of the relative dielectric constant of snow as a function of liquid water content at 6 GHz and 9.4 GHz.

Above 1 GHz

In the microwave region, both real and imaginary parts of ϵ_{ws} are frequency-dependent, therefore frequency extrapolation is questionable. Four sets of data have been reported in the literature for ϵ_{ws} as a function of snow liquid water content V_w. Cumming [14] reported the variation in loss-tangent in response to V_w; however, his data covered a narrow range extending between $V_w = 0$ and 0.006. Figure 8 presents dielectric measurements given by Sweeney and Colbeck [23] at 6 GHz and Tobarias et al. [30] at 9.4 GHz, together with

the results reported by Linlor [31] for both frequencies. Also shown are curves computed using the mixing formulas indicated on the figure. The curves due to Linlor [31] were computed from expressions he had developed on the basis of experimental data acquired over the 4-to 12-GHz region. These expressions are:

$$\epsilon'_{ws} = 1 + 2\varrho_s + bV_w^{3/2} \qquad (9)$$

$$\epsilon''_{ws} = \frac{1.0994\alpha}{f} \sqrt{\epsilon'_{ws}} \qquad (10)$$

98

where

$$b = 5.87 \times 10^{-2} - 3.10 \times 10^{-4}(f-4)^2$$

$$\alpha = V_w[0.045(f-4) + 0.066(1+a)]\text{dB/cm} \qquad (11)$$

with f in GHz and with a representing the average grain diameter in mm. The ranges of validity are stated to be: 0.1 mm $\leq a \leq$ 1.0 mm and $0 \leq V_w \leq 0.12$ [31].

The experimental data in Figure 8 show significant differences at both frequencies, especially for the imaginary part. In addition, the curves generated from mixing Formulas 5, 6 and 9 also show some discrepancies. The behavior at 6 GHz shows that Formulas 5 and 6 give similar results as expected because of their common basis. Formula 6 was applied using spherical ice particles ($A_{i1} = \frac{1}{3}$), ellipsoidal water particles ($A_{j1} = 0.04$, an average from Figure 7), and the constituent dielectric properties. The results from this formula fall near an upper bound on the data, indicating that at the higher values of V_w a different value of A is needed. Formula 9 shows good agreement with ϵ' data from Linlor [31] up to about $V_w = 0.1$; however, the curvature does not follow the correct trend and therefore should only be used with great caution. Its prediction for ϵ''_{ws} is even further in error.

At 9.4 GHz, again the data from Linlor [31] are much lower than the other data. Formula 9 gives a better fit to Linlor's data than at 6 GHz, while Formula 6 fits the data of Tobarias et al. [30] fairly well with the same depolarization factors used at 6 GHz.

The differences in dielectric constants for these sets of data suggest that the dielectric behavior of wet snow in the microwave region is influenced by some parameter(s) besides snow density. Dielectric mixing theory and observations of Ambach and Denoth [36] indicate that snow grain size or structure should not affect the properties. It is the author's belief that grain structure does indirectly influence the dielectric properties. The method of preparing the samples of reference [23] was to flood the snow sample and then drain it. Colbeck [37] states that this leads to multi-grain clusters of three and more particles and the liquid inclusions exist at grain boundaries. This results in ellipsoidal liquid inclusions which may explain the better fits obtained by Formulas 5 and 6. Colbeck [37] also states that in seasonal snowpack two-grain clusters are more probable, indicating that the water will take on a ring-like shape. The data obtained by Linlor [31] were for snow that had been subjected to "vigorous" manual mixing, which probably resulted in single ice grains with a coating of water which lends itself to a good fit by Formula 9. It should be noted, however, that this is not an equilibrium state for water distribution [37] and although it may be valid for freshly wetted snow, it should be considered at most a lower limit for ϵ'_{ws} and ϵ''_{ws}.

Current understanding of the microwave dielectric behavior of snow may be summarized as follows:

1. For dry snow, ϵ'_{ds} is independent of frequency, approximately temperature-independent, and its variation with snow density is fairly well established (Figure 5) and may be approximated by Equation 7 or Formula 6.

2. For dry snow, ϵ''_{ds} varies with temperature, frequency and density. Very few experimental data are available, particularly above 10 GHz.

3. For wet snow, the presence of water adds another dimension to the complexity of the dielectric behavior of snow, and yet available data on ϵ'_{ws} and ϵ''_{ws} are even fewer than those reported for dry snow, thereby resulting in a rather sketchy understanding of the variation of ϵ_{ws} with frequency, and water content. However, Formulas 5 and 6 appear to provide the best fit to non-mixed snow.

Clearly, a vigorous experimental program designed to establish the dielectric behavior of snow is called for, particularly when free water is present.

PENETRATION DEPTH
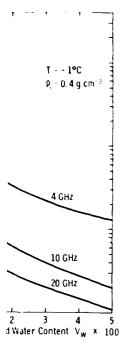
The penetration depth in a medium is defined as the depth at which the average power of a wave traveling downward in the medium is equal to $1/e$ of the power at a point just beneath the surface of the medium. For a medium with uniform extinction coefficient κ_e, the penetration depth δ_p is given by

$$\delta_p = 1/\kappa_e.$$

In the general case, κ_e consists of an absorption coefficient κ_a and a scattering coefficient κ_s,

$$\kappa_e = \kappa_a + \kappa_s.$$

As a first order estimate of κ_e, κ_s usually is ignored because its computation involves the dielectric properties of the ice particles and their size and shape distributions relative to the wavelength. For wet snow, setting $\kappa_e \approx \kappa_a$ is a fair approximation because $\kappa_s << \kappa_a$ under most snow conditions in the microwave region. The same approximation holds true for dry snow at frequencies in the lower part of the microwave spectrum (<5 GHz), but for frequencies above 10 GHz, κ_s may be comparable in magnitude to κ_a for some dry snow conditions (large particle sizes). Thus, when the penetration depth is calculated from $\delta_p = 1/\kappa_a$, the values then obtained should be regarded as upper limits since they do not account for scattering losses in the medium.

99

T - -1°C
ρ · 0.4 g cm⁻³

4 GHz

10 GHz

20 GHz

2   3   4   5
d Water Content V_w x 100

ed values of penetration
1 function of V_w for

ient is defined as:

$$+ \left(\frac{\epsilon''}{\epsilon''}\right)^2\right]^{1/2} - 1\right\}\right]^{1/2}$$

ι in free space. If $(\epsilon''/\epsilon') \ll 1$,
ıces to

)

· snow throughout the micro-
ıow for $V_w < 2\%$.
ted values of δ_p plotted as a
microwave frequencies. The
ry snow conditions ($V_w = 0$)
= 1.74 (from equation 6) and
ι $\varrho_s = 0.4$ g cm⁻³ and ϵ_i'' as
, > 0, equations 9–11 due to
computing ϵ_{ws}' and ϵ_{ws}''. These
all three frequencies even
measurements over the 4- to
hermore, as noted earlier, be-
nents are representative of
wet snow which exhibit lower
ınder natural conditions, the
ıre 9 are larger than would be
'. That is, these curves should
)f the upper limit of δ_p.

Perhaps the most significant information one can de-
duce from Figure 9 is that the penetration depth can de-
crease by more than an order of magnitude as V_w in-
creases from 0 to 0.5%, followed by a much slower rate
of decrease as a function of increasing V_w.

ENGINEERING APPLICATIONS

Two of the uses of dielectric properties of snow are:
1) development of sensors to measure snow liquid
water content and 2) interpretation and modeling of
microwave remote sensing data. For liquid water deter-
mination, frequencies below 100 MHz have been found
useful, while for remote sensing observations only fre-
quencies above 1 GHz are usually employed.

Knowledge of the liquid water content of snow is of
interest in many areas of snow research, including snow
strength, snow melt, rate of metamorphism, water flow
in snow, avalanche prediction and as a ground-truth
factor for remote sensing observations at the higher
frequencies. Ambach and Denoth [25] have worked for
several years to develop a dielectric measuring device
that can be used to ascertain the liquid water content of
snow. This indirect method has numerous advantages
over traditional methods such as calorimetric and cen-
trifugal separation, among which are rapidity of meas-
urement and reduction in the required ancillary equip-
ment (dry ice, silicone, etc.). Also, when evaluated
against the freezing calorimeter as a reference, an ab-
solute accuracy of ±0.5% for V_w was observed [25].
This accuracy is comparable to that of a field
calorimeter and, although contact with the snow is re-
quired for measurement, the time savings represented
by this in-situ method, as compared with calorimetric
methods, are very important in field operations.

This technique is based upon the substantial differ-
ence in the magnitude of the dielectric properties of
water and dry snow as discussed in the preceding sec-
tion. Ambach and Denoth's device consists of a bridge
circuit that measures the capacitance of a probe filled
with a snow sample. The change in capacitance due to
the presence of the snow sample is used to compute ϵ'
of the snow sample. Using equation 10, and either
measuring or estimating the snow density ϱ_s, the snow
liquid water content V_w is obtained. In one configura-
tion, the probe consists of five parallel plates with a
3-cm spacing and an effective volume of approximately
1000 cm. This volume was found to be near the lower
practical limit based on constraints of minimal com-
paction of the snow sample and negligible fringing
fields.

In many cases liquid water determination in thinner
layers is desired; near the surface of a snowpack, the li-
quid water content can have a large gradient with

ir comb-shaped capacitors have been devel-
at, through control of widths and spacings,
g effective measurement depths. Liquid
its in layer thicknesses as small as millime-
ceptually be obtained. Hence, the potential
easuring a very detailed liquid water profile
pack near-surface layer which would be
in the interpretation of microwave remote
rvations.

e radiometers and radars have shown
mapping snow depth, or water equivalent,
ireas for hydrologic applications [32-34].
crystals in snow being comparable in size
ength in the microwave region, particularly
meter wavelength range, propagation in
racterized by both absorption and scatter-
he radar backscatter and radiometric emis-
now are governed by the mean dielectric
the snow volume as well as the spatial vari-
dielectric constant within the volume. Dry
et snow at low microwave frequencies in
rhood of 1 GHz) is a relatively low-loss me-
means that the observed backscatter and
m a snowpack usually consist of contribu-
he entire pack as well as from the ground
detailed knowledge of the snow structure
dielectric depth profile is the key to success-
g of the microwave interaction with snow
rate interpretation of microwave observa-
to the lack of experimentally established
t can adequately describe the dielectric
snow as a function of frequency and liquid
ent, most research activities related to
emote sensing of snow have been limited to
" investigations.

irst-order investigations, the mean dielectric
ually is assumed to be uniform with depth
w crystals are assumed spherical in shape
m in size. These assumptions are used in
and empirical models developed to interpret
al results. Such investigations have estab-
verall behavior of backscattering and emis-
snow, but in order to use remotely sensed
dict snow parameters—such as water equiv-
quid water content—and to assess the state
rlying ground medium (frozen or thawed),
ecessary to use multi-frequency and multi-
bservations in a prediction algorithm that
s in greater detail the role of frequency and
ofile shape than is currently possible. Thus,
r research of the microwave dielectric prop-
iow is conducted, development of remote
lications of snow can only proceed at a slow

CONCLUDING REMARKS

The electrical properties of snow have been evaluated
as functions of the following physical properties: snow
density, temperature, ice particle shape, liquid water
content, and the shape of the liquid water inclusions.
Analyses of the dielectric dependence on the above par-
ameters indicates that the liquid water content exercises
the single most important influence, and consequently
the discussions were divided into wet and dry snow sec-
tions. Additionally, two spectral regions were exam-
ined in terms of potential applications.

In the lower of the two regions, 100 kHz to 1 GHz,
dielectric measurements have been used to measure the
liquid water content of snow. By further restricting this
range to above 10 MHz, the dependence of ϵ_{ws} on ice
particle shape becomes negligible. Hence, for a specific
snow sample, only snow density ρ_s must be measured
for a calculation of liquid water content. Although not
available commercially, operational sensors have been
built, are in use for measuring liquid water in the snow,
and hopefully will provide a good alternative to tradi-
tional techniques.

In the spectral region applicable to remote sensing, 1
GHz to 35 GHz, the general electrical characteristics of
snow are known; however additional measurements are
needed, especially for the imaginary part of the dielec-
tric constant above 10 GHz. Application of this infor-
mation is not direct as in the liquid water measurement,
but it is needed for refinement of the models used to de-
scribe the electromagnetic wave interaction with snow.
The sensitivity of microwave sensors to changes in the
dielectric properties of snow (due to changes in liquid
water content) may be illustrated by the following ex-
ample. Corresponding to a change in liquid water con-
tent of the snow surface layer from V_w = 0 (dry snow)
to V_w = 2%, the radar backscattering coefficient has
been observed to change by a factor of 30 (15 dB) at 35
GHz and the radiometric temperature increased by 120
K [35]. These results indicate that dry-wet snow deter-
mination is a relatively simple task, but quantifying the
wetness of measuring the water equivalent of the snow-
pack is not as straightforward. To realize these latter
objectives with a usable degree of prediction accuracy,
improved knowledge of the microwave dielectric prop-
erties of snow is needed.

REFERENCES

[1] Evans, S. (1965) Dielectric properties of ice and
    snow—A review. *Journal of Glaciology*. vol. 5, p.
    773-792.
[2] Royer, G.M. (1973) The dielectric properties of

ice, snow, and water at microwave frequencies and the measurement of the thickness of ice and snow layers with radar. Communications Research Centre, Ottawa, Canada, Technical Report No. 1242.

[3] Glen, J.W. and P.G. Paren (1975) The electrical properties of snow and ice. *Journal of Glaciology,* vol. 15, p. 15-38.

[4] Stiles, W.H. and F.T. Ulaby (1980) Microwave remote sensing of snowpacks. NASA Contractor Report CR 3263, for Goddard Space Flight Center, Greenbelt, Maryland, June.

[5] Hasted, J.B. (1973) *Aqueous Dielectrics.* London: Chapman and Hall.

[6] Lane, J.A. and J.A. Saxton (1952) Dielectric dispersion in pure polar liquids at very high radiofrequencies. I. Measurement of water, methyl and ethyl alcohols. *Proceedings of the Royal Society,* Series A, vol. 213, p. 400-408.

[7] Stogryn, A. (1971) Equations for calculating the dielectric constant of saline water. *IEEE Transactions on Microwave Theory and Techniques,* vol. MTT-19, p. 733-736.

[8] Klein, L.A. and C.T Swift (1977) An improved model for the dielectric constant of sea water at microwave frequencies. *IEEE Transactions on Antennas and Propagation,* vol. AP-25, p. 104-111.

[9] Ulaby, F.T., R.K. Moore and A.K. Fung (In press) *Microwave Remote Sensing: Active and Passive.* Reading, Massachusetts: Addison-Wesley Publishing Company.

[10] Cole, K.S. and R.H. Cole (1941) Dispersion and absorption in dielectrics. I. Alternating current characteristics. *Journal of Chemical Physics,* vol. 9, p. 341-351.

[11] Auty, R.P. and R.H. Cole (1952) Dielectric properties of ice and solid D_2O. *The Journal of Chemical Physics,* vol. 20, no. 8, p. 1309-1314.

[12] Paren, J.G. and J.W. Glen (1978) Electrical behavior of finely divided ice. *Journal of Glaciology,* vol. 21, no. 85, p. 173-192.

[13] Loria, A., E. Mazzega, U. del Pennino and G. Andreotti (1978) Measurements of the electrical properties of ice Ih single crystals by admittance and thermally stimulated depolarization techniques. *Journal of Glaciology,* vol. 21, no. 85.

[14] Cumming, W. (1952) The dielectric properties of ice and snow at 3.2 cm. *Journal of Applied Physics,* vol. 23, p. 768-773.

[15] Perry, J. and A. Straiton (1973) Revision of the 'dielectric constant' of ice in the millimeter-wave spectrum. *Journal of Applied Physics,* vol. 44, p. 5180.

[16] Vant, M.R., R.B. Gray, R.O. Ramseier and V. Makios (1974) Dielectric properties of fresh and sea ice at 10 and 35 GHz. *Journal of Applied Physics,* vol. 45, p. 4712-4717.

[17] Lamb, J. (1946) Measurements of the dielectric properties of ice. *Transactions of the Faraday Society,* vol. 42A, p. 238-244.

[18] Lamb, J. and A. Turney (1949) The dielectric properties of ice at 1.25-cm wavelength. *Proceedings of the Physical Society,* Section B, vol. 62, p. 272-273.

[19] Blue, M.D. (1979) Reflectance of ice and sea water at millimeter wavelengths. *Proceedings of IEEE MTT-S Symposium,* Orlando, Florida, May 1979.

[20] Von Hipple, A.R. (1954) *Dielectric Materials and Applications.* Cambridge, Massachusetts: MIT Press.

[21] Bertie, J., H. Labbe and E. Whalley (1969) Absorptivity of Ice I in the range 4000-30 cm⁻¹. *Journal of Chemical Physics,* vol. 50, p. 4508.

[22] Edgerton, A.T., A. Stogryn and G. Poe (1971) Microwave radiometric investigations of snowpacks. Final Report No. 1285 R-4 for USGS Contract No. 14-08-001-11828, Aerojet General Corporation, Microwave Division, El Monte, California.

[23] Sweeney, B.D. and S.C. Colbeck (1974) Measurements of the dielectric properties of wet snow using a microwave technique. U.S. Army Cold Regions Research and Engineering Laboratory, Hanover, New Hampshire, Research Report 325.

[24] Colbeck, S.C. (1980) Liquid distribution and the dielectric constant of wet snow. *Proceedings of NASA Workshop on the Microwave Remote Sensing of Snowpack Properties, Fort Collins, Colorado, 20-22 May 1980* (A. Rango, Ed.). NASA Goddard Space Flight Center, Greenbelt, Maryland, NASA CP-2153.

[25] Ambach, W. and A. Denoth (1980) The dielectric behavior of snow: A study versus liquid water content. *Proceedings of NASA Workshop on the Microwave Remote Sensing of Snowpack Properties, Fort Collins, Colorado, 20-22 May 1980* (A. Rango, Ed.). NASA Goddard Space Flight Center, Greenbelt, Maryland, NASA CP-2153.

[26] Tinga, W.R. and W.A.G. Voss (1973) General approach to multiphase dielectric mixture theory. *Journal of Applied Physics,* vol. 44, no. 9, p. 3897-3902.

[27] Tiuri, M. and H. Schultz (1980) Theoretical and experimental studies of microwave radiation from a natural snow field. *Proceedings of NASA Workshop on the Microwave Remote Sensing of Snowpack Properties, Fort Collins, Colorado, 20-22 May 1980* (A. Rango, Ed.). NASA Goddard Space Flight Center, Greenbelt, Maryland, NASA CP 2153.

[28] Keeler, C.M. (1969) Some physical properties of alpine snow. U.S. Army Cold Regions Research and Engineering Laboratory, Research Report 271.

[29] Kuroiwa, D. (1956) The dielectric property of snow. Union Géodésique et Géophysique Internationale, Association Internationale d'Hydrologie Scientifique, Assemblée générale de Rome, Tom. 4, p. 52-63.

[30] Tobarias, J., P. Saguet and J. Chilo (1978) Determination of the water content of snow from the study of electromagnetic wave propagation in the snow cover. *Journal of Glaciology*, vol. 20, p. 585-592.

[31] Linlor, W.I. (1980) Permittivity and attenuation of wet snow between 4 and 12 GHz. *Journal of Applied Physics*, vol. 51.

[32] Rango, A., A.T.C. Chang and J.L. Foster (1979) The utilization of spaceborne microwave radiometers for monitoring snowpack properties. *Nordic Hydrology*, vol. 10, p. 25-40.

[33] Ulaby, F.T. and H. Stiles (1980) Microwave radiometric observations of snowpacks. *Proceedings of NASA Workshop on the Microwave Remote Sensing of Snowpack Properties, Fort Collins, Colorado, 20-22 May 1980* (A. Rango, Ed.). NASA Goddard Space Flight Center, Greenbelt, Maryland, NASA CP-2153.

[34] Stiles, W.H. and F.T. Ulaby (1980) Radar observations of snowpacks. *Proceedings of NASA Workshop on the Microwave Remote Sensing of Snowpack Properties, Ft. Collins, Colorado, 20-22 May 1980* (A. Rango, Ed.). NASA Goddard Space Flight Center, Greenbelt, Maryland, NASA CP-2153.

[35] Stiles, W.H. and F.T. Ulaby (1980) The active and passive microwave response to snow parameters. 1. Wetness. *Journal of Geophysical Research*, vol. 85, no. C2, p. 1037-1044.

[36] Ambach, W. and H. Schittelkopf (1978) Neue Ergebnisse zum dielektrischen Relaxationsverhalten von Schneeproben. ZGG 14, no. 2, p. 201-208.

[37] Colbeck, S.C. (1979) Grain clusters in wet snow. *Journal of Colloid and Interface Science*, vol. 72, no. 3.

NOMENCLATURE

A_{kj} = depolarization factor

k = index where i = ice and w = water

$$A_j = \tfrac{1}{2}\,abc \int\limits_0^\infty \frac{ds}{(a^2 + S)^{1/2}(b^2 + S)^{1/2}(c^2 + S)^{1/2}(j^2 + S)}$$

where a, b and c are ellipsoid axes and S is distance along the respective axis

a = molecular radius, constant

F = form factor

f = frequency

f_0 = relaxation frequency

k = Boltzmann's constant

r_k = radius of i = ice, a = air, w = water, where

$$r_w = r_i\left(1 + \frac{0.916\,W_w}{100 - W_w}\right)^{1/3}$$

$$r_a = r_i\left(\frac{0.0916}{\varrho_s}\right)^{1/3}\left(1 + \frac{W_w}{100 - W_w}\right)^{1/3}$$

T = temperature

V_i = volumetric fraction of i = ice, w = water

W_w = percent liquid water by weight

α = attenuation coefficient

δ_p = penetration depth

ϵ_k = dielectric constant of i = ice, w = water, ds = dry snow, ws = wet snow, 0 = static value, ∞ = optical limit

ϵ' = real part of ϵ

ϵ'' = imaginary part of ϵ

η = viscosity

x_e = extinction coefficient

x_a = absorption coefficient

x_s = scattering coefficient

λ_0 = wavelength in free space

ϱ_k = density of s = snow, i = ice

τ = relaxation time

Committee Chairman Report on
Mechanical Properties

R. Oakberg

*CE/EM Department, Montana State University,
Bozeman, Montana 59717*

If this report were to summarize the agreements reached by the committee on mechanical properties, it would be very brief indeed. If it were to detail the discussions and mention all of the disagreements, it would be lengthy, complex and convoluted.

A sense of frustration, felt by practitioners and researchers alike, pervaded the meetings. The practitioners—who forecast avalanche hazard, evaluate static pressures on obstacles, predict vehicle mobility, etc.—repeatedly asked for standard field procedures that would give an accurate indication of the state of the snow. The researchers would like to help the practitioners, but are frustrated because they cannot suggest suitable procedures.

The practitioners want "index properties" that would provide sound bases for predictions. Salm defined an index property in the following way: it would be closely related to a physical property, but not one of the parameters in a constitutive equation; field measurements would be simple, and would always be conducted in the same way; the value obtained would not be affected by variations in sampling technique. The practitioners want procedures that are speedy and inexpensive, so they can evaluate index properties over a wide area. Any required analysis of the data should be so simple that it can be performed in the field.

An identification of possible index properties was attempted and a table was constructed to focus the discussion. The attempt floundered in a wash of potentially important physical parameters, deformation mechanisms, and interactions. The attempt was not completely fruitless—it identified the source of the researchers' frustrations.

The researchers are a long way from being able to suggest index properties, because they have not been able to define the problems. Either the problems are formidably complex, or crucial interactions are yet to be identified. Adequate models have not been developed.

For example, consider the release of a dry-slab avalanche. Each person who addressed this problem had a different mental picture of the processes involved. Some envision a large-scale phenomenon—some sort of shear failure develops over a large area, and this precipitates the other failures required for avalanche release. Others think that a failure nucleates locally, spreading as a brittle fracture or by coalescence of local failures into the full-scale avalanche. The practitioners decry current techniques, which require an extensive investigation of a single snow pit. They want to be able to make their measurements with portable instruments, so they can visit a large number of sites and establish the areal distribution of snowpack parameters. However, the practitioners don't mention what they expect to find. Do they want to establish the extent of an unstable zone, or do they want to increase the probability of finding a "hot" spot? There is consensus neither on the size of the failure zone nor about the controlling failure mechanisms. The lack of consensus isn't surprising—the progress of an avalanche obliterates all of the evidence.

In retrospect, the committee spent very little time discussing material properties. There may have been an unspoken consensus: It's inappropriate to concentrate upon material properties when the controlling mechanisms aren't understood.

If the researchers were given a complete statement of a problem, it could be solved. The complete statement would include: specification of the system; the applicable field equations (equations of equilibrium or motion, the strain–displacement or rate of deformation–velocity relations, constitutive equations that relate the stresses, stress rates, strains, strain rates, temperature, etc.); the boundary conditions, including relations between tractions and the slip rates. The solution may have to be a numerical one, and it may require the use of impractically complicated techniques, but it could be obtained.

It is instructive to ask the following question: "What parts of the boundary value problem do we have confidence in?" We trust the equations of equilibrium or motion and the kinematic equations—

they are based upon fundamental physical principles and upon geometry. However, we can't specify the system—we don't even know the extent of the critical zone. We can't select or develop the simplest constitutive equations that include the controlling physical effects—we don't know what failure and deformation mechanisms are involved. We can't select boundary conditions with confidence—again, we don't know what failure mechanisms are involved.

The speculations of a decade ago haven't developed into a consensus. Some of the more plausible hypotheses have been tested, and most of these have failed. Perla pointed out that even if parameters are obtained only from the tracks of recent avalanches, no correlation between avalanche events and the predictions of the current theories can be obtained. A great deal of effort has been spent developing improved instruments and sampling techniques, but these haven't led to accurate predictions. A notable exception is Sommerfeld's shear frame; however, some practitioners object to the large number of measurements that are required at a single site, which must be at the failure zone.

St. Lawrence dramatized the plight of the practitioner by saying that he has to solve the boundary problem—in his head! Perhaps this is the root of the problem. Have we pruned the problem until it will fit into our heads, but lopped the controlling features and crucial interactions in the process? Do all of our tractable models omit the essential physics?

A renewal of speculation is required. The problems must be reconsidered in all of their complexities. This time, the effect of no parameter should be neglected until it can be *shown* to be insignificant. Nor, should any possible interaction among the parameters be neglected unless it can be *shown* to be nonexistent or of minor importance.

The problems are very complex; as LaChapelle suggested, our approach must be holistic. For each problem, our goal should be to develop the simplest model that includes the essential physics. Dependencies among the parameters must be identified; nonessential parameters and interactions must be identified and eliminated from the model.

Two approaches can be used to eliminate irrelevant parameters from models. First, statistical methods can be used to identify dependent parameters. Second, the problem can be resolved into its simplest components and each component can be studied in isolation. Once the behaviors of the individual components are understood, they can be combined in order to study interactions among the components. The proper relationship between theory and experimentation should be maintained. It should be possible to falsify each theory; each experiment should test a hypothesis.

Although the committee spent more time discussing mechanisms than it did discussing material properties, some new and important research areas were identified.

One task would be to correlate the electrical and mechanical properties of snow. If these properties can be correlated, it might be possible to devise instruments that will enable a practitioner to assess the properties of a snowpack quickly; this would enable a practitioner to evaluate the areal distribution of the properties.

Another task would be to study the dissipation characteristics of snow. This research is prompted by the fact that the field equations and boundary value problems appear to be much too complicated to be of practical value. The dissipation or dissipation rate is a phenomenological property that represents the energy required to change the state of snow. The use of an energy method could avoid the complexities of the field equations, and the complexities of attempting to relate the details of the deformation mechanism to the behavior of the system.

Allied to the dissipation is the disaggregation energy, the amount of energy required to transform a unit volume of cohesive snow into individual particles. Knowledge of the disaggregation energy would have obvious application in blowing snow problems, since saltation erodes snow surfaces. It could also have relevance to avalanche problems. It could serve as an index property for snow slabs and layers, and could also indicate how much potential energy is expended in pulverizing a slab in the acceleration phase of an avalanche. Again, use of the disaggregation energy could eliminate the complexities of relating the strengths of individual bonds to the behavior of a snow mass.

The effects of a sudden temperature increase on the surface of a snow slab should be investigated. There is an abundance of circumstantial evidence—including diurnal variations of the acoustic emissions from snowpacks—suggesting that a sudden change in the temperature of the surface layers of a snowpack has an unexpectedly large effect upon its stability.

In conclusion, a sense of frustration pervaded the ~~committee meetings.~~ The practitioners are frustrated because they have no reliable index properties and feel that the researchers haven't addressed their needs. The researchers are frustrated because they haven't been able to help the practitioners and feel that the practitioners haven't helped them define the problems. Although the index properties desired by the practitioners won't be forthcoming until the mechanisms are fully understood, the value of the efforts to date must be recognized. At least the strenuous plowing has identified infertile ground.

Committee Chairman Report on
Viscous, Frictional, and Blowing Snow Properties

David M. McClung

Canmore, Alberta, Canada T0L 0M0

INTRODUCTION

This session dealt with three basic topics: a) sliding friction of snow dealing with the basic problems of static grip and kinetic glide coefficient of skis and runners on snow as well as the problem of friction of snow on snow at slow speeds; b) properties of flowing snow as related to avalanche dynamics; and c) properties of blowing snow. These topics are all interrelated to some degree, particularly b and c. A summary of the committee discussions relevant to each topic appears below.

a. Sliding friction

There was surprising interest in this topic among the participants, although none of the participants are actively engaged in full-time research on this topic. There was considerable discussion about the physical mechanisms involved and a variety of ideas were proposed to explain the various features of the apparent low coefficient of friction for runners and skis on snow. It quickly became evident that the number of parameters and variety of test conditions involved make it a very complex problem, in which careful experimental work is essential. Theoretical work unsupported by data would very likely not be very appropriate on many aspects of the subject.

Specific points of note from the discussion were as follows:

Bard Glenne presented a short summary of the problem. He emphasized the large numbers of parameters involved the necessity to measure a large number of parameters in any given experiment. Other points he mentioned were: 1) there will be several mechanisms operating simultaneously and each area of a ski may have a different dominant mechanism; 2) there is a possibility that friction may increase with increase in water film thickness under limited conditions based on ski testing. This is thought to occur under very wet conditions.

Ray Yong pointed out that the U.S. Army was doing experimental work on sliding friction at Ft. Greely, Alaska. This work may be of interest because the possibility of cooperative efforts between that group and those more theoretically inclined might provide a focal point for a good research effort.

Walter Ambach made a presentation based on the doctoral thesis of his colleague, Dr. Mayr, on measurement of water film thickness on skis. The measurements employed a parallel plate capacitance pickup system mounted on the ski. The results showed: 1) A water film thickness under the middle section of the ski of 4–16 μm. Thickness increased with speed and temperature. 2) Much steadier conditions were encountered in soft snow than on hard pack due to better ski contact. 3) Variations in film thickness with wax color and air and snow temperatures were also shown.

K. Tusima made a short theoretical presentation for ski resistance and plowing (deformation) resistance. The theory does not, however, take into account water film effects.

J. Dent and T. Lang made a presentation on the question of formation of a thin mobile layer for sliding blocks of snow on snow. This work was undertaken for speeds up to ¼ m/s and provides estimates of the dynamic coefficient of friction for snow on snow. It was also noted that this work may be of use to study the question of the disaggregation energy to remove particles from the surface for blowing snow problems.

Summary

There was surprising interest in this topic in general and it was felt that the group had the theoretical capability to greatly advance research in this area should interest be shown by funding agencies. The absence of those doing experimental work on this topic (such as those from the ski wax companies in Scandinavia and Finland as well as those from the U.S. Army) was felt and prevented great progress in the discussion.

No specific research areas were identified for immediate recommendation in this area. There seemed to be a general feeling that studies of a rather basic, general nature are still appropriate in this field which is in its infancy. Good basic experiments carefully done and well planned seem appropriate on many individual aspects of the problem. In this way more specific problem areas may be identified. It should be emphasized, however, that had the committee included experimentalists actively engaged in research on these topics this assessment might be radically changed.

b. Properties of blowing snow as related to avalanche dynamics

This part of the session provided the best interaction because most of the committee members have worked in this area or have high interest in it. Practical problems as well as theoretical problems were discussed but the emphasis was on measurements. The discussion on measurements was based upon not only what has been measured but also what should be measured.

On the theoretical side there was considerable discussion about modeling of flowing snow in avalanches and how to characterize it. In this regard the following comments seem in order.

1. There seems to be a trend away from purely dynamic modeling and toward treatment of the problem as a two- or perhaps multi-phase flow problem. This will require a better knowledge of the flow characteristics of a system of particles in a fluid which is what flowing avalanches consist of. The discussion seemed to indicate that field data show at least some correlation of particle size with runout characteristics, for example. Such modeling would not negate the fluid dynamic models which have dominated for the past 25 years but seems to point the way toward the foundations of future research.

2. There was considerable discussion as to how to characterize the flow in terms of the ratio of internal to viscous forces which may be a Reynolds number in fluid dynamics or a Bagnold number when particle collisions enter in. There was a rather general feeling that for the large avalanches of importance the ratio is very high and the problem is strongly inertial. This would imply viscosity will not enter significantly in the modeling.

3. It was pointed out that there is a transition in states in the problem for large avalanches. At the starting zone and runout zone the deformation resembles a sliding block or the flow condenses by a locking mechanism to nearly the same thing. In the middle section of the path near terminal speed the motion is fluid-like. It was noted that the lengths of these zones or sections are related to path length. It seems thus that one may not be able to accurately model all avalanches with the same simple model. For example, a fluid-like model would not be valid in problems with very short path lengths since this appears to be a sliding problem.

4. The discussion about measurements dominated the session. The measurement of velocity and density of flowing snow was identified as the most important area for future research, both from large-scale field measurements as well as small-scale controlled experiments. Two points which were emphasized were: a) It is not possible to determine the parameters even in the simple models now employed without speed measurements such as speed of the center of mass of the avalanche along the incline, and b) knowledge of the flow mechanisms is not possible without velocity and density profiles through the cross section of the avalanche.

Specific points of note from the discussions

Art Mears presented a field estimate of velocity and friction coefficient for a large glacier avalanche with a path length of 8 km and an apparent coefficient of friction near 0.1.

J. Dent and T. Lang illustrated small-scale field experiments on flowing snow. These experiments showed that a Bagnold type collision or grinding mechanism applies at slow speeds (< 20 m/s) with many snow balls of initial diameter 0.1 m ground to powder on a path length of 85 m.

Hal Boyne presented an innovative idea based upon the concept of a Michelson interferometer (microwave range) which holds promise to get at the important question of velocity and density profiles in flowing snow.

Bruno Salm briefly mentioned new work to be done in Switzerland on measurement of avalanche transport velocity by radar techniques as well as small-scale laboratory modeling with fluid–granular mixtures.

Dave McClung presented the descriptive aspects of the characteristics of flowing snow measured in full-scale impact experiments at Rogers Pass, B.C. The contrasting behavior between wet and dry snow was noted. Dry avalanches appear to consist of bursts of particles similar to turbulence bursts in turbulent fluids. Wet avalanches have a more continuous type of flow. Both types of avalanches are characterized by steep vertical gradients of the relative volume concentration of solids. Also mentioned were data on correlation of impact of wet snow on a large plate (0.5 m diameter) with smaller load cells. Impact signals correlate well but a steadier flow is obtained on the large plate because many particle collisions are simultaneously integrated.

Summary

There was high interest in this topic because many of the participants had done work in this area. The specific research areas identified for immediate concern

were: 1) velocity data, both of the center of mass of transport velocity along the incline as well as velocity profiles through the avalanche cross section, are needed to determine the parameters in the existing models as well as to advance the state of the art for flow and runout models; and 2) profiles of the density distribution of flowing snow are needed to determine flow mechanisms. These data, in concert with velocity data through the cross section of the avalanche, seem essential before serious detailed flow models are developed. It should also be mentioned that participants emphasized throughout the discussion the extreme difficulties which will be encountered in performing such experiments in full-scale avalanche flows in the field as well as the inherent personal risks involved.

c. Properties of blowing snow

Some of the discussion on the topic of blowing snow was integrated into the discussion on flowing snow. The committee discussions revealed that this topic is one of great practical importance as well as one with great intellectual challenge. In-depth progress to any great degree was somewhat hampered by the small number of committee members actually engaged in research in this area. Specific points of note from the discussion follow.

The major portion of the discussion, which was led by R.A. Schmidt, focused on relating physical properties to engineering indices. Three basic classes of problems were identified: 1) estimation of total transport mass from upwind contributing areas, 2) estimates of trapping efficiency which is the fraction of blowing snow caught in a catchment basin or control structure, 3) estimation of transport rate.

Of these three classes of problems the least understood seems to be the estimates of transport rate. The application of engineering indices to predictions for flow over complex terrain appears to be a worrisome and important research problem. For terrain such as mountain ridge crests there is experimental evidence from Switzerland which indicates that there is uncertainty in describing the drift flux distribution with height. Current data indicate a maximum far above the surface in some cases which is contrary to hori-

zontal surface measurements. This will strongly affect trapping efficiency modeling as well as transport rate modeling, of course. In order to apply blowing snow modeling effectively to the avalanche formation problem, and many other practical problems for example, research in this area is needed. In this regard R.A. Schmidt discussed some preliminary ideas and possibilities for measuring drift flux in the lowest half meter. He emphasized that this will be a difficult experimental problem, however.

Summary

The general area of extension of current prediction techniques to complex terrain was identified as an important research area for blowing snow. More specifically, estimates of transport rate and related drift flux measurements above the surface for such terrain seem to be particularly difficult and important areas. The mechanism which elevates the drift flux to produce a maximum far above the ridge crest is presently unknown, which indicates that theoretical work will have to be undertaken to solve the problem as well.

In order to apply engineering indices to the total transport rate, current theoretical models call for the threshold wind speed to produce blowing snow, which will be a function of many parameters and fundamentally related to surface strength. Data related to this problem directly or indirectly seem very scarce if not non-existent, and such data seem essential if progress is to be made in this area. The experiments reported at this session on formation of a thin mobile grain layer provide a small beginning on one aspect of this problem.

Other related experiments outlined in the review paper by Schmidt seem worthwhile to clarify the physics involved in blowing snow and to extend and understand the limitations of the main theories proposed to date. For the topic of blowing snow as with the two others in this session the complexity of the problems both experimentally and theoretically mean that real progress will be hard to achieve and perhaps cooperative efforts, even internationally, will be called for in view of the small number of workers in those fields on a worldwide basis.

Report of Committee Meeting

Electrical, Optical and Acoustical Properties of Snow

H. Gubler

*Eidg. Institut fur Schnee-und Lawinenforschung,
Davos, Switzerland*

ABSTRACT

Measurements and modeling of the complex dielectric constant of dry and wet snow in the frequency range up to 100 MHz allow accurate (1% accuracy) determinations of the snow wetness in the range of 0.5 to 30% water content as well as particle shape and possible surface parameters. Ground-based active radar systems are in use for snow profiling and water-equivalent determinations. Radar radiometers and active radar systems (ground-, aircraft- and satellite-based) show improved performance for snow water-equivalent, wetness, melt-freeze cycle determinations and snow cover mapping. More work is needed to include and correct for the stratification of the snow cover and the structure of the snow. The most important model parameter is the correlation length distribution which can be directly determined from thin sections. Radar measurements are also used for avalanche speed measurements.

Visible and near-infrared measurements of albedo are generally well-explained by model calculations, but further observations and modeling efforts are needed. The most important snow parameter is optical grain size; a second important parameter is impurity content. The influence of snow surface structure on the albedo is less than the influence of these other two parameters, but may be important for very low sun angles. Thermal emissivity of snow is about 99%, essentially independent of snowpack parameters.

The only practical applications of the acoustical properties of snow so far are low and high frequency acoustic emission measurements in natural avalanche release zones and artificially stressed snow samples respectively. These types of measurements are used to investigate the stability of sloping snow covers and to formulate constitutive equations for snow. The acoustical properties of snow show some potential for investigating or at least indexing snow structure.

INTRODUCTORY REMARKS

This report consists of three parts:
  I The Committee Chairman Report
  II Short Contributions by Other Authors
  III Summary of today's and near-future measuring and modeling techniques and their practical application (Tables I, II), summary of the problems to be solved in the near future (Table III), and conclusions

The main research fields and applications depending on electrical, optical or acoustical properties of snow are snow mechanics, snow avalanche research, snow hydrology, and climatology.

I. COMMITTEE CHAIRMAN REPORT

Introduction

The main goals of the workshop session on electrical, optical and acoustical properties of snow as part of the Joint U.S.–Canadian Workshop on the Properties of Snow can be described as:

a) definition of the parameters meeting the requirements of the users (snow mechanics, snow avalanche research, snow hydrology, climatology);

b) presentation of recent results not covered by the review papers (Stiles, Warren and Sommerfeld) and critical analysis of the compatibility of the data;

c) discussion of the possibilities, problems and limitations of today's and near-future measurement and modeling techniques;

d) ideas for future research activities to fit the requirements of scientific and user communities.

Electrical properties

The different measurement techniques and the types of parameters to be determined admit a subdivision of the electrical properties of snow into four parts: 1) direct current properties, 2) AC properties below 1 GHz, 3) microwave properties, and 4) miscellaneous.

111

1. Direct current properties

Only very few direct current measurements have been done in snow (Siksua 1957, Kopp 1962, Mellor 1964, Glen 1975). Kopp concluded from his conductivity measurements in snow that the bulk conductivity of ice is too small to account for the measured snow conductivities. He also found that the activation energy for snow does not correspond to the value for bulk ice and is different for new snow and recrystallized snow. He proposed that conductivity of snow occurs mainly in the disordered surface layer of the ice crystals (Fletcher 1968, Kulividze 1974, Mazzega 1976, Golecki 1977, Maeno 1978, Beaglehole 1980). Knowing the impurity content of the snow under investigation (e.g. by determination of the conductivity of the corresponding melt-water) it seems to be possible to determine the specific surface of the snow as well as the state of recrystallization (metamorphism) of the snow.

Unfortunately other fields, like the thermoelectric effect or volta effect or charging of ice particles (Mellor 1964, Hobbs 1974), have not been covered by the review paper and during the session.

2. AC properties below 1 GHz

In the low frequency range (< 500 kHz) the static dielectric constant ϵ_0 determined from the measured distribution of relaxation time for snow depends strongly on the shape factor (depolarization factor, e.g. for the Polder and van Santen mixing model) of the ice particles (Denoth, short contribution). A determination of the shape factors by measuring the dielectric constant as a function of frequency and using an appropriate mixing model looks promising. Preliminary measurements of the absorption coefficient by Denoth in the frequency range 1 MHz to 100 MHz show a dependence on the shape of the ice particles independent of wetness. Particle shapes and particle sizes (snow structure) are of high interest in snow mechanics and also for the modeling of the microwave properties of snow (calculation of the ice–pore correlation length in the case of isotropy [Kong 1980]) as well as the optical properties (albedo and emissivity).

In the frequency range above 1 MHz the permittivity depends only very weakly on the shape of the ice particles and has a dependence on the shape of the water inclusions (pendular, funicular wetness regime [Colbeck 1980]) but depends strongly on the liquid water content. The accuracy of the wetness determination using the Polder and van Santen mixing model in the range of liquid water saturations of 0.5 to 30 vol % is about 0.5%. The announced (Denoth) development of an easy to handle microprocessor-based device using a 10^{-3} m^3 5-to-7 plate condenser as a sampling probe will provide an accurate (≤ 1 vol % absolute error) standard instrument for wetness determinations in the near

future. Another topic, propagation of radio waves in and over a snow cover, has not been covered by this workshop but has practical importance (communication; rescue beacons [M. Bockert 1964/65, Good 1977]).

3. Microwave properties

In the microwave range research has been intensified during the last 10 years, stimulated by the possibilities of remote sensing from spacecraft. Different types of measurements are possible and have been investigated (short contribution of H. Boyne). Basically there are two types of applications: remote measurements from satellites and aircraft, and measurements using instrumentation at given locations on the ground.

The ground-based measurements include local determinations of the density profile or the stratification of the snow cover, the water-equivalent and the depth of a dry snow cover using FM–CW radar in the frequency range 1–15 GHz. These types of measurements are of great promise for localized ground truth measurements of the water-equivalent, replacing pressure pillows and indirect water-equivalent estimates, and to calibrate remote areal measurements from satellites for water resource management. They may also simplify snow profiling in connection with stability evaluations for avalanche research. Devices may be used either buried in the ground looking upward through the snow cover or installed above the snow cover, looking downward. They could also be carried by men or helicopters. Linlor (1977) measured the coherent microwave backscatter of natural snowpacks using modulated and unmodulated swept frequency sources in the range from 4 to 12 GHz to determine the layering of a natural snowpack. In this experiment interference patterns caused by the backscatter of the different layers as a function of frequency are measured, whereas the FM–CW device basically measures distances from the antenna system to the backscatterer. Both systems looking upward through the snow cover also show promise for investigations of the drainage of water through snow or of the growth of the wet snow layer from the snow surface downward.

Linlor also performed transmission and resonance (snow-filled microwave cavity) measurements in the range 1–12 GHz to determine snow wetness, grain size, attenuation, complex dielectric constant, drainage speeds and water flow speeds. Drainage speeds in snow are very important again for watershed management and also for flood forecasting. Attempts are made to use X-band doppler radar systems to measure velocity distributions in flowing snow avalanches (Gubler 1980). FM–CW systems will be used to measure flow height and particle size distributions. Remote measurements mainly used for snow hydrology include

water-equivalent and wetness estimations and snow cover mapping. Both active and passive systems are under investigation or are proposed.

Wetness measurements are so far restricted to near-surface layers and the determination of the water-equivalent depends strongly on the snow stratification (Maetz..r 1980, 1981). Improvements of modeling techniques (Kong 1980) and accurate measurements of the loss factor for snow above 10 GHz are necessary to further improve these types of measurements, which are of fundamental importance for snow hydrology. Common suggestions for all types of measurements in the microwave range are:

1. For wet snow sample preparation, the committee proposes to use the technique introduced by Colbeck (1979).

2. Dry snow is best characterized by photographs of stereological planes or thin sections.

3. For modeling the microwave properties the distribution of the correlation lengths in three dimensions (determined from thin sections or stereological planes) as well as the complex dielectric constant of ice have to be known.

4. The vertical particle size profile in the snowpack is important for snow water-equivalent determinations (partially determines the correlation length distribution).

A summary of applications and methods of measurement is given in Table I.

4. Miscellaneous

The different methods, basically belonging to the electromagnetic properties of snow, were neither covered by the review papers nor were they discussed by the committee. Some of the most important methods and properties will therefore be summarized here. Various types of γ-snow profiling gauges are in use (Armstrong 1976, Brown 1980). The attenuation of a γ-ray emitted by a radioactive source and received by a rate meter is measured. The attenuation depends on the mean density of the snow between source and rate meter. Emitter and receiver are either moved in separate vertical tubes through the snow cover or have fixed location. Depending on the type of instrumentation, the water-equivalent and the density profile can be determined.

Areal water-equivalent measurements from aircraft have been made by determining the attenuation of the natural γ-emission of the ground due to the snow cover (Brown 1980).

Different researchers developed neutron counters buried below the snow cover to measure the changes in the incident natural neutron flux by the snow cover (Brown 1980, Kodama 1980, Fritzsche 1981). The accuracy depends on the integration time and amounts to

a few centimeters of water-equivalent. Both types of water-equivalent determinations do not depend on the snow wetness

Nuclear Magnetic Resonance (NMR) measurements have been used by Kulividze (1974) to determine the thickness of the disordered layer on ice crystals. It has been proposesd to use low magnetic field NMR to measure very low liquid water contents of snow (<< 1%), which have a strong effect on the microwave properties above a few GHz.

Optical properties

The optical properties of snow are important for many different fields of snow and avalanche research and other environmental sciences. The review paper, as well as the committee discussion, concentrated on snow albedo and emissivity calculation. Other important areas, such as flux extinction (Mellor 1970, Warren review paper) and radiative heating (Colbeck 1976) were not been discussed at the meeting. Nevertheless, these parameters are very important for runoff forecasting and for stability evaluations in avalanche release zones for dry and wet snow avalanches (Gubler 1980). Some of the controversy concerning the different models is discussed in the short contribution by Chang. Instrumentation and measuring problems are outlined in the short contribution by Ambach. The optical grain-size and, in some cases, the surface and near-surface structure at the snow cover seem to be the most important input parameters to the different models in addition to the complex dielectric constant of ice which has not been measured accurately in some wave length ranges. The particle size and shape and structure parameters can be deduced from thin sections or stereological planes. Type and amount of impurities also have a large effect on the optical properties. Because of the high emissivity of snow in the thermal infrared, radiative cooling of the snow surface may permanently alter the snow surface structure. This fact is again very important for avalanche stability evaluations. Other applications depending on the knowledge of the optical properties of snow are: mapping of the snow cover, estimates of water-equivalents for shallow snow covers, estimates of impurity contents and grain sizes near the snow surface, alterations of the surface of the snow cover in spring (Firnspiegel, surface ripple). Optical systems are also in use to digitize thin sections and stereological planes of snow samples (Good 1980, Perla 1980), for blowing snow particle counters (Schmidt 1977, Gubler 1981), for snow depth measurements (Good 1973, Aburakawa 1979), for stereophotogrammetric systems to measure avalanche speeds (CTGREF 1980) and may be used in the future for measurements in powder snow avalanches (Abe 1978).

Acoustical properties of snow

Investigations and applications of the acoustical properties of snow have so far been very limited. There is no sharp separation between mechanical and acoustical properties. The investigations can be divided into two main classes: propagation properties of acoustic and shock waves in snow, and acoustic emission of stressed snow.

The special contribution of J. Johnson lists the parameters to be measured to characterize sound propagation in snow.

In the past, many measurements were restricted to some kinds of measurements (not well-defined) of a propagation velocity and an attenuation using either explosives or sonic bursts (Sommerfeld review paper). The interpretation of these data is, in many cases, very difficult because it is not clear which wave type was dominant in the experiment. Better defined measurements of the wave impedance and dispersion have been made using wave tubes (Ishida 1965, Johnson 1978, Buser 1981). Applications include investigations of the effect of explosives on the snow cover for military purposes and artificial avalanche release (Montmollin 1976, Gubler 1977, Brown 1980, Johnson 1981); propagation of sound over a snow surface (Mellor 1965), propagation of sound through the air/snow interface (Johnson 1978) with respect to the problem of the location of avalanche victims; snow depth measurements using ultrasonic signals (Marbouty 1978, Gubler 1981); propagation of acoustic energy at low frequencies originating from limited fracturing or from snow creep and glide in avalanche release zones, propagation of very high frequency signals originating from dislocations in ice crystals or breaking bonds between crystals in loaded snow samples.

Attempts to quantitatively correlate snow structure with acoustic properties look promising but were so far only partially successful (Ishida 1965, Johnson 1978) or are very preliminary (Buser 1981).

Modeling problems arise mainly at very low snow densities (< 200 kg) where the ice network can not be considered as rigid or purely elastic and a main portion of the acoustic energy propagates through the pore space. Possible future experiments may include nondestructive in situ snow structure measurements.

The frequency spectra of the acoustic emission of snow depend on the size of the energy releasing volume. Breaking of single bonds or energy releases in single crystals causes high frequency signals, whereas larger fractures in the snow cover or creep and glide of the snow cover cause low frequency signals. The high frequency signals have a very short detectable range of a few centimeters and are detected by piezoelectric pressure transducers. This type of measurement is used to investigate adaptation of the snow structure to a given stress state. More research is necessary for a complete understanding of the mechanisms involved.

To register the low frequency signals in avalanche release zones, sensitive seismic transducers embedded in the snow or in the ground are used. Recent results (Gubler and Sommerfeld) show that at least two types of signals occur: isolated spikes, possibly from limited fractures, and continuous low frequency noise from gliding, possibly creeping snow. The signal increase preceding a full-depth avalanche developing from a gliding snow cover looks very similar to the type of signal measured preceding earth slides or ice avalanches. The signals from gliding snow have large amplitudes and can easily be measured with seismometers buried in the ground even at distances on the order of 100 m from the source. The isolated spikes, possibly originating from limited fractures and redistribution of stresses in a release zone, have very low amplitudes and are, in general, only observed with transducers embedded in the snow cover near the active zones. More research is needed for a better understanding of the source mechanism and the signal interpretation with respect to the development of natural stability, and also to discriminate the snow signals against different sources of environmental noise.

II. SHORT CONTRIBUTIONS

IIa. Snow structure and electrical properties (by A. Denoth)

1. Introduction

Grain size, grain shape, porosity and liquid water content control most of the electrical properties of snow. In order to determine the influence of these quantities on the electrical behavior, the complex dielectric constant of various snow samples was measured in the frequency range of 100 Hz up to 100 MHz. The mean grain size and the axial ratio of the grains were determined by analyzing photographs of the surface of the snow samples. Assuming the ice grains or grain clusters can be approximated by spheroids, the shape factor or the depolarizing factor g_s can be calculated from the axial ratio m by (Stoner 1945)

$$g_s = \frac{1}{1-m^2}\left(1 - \frac{m}{(1-m^2)^{1/2}} \cdot \cos^{-1}m\right) \quad m < 1.$$

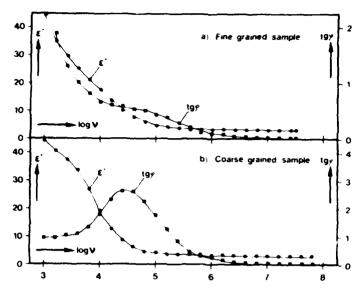The liquid water content was determined by a freezing calorimeter within an absolute error of 0.5% by volume.

114

Figure 1. Frequency dependence of the relative permittivity ϵ' and the loss tangent $tg\varphi$ of a fine-grained (a) and a coarse-grained (b) snow sample.

2. Experimental results

The experiments were carried out in the natural snow cover in the Stubai Alps (Schaufelferner/Daunferner) at 3000 m a.s.l.

2.1. The complex dielectric constant. Figure 1 shows the frequency dependence of the relative permittivity ϵ' and the loss tangent $tg\varphi = \epsilon'/\epsilon''$ (ϵ'' loss factor) of a fine-grained (Fig. 1a) and a coarse-grained (Fig. 1b) snow sample. Fine-grained snow samples are defined as samples that have not undergone appreciable metamorphism and with a shape factor $g_x \leq 0.03$. Coarse-grained samples are defined as samples with a mean grain size greater than 0.5 mm and with a shape factor $g_x \geq 0.20$. In comparison with the coarse-grained sample, the fine-grained sample shows a wide relaxation regime and the loss tangent decreases monotonically without passing through a marked maximum. This means that in the case of a fine-grained sample the relaxation behavior is controlled by a spectrum of relaxation times, and in the case of a coarse-grained sample only by a single relaxation time.

From a detailed analysis of the frequency dependence of the complex dielectric constant results, the model of Cole-Cole, which is based on a spectrum of relaxation times, can be applied to snow (Ambach 1972):
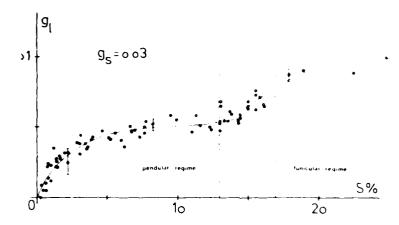
$$\epsilon(\omega) = \epsilon' - i\epsilon'' = \epsilon_\infty + \frac{\epsilon_s - \epsilon_\infty}{1 + (i\omega\tau)^{1-\alpha}}$$

where ϵ_s and ϵ_∞ are the limiting values of the relative permittivity for very low ($\omega \to 0$) and very high ($\omega \to$

∞) frequencies respectively, τ is the main relaxation time and α the distribution parameter of relaxation times. In the case of $\alpha = 0$, the model of Cole-Cole converts into the model of Debye, which is characterized by a single relaxation time. The static (ϵ_s) and high frequency (ϵ_∞) relative permittivity, τ, and the distribution parameter α can be derived from the experimental data by a least-square fit.

2.2. The high frequency relative permittivity ϵ_∞. The high frequency relative permittivity is controlled by the porosity, the liquid water content and the relative permittivities of the components ice, air and water (Ambach 1975). The influence of snow structure properties such as size and shape of the ice grains is negligibly small. In contrast to that, the shape of the liquid inclusions plays an important role—it depends on water saturation (water volume/pore volume) and on the kind of snow (Denoth 1980).

The dependence of the shape factor g_l of the liquid inclusions on water saturation is shown in Figure 2 for fine-grained snow and in Figure 3 for coarse-grained snow. The kind of snow is characterized by the mean grain size and the shape factor g_x of the ice grains. The solid line in Figure 2 and Figure 3 is a least-square fit using Tchebycheff polynomials. At low liquid saturation the shape factor g_l increases monotonically, whereas at higher saturations a significant change is marked. This change may be attributed to the pendular-funicular liquid transition (Denoth 1978, 1980). This transition occurs between 8% and 12% saturation in the case of snow in an advanced stage of metamorphism ($g_x \geq 0.20$) and between 13% and 17% in the

115

Figure 2. Dependence of the shape factor g_l of the liquid inclusions on water saturation for fine-grained snow samples. Fine-grained samples are characterized by a shape factor for the ice grains $g_s \leq 0.03$. The pendular-funicular transition occurs in the range of 13% to 17% liquid saturation.
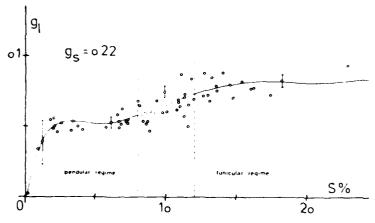
Figure 3. Dependence of the shape factor g_l of the liquid inclusions on water saturation for coarse-grained snow samples. Coarse-grained samples are characterized by a shape factor for the ice grains $g_s \geq 0.20$. The pendular-funicular transition occurs in the range of 8% to 12% liquid saturation.

has not undergone appreciable
).03).
ous mixing formula for calculat-
tivity of snow from the relative
components, the corresponding
, and shape factors shows that
nd van Santen is especially suited
and Schittelkopf 1978).
'ative permittivity ϵ_s. Figure 4
of the static relative permittivity
sults of a detailed analysis show

that ϵ_s depends mainly on the porosity and on the shape factor g_s of the ice grains: ϵ_s reflects structure properties. The influence of liquid water saturation is comparably small. Calculations of ϵ_s according to the three-component mixture theory of Polder and van Santen are also given in Figure 4. This model is especially suited for application to snow, as it allows the calculation of both the high frequency and static relative permittivity ϵ_∞ and ϵ_s respectively with the same parameters g_l and g_s.
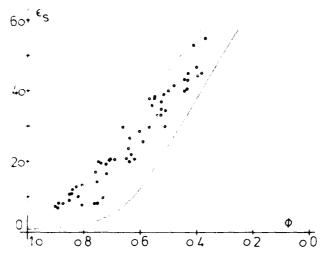
Figure 4. Dependence of the static relative permittivity ϵ_s on the porosity o. Full symbols represent dry snow, open symbols wet snow. The lines represent calculations of ϵ_s according to the theory of Polder and van Santen for liquid water content W and shape factors g_s naturally occurring: broken line represents wet snow (W = 0.01) and oblate ice grains (g_s = 0.00), the solid line represents dry snow (W = 0.00) and spherical ice grains (g_s = 0.33).

ions
lel of Cole-Cole combined with the three-
mixture theory of Polder and van Santen is
scribe quantitatively the frequency depend-
: complex dielectric constant of snow. The
r g_s accounts for the shape of the ice grains,
,hape of liquid inclusions. A significant in-
the grain size on the relative permittivity
und in the frequency range of up to 100

:c relative permittivity ϵ_s is determined by
d the shape of the solid ice matrix. So, if ϵ_s
ith a reasonable accuracy, the shape factor
J ice matrix can be calculated. This shape
be used to characterize the structure of
les.
frequency relative permittivity ϵ_∞ is main-
ed by porosity, liquid water saturation and
of water inclusions. Therefore, compared
methods, the measurement of the relative
ϵ_∞ of snow is a more economical method
rmination of liquid water content (Ambach
th in press). This dielectric method is par-
ited for field measurements and the results
factory accuracy.

'gment
nds zur Forderung der Wissenschaftlichen

IIb. Active microwave systems (by H. Boyne)

Active microwave systems in the frequency range 1
GHz to 100 GHz have been used to investigate stratifi-
cation, density, water equivalent and liquid water con-
tent in the snow cover. The types of active microwave
measurements include radar reflection coefficient and
backscatter and snow profiles. These measurements
are then interpreted using knowledge of the relation-
ship between electromagnetic and physical characteris-
tics of the snowpack. Since these characteristics are all
interwoven, accurate and detailed ground truth is
needed to interpret the results properly.

Reflection coefficient and
backscatter measurements

The measurement of radar coefficient and backscat-
ter indicates a sensitivity to snow wetness at the sur-
face. Both types of measurements give similar infor-
mation. Radar backscatter measurements will be
stressed since they are the most common field meas-
urements.

In the frequency range 1-18 GHz, significant trans-
mission into the pack can occur for dry snow condi-
tions. For wet snow, absorption increases with increas-
ing frequency. Above 18 GHz the underlying snow-

117

pack can be treated as infinite in extent except for very shallow snowpacks.

Radar reflection and backscatter respond similarly to snowpack water equivalence and snow wetness. The backscatter coefficient, for example, increases with increasing snowpack water equivalence and decreases with increasing liquid water in the snowpack (Stiles and Ulaby 1980).

The radar backscatter coefficient is most sensitive to liquid water near the snow surace since the presence of liquid water makes the medium highly absorbent. No experiments have been done by any method where a liquid water profile of the snowpack has been measured. This is due mainly to the difficulty in measuring liquid water content with a freezing calorimeter technique.

Measurements of reflection coefficient and backscatter have been made from ground-based platforms at selected frequencies in the range from 1.0 to 145 GHz, the most common being 1-18 GHz in 1-GHz steps, 35 GHz, 95 GHz and 145 GHz (Hayes et al. 1979, Stiles and Ulaby 1980).

Experiments to determine snowpack stratigraphy and water equivalence have been done using short-pulse and FM-CW radar (Venier and Cross 1972, Vickers and Rose 1977, Ellerbruch and Boyne 1979). In addition, experiments on snowpack liquid water content have been conduced using a CW swept frequency technique (Linlor et al. 1980).

The technique showing the most promise for snow research is the FM-CW technique. Experiments have demonstrated the measurement of snow stratigraphy, surface liquid water content, and snowpack water equivalence of dry snow (Ellerbruch and Boyne 1979).

The reflection, backscatter and FM-CW techniques have the advantage of noncontacting and nondestructive measurements of snowpack properties. The chief limitations in using these techniques are 1) the lack of an adequate data base for the real and imaginary parts of the dielectric constant in the range of frequencies of interest and 2) the lack of an adequate interpretation of the dielectric properties in terms of the physical properties of the snowpack. A better knowledge of properties is needed in order to test and verify theoretical models used to interpret and delineate snowpack water equivalence and liquid water content.

A microwave measurement of snow wetness has been proposed and tested (Linlor et al. 1980) in which measurements were made of phase shift and attenuation in the frequency range 4-12 GHz of a sample of snow which was specially prepared. Experimental measurements of liquid water content in the sample are presented. A theoretical interpretation of the experimental results is also presented. While the results are interesting, the main disadvantge of the techniques is the destructive nature of the test.

IIc. Models in visible and thermal regions
(by A. Chang)

Recent advancement in satellite observation techniques provides an opportunity to obtain global information on snow-covered areas. Understanding of the interaction of electromagnetic waves (EM) with a snow cover is required to properly interpret these data. The physical properties of snow studied by researchers in this area are mainly reflection and transmission of shortwave radiation (0.3 to 3 μm) and emission of longwave radiation (3 to 50 μm). Progress has been made in modeling the optical responses of snow in the visible and infrared regions of the EM spectrum.

At present most of the theoretical models dealing with the optical properties of snow are bsed on calculations made from approximate solutions of the radiative transfer equations. The lack of detailed measurements of optical responses (such as bidirectional reflectance) and physical parameters (such as grain size and density) of a snowpack simultaneously results at best in qualitatively matching portions of the available data for each model calculation. Dunkle and Bevans (1956) were the first to have applied two stream approximation to calculate the albedo of a homogeneous slab of snow. Later Giddings and LaChapelle (1961) utilized a diffusion model on this problem. Bohren and Barkstrom (1974) began treating the snow grains as individual scatterers in solving the radiation transfer equation. Choudhury and Chang (1980) and Wiscombe and Warren (1980) both treat the multiple scattering by the "delta-Eddington" approximation. Choudhury and Chang (1980), who separate the glitter contribution by assuming a surface reflection in their calculations, seem to match the data best at this time. This assumption is consistent with the two well-known, generally accepted approaches for modeling EM wave interaction with dielectric media. Macroscopic models deal with dielectric media with interfaces whereas microscopic models deal with individual particles in the media. Both viewpoints are well accepted by the EM researchers. In the snow case, the size of a typical snow crystal (~ 1 mm) is about one thousand times larger than the wavelength in the visible and near-infrared region. Therefore, a reflecting surface is not an unreasonable assumption. Warren resorted to specular reflection to resolve the albedo problems at low sun angle.

In the workshop, different opinions countered Warren's (1981) view of the non-existence of a reflecting surface in a snowpack. Since there is no reported observation concerning the surface characteristics of snowpack in this spectral region, it is strongly recommended that an experiment should be conducted in the near future to answer this question.

A shadowing effect was proposed by Warren and Wiscombe (1980) for adjusting the albedo calcula-

tions. I believe this shadowing correction comes in only because they ignore the near-field effects in their calculations. The region where a plane wave is disturbed by an obstacle is classified as near-field. Shadowing obviously happens within this region. The near-field effect can only be resolved by solving the Maxwell equation; a radiative transfer technique which treats radiation incoherently cannot be used to solve this coherent interference.

Next, directional reflectance and transmission of a snowpack of variable depth and different snow conditions should be measured. In addition, the angular dependence of the emissivity of snowpack in the infrared region should be investigated.

IId. Measurements of the albedo and the extinction coefficient of a snowpack
(by W. Ambach)

The following aspects must be taken into account when the albedo is obtained from measurements by thermopiles:

• For direct solar radiation, the sensitivity of the thermopile depends strongly on the zenithal angle of the beam, when the zenithal angle exceeds approximately 70°. Under a clear sky, hourly variations of the albedo as a function of the zenithal angle can only be obtained when this change of sensitivity is taken into account.

• At large zenithal angles with a clear sky, the contribution of the diffuse sky radiation is of importance for the incoming radiation flux. In this case the diffuse sky radiation has to be evaluated with the proper sensitivity of the thermopile which can be calculated from the function of sensitivity versus zenithal angle.

• For the upward-directed radiation flux, scattered from the snowpack, an isotropic distribution can be assumed as a good approximation. However, the sensitivity for the isotropic distribution has also to be calculated from the function of sensitivity versus zenithal angle.

• No exact data are known about the difference in sensitivity between the upward- and the downward-directed thermopiles. The downward-directed thermopile may have a higher sensitivity (of some percent) because of the greater thermal stability in that position.

Only few data are available about the angular distribution of the scattered radiation within the snowpack. It would be highly appreciated to obtain further spectral measurements of the angular distribution of the scattered radiation as a function of depth. In the case of the direct incoming solar beam, the relative angular distribution varies strongly with depth within the uppermost snow layers and only becomes independent of depth deeper in the snowpack.

Measurements of the radiation fluxes within the snowpack for different spatial orientations of probes

would also be highly appreciated. Measurements of the upward- and downward-directed radiation fluxes may give different values of the extinction coefficient due to changes of the relative angular distribution of the scattered radiation with depth. Records of the radiation balance within the snowpack and of the integrated radiation over the whole angular distribution (4π), which can be obtained by using a spherical probe, may be a great help in deciding between different multiple scattering models based on different phase functions.

IIe. Acoustical properties of snow
(by J.B. Johnson)

The important measurement parameters which are required to define the acoustical properties of snow independent of theoretical models include:

1. Wave impedance (the complex ratio of pressure-to-particle velocity; this measurement is a material constant and is independent of position).

2. Phase velocity and dispersion (shear waves, fast dilatational waves for which the primary energy is associated with the ice framework, and slow dilatational waves, for which the primary energy is associated with the air pores, have been observed experimentally).

3. Attenuation characteristics for the three wave types.

4. Structural properties of samples (this measurement will aid in examining theoretical models and determine the anisotropy of a given sample).

Model-dependent parameters

The best theoretical description of acoustical wave propagation in snow is presently Biot's model describing wave propagation in a fluid-saturated porous medium. The parameters needed to apply the porous medium model must be measured so that the model can be compared to experimental measurements.

The parameters used to apply Biot's porous medium model to snow include:

1) The dilatational and shear Lamé coefficients
2) The fluid–solid coupling coefficient
3) The pressure required to force a given volume of fluid in an aggregate of constant volume
4) The permeability of the sample
5) Fluid viscosity
6) Density of the solid material (ice framework)
7) Density of the fluid material.

Additional notes

1. The experimental techniques should be described in detail. This will minimize interpretation problems.

2. Experiments should be conducted on homogeneous samples when measuring fundamental parameters (this can be checked with the textural analysis).

119

Table 1. Summary of electromagnetic and optical properties of snow, including applications.

field of application / type of parameter range	snow mechanics / avalanche research			hydrology		climatology	
	snow structure	stratification	moving snow	wetness	water-equivalent	snow mapping	radiation balance
direct current	conductivity, activation energy: surface structure of crystals, specific surface, recrystallization of snow						
0 - 1 MHz	complex dielectric const., relaxation time mixing model: depolarisation factor, shape factor of particles						
1 - 100 MHz	imag. part of dielectr. constant: shape, structure independent of wetness	density, permittivity: wetness profile (destructive, snow pit)		density, permittivity (wetness regime) mixing model: wetness standard			
1 - 10 GHz		FM-CW: amplitude and phase spectra (distance measurement) sweep: interference pattern: density profile, snow depth, layering	FM-CW, Doppler radar, amplitude and phase spectra. backscatter: flowing snow avalanches: flow height, density profile,size distribution, velocity profile	backscatter, brightness temp.(polaris.), FM-CW, resonance,interferometer: vol % wetness, ground condition (frozen/wet.) melt-freeze cycle rain on snow	FM-CW, backscatter: water-equivalent for dry (wet) snow		
10 - 50 GHz	brightness temp.(nadir, polarization) backscatter: grain size	brightness temp.(nadir, polarization) backscatter: grain size profile	FM-CW, Doppler, backscatter: speed, size distribution in flowing snow avalanches		brightness temp. (nadir, polarisation): dry snow water-equivalent	SAR: wet/dry snow mapping	
> 50 GHz	similar to 10-50 GHz				similar to 10-50 GHz		
Optics							
> 3 µ	emissivity			extinction coefficient, radiative heating: snow melt			emissivity, backscatter
3 - 0.6 µ	albedo optical grain size					photograph	
0.6 - 0.1 µ	albedo, impurities, grain size	albedo (nadir), surface condition	Doppler interferometry: speed of snow particles, stereophotogrammetry, avalanche speed		albedo: water-equivalent of shallow snow cover	photograph	

Table 2. Summary of acoustical properties of snow, including applications.

field of application / type of measurement	snow structure	snow [...]	slope stability / fracture mechanics	instrument [...]
wave impedance, phase velocity, dispersion, attenuation,	nondestructive structure classification depending on statistic or deterministic model assumption, snow type, stratification	determination of mechanical parameters, model dependent, explosive control		wave tube, propagation time measurement, attenuation measurement
reflection of snow surface				snow depth measurement
high frequency acoustic emission	fracture of grain bonds, intergranular dislocations			special high frequency microphones (100 kHz – 1 MHz)
	small fractures, evolution of structure under load	changes of mechanical behaviour of snow under load		
low frequency acoustic emission			a) low frequency noise from gliding/creeping snow : short term forecast of full depth avalanches starting from gliding snow	a) seismic sensor in the ground or snow
			b) isolated spikes indicating limited fracture, stress-redistributions : stability evaluation	b) seismic sensor in the snow (adapted to snow)

Table 3. Priority list of problems to be solved.

subject	problem	priority a > b > c
direct current	physical properties of the topmost surface layer on ice	a
dielectric properties ≤ 100 MHz	development of standard wetness gauge with direct reading	a
	shape factor determination	b
microwave	accurate determination of loss factor for $v > 10$ GHz	a
	improved models including passive and active radar response as a function of structure, stratification, wetness	a
	improvement of water-equivalent measurements, experiments depending on models	b
	determination of phase spectra in FM-CW measurements for simultaneous layering and water-equivalent measurements	c
optical properties	accurate measurements of complex index of refraction	a
	improved albedo and emissivity measurements as a function of nadir, bidirectional reflection measurements (grain size, texture, impurity)	a
	improved modeling including near field approximation or solution of Maxwell equation	b
	improved penetration depth / extinction coefficient measurements	b
acoustical properties	improved physical model for low density snow	a
	accurate measurements of wave impedance, phase velocity and dispersion, attenuation and model dependend parameters	b
acoustic emission	investigation of the source mechanism for low and high frequency emission	a
	discrimination against environmental noise at low frequencies	b

3. Techniques for measuring the above parameters are well-known and have been discussed, in the acoustics, seismology and snow physics literature. These techniques should be utilized.

4. Resonance techniques should not be used to determine phase velocity since the result depends on model descriptions for the sample.

5. Attenuation measurements should clearly differentiate between geometrical effects (either wave form or boundary condition influence of the sample) and internal losses.

III. SUMMARY AND CONCLUSIONS

Table 1 is a summary of electromagnetic and optical properties of snow, including applications. Included are the parameters to be measured or types of measurements involved, specific conditions and applications. Table 2 summarizes acoustical properties of snow, including applications. Table 3 is a priority list of problems to be solved to improve accuracy in practical applications.

The electromagnetic, optical and acoustical properties are very important for many practical applications in snow and avalanche research, snow hydrology and even in climatology. More research, and above all, a better understanding of the physical processes involved, are necessary to improve accuracy of practical

applications beyond the use of index properties that always have to be recalibrated if conditions change.

REFERENCES

Abe, T. (1978) Measurement of falling velocity of snow using a laser doppler velocimeter. *SEPPYO, Journal of the Japanese Society of Snow and Ice*, vol. 40, p. 12–15.

Ambach, W. and A. Denoth (1972) Frequenzgang und Relaxationszeiten der Dielektrizitatskonstante von Schneeproben nach dem Modell von Cole-Cole. *Acta Physica Austriaca*, vol. 35, p. 249–261.

Ambach, W. and A. Denoth (1975) On the dielectric constant of wet snow. IAHS–AISH Publication No. 114, p. 136–142.

Ambach, W. and A. Denoth (1980) The dielectric behavior of snow: A study versus liquid water content. In *Proceedings of NASA Workshop on the Microwave Remote Sensing of Snowpack Properties, Fort Collins, Colorado, 20–22 May 1980* (A. Rango, Ed.). NASA Goddard Space Flight Center, Greenbelt, Maryland, NASA CP 2153, p. 69–92.

Armstrong, R.L. (1976) The application of isotopic profiling snow gauge data to avalanche research. Report to the Bureau of Reclamation, Institute of Arctic and Alpine Research, University of Colorado, Occasional Paper No. 19, p. 131–143.

Aburakawa, H. (1979) D-type snow depth recorder using optical fibers. *Low Temperature Science*, vol. A38, p. 73–79.

Beaglehole, D. et al. (1980) Transition layer on the surface of ice. *Surface Science*, vol. 96, p. 357–363.

Borchert, M. et al. (1964–65) Forschungs- und Entwicklungsarbeiten über Möglichkeiten der Ortung von Lawinenverschütteten. *Bericht für Fondat. Int. Vanni Eigenmann*, I Teil, 79 p. II. Teil, 110 p.

Brown, A.J. et al. (1980) California's transition from conventional snowpack measurements to a developing remote sensing capability for water forecasting. In *Proceedings of NASA Workshop on the Microwave Remote Sensing of Snowpack Properties, Fort Collins, Colorado, 20–22 May 1980* (A. Rango, Ed.). NASA Goddard Space Flight Center, Greenbelt, Maryland, NASA CP 2153, p. 11–19.

Brown, R.L. (1980) Pressure waves in snow. *Journal of Glaciology*, vol. 25, p. 99–107.

Buser, O. (1981) Personal communication. Federal Institute for Snow and Avalanche Research/Davos.

Colbeck, S.C. (1976) Effects of radiation penetration on snowmelt runoff hydrographs. U.S. Army Cold Regions Research and Engineering Laboratory, CRREL Report 76-11.

Colbeck, S.C. (1979) Sintering and compaction of snow containing liquid water. *Philosophical Magazine*, vol. 39, p. 13–32.

Colbeck, S.C. et al. (1980) Liquid distribution and the dielectric constant of wet snow. In *Proceedings of NASA Workshop on the Microwave Remote Sensing of Snowpack Properties, Fort Collins, Colorado, 20–22 May 1980* (A. Rango, Ed.). NASA Goddard Space Flight Center, Greenbelt, Maryland, NASA CP 2153, p. 21–29.

CTGREF (1980) La stéréophotogrammetrie a cadence rapide d'avalanches. Information Technique, CTG REF/St. Margin d'Heres, Cahier 39, No. 8.

Denoth, A. (1978) On the calculation of the dielectric constant of snow. *Comptes Rendus* ANENA, 2me Renc. Int. sur la Neige et les Avalanches, Grenoble, France.

Denoth, A. (1979) Problematik der Messung des Gehalts an freiem Wasser in der naturlichen Schneedecke. *Proceedings, "Elektronik und Lawinen," Graz, Austria.*

Denoth, A. (1980) The pendular-funicular liquid transition in snow. *Journal of Glaciology*, vol. 25, no. 91, p. 93–97.

Denoth, A. and H. Schittelkopf (1978) Mixing formulas for determining the free water content of wet snow from measurements of the dielectric constant. *ZGG*, vol. 14, no. 1, p. 73–80.

Ellerbruch, D.A. and H.S. Boyne (1979) Snow stratigraphy and water equivalence measured with an active microwave system. Symposium on Snow in Motion. *Journal of Glaciology*, vol. 94, p. 225–234.

Ellerbruch, D.A. and H.S. Boyne (1980) Snow stratigraphy and water equivalence measured with an active microwave system. *Journal of Glaciology*, vol. 26, p. 225–233.

Fletcher, N.H. (1968) Surface of water and ice. A revised model. *Philosophical Magazine*, vol. 18, no. 156, p. 1287–1300.

Fritzsche, W. (1981) Personal communication. Inst. f. Hochfrequenz und Elektronik, Graz/Oesterreich.

Glen, J.W. et al. (1975) The electrical properties of snow and ice. *Journal of Glaciology*, vol. 15, p. 15–38.

Golecki, I. and C. Jaccard (1977) The surface of ice near 0 °C studied by 100 keV proton channeling. *Phys. Letters*, vol. 63A, p. 374–376.

Good, W. et al. (1973) Ein optoelektronischer Schneehöhenmesser. Winterbericht Nr. 37 (1972/73), EISLF/Davos, p. 150–156.

Good, W. (1977) Probleme des Sender-Empfanger-Prinzips, Symp. Sulden 1975, Fondat. Int. Vanni Eigenmann: "Lawinen," p. 85–108.

Good, W. (1980) Structural investigations of snow, a comparison of different parameter sets. In *Pattern Recognition in Practice* (E.S. Gelsema and L.N. Kanal, Eds.). North Holland Publishing Company, p. 161–170.

Gubler, H. (1977) Artificial release of avalanches by explosives. *Journal of Glaciology*, vol. 19, p. 419–429.

Gubler, H. (1980) Proposal to use CW doppler radar

to measure velocities of flowing snow avalanches. Int. Ber. Nr. 586, EISLF/Davos.

Gubler, H. (1980) Simultaneous measurements of stability indices and characteristic parameters describing the snow cover and the weather in fracture zones of avalanches. *Journal of Glaciology*, vol. 26, p. 65-74.

Gubler, H. (1981) An inexpensive snow depth gauge based on ultrasonic wave reflection from the snow surface. *Journal of Glaciology*, vol. 27, no. 95, p. 157-163.

Gubler, H. (1981) An electronic remote snow drift gauge. *Journal of Glaciology*, vol. 27, no. 95, p. 164-174.

Hayes, D., V.H.W. Lammers, R. Marr and J. McNally (1979) Millimeter wave backscatter from snow. *Proceedings of the Workshop on Radar Backscatter from Terrain*. RSL Technical Report 374-2, University of Kansas Center for Research, Lawrence, Kansas.

Hobbs, P.V. (1974) *Ice Physics*. London: Oxford University Press.

Ishida, T. (1965) Acoustic properties of snow. *Contributions of the Institute of Low Temperature Science*, Series A, vol. 20, p. 23-63.

Johnson, J.B. (1978) Stress waves in snow. Thesis, University of Washington.

Johnson, J.B. (1980) A model for snow-slab failure under conditions of dynamic loading. *Journal of Glaciology*, vol. 26, p. 245-254.

Kodama, M. (1980) Continuous monitoring of snow water equivalent using cosmic ray neutrons. *Cold Regions Science and Technology*, vol. 3, p. 295-303.

Kong, J.A. et al. (1980) Theoretical models for microwave snow response and applications to remote sensing. In *Proceedings of NASA Workshop on the Microwave Remote Sensing of Snowpack Properties, Fort Collins, Colorado, 20-22 May 1980* (A. Rango, Ed.). NASA Goddard Space Flight Center, Greenbelt, Maryland, NASA CP 2153, p. 147-155.

Kopp, M. (1962) Conductivité electrique de la neige au courant continu. ZAMP, XIII, 5, p. 431-441.

Kulividze, V.I. et al. (1974) The mobile water phase on ice surface. *Surface Science*, vol. 44, p. 60-68.

Linlor, W.I. (1977) Coherent microwave backscatter of natural snowpacks. Memorandum No. USB/ERL M77/75, Electronics Research Laboratory, College of Engineering, University of California (Berkeley).

Linlor, W.I., J.L. Smith, F.D. Clapp and D.J. Angelekos (1980) Snow electromagnetic measurements. In *Proceedings of NASA Workshop on the Microwave Remote Sensing of Snowpack Properties, Fort Collins, Colorado, 20-22 May 1980* (A. Rango, Ed.). NASA Goddard Space Flight Center, Greenbelt, Maryland, NASA CP 2153, p. 93-117.

Maeno, N. et al. (1978) The electrical properties of ice surfaces. *Journal of Glaciology*, vol. 21, p. 193-205.

Maetzler, C. et al. (1980) Microwave signatures of the natural snow cover at Weissfluhjoch. In *Proceedings of NASA Workshop on the Microwave Remote Sensing of Snowpack Properties, Fort Collins, Colorado, 20-22 May 1980* (A. Rango, Ed.). NASA Goddard Space Flight Center, Greenbelt, Maryland, NASA CP 2153, p. 202-223.

Maetzler, C. et al. (In press) Towards the definition of optimum sensor specifications for microwave remote sensing of snow.

Marbouty, D. et al. (1978) Mesure de la hauteur de neige par ultrasons. 2^e Rencontre Int. sur la Neige et les Avalanches, Avril 1978. ANENA/Grenoble. *Comptes Rendus*, p. 49-59.

Mazzega, N. et al. (1976) Volta effect and liquid-like layer at the ice surface. *Surface Science*, vol. 64, p. 1028-1031.

Mellor, M. (1964) Properties of snow. CRREL Cold Regions Science and Engineering Monograph III-A1.

Mellor, M. (1965) Explosions in snow. CRREL Cold Regions Science and Engineering Monograph III-A3a.

Mellor, M. (1970) Optical measurements on snow. Ice-field ranges research project, scientific results. American Geographical Society/New York, and Arctic Institute of North America/Montreal, vol. 2, p. 43-50.

Montmollin de, M. Stabilité d'une pente de neige: Effet du bang sonique sur le déclenchement d'avalanches. Note CENG/ASP No. 76-09, Grenoble.

Perla, R. (In press) Preparation of snow specimens for stereology.

Schmidt, R.A. (1977) A system that measures blowing snow. USDA Forest Service Research Paper RM-194.

Siksna, R. (1957) Conduction of electricity through ice and snow. *Arkiv for Fysik*, vol. 11, p. 495-528 and 567-585.

Sommerfeld, R.A. (1982) A review of snow acoustics; Review paper. This volume.

Stiles, W.H. et al. (1980) Radar observations of snowpacks. In *Proceedings of NASA Workshop on the Microwave Remote Sensing of Snowpack Properties, Fort Collins, Colorado, 20-22 May 1980* (A. Rango, Ed.). NASA Goddard Space Flight Center, Greenbelt, Maryland, NASA CP 2153, p. 131-146.

Stiles, W.H. and F.T. Ulaby (1982) Electrical properties of snow. Review paper. This volume.

Stiles, W.H. and F.T. Ulaby. *Microwave Remote Sensing of Snowpack*. NASA Contractor Report 3263.

Stoner, E.C. (1945) The demagnetizing factors for ellipsoids. *Philosophical Magazine*, Ser. 7, vol. 36, p. 803-821.

Venier, G.O. et al. (1972) An experimental look at the use of radar to measure snow and ice depths. Communications Research Center, Technical Note No. 646, Ottawa, Canada.

Vickers, R.S. and G.C. Rose (1972) High resolution measurements of snowpack stratigraphy using a short pulse radar. *Proceedings, 8th International Symposium on Remote Sensing of Environment, Ann Arbor, Michigan.*

Warren, S.G. (1982) Optical properties of snow. Review paper. This volume.

Warren, S.G. and W.J. Wiscombe (1980) A model for spectral albedo of snow. II: Snow containing atmospheric aerosols, *Journal of Atmospheric Science*, vol. 37, p. 2734–2745.

Committee Chairman Report on

Snow Metamorphism

E.R. LaChapelle

*Department of Atmospheric Science, University of Washington,
Seattle, Washington 98195*

The subject was introduced on 8 April by an invited paper entitled "An Overview of Snow Metamorphism," by S.C. Colbeck.

Two discussion sessions were held on the morning and afternoon of 9 April. These sessions were marked by a wide diversity of opinion, a general lack of clear agreement on the part of the participants on which directions developments in snow thermodynamics ought to take, and some limited agreement on priorities for future research. While the top priority was in the theoretical realm, the rest of the current needs were clearly grouped around practical understanding of snow behavior and quantitative data collection. The clearest product of the discussions was the recognition that the science of snow thermodynamics is hampered by a dearth of comprehensive, quantitative observations in the laboratory and field. The following specific topics were taken up during the discussion periods.

1. *Classifying stages of snow metamorphism.* Current classification schemes are largely morphological. Interpretive skills tend to be subjective and are difficult to communicate. A process-based classification scheme (genetic scheme) would be desirable but currently lacks a good theoretical foundation.

2. *Convection and pumping of interstitial air.* Conflicting evidence exists about the magnitude and even the existence of air convection within the snow cover. Some definitive experimental work is needed in this area.

Practical field evidence suggests that air may sometimes be exchanged between surface snow layers and the atmosphere, with significant effects on snow properties, but there does not appear to be any theoretical analysis or observational data to define this phenomenon.

3. *Snow metamorphism.* The major parts of the discussions were devoted to the topic of snow metamorphism. The following items were introduced by one or more of the participants.

a. The study of snow deals largely with a porous medium. While the engineering aspects of this (e.g.,

forced ventilation in snow) have been examined, little work has been done on snow from the standpoint of the physics of porous media. Snow represents a case of special interest because one constituent of the pore volume is the vapor phase of the granular solid.

b. Theoretical examinations of snow tend to treat it from the standpoint of equilibrium thermodynamics because this is the simpler approach. Many of the phenomena associated with metamorphism, however, are best described by non-equilibrium thermodynamics.

c. Snow can be viewed from two entirely different standpoints. Many mechanical considerations treat it as a bulk continuum. But the metamorphism processes that profoundly affect mechanical properties must be examined from the standpoint of particle thermodynamics in a finely divided medium.

d. There is a common tendency to describe snow in terms of individual crystals and their behavior, but snow in fact is a dispersed particulate system with a very large surface area, and must be so treated in analysis.

The discussions led to the following suggestions, in order of priority, for future work in snow thermodynamics.

1. Apply current knowledge in surface physics and non-equilibrium thermodynamics to developing a basic theory of snow metamorphism.

2. Collect quantitative field data on common phenomena in snow metamorphism which presently are largely known only in a qualitative sense.

3. Perform some basic experiments and analysis on the phenomena of convection and pumping of interstitial air in the snow cover.

4. Collect synoptic snow temperature data in a wide diversity of terrain and snow climates.

5. Examine in depth the known profound effects of trace contaminants on snow metamorphism in all of its phases.

Committee Chairman Report on

Experimental Methods,

Data Reporting and Snow Classification

F.W. Smith

Mechanical Engineering Department, Colorado State University,
Fort Collins, Colorado 80526

ABSTRACT

During the conference, a session was held to determine if there is a common ground with respect to the kinds of experiments which should be conducted to determine snow properties. It was intended that this session result in brief statements of types of experiments, control of conditions necessary, and the proper reporting of data required to make the results of experiments conducted have maximum value to the snow research community.

These brief reports cover the subjects of blowing snow, acoustics of snow and acoustical emissions, reflectance and thermal emission, snow classification, sliding ski resistance, electrical properties tests, mechanical properties tests, measurement of density and velocity in moving snow, and snowpack temperature profiles.

BLOWING SNOW (R.A. Schmidt)

Because threshold windspeed appears to be a very important parameter which explains some of the variation in measurements of blowing snow transport rate as a function of wind speed, some measure and reporting of this parameter in future experiments is strongly recommended.

ACOUSTICS OF SNOW
AND ACOUSTICAL EMISSIONS
(R.A. Schmidt)

I. Acoustical Properties
  A. Important measurement parameters required to define the acoustical properties of snow independent of theoretical models
    1. Wave impedance: this is a material property and is independent of position
    2. Phase velocity: resonance techniques should not be used (model-dependent)
      a. dilatational waves of the first kind (mainly in ice framework)
      b. dilatational waves of the second kind (mainly in air pores)
      c. shear waves

3. Phase velocity dispersion: variation of phase velocity with frequency
4. Attenuation of wave types: excluding geometrical attenuation associated with non-planar waves
5. Textural properties of snow
  a. the above experiments should be conducted on homogeneous, isotropic samples
  b. experimental techniques and associated uncertainties should be described in detail
  c. techniques for the above tests are well-known in acoustics, seismology and snow physics and should be utilized
  B. Important model-dependent parameters to test and apply Blot's porous media model to snow
    1. The Lamé coefficients A, N
    2. The fluid–solid coupling coefficient Q
    3. The coefficient R which is a measure of the force required to force fluid into an aggregate at constant volume R
    4. Permeability
    5. Density of fluid
    6. Density of framework solid
    7. Viscosity and compressibility of fluid
The techniques for determining A, N, Q and R statically or dynamically are known and should be utilized.

127

II. Acoustic emissions (important items to measure and/or report)
   A. Specify sensor type and calibration
   B. Describe coupling of sensor to snow
   C. Specify noise of the system referred to input with respect to a specific sensor
   D. Specify the location of the sensor in the snow-pack
   E. Report measurements as RMS values or event rate (RMS for discrete events)
   F. Specify frequency bandwidth of the system

REFLECTANCE AND THERMAL EMISSION
(J. Dozier, A. Chang, D. Marks and D.S.G. Warren)

Recommendation #1

Reflectance and emission experiments should be co-ordinated with measurements of snow properties in the near-surface zone. These would include:

a) Profile of grain size with depth, made via thin sections if possible, because we don't really have a good definition of grain size.

b) If liquid water present, need to know continuity.

c) Orientation (if any) of surface grains.

d) Contaminants—if measuring in visible spectrum (amount, composition, profile)

Recommendation #2

A basic parameter which needs to be more accurately determined is absorption, coefficient of ice at 0.17–0.4 μm, 1.4–2.8 μm, and 33–150 μm (for near-melt temperatures).

Recommendation #3

Reflectance measurements needed the following:

a) Bidirectional reflectance distribution function, at range of wavelengths, illumination angles, and snow types. (These might best be done at night.)

b) Some of these measurements should be made with polarized light, to see if the Brewster cycle exists.

c) Need transmittance measurement.

d) Need to investigate near-field effect, through measurements and models (wave equation and radiative transfer).

Recommendation #4

Thermal emission measurements are needed at various view angles and grain sizes.

SNOW CLASSIFICATION
(E.R. LaChapelle)

1. The present* classification scheme is functional, meets most needs and should be retained.

---

* The International Classification for Snow, National Research Council, Ottawa, Canada, August 1954, as modified by Sommerfeld and LaChapelle.

2. For specific applications (mobility and remote sensing, for instance) a simplified scheme dealing with bulk properties would be useful.

3. Such a simplified scheme should be derived from the present classification.

4. The weakest point in snow description is the measurement of free water content. Reliable, fast measurement methods need to be developed.

FRICTION AND SLIDING SKI RESISTANCE ON SNOW (B. Glenn)

I. Definition
   To quantify the kinematic resistance (static, dynamic) to sliding of a ski (runner) on snow as a function of loading, ski and snow properties.

II. Conditions
   The towing or downhill release of a ski (runner) or skis on a prepared or unprepared track such that the frictional resistance due to deformation (plowing) and sliding may be calculated. (For appreciable velocities the air resistance must be subtracted.) Preferable velocities should be up to 50–70 m/s to simulate airplane ski velocities.

III. Data
   A. Track description
      1. Slope, length
      2. Smoothness
   B. Interface properties
      1. Surface type
      2. Surface preparation
      3. Adhesion (contact, angle)
   C. Kinematic characteristics
      1. Static resistance
      2. Dynamic resistance (as functions of time and velocity)
      3. Air resistance (as function of velocity)
   D. Meteorological data
      1. Temperatures (snow and air)
      2. Air humidity
      3. Test site wind and direction
   E. Snow properties
      1. Snow track compressibility
      2. Snow density
      3. Free-water content
      4. Snow crystal size, age, form
   F. Ski properties
      1. Width and length, to indicate surface area (contact area)
      2. Stiffness and camber to indicate pressure distribution
      3. Vibration characteristics

ELECTRICAL PROPERTIES TESTS

(H.S. Boyne, A. Denoth, W.H. Stiles,
C. Raymond, J.A. Kong and H. Gubler)

In the range from 10 MHz to 1 GHz, capacitance measurements for determining liquid water content can be made with an accuracy of 0.5% with a 99% confidence interval. The capacitor contains 5 to 7 plates and has about 1 liter volume. The capacitance measurement must be accompanied by density measurement to correct for packing of snow between the capacitor plates. There is a linear relation between dielectric constant and the density which is $E = 1 + 2.000 \times \varrho$ at 10 MHz. The theory of Polder and Van Santen for a snow–water mixture agrees best with experimental data for both high-frequency and DC measurements. The capacitor is calibrated to absolute liquid water content by comparing its reading with the freezing water calorimetric technique (Ambach and Denoth (1975).

A second technique is the use of a flat plate microstrip type capacitor. It has the advantage of not disturbing the snowpack during the measurement, but is limited to a range of less than 10% liquid water. Penetration depth depends on electrode size and electrode spacing. The penetration depth will be 1 mm or greater.

Static Dielectric Constant depends on grain size, shape and porosity. More research is needed to correlate theoretical predictions with visually determined grain shape, size and porosity characteristics. In the range above 1.0 GHz it is important for interpretation of theoretical models of electromagnetic wave interaction with the snowpack to determine correlation characteristics. A correlation length can be determined by preparing a thin section and then digitizing the sample to obtain a distribution histogram. One can then calculate correlation length or autocorrelation along a line in the thin section (Ambach and Denoth 1980).

**Possible ways to measure real and imaginary parts
(ϵ' and ϵ'' respectively)**

1. Cavity measurements

Cavity measurements can be used to measure ϵ' and ϵ'' at a fixed frequency. The measurements can be made very accurately in a laboratory situation. Samples of snow must be prepared and inserted in the cavity. Therefore, the frequency range is limited because the sample size has to be small enough that it does not seriously perturb the electromagnetic field distribution within the cavity.

2. Reflection measurements

Amplitude and phase measurements on reflection at a surface can be used to determine the dielectric con-

stant at the surface. The measurement needs careful analysis because scattering at the surface is also involved. One has to insure that reflection losses are only used in the measurement.

3. Interferometer measurements

By inserting a snow sample in an interferometer measurement device, one can determine both ϵ' and ϵ''. The change in the electromagnetic path lanes which is measured by changes in the number of fringes on one arm of a Michaelson interferometer, for example, is related to ϵ'. Changes in amplitude of the electromagnetic radiation give information about ϵ'. One advantage of this method over cavity measurements (No. 1 above) is that generally an interferometer can be designed to accommodate larger samples than those used in the cavity measurements.

4. Transmission measurements

One can make an amplitude and phase comparison of electromagnetic radiation transmitted through a snow sample with the amplitude and phase of a wave traveling in free space. Like the reflection method, this method includes surface scattering and one must carefully assess the contribution due to scattering.

5. Wave guide method

By measuring the change in phase and amplitude of an electromagnetic wave due to the insertion of a snow sample in a wave guide, one can make accurate measurements of ϵ' and ϵ''. Like the cavity measurements and the interferometer measurements, a sample must be prepared for insertion into the wave guide.

MECHANICAL PROPERTIES TEST

(F.W. Smith, R.G. Oakberg, R.L. Brown,
J.A. Kong, W.L. Harrison and B. Glenne)

The following statements apply to tension, compression and shear tests of snow conducted to obtain quantitative information regarding constitutive behavior.

A. Conditions of experiment to be reported
  1. Snow sample information
    a. Shape and dimensions of sample and sampling device
    b. Sampling procedure
    c. Sample taken from where in the snowpack and what orientation relative to the layers?
    d. Handling of samples; i.e. is the snow natural or reprocessed, tested in the field, stored in freezer, other?
    e. Snow classification (very important)
    f. Snow density (very important)
    g. Grain size from photographs of grains or

from thin sections which would also give information on grain bonds

   h. Free water content; at least use the snowball test

2. Ambient temperature during test

3. Testing apparatus information

   a. Size, shape and operating principles of apparatus

   b. Details of loading attachments to the sample including attachment procedures

   c. Procedures for strain rate or stress rate control (very important)

   d. Technique for measurement of strain including gauge length for strain measurement

B. Data from experiment to be reported

1. Load or stress (stress preferred)

2. Displacement or strain (strain preferred)

3. Displacement rate or strain rate (strain rate preferred), OR load rate or stress rate

4. Lateral strain in unconfined tension or compression tests, OR lateral pressure in confined tests

5. Condition of rupture with careful definition of rupture for the particular testing situation

MEASUREMENT OF DENSITY AND VELOCITY IN MOVING SNOW
(J. Dent)

The committee agreed that the problem was extremely difficult, and would not be solved in one committee meeting. It will be necessary for many more meetings to be held.

The approach to the problem can be twofold depending upon money and time available. The simplest tests to be made are:

1) flow depths

2) release masses

3) average densities

4) front edge velocities

5) particle sizes

These measurements may not be easy to make. The following lists possible methods of measuring velocity and density profiles inside a flowing avalanche. The development of these methods will take much more time and money. These methods are:

1. Microwave interferometer and/or FM-CW RADAR looking upward from the bottom of the avalanche track.

2. Banks of pressure transducers set in an avalanche path, trying to measure pressure correlations at multiple levels between upstream and downstream sensors. Can measure velocities and may be able to get density estimates.

3. Placing a glass window in an enbankment in an avalanche and using optical correlation techniques to measure velocities.

4. An inertial system consisting of a gyroscope and accelerometers.

SNOWPACK TEMPERATURE PROFILES
(H.B. Grandberg)

Snow is a translucent, structurally and thermodynamically unstable material with low thermal conductivity and low volumetric heat capacity. Thermometry in such a material requires that attention be paid to the heat balance of the temperature sensors, to avoid a condition in which the measured temperature differs from the undisturbed temperature of the medium.

Absorption of solar radiation by the sensor is a common source of error in snow temperature measurements. This error can be minimized by minimizing the physical size of the sensor and by maximizing its albedo.

Heat production by the sensor itself occurs when thermistors and other resistance thermometers are used. This error can be minimized by minimizing the current through the thermistor and the time taken for the measurement.

A high thermal inertia of the sensor causes a smoothing of the actual temperature variations and also causes a long time lag before a temperature probe comes into equilibrium with its surroundings. Thermal inertial effects are minimized by minimizing the size of the sensor.

Heat conduction along the leads or along the probe may significantly distort the local temperature field. This error is minimized by minimizing the thermal conductivity and the area of the probe/leads. It can also be minimized by arranging the temperature-measuring device so that steep temperature gradients do not occur along the leads near the sensor.

Conduction of meltwater along the thermometric device is a common cause of error in snow temperature measurements during surface melting events. This error can be minimized by designing the thermometric device so that it does not encourage downward percolation of meltwater.

The purpose of the temperature measurement dictates the design of the instrument. Because of the properties of the snow cover, off-the-shelf thermometric devices are often inadequate. Researchers are often forced to design their own thermometric equipment. The following are two suggestions for thermometers that give satisfying results.

rements

!6 copper-constantan ther-
mermos bottle with crushed
nctions should be painted
electrically insulating lac-
isted and soldered. Cut the
bout 3 mm and gently push
yer of the snow, each of the
)arately, so that the part
:onstantan is at the surface.
surface thermometer while
can easily be lifted off the
The radiation error of this
' under most conditions.

irements (intermittent)

i be made from a white, hol-
a suitable small thermistor.
il—precision calibrated are
p off the rod and drill a seat
the thermistor to thin leads
il shock), smear the thermis-
and pull it back into the
ilicone. Sand the tip portion
te thin to minimize the ther-
'he probe is a tool for insert-
desired position in the snow
in steel rod to poke holes

g error, let the probe come to
of minutes before the resis-
nt is connected. The error of
ambient conditions, but with
i 0.5 °C is attainable.

Permanent installations for temperature profile measurements

Permanent installations face structural and depth control problems because of the gradual compaction of the snow cover. Alterations of the surrounding snow caused by the thermometric device may cause local changes in the processes under study. No particular recommendations are given here beyond those already available in the literature.

There is a need to develop instrumentation for measurement of thermal events associated with metamorphic processes in the snow cover. Of particular interest is the spatial variation in the surface temperature of the ice matrix and how these temperatures vary through time.

Efforts should be made to develop and make commercially available thermometric instrumentation adequate for in-snow use.

REFERENCES

Ambach, W. and A. Denoth (1975) On the dielectric constant of wet snow. In *Snow Mechanics Symposium: Proceedings, Grindelwald Conference, April 1974.* IAHS Publication No. 114, p. 136-142.

Ambach, W. and A. Denoth (1980) The dielectric behavior of snow: A study versus liquid water content. In *Proceedings of NASA Workshop on the Microwave Remote Sensing of Snowpack Properties, Fort Collins, Colorado, 20-22 May 1980* (A. Rango, Ed.). NASA Goddard Space Flight Center, Greenbelt, Maryland, NASA CP 2153, p. 69-81.

Final Position Paper

idenced during the workshop, a large
nteresting and important research topics
l were discussed in some detail. Problems
ics such as mechanical properties, micro-
operties, blowing snow, acoustic, optical
ıl properties and snow metamorphism. By
ıe workshop, the list of unsolved problems
f study was quite extensive. However, the
promise for a number of new and innova-
s of study.
vill attempt to provide an overall summary
ıroblems, their importance and an assess-
ogress that can be expected in the next
consider each area separately and focus on
e major unsolved problems.

ICAL PROPERTIES

:al properties have direct application to a
er of engineering problems, including ava-
hanics, vehicle mobility, snow plowing, and
·ts of snow handling. In the past, most of
n mechanical properties has been done by
interested in the avalanche problem. How-
apparent increasing effort on other engi-
ıblems, new people are taking a look at
:rties.
y, there are many gaps in the knowledge of
ıical properties of snow. Fracture proper-
ate properties, and metamorphism effects
·w. When one considers all the forms snow
ınd can be found in and the wide variety of
:ions and temperatures it is subjected to, a
ıracterization in the near future appears

-specific properties, however, can be de-
efforts in characterizing the properties of
pecific applications should be encouraged.
:e, in vehicle mobility, high rate volumetric
ıric properties of snow are needed. The con-
uation must necessarily be capable of de-
: response of snow to large strains and com-
)n the other hand, when significant vehicle
incurred, the snow near the track grousers
ghly disaggregated, and the behavior then
ore like that of a non-Newtonian fluid.

Conversely, analysis of slope glide or snowpack deformation presents a much different problem. In this case strains occur over much lower rates and the material characterization in this case may be represented by linear viscous or viscoelastic models, or better yet, creep compliance.

Shockwave propagation represents the other end of the spectrum. To date little effort has been devoted to this problem, and much remains to be done.

In regard to mechanical properties, there appears to be a lack of agreement over just what emphasis should be made to characterize snow. For instance, there is a definite need for tractable constitutive relations that can be applied directly to a large number of engineering problems. This should certainly be the bottom line of research, i.e. it has to lead to a usable, applicable and practical result. However, at the same time there needs to evolve from this work a better understanding about the physical nature of the material, i.e. how the microstructure determines the material properties. While future work on mechanical properties should point toward usable engineering results, the investigation of the microdynamical aspects of the material behavior should not be totally disregarded. Much can be learned from ongoing research on granular materials.

By and large, there appears to be no proper consensus of what constitute the shear strength parameters for snow. Traditional concepts of friction and cohesion as applied to snow cannot be used indiscriminately since these should be restricted to application in situations where little or no volume change occurs upon shearing. The traditional model used for the determination of the friction and cohesive parameters is the Mohr–Coulomb model. It should be observed that in the derivation of these shear strength parameters, tests should be performed on snow initially compressed to a state where little or no volume change occurs upon shearing. Where these test conditions are not met, and if these parameters are derived from tests where these conditions are not met, those parameters should be considered invalid. It is not therefore remarkable to observe that while the model requirements are indeed both rigorous and demanding, most testers, both in the laboratory and in the field, tend to ignore these requirements and produce various sets of shear strength parameters purporting to represent friction and cohesion. The difficulties arising therefrom can be most

embarrassing. Also, the test boundary conditions, in the laboratory and in the field, have never been fully identified or specified. This does not permit the modeler to properly represent the snow in his specification of the analytical stress/strain relationship.

The simplest view and application for derivation of the mechanical properties of snow are in terms of energy relationships. The two significant components for these are the compressibility of the snow and the shear resistance. These should be, and can be, derived in terms of the compression energy requirements for compaction of the snow, and the shear energy requirements to create shear distortion and failure in the snow. In viewing these in terms of energy requirements and demands, one is essentially encapsulating all the various historic facts determining the properties of the snow into two readily determinable quantities. It is unfortunate that all the various kinds of tests and techniques, with their indeterminate boundary conditions and unspecified constraints, cannot and have not been able to view and analyze the test results in terms of the two simple components of the energy spectrum. It would be helpful if these concepts could indeed be implemented in the future tests for determination of mechanical properties of snow.

ELECTRICAL, OPTICAL AND ACOUSTICAL PROPERTIES OF SNOW

This area of research holds much promise for significant usable results in the next ten years. During the past ten to fifteen years, research in these areas has intensified. While much about these properties remains undetermined, current research appears directed toward the development of new means of monitoring snowpack properties. As it now stands microwave systems show substantial potential as the only effective means of remote, nondestructive interpretation of many important snowpack properties such as free water content, density, layering, depth, etc.

In addition, microwave systems also seem to show some promise for analyzing flowing avalanche characteristics. To date this has been a particularly troublesome problem for avalance researchers, since no apparent means of monitoring flow characteristics such as velocity profile, turbulence, etc., has been possible.

As was apparent during the committee sessions, the optical properties have important implications on problems such as snow hydrology, snowpack stability, water equivalent content, etc. However, it appears that useful application to these problems must wait for a more thorough understanding of just what determines the optical properties of snow. Emissivity, for instance, is determined by a number of parameters (grain size, grain shape, water content, impurities) and

to date the effect of these factors and modeling of these parameters has not been done quantitatively to an accurate degree. Gubler's review gives a good summary of this.

Acoustical properties of snow have not received as much attention as other areas in the past ten years. This area of research includes problems of shock wave propagation, seismic waves, acoustical waves, and acoustic emissions associated with deformation processes. Hence, it is difficult to separate acoustic properties from mechanical properties. This work has much potential application, the extent of which cannot be covered here. This type of research could go a long way toward describing material properties, crack propagation in snowpack, snowpack stability, and some physical properties of snowpack. To date this area of research is in its infancy.

In conclusion, an intensified research effort on the electrical, optical and acoustical properties of snow could lead to truly usable results by the end of this decade. In all three subfields discussed here, research could result with instrumentation that can be used to solve a number of engineering problems of practical importance.

Finally, since snow directly influences climatic parameters such as radiation balance, surface and air temperature, cloudiness, soil moisture, water storage and precipitation, certain critical properties of snow become very important in relation to climatological requirements. These snow properties are snow depth, snow water equivalence, area covered, density, albedo, and temperature distribution. It is important that these kinds of information be made available and in a form for ready use by the modelers involved in climatological studies.

SLIDING FRICTION, FLOWING SNOW AND BLOWING SNOW

The problem of sliding friction is still not thoroughly understood. However, research in several countries (Canada, Sweden and the U.S.) is currently in progress to determine the predominant mechanisms which govern the process of sliding friction. At this point in time still more careful and detailed experimentation is needed before these questions can be answered. All analytical representations of sliding friction are not accurate.

The properties of flowing snow was the topic which generated the most discussion. Many unanswered questions surfaced during the discussion sessions. For instance, the importance of particle size in disaggregated flowing snow was discussed in detail. The relative importance of inertial and viscous effects in flowing avalanches was also a hot topic of discussion, and

the problem of in situ measurements to clarify these questions was also a significant part of the discussion. It is generally felt that without improved measurement techniques, the proper characterization of avalanche dynamics will not be achieved. The properties of fluidized snow also have application to other problems such as vehicle mobility, thereby making this of more general interest.

Of the three areas of research discussed by this committee, the problem of blowing snow and snow transport and deposition has received the least attention during the past decade. Currently research is ongoing at several research institutes, but the ability to predict snow transport and deposition patterns still is not available. Research into the mechanics of snow ablation and defining the snow–air interaction needs to be continued, but at a higher level of effort. Possibly, newer techniques such as mixture theory could lead to new advances in this area. Methods of experimentally monitoring snow transport and deposition seem to be well-developed. However, analytical techniques for predicting snow transport are lacking. Good results have been achieved in some instances by using purely empirical recursion techniques, but these are of limited use and do not necessarily improve understanding of the physics of the problem. More effort is needed to develop methods based on the mechanics of two-phase flow, and a considerable research effort will be required before useful engineering solutions are available for predicting snow deposition patterns in mountainous terrain.

SNOW METAMORPHISM

This area of snow research has received some basic scientific investigation rather than just engineering analysis. This is not surprising, since the mechanisms of crystal growth involve intricate thermodynamic processes which appeal to scientific studies. All forms of snow metamorphism have direct application to a large number of practical problems because all of the important material properties of snow are greatly affected by the constant changes brought by snow metamorphism.

Snow has a large specific surface area and is at or close to its melting temperature. Accordingly, it is very active thermodynamically and undergoes constant changes in response to changing environmental conditions. Even at a constant temperature such as the melting point, its specific surface area is continuously reduced as grain growth and densification occur. When large temperature gradients are imposed on snow (the "Soret effect"), the supersaturations are sufficient to cause facet or kinetic crystal growth close to the ground surface. The resulting cohesionless crystals (called depth hoar) are perhaps the most striking example of snow metamorphism.

Because snow metamorphism so greatly affects all of the snow properties that concern us, a thorough understanding of snow metamorphism should be achieved. The basic physics of the problem should be understood, and quantitative models of the processes should be available for the people who need to predict snow properties for problems such as snowmelt, runoff, and avalanche forecasting. In particular, grain growth and densification in freely draining wet snow and the growth and development of faceted crystals in dry snow should be investigated. The responsible processes are worth investigating not only for the sake of understanding snow, but for the information that could be provided about other processes such as hot press sintering and crystal growth at low supersaturations.

FINAL SUMMARY

During the past ten years, much of the research effort on snow has been of a scientific nature. This is evident in published results on the mechanical, optical, electrical, acoustical and thermodynamic properties. In many areas, significant advancements have been made. However, application to practical problems has not progressed as rapidly as one could hope for. The upcoming decade shows good promise for solution of many relevant problems, provided funding is made available to support the work necessary for this effort.

It is the opinion of the committee that scientific basic research should continue to be emphasized. This is especially true in the areas of friction, acoustics, and electrical and optical properties, where fundamental processes are not yet fully understood. However, development of engineering solutions to many problems appears now to be at hand if only an increased effort can be encouraged. Quite possibly a follow-on workshop which addresses the question "Where do we go from here?" could help facilitate this process.